Taming Torridity
New Housing Forms for Heat Resilience

by

Jonathon Brearley

Bachelor of Science in Architecture
Portland State University, 2018

Submitted to the Department of Architecture
in Partial Fulfillment of the Requirements for the Degree of

**Master of Architecture and
Master of Science in Building Technology**

at the

Massachusetts Institute of Technology

May 2022

Signature of Author: _____
Department of Architecture
May 6, 2022

Certified by: _____
Miho Mazereeuw
Associate Professor of Architecture and Urbanism
Thesis Supervisor

Certified by: _____
Leslie K. Norford
Professor of Building Technology
Thesis Supervisor

Accepted by: _____
Leslie K. Norford
Professor of Building Technology
Chair, Department Committee on Graduate Students

Thesis Committee

Advisor (M.Arch):
Miho Mazereeuw
Associate Professor of Architecture and Urbanism

Advisor (S.M.B.T.):
Leslie K. Norford
Professor of Building Technology

Reader:
Caitlin Mueller, PhD
Associate Professor of Building Technology

Taming Torridity
New Housing Forms for Heat Resilience

By Jonathon Brearley

Submitted to the Department of Architecture on May 25, 2022
in Partial Fulfillment of the Requirements for the Degree of
Master of Architecture and Master of Science in Building Technology

Abstract

Intervening on the contemporary US housing typology of the single-family home, this work imagines new building forms that foster resilience to extreme heat through social proximity, housing heterogeneity, and novel space cooling strategies. As we move into a new climate paradigm of increased weather variation and higher temperatures, extreme heat events will become more frequent and extreme. Increased cooling demand during such heat events contributes to electrical grid instability and, in some cases, causes blackouts or rolling brownouts. An established pathway to addressing this problem is more efficient envelopes and building systems, a strategy captured by the Passive House standard. Passive House is not without its constraints, primarily in upfront capital costs, skilled labor availability, and more complex building details. Using two metrics, cooling energy demand and heat index, to model resilience in grid-on (active) and grid-off (passive) scenarios, a heat vulnerability study of single-family houses in four US cities modeled to both Passive House standards and International Energy Conservation Code (IECC) is conducted over a representative hot week in each location. Models are simulated under four climate scenarios (Historic TMY3, and morphed 2020-80 HadCM2 A2) and show that Passive House models improved active resilience by decreasing both peak and total cooling energy over the week in all-weather scenarios by an average of 30% and 33%, respectively. Passive House standard increases passive resilience when houses are ground-coupled through the slab or basement, but otherwise produced worse interior conditions than the IECC model. While it is demonstrated that the Passive House standard is a viable strategy for increasing heat resilience with small deviations from the conventional Passive House logic, this thesis pursues an alternative pathway to heat resilience in US homes by emphasizing building form and architecture that is designed for flexible, resilient functions by exploring three fundamental strategies. Earlier findings on the significant impacts on ground coupling in heat resilience are translated into an architectural and operational strategy that reduces cooling energy and improves passive survivability by leveraging the ground as a heat sink. The second strategy uses zone nesting and thermal buffers conceptualized as layered thermal spaces. Finally, recognizing that social resilience is integral to increasing positive outcomes in extreme events, party walls and unit adjacent reduce exposure and cooling loads while embedding community proximity. The sum of these approaches is presented in a housing proposal that recognizes the forces at play in the desire for low-density, low-rise housing while attempting to subtly undermine kernels of the low-rise, single-family typology such as its resource intensity and homogeneity.

Thesis Supervisor: **Miho Mazereeuw**
Title: Associate Professor of Architecture and Urbanism

Thesis Supervisor: **Leslie K. Norford**
Title: Professor of Building Technology

Page intentionally left blank

All images are produced by the author unless otherwise noted.

Thank you!!!

Page intentionally left blank

Taming Torridity

New Housing Forms for Heat Resilience

Table of Contents

Page intentionally left blank

List of Tables

List of Tables

Page intentionally left blank

List of Figures

List of Figures

List of Abbreviations

List of Abbreviations

IECC	International Energy Conservation Code
TMY	Typical Meteorological Year
SHGC	Solar Heat Gain Coefficient
PHIUS	Passive House Institute United States
ZERH	Zero Energy Ready Home
CONUS	Continental United States
PNAS	Proceedings of the National Academy of Sciences
DOE	Department of Education
NREL	National Renewable Energy Laboratory
ASHRAE	American Society of Heating, Refrigerating and Air-Conditioning Engineers
LEED	Leadership in Energy and Environmental Design
CIBSE	Chartered Institution of Building Services Engineers
IPCC	Intergovernmental Panel for Climate Change
CCWWG	Climate Change World Weather Generator
RCP	Representative Concentration Pathway
HadCM2	Hadley Centre Coupled Model version 3
AR5	Fifth Assessment Report
CFD	Cumulative Frequency Distributions
VRF	Variable Refrigerant Flow
DOAS	Dedicated Outdoor Air System
COP	Coefficient of Performance
EP	EnergyPlus
HHH	Heat Hazard Hours
HHH28	Heat Hazard Hours above 32
HHH32	Heat Hazard Hours above 28
UHI	Urban Heat Island
HVAC	Heat Vulnerability and Air Conditioning
SSP	Shared Socioeconomic Pathway
ICC	International Code Council
GCM	Global Circulation Model
SRES	Special Report Emission Scenario

DBT	Dry Bulb Temperature
RH	Relative Humidity
CMIP	Couples Model Intercomparison Projects
EER	Energy Efficiency Ratio
BTUs	British Thermal Units
SEER	Seasonal Energy Efficiency Ratio
ANSI	American National Standard Institutes
WBGT	Wet Bulb Globe Temperature
SET	Standard Effective Temperature
HI	Heat Index
PCE	Peak Cooling Energy
TCE	Total Cooling Energy
NV	Natural Ventilation
CTF	Conduction Transfer Function
FD	Finite Difference
FE	Finite Element
EUI	Energy Use Intensity
RMSE	Root Mean Square Error

Page intentionally left blank

Chapter 1
Introduction

Chapter 1. Introduction

"Extreme exogenous forces such as the climate have become so disastrous partly because the emerging isolation and privatization, the extreme social and economic inequalities, and the concentrated zones of affluence and poverty pervasive in contemporary cities."

-Eric Kleinberg, *Heat Wave: A Social Autopsy of Disaster in Chicago*[1]

Section 1.1. Extreme Heat as Natural Disaster

Extreme heat events are natural disasters. The World Health Organization calls heatwaves "among the most dangerous of natural hazards" and notes that they are often not heralded as cause for action despite the fact that heat-related mortalities are one of the highest among climate-related disasters in the world.[2] Most loss of life stems from heat-related causes (HRC) where vulnerable populations have their conditions exacerbated.[3] A well-documented spike in hospitalizations and deaths occur on the day and the few days following a heatwave peak and has become the impetus for cross-disciplinary investments in research on multiple aspects of extreme heat and the possibilities of risk reduction at multiple scales.[4] Beyond loss of life by heat and heat-related causes, our material environments also suffer from extreme heat. Eric Keinenberg's book *Heat Wave: a Social Autopsy of Disaster in Chicago* explicates the Chicago heat wave in 1995 where he describes a heat-induced pandemonium; "Thousands of cars broke down in the streets. Several roads buckled. City workers watered bridges spanning the Chicago River to prevent them from locking when their plates expanded...The City soon experiences scattered outages as a result of unprecedented electrical use"[5] In a more recent example during a west coast heatwave in June 2021, streetcar power lines were melted in Portland, OR, rain tracks buckled as did roads.[6] Extreme heat waves, albeit quiet and creeping, have proven to be one of the more deadly and formidable natural forces with serious consequences.

---

[1] Eric Klinenberg, *Heat Wave: A Social Autopsy of Disaster in Chicago* (Chicago, IL: University of Chicago Press, 2002).
[2] Mami Miutori and Deberati Guha-Sapir, eds., "Economic Losses, Poverty & Disasters 1998-2017" (Center for Research on the Epidemiology of Disasters, 2018).
[3] Rupa Basu and Jonathan M. Samet, "Relation between Elevated Ambient Temperature and Mortality: A Review of the Epidemiologic Evidence," *Epidemiologic Reviews* 24, no. 2 (December 1, 2002): 190–202, https://doi.org/10.1093/epirev/mxf007.
[4] Nadja Popovich and Winston Choi-Schagrin, "Hidden Toll of the Northwest Heat Wave: Hundreds of Extra Deaths," *The New York Times*, August 11, 2021, sec. Climate, https://www.nytimes.com/interactive/2021/08/11/climate/deaths-pacific-northwest-heat-wave.html.
[5] Klinenberg, Eric. Heat Wave: A Social Autopsy. Chicago, IL: Univeristy of Chicago Press, 2002.
[6] Josie Fischels, "PHOTOS: The Record-Breaking Heat Wave That's Scorching The Pacific Northwest," *NPR*, June 29, 2021, sec. Environment, https://www.npr.org/2021/06/29/1011269025/photos-the-pacific-northwest-heatwave-is-melting-power-cables-and-buckling-roads.

Section 1.2. Heat Vulnerability

As one might imagine there are a multitude of factors that contribute to heat vulnerability. Factors that contribute to vulnerability include environmental, demographic, economic, pre-existing health conditions, and other factors associated with the existing social fabric.[7] Age and ability are very important in determining heat vulnerability because a person's age affects their ability to shed heat and cool themselves down. Age can also be a predictor in the strength of a person's social network, as well as underlying conditions that elevate risk. These conditions can create vulnerability in many ways, for example, a person might have mobility issues making it difficult to move to a cooler place or a person might not be able to fully assess the effects that heat might be having on them.

Economic factors are also a significant predictor of heat vulnerability and encompass many subfactors such as: income, education level, occupation type, homeownership, housing location, and urban characteristics. Around the word, migrant status is a significant indicator of vulnerability especially in locations where the physical labor force is composed primarily of migrant workers.

> More devastation is seen when the migrant worker population was carefully examined for the effects of extreme heat in Kuwait. Non-Kuwaiti males, who make up the majority of outdoor workers, were disproportionately affected by extremely hot temperatures, with the risk of dying being three times higher during extreme heat compared to optimum temperatures.[8]

This relates strongly to economic status but has the added layer of the vulnerability of workers who might be undocumented or lacking sufficient protections from governing bodies.[9]

The presence and adoption of air conditioning is an essential component of reducing heat vulnerability. A significant reduction in heat-related illness and mortality can be seen in areas with a higher presence of air conditioning. Air conditioning, versus natural ventilation, which becomes untenable at extreme levels of heat, reduces exposure to potential air pollution which can often increase during a heatwave.[10] However, air conditioning has its drawbacks, primarily because of increased demand for energy which puts strain on a grid with increased vulnerability.

Section 1.3. The Electrical Grid

One of the most crucial aspects in thinking about heat resilience is understanding how the electrical grid becomes increasingly vulnerable during periods of elevated temperatures. Much of the electrical infrastructure in the US is based on very early models that date back to the early 20th century where power plants that burn fossil fuels generate electricity which is sent via large transmission lines to specific localities which it is transformed and distributed to electricity consumers. At almost every stage in the process, from generation to consumption, elevated temperatures reduce the efficiency of the grid to be able to produce and distribute electricity.

---

[7] Kathryn C. Conlon et al., "Mapping Human Vulnerability to Extreme Heat: A Critical Assessment of Heat Vulnerability Indices Created Using Principal Components Analysis," *Environmental Health Perspectives* 128, no. 9 (September 2020): 097001, https://doi.org/10.1289/EHP4030.

[8] "Migrant Workers Bear the Brunt of Extreme Heat in Kuwait," August 2021, https://www.who.int/news-room/feature-stories/detail/migrant-workers-bear-brunt-extreme-heat-kuwait.

[9] "Migrant Workers Bear the Brunt of Extreme Heat in Kuwait."

[10] Carina J. Gronlund, "Racial and Socioeconomic Disparities in Heat-Related Health Effects and Their Mechanisms: A Review," *Current Epidemiology Reports* 1, no. 3 (September 2014): 165–73, https://doi.org/10.1007/s40471-014-0014-4.

Almost every method of electricity generation from thermoelectric, to hydroelectric, wind, and solar suffer from high temperatures. Notably, this issue does not discriminate between fuel burning and renewable methods. Combustion methods, though, rely on steam turbines whose efficiency is dependent on the temperature of coolants which begins to rise with higher ambient temperatures.[11]

> Thermal discharge limits vary by world geopolitical region but in the U.S., surface water is typically required to remain under 32.23°C. Plants that use once-through cooling technologies typically return water to the source at a temperature that is 8 to 12°C warmer than the original intake water temperature.[12]

Additional efficiency is also lost by the simple fact of reduced air mass with increased temperatures. Lower air mass means there is less oxygen to burn, which lowers the ability for fuels to output to their fullest potential. The same principle applies to a gasoline-powered car that gets poorer gas mileage in higher temperatures.[13] The relationship between power generation and elevated temperatures is generally linear. As such, high-temperature efficiencies can be understood as percent reductions per degree of temperature increase. According to the Oak Ridge National Laboratory, depending on the generation type, reductions can range from 0.3% to 0.7% per degree °C.

Electrical Grid

1. Generation   2. Transmission   3. Distribution   3. Consumption
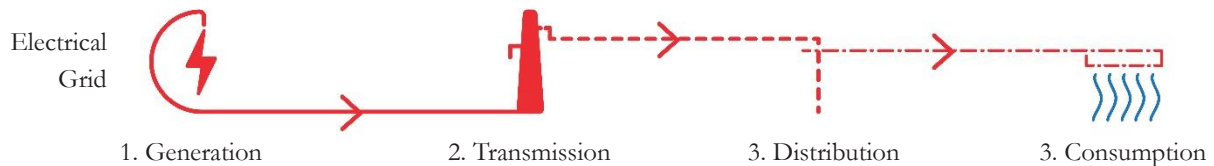
Figure 1. Diagram of electrical grid from generation to consumption

A similar reduction in efficiency can be found in both transmission and distribution, and consistently high temperatures can have lasting effects on transmission and distribution infrastructure eventually leading to failure and faster aging. Again, the relationship between higher temperatures and reduced efficiency of transmission and distribution lines is a linear one, and so can be understood as percent reduction per degree. In this case, transmission and distribution reduction efficiency reduces by 0.7% to 1% per degree Celsius[14]. One reason for this reduction is increased resistance in power lines which reduces electrical throughput.[15] Finally, we can see a significant increase in electrical demand mostly for cooling equipment which sees both an increase in usage, but also a reduction in efficiency per degree of temperature increase.[16]

---

[11] Melissa Dumas, Binita Kc, and Colin I. Cunliff, "Extreme Weather and Climate Vulnerabilities of the Electric Grid: A Summary of Environmental Sensitivity Quantification Methods," August 1, 2019, https://doi.org/10.2172/1558514.

[12] Dumas, Kc, and Cunliff.

[13] Dumas, Kc, and Cunliff.

[14] Dumas, Kc, and Cunliff.

[15] Dumas, Kc, and Cunliff.

[16] Mohd Hazwan Yusof et al., "The Effect of Outdoor Temperature on the Performance of a Split-Unit Type Air Conditioner Using R22 Refrigerant," ed. S.A. Abdul Karim et al., *MATEC Web of Conferences* 225 (2018): 02012, https://doi.org/10.1051/matecconf/201822502012;
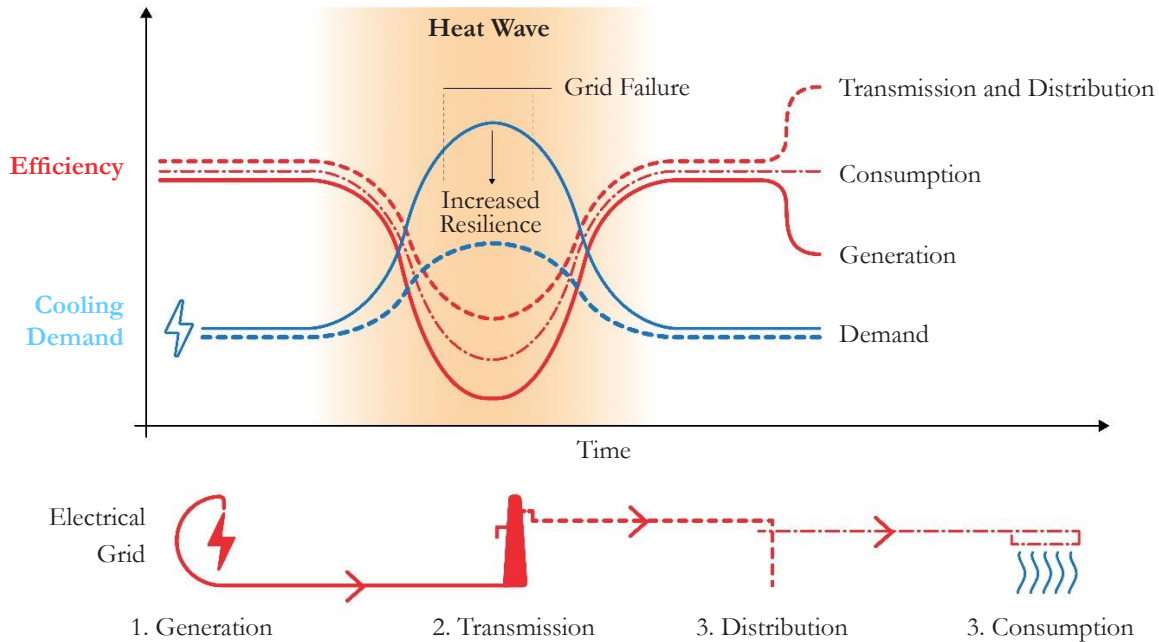
Figure 2. Diagram of the impact heat waves have on grid efficiency and grid demand

Therefore, it is an overarching goal of heat resilience to reduce the peak load demand on the grid which helps to reduce the stress put on the grid to both increase production while battling against reduced efficiency at almost every level from generation to consumption. However, in the event of a grid failure, or more generally considering places with low air conditioning penetration, another aspect of heat resilience is to ensure that buildings have some space that will remain cool through the course of a heatwave.

Section 1.4. Active and Passive Building Resilience.

A comprehensive paper written by Attia, et al. *Resilient cooling of buildings to protect against heat waves and power outages: Key concepts and definitions* provides a holistic sense of what cooling factors play a role in resilient active strategies. The paper also goes to great lengths to provide definitions and frameworks for building resilience from an extensive literature review. A key concept of resilience in the paper is the notion of a system or building's ability to return to equilibrium or find a new equilibrium after an event that might shock them from stability.[17]

> The cooling of a building is resilient when the capacity of the cooling system integrated in the building allows it to withstand or recover from disturbances due to disruptions, including heatwaves and power outages, and to adopt the appropriate strategies after failure (robustness) to mitigate degradation of building performance (deterioration of indoor environmental quality and /or increased need for space cooling energy (recoverability).[18]

Attia, et al. provide a useful framework for conceptualizing the resilient design, using four buckets of building resilience:1) vulnerability, 2) resistance, 3) robustness, 4) recovery. Vulnerability should be considered in the design stage to be able to make decisions toward resilience. Resistance is the ability of the building to maintain

---

[17] Shady Attia et al., "Resilient Cooling of Buildings to Protect against Heat Waves and Power Outages: Key Concepts and Definition," *Energy and Buildings* 239 (May 2021): 110869, https://doi.org/10.1016/j.enbuild.2021.110869.
[18] Attia et al.

equilibrium during normal or predicted extreme weather. Robustness describes the pace and manner in which a building fails under extreme events. Recoverability describes the way that a building returns to equilibrium after an extreme event, which usually relies on robustness. These definitions differ from what might be used at an Urban Scale where "two other resilience definition criteria are found in literature and are used on an urban scale: (1) adaptability, efficiency, flexibility, and redundancy; and (2) preparation, adaptation, recovery, and mitigation."[19]
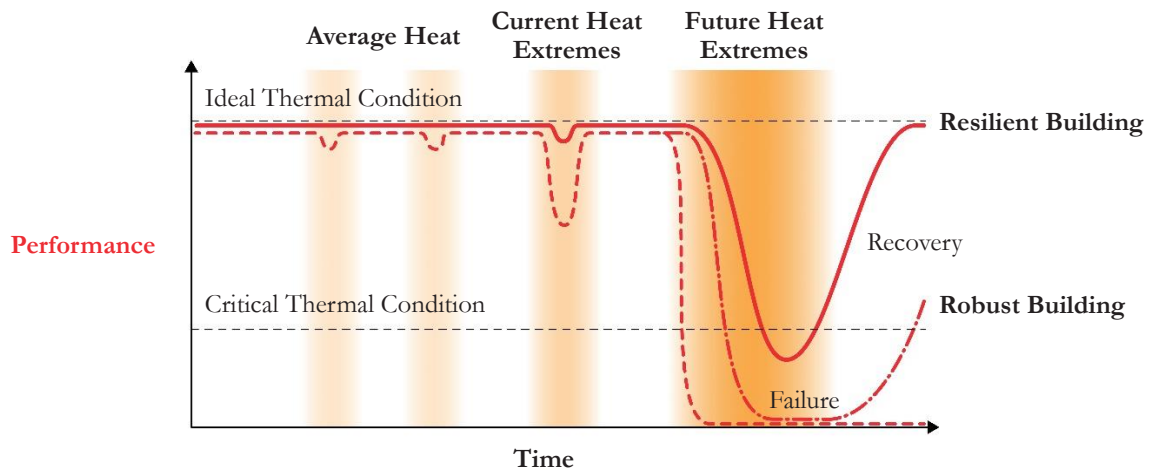
Figure 3. A diagram adapted from Attia, S. et al that shows show forms of resilience in buildings.

The *Annex 80 on Resilient Cooling for Residential and Small Non-Residential Buildings* from the International Energy Agency's Energy in Buildings and Communities Program gives a long list of potential technologies and solutions to resilient cooling with the goals of reducing solar gains, removing sensible heat, and mitigating latent heat of indoor environments. These include solar shades, ventilated facades, micro cooling, and personal comfort control, natural heat sinks, and solar cooling.[20] Many of these strategies straddle between active and passive resilience.

The LEED v4 credit 100 offers a robust framework for approaching passive building resilience. The credit is called *Passive Survivability and Back-up Power During Disruptions* and targets occupant thermal comfort in the event of a power outage. The three paths for achieving the passive survivability credit are: 1) demonstrating that the building does not cross a Heat Index, Wet Bulb Globe Temperature, or Standard Effective Temperature threshold. The credit further specifies that a building should provide backup power for critical loads for systems that are capable of providing cooling or targeted heating.[21]

This thesis uses a very similar building resilience framework that essentially understands building resilience in both active cooling energy resilience and passive resilience in the context of a power outage during a heatwave. A more resilient building stays below a cautionary upper threshold for a longer period of time. Put another way, a building that has a reduced rate of temperature increase is considered to be more resilient. Many of the strategies overlap with those found in Annex 80 in some form.

---

[19] Attia et al.

[20] Peter Holzer, Phillip Stern, and Gerhard Hofer, "Annex 80 on Resilient Cooling for Residential and Small Non-Residential Buildings" (International Energy Agency, June 2019).

[21] U.S. Green Building Council, *LEED Reference Guide for Building Design and Construction.*, 2019.
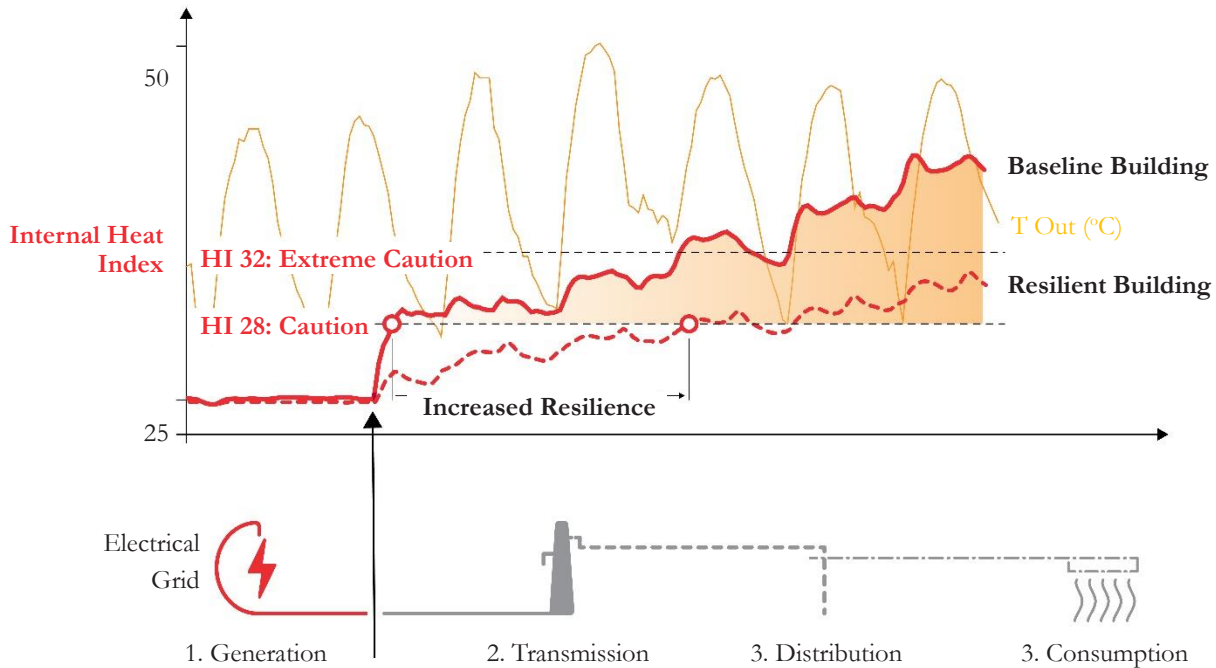
Figure 4. A diagram of internal building conditions in heat index taken from work performed for DAR Engineering on Kuwaiti Villas

Section 1.5. Heat-Related Illness and Treatment

There are several possible heat-related illnesses that might develop with extended exposure to heat. Some illnesses are differentiable progressions of an earlier illness. For example, heat exhaustion is usually a precursor to heatstroke. A journal article in the American Family Physician from Becker and Stewart from 2011 entitled *Heat-Related Illness* offers detail in both the characteristics of heat-related illness as well as their treatment and prevention. Simply, the body's thermoregulation follows the same thermal processes that a building does: conduction, convection, and radiation. In the context of heat-related illness, conduction becomes extremely important because it is the most efficient way to transfer heat away from the body.

> Perspiration is an evaporative mechanism that is dependent on sweat production and water vapor pressure gradient. In high ambient temperatures, heat loss is almost solely based on the rate of sweating. As humidity increases, evaporation becomes increasingly ineffective, thus perspiration serves as the most effective way humans release heat.[22]

Becker and Steward write that body core temperatures of 104°F (40°C) are the effective threshold between mild and severe heat-related illness. "In an effort to preserve central perfusion [blood flow to major organs], there is vasoconstriction of the peripheral vasculature creating hypoperfusion [reduced blood flow]. When a person's core temperature is 104°F or greater, cellular damage occurs." [23]

Mild heat-related illnesses are heat exhaustion and heat cramps. Heat exhaustion is characterized by "headache, weakness, dizziness, goose flesh, nausea, vomiting, diarrhea, irritability, and loss of coordination. The skin may

---

[22] Jonathan A Becker and Lynsey K Stewart, "Heat-Related Illness" 83, no. 11 (2011): 6.
[23] Becker and Stewart.

appear pale or ashen, with associated tachycardia or hypotension."[24] the treatment for which is lying in a cool, shaded place with legs elevated and drinking water. Heat cramps result from diminished salts and electrolytes from excessive sweating. Treatment for heat cramps includes drinking electrolytes and stretching, but if both heat stroke or heat cramps do not get better after half an hour or so, further treatment might be necessary.[25]

Heat stroke is extremely serious and can be diagnosed by a core temperature of over 104°F. People with heat stroke might slur their words, be delirious, pass out, or profusely sweat. The best way to treat heatstroke is by rapid cooling, preferably in a cold tank of water, "cooling rates for cold water immersion have been shown to be superior, applying ice packs or cold, wet towels to the head, neck, axilla, and groin is an alternative option. Rapid air movement with a fan, in combination with spraying a moderate-temperature mist of water, encourages evaporative and convective cooling and is also effective".[26] In general, having the ability to be cooled down rapidly can prevent mild heat-related illness from progressing to heatstroke and begin recovery from heatstroke, though further treatment would be needed.
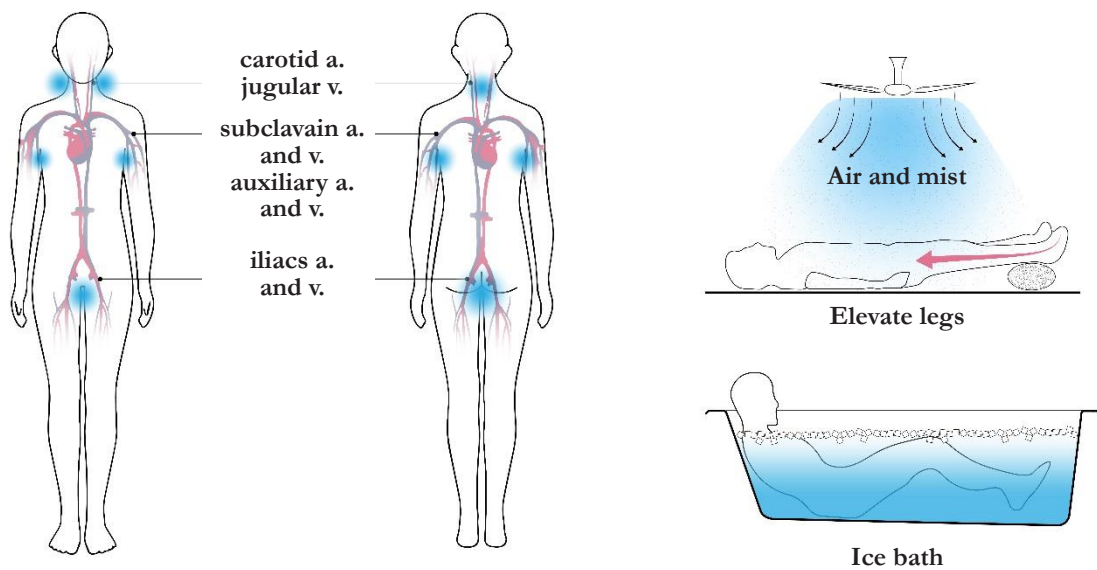
Figure 5. Cooling points and heat related illness treatments

Section 1.6. Urban Heat Island

Urban Heat Island (UHI) is often cited as one of the major heat-related concerns for cities. [27] [28] [29] Hence, heat-related design and heat resilience plans usually center on reducing UHI through urban forestation and roofs that are either high albedo or vegetated. The consequences of heat islands are widely studied and have advanced dramatically since the introduction of the term into literature in 1969.[30] UHI increases energy use across an urban environment by increasing the cooling demand needed to maintain comfortable temperatures.

---

[24] Becker and Stewart.
[25] Becker and Stewart.
[26] Becker and Stewart.
[27] Dean Fuleihan et al., "One NYC 2050 Climate Report," n.d., 332.
[28] John Bolduc et al., "Resilient Cambridge: Climate Change Preparedness and Resiliency Plan," n.d., 70.
[29] Mayor Eric Garcetti, "L.A.'s Green New Deal: Sustainable City PLAn 2019," 2019, 152.
[30] Leonard Myrup, "A Numerical Model of Urban Heat Island," *Journal of Applied Meteorology* 8 (July 24, 1969), https://doi.org/10.1175/1520-0450(1969)008<0908:ANMOTU>2.0.CO;2.

Some studies suggest that cooling energy can triple in extreme cases of UHI.[31] Even localized heat mitigation strategies like building shading and vegetation only partially offset the effects of UHI. One of the most significant phenomena of UHI on buildings is elevated nighttime temperatures that would usually provide passive cooling and opportunities for night flushing.[32] There are many other adverse effects of UHI including decreased air quality and ecological degradation

Significantly, in some large desert cities, the UHI effect is inverted and becomes an Urban Cool Island effect during the day. This is not to say that the urban environment is necessarily "cool" but that relative to the dry and bare sand or soil, urban areas have more vegetation and diversity in the ground cover which ultimately results in lower daytime temperatures.[33] This inversion of UHI results in a smaller temperature delta between day and night because UHI effects are most pronounced in the nighttime. The implications of this observation support significant investments in cultivating the urban cool island effect as well as finding mechanisms to reduce nighttime urban heat island.

Section 1.7. Single-Family Homes.

The single-family home is the most resource intensive form of housing in the United States.[34] It carries with it not just a legacy of resource intensity but a legacy as a tool for racially exclusive wealth creation and "state-sponsored system of discrimination".[35] In aggregate, with some help from the automobile and the National Housing Act, the suburban type of the post-war expansion remains the status quo. White flight and so-called urbanization set in motion a number of crises of which the single-family home was the backdrop. Notablyq, the single-family home, the product and the image, was central to the beginning of the past decade and a half's economic instability and has created the backdrop crisis after crisis.

In the United States, single-family homes dominate housing unit types. Nationally, single family homes account for 61% of all housing unit stock and have been the majority of housing unit construction since 1990 (Figure 6). Additionally, its aggregate typology (low-density suburb) is one of the most energy intensive housing types per capita.[36] Despite the International Energy Conservation Code's (IECC) gradual increase in stringency towards more efficient homes, the relative age of the U.S housing stock and the dominance of the single-family typology present concerns for both active and passive resilience in extreme heat events (Figure 7 and Figure 8).

---

[31] M Santamouris et al., "On the Impact of Urban Climate on the Energy Consumption of Buildings," *Solar Energy* 70, no. 3 (2001): 201–16, https://doi.org/10.1016/S0038-092X(00)00095-5.
[32] M. Kolokotroni, I. Giannitsaris, and R. Watkins, "The Effect of the London Urban Heat Island on Building Summer Cooling Demand and Night Ventilation Strategies," *Solar Energy* 80, no. 4 (April 2006): 383–92, https://doi.org/10.1016/j.solener.2005.03.010.
[33] Michele Lazzarini et al., "Urban Climate Modifications in Hot Desert Cities: The Role of Land Cover, Local Climate, and Seasonality: URBAN CLIMATE OF DESERT CITIES," *Geophysical Research Letters* 42, no. 22 (November 28, 2015): 9980–89, https://doi.org/10.1002/2015GL066534.
[34]Jonathan Norman, Heather L. MacLean, and Christopher A. Kennedy, "Comparing High and Low Residential Density: Life-Cycle Analysis of Energy Use and Greenhouse Gas Emissions," *Journal of Urban Planning and Development* 132, no. 1 (March 2006): 10–21, https://doi.org/10.1061/(ASCE)0733-9488(2006)132:1(10)..
[35] Richard Rothstein, *The Color of Law: A Forgotten History of How Our Government Segregated America*, 2017, https://www.epi.org/publication/the-color-of-law-a-forgotten-history-of-how-our-government-segregated-america/.
[36] Norman, MacLean, and Kennedy, "Comparing High and Low Residential Density."
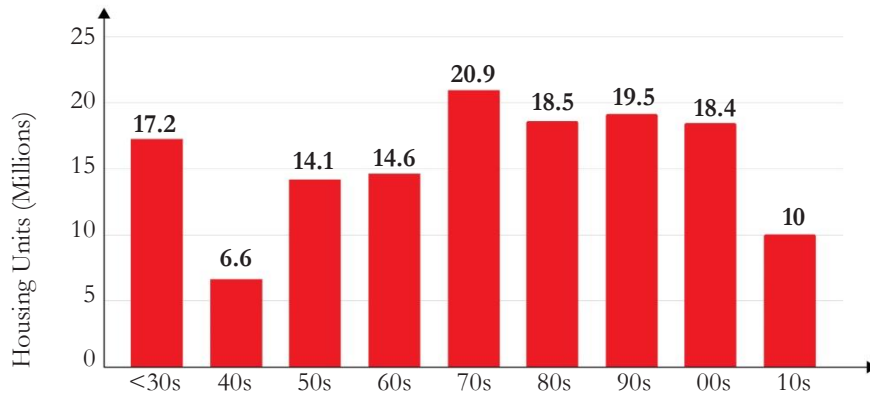
Figure 6. US Housing Unit Quantity by Vintage

Multifamaily   Single fmaily
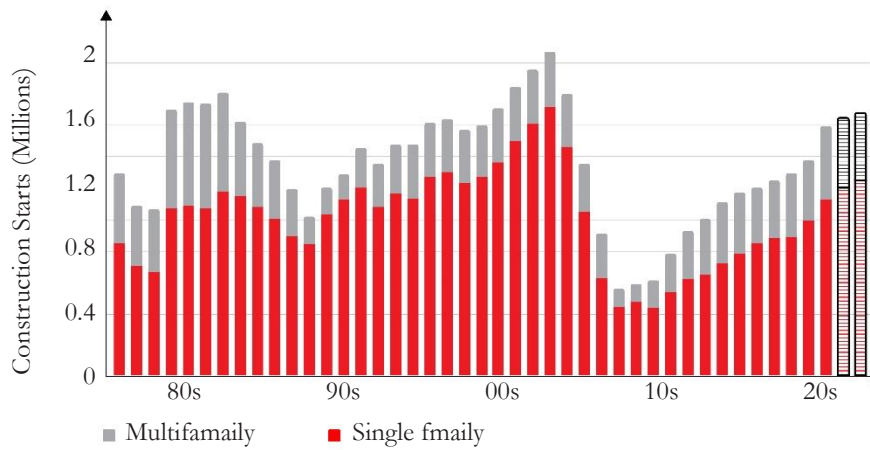
Figure 7. US Number of Housing Starts by Type over Time
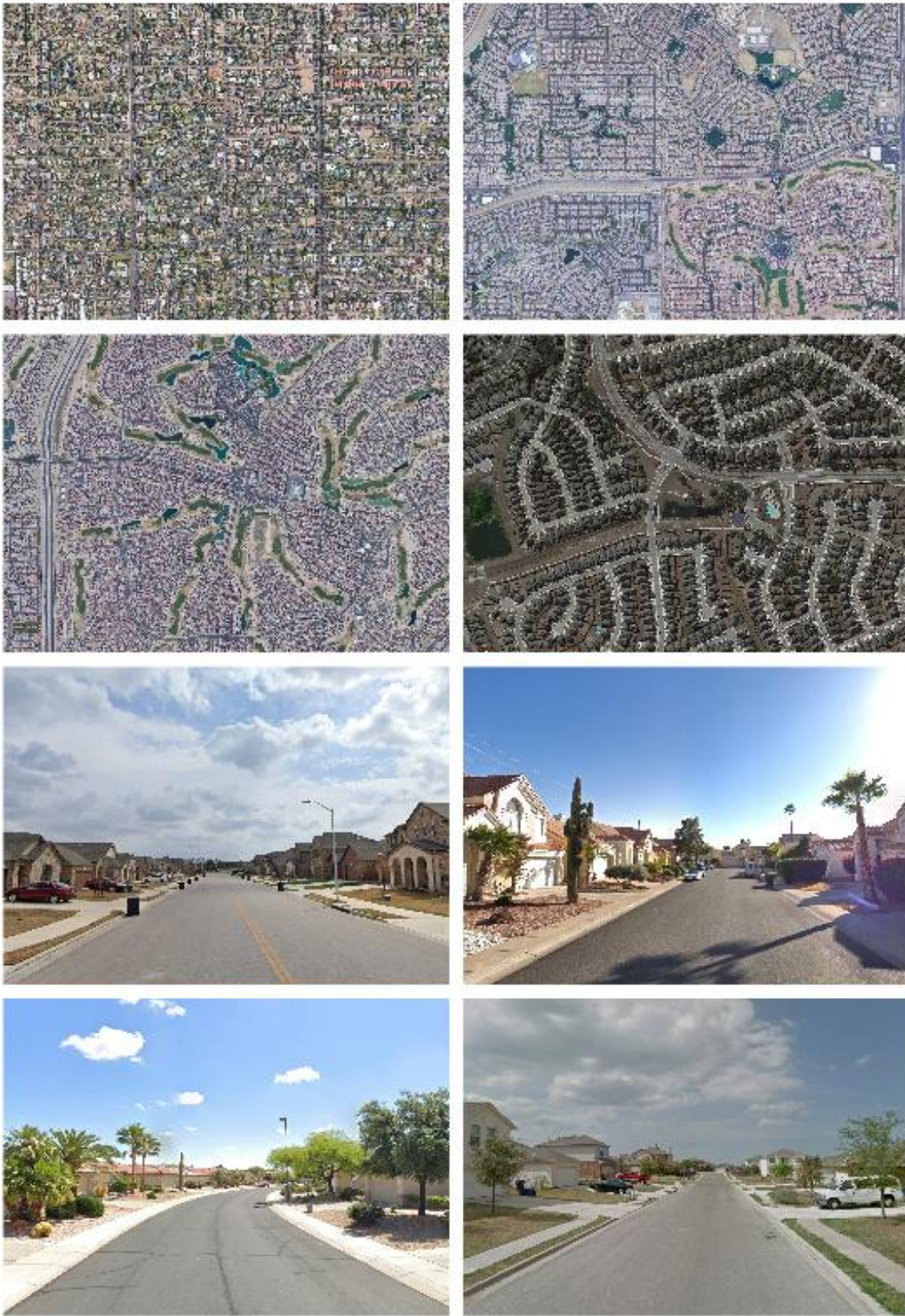
Figure 8. Low-rise, low-density housing in the US Sunbelt – Source: Google Earth

Section 1.8. Thesis Motivation

As we move into a new climate paradigm of increased weather variation and higher temperatures, extreme heat events will become more frequent and extreme. Increased cooling demand during such heat events contributes to electrical grid instability and, in some cases, causes blackouts or rolling brownouts. Single family homes are the focus of this work, and they are examined through the lenses of active resilience and passive resilience. It is imperative to consider passive resilience to ensure that homes are not, at the very least, the cause of heat related illnesses, and that they ideally remain within upper levels of comfortable if the worst-case scenario occurs. As will be discussed in the following chapters, there are several approaches to improving resilience in US single-family housing, one is through high performing envelopes and HVAC systems. This thesis proposes a pathway that emphasizes building form, acknowledges the role of social resilience, and attempts to challenge kernels of the low-rise, single-family typology such as its resource intensity and homogeneity.

Section 1.9. Thesis Organization

There are 8 chapters in this thesis:

1. Introduction – Contextualizes the multifaceted aspects of heat resilience and introduces key concepts in the project

2. Literature Review – Conducts a brief survey of existing literature with which the thesis is in dialogue.

3. Heat Vulnerability in US Single Family Homes – Presents a study of heat vulnerability in US single-family homes and contributes a novel comparison of energy efficiency and passive survivability in future climate scenarios.

4. Ground Coupling and Simulation Methods – Builds on insights gleaned from Chapter 3 on the impact of ground coupling and simulation methods.

5. Jerboa; a simulation tool for advanced ground modeling in a Grasshopper environment – Provides a brief overview of the simulation tool developed as part of the thesis in order to conduct ground modeling simulation in a parametric environment.

6. Strategies and Building Forms for Heat Resilience – Explores three building form strategies that, in concert with building occupant behavior, provide improved heat resilience

7. Heat Resilience Hamlet – Deploys the strategies from Chapter 6 in a low-rise, heat resilience housing proposal as an alternative to the single family-home

8. Conclusion – Reflects on process, outcomes, and takeaways from the project and its various studies.

Chapter 2
Literature Review and Research Opportunity

Chapter 2. Literature Review and Research Opportunity

The field of heat resilience and building simulation is rich and full of work that provides valuable touchpoints to begin this thesis. This brief chapter contextualizes this work in a broader context and identifies two main research themes:

1. The relationships between energy efficiency and heat resilience
2. Assessing current building stock for heat risk and characterizing mitigation strategies towards more heat resilient homes of older vintages.

Both research streams emphasize dwellings in some form, usually diagrammed as single family or multifamily. In most cases, in the US particularly, homes are modeled to International Energy Conservation Code (IECC) minimums, and either take generic forms or use Department of Energy (DOE) reference buildings.

Section 2.1. Energy Efficiency and Heat Resilience

A broad discourse community addresses a tension between the pursuit of energy efficiency and its effects on heat resilience. Baniassadi, Heusinger, and Sailor (2018) conduct a study of new and historic single-family homes in Phoenix, AZ and Houston, TX to assess the performance of each home during a three-day heat wave. Their results show that homes with increased efficiency provide better resilience than older homes. Their parameters of adjustments are in the constructions of the homes: roof and wall R-value, roof absorptivity, window U-value and SHGC, and infiltration rates.[37] A second 2018 paper from Baniassadi and Sailor address a similar question to the previously mentioned paper and survey a higher density housing model across 15 cities during a power outage in order to assess overheating risk across the United States. Their results show that in heating dominated climates, high density housing has higher risk of overheating in hot weather events than those in cooling dominated climates. Baniassadi and Sailor note that buildings in all cities experiences overheating.[38]

Baniassadi and Sailor are in good company with interest in heat risk in high density housing. In Toronto, Canada, O'Brien and Bennet (2018) show through testing of four façade scenarios, two high performance and two minimum standards, perform significantly better when occupants have the ability to open and shade their windows during a power outage. The two façade scenarios create overheating and dangerous interior conditions without occupant intervention. High performance façades perform better with appropriate occupant behavior, but worse when occupants do not shade or naturally ventilate their space. The paper highlights two important aspects of heat resilience: 1) the importance of occupant engagement in the event of a power outage, and 2) window operability should not be sacrificed in the pursuit of efficiency in high rise buildings.[39]

A 2015 report from Wright and Klingenberg detail a range of climate specific passive building standards and show that conventional Passive House wisdom may result in overheating in extreme climates. Wright and Klingenberg show that the German origins of Passive House standards, widely considered to be a gold standard in terms of energy efficiency, can produce negative passive survivability outcomes with its emphasis on passive

[37] Amir Baniassadi, Jannik Heusinger, and David J. Sailor, "Energy Efficiency vs Resiliency to Extreme Heat and Power Outages: The Role of Evolving Building Energy Codes," *Building and Environment* 139 (July 2018): 86–94, https://doi.org/10.1016/j.buildenv.2018.05.024.

[38] Amir Baniassadi and David J. Sailor, "Synergies and Trade-Offs between Energy Efficiency and Resiliency to Extreme Heat - A Case Study," *Building and Environment* 132 (March 15, 2018): 263–72, https://doi.org/10.1016/j.buildenv.2018.01.037.

[39] William O'Brien and Isis Bennet, "Simulation-Based Evaluation of High-Rise Residential Building Thermal Resilience," *ASHRAE Transactions; Atlanta* 122 (2016): 455–68.

heating, where one strategy is to increase solar heat gain through south facing windows which can be detrimental during summer months.[40] A similar finding is shown by Mulville and Stravoravdis (2016) where UK buildings built to higher efficiency codes in order to reduce heating loses simulated under future weather scenarios, concluding that overheating risks increase in new buildings in future weather.[41]

Section 2.2. Assessing Existing Risk and Mitigation Strategies

While section 2.1 focuses largely on the implications of new building codes and standards of heat resilience, a second discourse community concerns itself with assessing risk and potential mitigation strategies. Sun et al. (2021) address issues related to underserved and vulnerable communities in Fresno, California where they examine vulnerability and potential mitigation methods for existing building of primarily 1950s and 1970s vintage. The authors show that roof insulation and low-emissivity window coatings reduce heat gains and improve efficiency and overheating hours in the homes tested. They note that roof insulation should only be considered if the roof is already being replaced, but after-market window coatings could be very powerful. They conclude that passive measures in the event of a power outage are likely not sufficient in creating complete passive survivability in homes of older vintage.[42] In the UK, Porritt et al. (2012), present a study on 19th century terraced homes concluding that many occupant level resilience actions can be taken in order to reduce overheating, notably controlling ventilation and window shading are the most effective. Porritt et al. importantly remark that occupancy and demographic are highly influential in determining risk in homes. Many older homes are owned by the elderly or aging meaning that they will likely be occupying the home during the hottest hours of the day.[43] The aforementioned Baniassadi, Heusinger, and Sailor (2018) paper similarly applies to discourse on houses of older vintages and their vulnerability to heat. Their findings are consistent with Sun et al. and Porritt et al. where they show that roof characteristics are very important as well as reducing solar heat gain.[44] There is also a discourse community focused on geographic heat vulnerability mapping, which is less pertinent to this thesis, but important to mention. Nahlik et al. (2016) show heat vulnerability across two cities, Los Angeles and Phoenix using building appropriate building stock archetypes. This work shows a strong relationship between building vintage and heat vulnerability where older buildings are much more heat vulnerable.[45] A related study from Johnson et al (2012) does not use building stock characteristics, but instead uses socioeconomic data and environmental data.[46]

There is agreement in the literature that increased efficiency standards, which largely consist of higher R-values, U-values, and tighter buildings (among many other factors), improve energy efficiency when relying on mechanical conditioning, but in the event of power outage, generally prevent heat dissipation without occupant intervention. It is also generally agreed that older homes have higher heat vulnerability, and so require mitigation strategies to both reduce peak cooling loads and improve passive survivability.

---

[40] Graham S Wright and Katrin Klingenberg, "Climate-Specific Passive Building Standards," July 2015, 88.

[41] Mark Mulville and Spyridon Stravoravdis, "The Impact of Regulations on Overheating Risk in Dwellings," *Building Research & Information* 44, no. 5–6 (August 17, 2016): 520–34, https://doi.org/10.1080/09613218.2016.1153355.

[42] Kaiyu Sun et al., "Passive Cooling Designs to Improve Heat Resilience of Homes in Underserved and Vulnerable Communities," *Energy and Buildings* 252 (2021): 111383, https://doi.org/10.1016/j.enbuild.2021.111383.

[43] S. M. Porritt et al., "Ranking of Interventions to Reduce Dwelling Overheating during Heat Waves," *Energy and Buildings*, Cool Roofs, Cool Pavements, Cool Cities, and Cool World, 55 (December 1, 2012): 16–27, https://doi.org/10.1016/j.enbuild.2012.01.043.

[44] Baniassadi and Sailor, "Synergies and Trade-Offs between Energy Efficiency and Resiliency to Extreme Heat - A Case Study."

[45] Matthew J. Nahlik et al., "Building Thermal Performance, Extreme Heat, and Climate Change," *Journal of Infrastructure Systems* 23, no. 3 (September 1, 2017): 04016043, https://doi.org/10.1061/(ASCE)IS.1943-555X.0000349.

[46] Daniel P. Johnson et al., "Developing an Applied Extreme Heat Vulnerability Index Utilizing Socioeconomic and Environmental Data," *Applied Geography* 35, no. 1–2 (November 2012): 23–31, https://doi.org/10.1016/j.apgeog.2012.04.006.

Section 2.3. Research Opportunity

Within these discourse communities, there is a focus on building constructions and components with minimal interest in form, limited primarily to window to wall ratios. The literature addresses a constrained range of building characteristics that leave little room for creativity or innovation. They successfully identify building parameters that effect heat resilience and passive survivability in homes which generally boil down to roof and window characteristics, as well as a somewhat vague notion of building occupant behavior. Herein lies an opportunity to both think critically on the impact of building form on both peak cooling loads (the objective of building codes that require greater efficiency) and how that building form may improve passive survivability and partner with occupant behavior towards increased resilience during a heat wave.

Chapter 3
Heat Vulnerability in U.S. Single Family Homes Under Current and Future Climate Predictions

Chapter 3. Heat Vulnerability in U.S. Single Family Homes Under Current and Future Climate Predictions

Section 3.1. Chapter Overview

This chapter performs three sets of simulations over one hot week on two models of single-family homes: IECC and Passive House. Four locations are chosen in unique climate zones: Phoenix, AZ (2B), Austin, TX (2A), Miami, FL (1A), and the DC/Baltimore, MD area. The three major objectives of the chapter are to:

1. Establish an understanding and relationship between climate morphing methods.
2. Show the effects of different natural ventilation strategies on interior heat index during a power outage in a single-family home.
3. Compare peak energy loads, total energy consumption, and passive survivability in single family homes during a hot week.

Together, these objectives produce a definition of heat vulnerability in single-family homes across four climate zones and show the potential impacts of climate change and future extreme heat events on peak energy loads, total energy, and passive survivability. Importantly, this study provides the ability to compare a minimum code (IECC) with a gold standard (Passive House) in order to tease out the impacts of highly efficient standards during extreme heat events.

Section 3.2. Chapter Motivation

The motivation for this study is to quantify heat vulnerability in terms of peak energy loads (affected primarily by cooling loads) and the risk of overheating during a power outage in representative single-family house models in four climate zones across the Continental United States (CONUS). A 2020 PNAS report "*The motley drivers of heat and cold exposure in 21st century US cities* "projects an increase in population heat exposure by a factor of 12.5 to 29.5 across the CONUS. Under RCP 8.5 in the 2090-2099 time period compared to the historical data from 2009-2019, exposures with outstanding increases are Austin TX, Miami FL, Washington DC, and Phoenix AZ, among several large cities in the US South.[47] While the PNAS study represents a worst-case scenario and IPCC warming projections have been updated with the latest 2021 Climate Report, an increase in heat severity and frequency has already been documented and is projected to worsen under most of the new Shared Socioeconomic Pathways. [48] Housing vulnerability is of primary concern when considering extreme heat, not just because populations tend to stay at home during heat wave days, but because elevated temperatures are linked to reduced sleep quality, sleep deprivation, and many other severe health concerns.[49]

A 2015 U.S. Department of Energy Report, *Climate Specific Passive Building Standards,* raises a tension between the pursuit of energy efficient buildings and the negative impacts of passive building methodologies on passive survivability during extreme heat events. The report shows that building characteristics derived from European standards like the Passive House standard from the Passive House Institute US (PHIUS) have the potential to

---

[47] Ashley Mark Broadbent, Eric Scott Krayenhoff, and Matei Georgescu, "The Motley Drivers of Heat and Cold Exposure in 21st Century US Cities," *Proceedings of the National Academy of Sciences* 117, no. 35 (September 1, 2020): 21108–17, https://doi.org/10.1073/pnas.2005492117.

[48] V Zhai, A Pirani, and S. L Connors, "IPCC, 2021: Summary for Policymakers. In: Climate Change 2021: The Physical Science Basis. Contribution of Working Group I to the Sixth Assessment Report of the Intergovernmental Panel on Climate Change," 2021.

[49] Guozhong Zheng, Ke Li, and Yajing Wang, "The Effects of High-Temperature Weather on Human Sleep Quality and Appetite," *International Journal of Environmental Research and Public Health* 16, no. 2 (January 2019): 270, https://doi.org/10.3390/ijerph16020270.

overheat when deployed in some of the warmer US climate zones.[50] Furthermore, risks in single family homes built either to IECC minimum standards or to a gold standard efficiency standard like Passive House are exacerbated by projected increased temperatures, increased frequency, and further intensity of extreme heat events. [51] Quantifying heat vulnerability in U.S. single family homes is important towards charting the direction for increasing resilience for predicted extremes.

Section 3.3. IECC and Passive House

The International Energy Conservation Code is one of several International Building Codes and has been almost ubiquitously adopted across the United States. There are some exceptions: California that uses its own Building Energy Efficiency Standards which are markedly more stringent than the IECC, New York City follows their New York City Energy Conservation Code and is required to be more stringent than IECC, Vermont uses their own code but has an alternative pathway for compliance under ASHRAE 90.1 2016 standards, and Washington State also uses their own code.[52] In some cases, states are late to adopt the latest IECC which are updated on a cycle of three years, and are sometimes modified by a locality, usually towards greater stringency. The IECC references the most up-to-date ASHRAE 90.1 standards. The ASHRAE 90.1 Standards are similarly updated on a three-year cycle, although shifted forward one year. As such, the IECC release follows the most recent ASHRAE 90.1 standard from two years prior, but also includes updates based on ASHRAE recommendations.[53] It is important that ASHRAE 90.1 is differentiated from a building code. Rather, the IECC is the policy vehicle for energy efficiency and might be seen as an enforceable ASHRAE 90.1 even though they evolve together. In some cases, the language of the IECC essentially says: *comply with the ASHRAE 90.1 Standard*!

The IECC, then, "is a comprehensive energy conservation code that establishes minimum regulations for energy-efficient buildings using prescriptive and performance-related provisions."[54] It was preceded by the Model Energy Code which was also produced by the International Code Council. The IECC is divided between commercial and residential (low-rise) buildings. Essentially the scope of the IECC covers the building's: envelope, lighting, and HVAC systems. The IECC primarily justifies itself through economic means, citing that it has saved US energy consumers over $44 billion and 36 million tons of carbon. They also claim consumers are more enticed by more sustainable solutions when they affect their economic bottom-line.[55] An IECC white paper from 2019 cites the role of the code in resilience. The paper refers to the importance of energy efficiency and envelope in extreme temperatures. "Using energy codes to provide enhanced passive survivability provides significant co-benefits. Community and individual resilience are enhanced while building owners and tenants reap energy efficiency related rewards every day in the form of lower energy bills and greater cost certainty."[56] The IECC's prevalence and scope make it an appropriate reference code for modeling a baseline US low-rise, single-family home.

[50] Wright and Klingenberg, "Climate-Specific Passive Building Standards."

[51] Broadbent, Krayenhoff, and Georgescu, "The Motley Drivers of Heat and Cold Exposure in 21st Century US Cities."

[52] Bill Beals, "The Building Envelope: Codes, Codes, and More Codes," *Insulation Outlook Magazine* (blog), 2019, https://insulation.org/io/articles/the-building-envelope-codes-codes-and-more-codes/.

[53] "U.S. Energy Codes Adopted by States," September 29, 2021, https://www.cove.tools/u-s-energy-codes-adopted-by-states-2021.

[54] International Code Council, "International Building Code," 2021, https://search.library.wisc.edu/catalog/999907647602121.

[55] International Code Council.

[56] Ryan Colker, "The Important Role of Energy Codes in Achieving Resilience" (IECC Safe, 2019), https://www.iccsafe.org/wp-content/uploads/19-18078_GR_ANCR_IECC_Resilience_White_Paper_BRO_Final_midres.pdf.

Like ASHRAE 90.1, Passive House is a standard which is referenced in building codes. As of 2022, three states explicitly reference Passive House Standard as an alternative pathway to energy code compliance: Massachusetts, New York State, and Washington State.[57] It might be argued that the ideological origins of Passive House date back to MIT's solar houses in the 1930s where The Solar Energy Fund led by Hoyt C. Hottel developed a series of experimental houses that were conditioned passively (by means of the sun) as an alternative to active conditioning in cold climates.[58] "[Hottel] summarized the purpose of the projects on the fund in the 1940 talk to the Boston Society of the Arts titled 'The Sun as Competitor of Fuels.'"[59] The American pursuit of passive housing strategies evolved in the 1970s towards super insulation and solar design less in the name of fuel alternatives, but toward energy efficiency.

In the 1990s, after some further evolution in North America, Bo Adamson and Wolfgang Feist developed the Passive House standard or "Passivhaus" in Germany and constructed the first prototypes.[60] The pillars, which still hold today, focus on reducing energy consumption through: high wall R-value, minimal thermal bridging, air tightness, high performance glazing, and ventilation with heat recovery. The Passive House standard was brought to North America by Katrin Klingenberg who built the first US Passive House in Urbana, Illinois and went on to establish the Passive House Institute United States (PHIUS) as a 501(c)(3) non-profit organization with builder Mike Kernagis in 2007. [61] The development of the Passive House standards has been an ongoing project and in 2012 PHIUS and DOE joined forces to help develop the standard and promote adoption through the joint program Zero Energy Ready Home (ZERH).[62] PHIUS promotes their standards as a mechanism that creates resilience in many scenarios including extreme heat scenarios. Adjustments have been made to the standards to better address cooling dominated climates, yet this continues to be an active area of research. "PHIUS+ buildings provide superior indoor air quality, resilience during power outages, and an extremely quiet, comfortable indoor environment."[63] The Passive House standard represents the gold standard for energy efficiency in United States buildings and the increasing number of Passive House projects makes it an appropriate reference standard to evaluate heat vulnerability of ultra-high efficiency homes in future climates.

---

[57] "Building Codes," The Passive House Network, accessed February 20, 2022, https://naphnetwork.org/codes/.
[58] Daniel A. Barber, *A House in the Sun: Modern Architecture and Solar Energy in the Cold War* (New York, NY: Oxford University Press, 2016).
[59] Barber.
[60] Katrin Klingenberg, "Passive House (Passivhaus)," *Sustainable Built Environments*, 2020, 23, https://doi.org/10.1007/978-1-0716-0684-1_351.
[61] . Klingenberg.
[62] "Mission & History: Passive House Alliance U.S.," 2022, https://www.phius.org/about/mission-history.
[63] "Mission & History: Passive House Alliance U.S."

Section 3.4. Methodology

3.4.1. Approach and Framing

To produce a high-level understanding of heat vulnerability in the US, four outstanding cities in 4 unique ASHRAE climate zones were selected from the 2020 PNAS report on potential heat exposure increases in the next century: Phoenix, AZ (2B), Austin, TX (2A), Miami, FL (1A), and the DC/Baltimore, MD area (4A). (Figure 9). The first set of simulations provides a comparison between morphed weather files in two locations and frames future weather extremes, the second set establishes natural ventilation as a key component in creating passive survivability and the third provides heat vulnerability analysis in terms of peak load and passive survivability between two housing models. One model uses the locally adopted IECC and the other uses regional Passive House standards. All simulations are run over a hot week unique to each location under four climate scenarios: historic, 2020 A2, 2050 A2, and 2080 A2. (Table 1). Simulations are run using EnergyPlus V9.5.0 via OpenStudio and Honeybee 1.4.0 for Grasshopper (See 3.3.4).
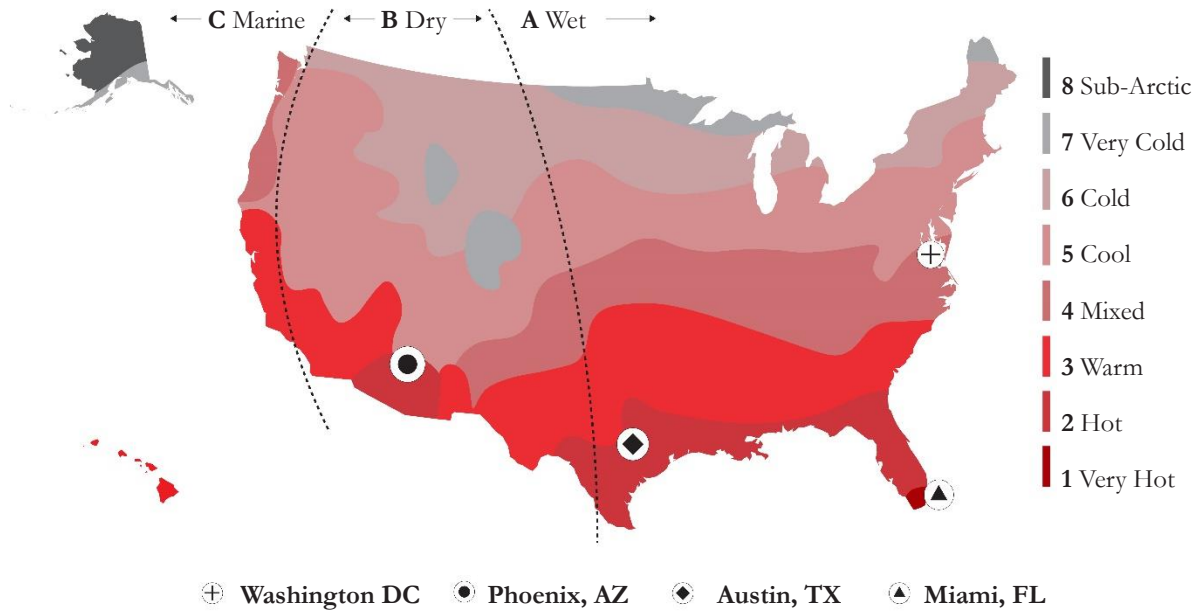
Figure 9. ASHRAE Climate Zone Map

Table 1. Hot weather weeks used in simulations

	DC	Miami	Austin	Phoenix
Hot Week	July 27 – August 2	August 23 - 29	July 25-31	August 5-11

3.4.2. Morphed Weather Data

TMY3 EPW files were used from the NREL TMY Data Set (2008) from the approximate period of 1973-2005. These serve as the basis for all Simulation Sets. Two major weather morphing sources are used: CCWorldWeatherGen (CCWWG) and WeatherShift™. The fundamental premise of morphing weather data is to preserve detailed time-series data found in EPW files and adjust daily and monthly data to match warming scenarios and emissions predictions.[64]

The CCWorldWeatherGen tool is well documented in the 2012 paper "Transforming existing weather data for worldwide locations to enable energy and building performance simulation under future climates" from Jentsh et al. [65] The CCWWG tool uses the Hadley Centre Coupled Model version 3 (HadCM3) global circulation model (GCM) developed by the Hadley Center in the UK. The "Coupled" model represents the coupling of the Hadley Centre's Atmosphere (HadAM3) and Ocean (HadOM3) Models. CCWWG uses the HadCM3 GCM to morph EPW files to the A2 emissions pathway from the IPCC's Special Report on Emissions Scenarios (SRES) published in 2000. The CCWWG Technical reference manual provides a detailed overview of morphed parameters that includes: DBT, Dew Point Temp., RH, Extraterrestrial Direct Normal Radiation, Horizontal Infrared Radiation, Total Precipitation Rate, and Wind Speed.[66] After morphing, the CCWWG EPW files were then run through the EnergyPlus Weather Statistics and Conversion Utility which outputs EPW files ready to be used in EnergyPlus Simulations.

WeatherShift™ is an Arup and Argos Analytics project based on the Coupled Model Intercomparison Project Phase 5 (CMIPs) which is a scientific consensus-based blend of GCMs that represent one of the most state-of-the-art climate projection mechanisms. Climate morphing through WeatherShift™ is available for three future time periods, 2026-2049, 2056-2075, and 2080-2099 for 5th, 10th, 25th, 50th, 75th, 90th, and 95th percentile projections under Representative Concentration Pathways (RCP) projections from the IPCC Fifth Assessment Report (AR5) that was released in 2014.[67] The WeatherShift™ tool uses cumulative frequency distributions (CFD) to offset monthly means based on percentile combinations of RCP projections. The WeatherShift™ files used for Simulation Set 1 (1.3.6) are all 50th percentile morphed EPW files.

The IPCC has recently updated its climate projections and scenario nomenclature in the most recent IPCC 2021 Climate Report. Emissions pathways are now called Shared Socioeconomic Pathways or SSPs. These pathways all ultimately have a warming scenario associated with them, though they differ in the mechanisms that result in each warming projection.[68] Figure 10 shows generally how each scenario relates to others and their respective warming implications. Roughly, the HadCM3 A2 Scenario generated by CCWorldWeatherGen falls slightly below projections for SSP and RCP 8.5. At the time, these scenarios represented "business as usual", but are now generally considered to be worst-case scenarios with a temperature rise between 4.5 and 5 ℃. RCP 4.5 does not have an SSP parallel and falls between RCP 2.6 and 6.0 with a warming projection of 2.5 ℃.[69]

---

[64] Robert Dickinson and Benjamin Brannon, "Generating Future Weather Files for Resilience," *Los Angeles*, 2016, 6.

[65] Mark F. Jentsch et al., "Transforming Existing Weather Data for Worldwide Locations to Enable Energy and Building Performance Simulation under Future Climates," *Renewable Energy* 55 (July 2013): 514–24, https://doi.org/10.1016/j.renene.2012.12.049.

[66] Mark F. Jentsch, "Climate Change Weather File Generators: Technical Reference Manual for the CCWeatherGen and CCWorldWeatherGen Tools" (Sustainable Energy Research Group, November 2012).

[67] Luke Troup, "Morphing Climate Data to Simulate Building Energy Consumption," 2020, 8.

[68] Zhai, Pirani, and Connors, "IPCC, 2021: Summary for Policymakers. In: Climate Change 2021: The Physical Science Basis. Contribution of Working Group I to the Sixth Assessment Report of the Intergovernmental Panel on Climate Change."

[69] Matthew J. Gidden et al., "Global Emissions Pathways under Different Socioeconomic Scenarios for Use in CMIP6: A Dataset of Harmonized Emissions Trajectories through the End of the Century," *Geoscientific Model Development* 12, no. 4 (April 12, 2019): 1443–75, https://doi.org/10.5194/gmd-12-1443-2019.
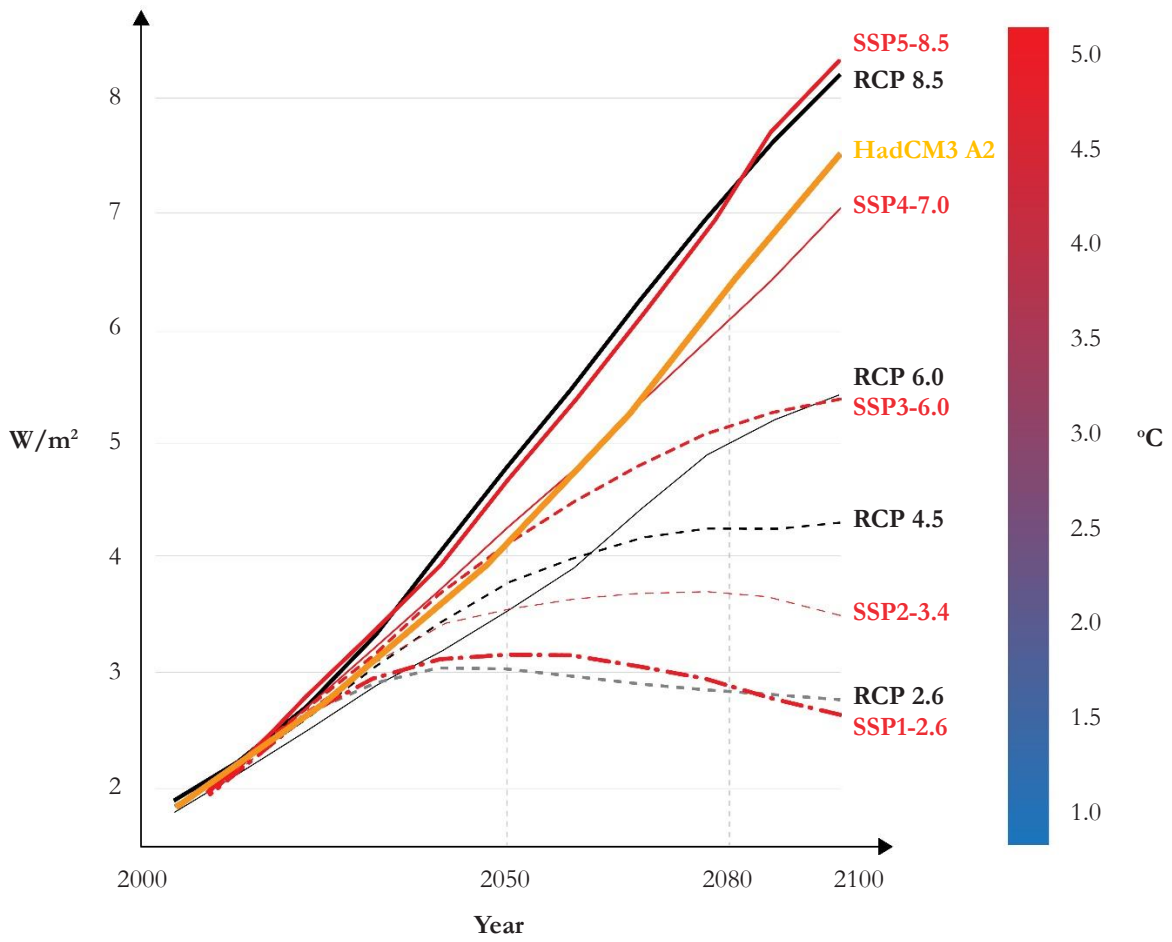
Figure 10. Warming Scenarios Radiative Forcing (W/m²) and Warming Projections (ºC)

3.4.3. Model Parameters

For each location, the house model has unique parameters that reference the IECC in its location, or the Passive House PHIUS+ 2018 Standard specific to that region (Figure 11, Table 2, Table 3).[70]
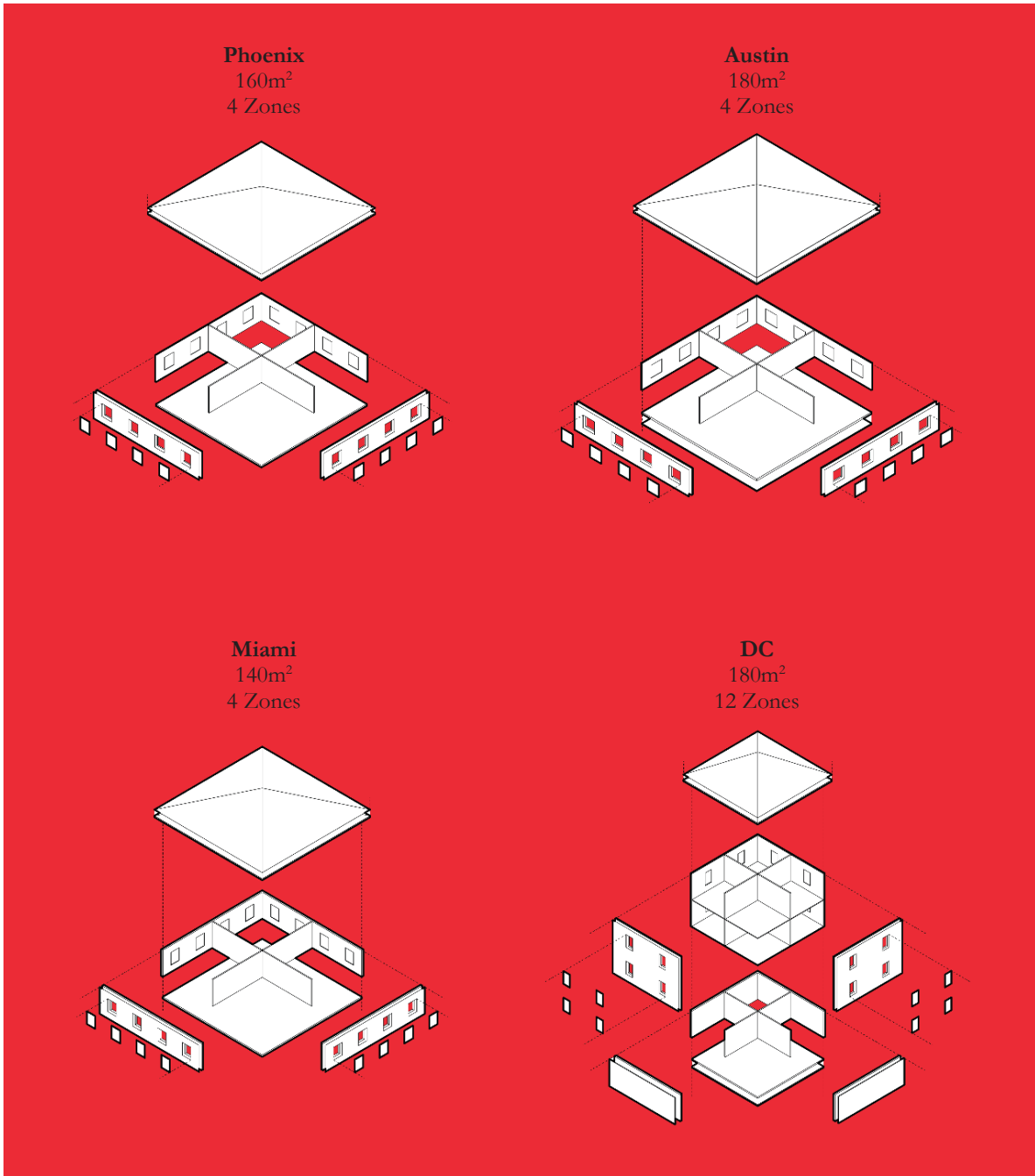
Figure 11. Physical characteristics of house models

[70] "PHIUS+ Certification Guidebook v2.0" (PHIUS, February 2019),
https://www.phius.org/PHIUS+2018/PHIUS+%20Certification%20Guidebook%20v2.0_final.pdf.

Table 2. State Adopted IECC codes (* indicates amendments have been made to code)

	Arizona	Texas	Florida	Maryland
Code[71]	N/A	IECC 2015*	IECC 2018*	IECC 2018*

Table 3. Locally Adopted IECC (* indicates amendments have been made to code)

	Phoenix, AZ	Austin, TX	Miami, FL	Baltimore, MD
Code	IECC 2018*[72] [73]	IECC 2021*[74]	Florida Building Code 2020[75]	IECC 2018[76]
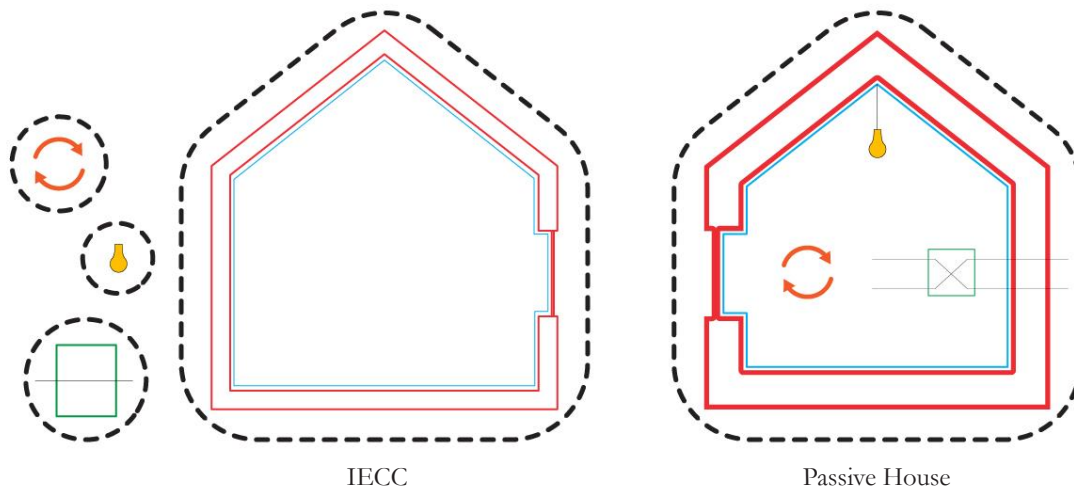
IECC   Passive House

Figure 12. IECC and Passive House graphical representation. IECC is a decoupled prescriptive minimum, where Passive House is performance-based standard.

---

[71] "Status of State Energy Code Adoption - Residential | Building Energy Codes Program," accessed March 28, 2022, https://www.energycodes.gov/status/residential.

[72] "2018 International Energy Conservation Code (IECC) | ICC Digital Codes," accessed March 28, 2022, https://codes.iccsafe.org/content/IECC2018P4.

[73] "2018 International Energy Conservation Code (IECC) Phoenix Amendments," 2018.

[74] "CHAPTER 25-12. - TECHNICAL CODES. | Land Development Code | Austin, TX | Municode Library," accessed March 28, 2022, https://library.municode.com/tx/austin/codes/land_development_code?nodeId=TIT25LADE_CH25-12TECO_ART12ENCO.

[75] "2020 Florida Building Code, Energy Conservation, 7th Edition | ICC Digital Codes," accessed March 28, 2022, https://codes.iccsafe.org/content/FLEC2020P1.

[76] "2018 International Energy Conservation Code (IECC) | ICC Digital Codes."

Table 4. Phoenix IECC and Passive House model parameters

Phoenix, AZ

Reference and Model Parameters

Parameter	Units	IECC Referenced	Modeled	Passive House Referenced	Modeled
Exterior Wall					
R-Value	hr ft² F⁰/Btu	13	14.4	27	27.5
Solar Absorption	%	.75	.75	-	.7
Emmitance	%	.9	.9	-	.9
Exterior Finish	-	-	Stucco	-	Stucco
Construction	-	-	Wood Framed	-	Wood Framed
Basement Wall					
R- Value	hr ft² F⁰/Btu	0	.6	0	.6
Insulation	yes/no	-	No	-	No
Construction	-				
Exterior Roof					
R- Value	hr ft² F⁰/Btu	38	39.1	70	70.7
Emittance	%	.9	.9	-	.9
Solar Absorption	%	.75	.75	-	.75
Exterior Finish	-	-	Asphault	-	Asphault
Interior Floors					
R- Value	hr ft² F⁰/Btu	13	13	13	13
Construction	-	-	Wood Framed	-	Wood Framed
Interior Walls					
R- Value	hr ft² F⁰/Btu	0	.62	0	.62
Construction	-	-	Wood Framed	-	Wood Framed
Slab					
R- Value	hr ft² F⁰/Btu	0	0	0	.78
Insulation	-	-	No	-	No
Construction	-		.8" Conc		.8" Conc
Glazing					
U-Value	hr ft² F⁰/Btu	.4	.4	.18	.18
SHGC	-	.24	.24	.3	.24
tvis		-	.6	.6	.6
Ratio		15% of FA	15% of FA	15% of FA	15% of FA
Infiltration					
ACH50	ACH/hr	5	5		.6
ACH4	ACH/hr	-	.25		.03
Envelope Area	m³/s/m²	-	.000174		.000026
HVAC					
Template	-	ACCA Man S	VRF + DOAS	<10W/m² peak	VRF + DOAS
COP	-	-	3.35	-	3.35
EER	(Btu/hr)/W	-	11.42	-	11.42
SEER	(Btu/hr)/W	14	13.41*	-	13.41*
Cooling Set-point	C	-	23	-	25
Ventilation	l/s	-	10	-	10
Heat Recovery Efficiency	%	-	-	yes	70 Sensible
DOAS	yes/no	-	yes	-	yes
DCV	yes/no	-	no	-	no

Table 5. Austin IECC and Passive House model parameters

Austin, TX

Reference and Model Parameters

Parameter	Units	IECC Referenced	Modeled	Passive House Referenced	Modeled
Exterior Wall					
R-Value	hr ft² F⁰/Btu	19	20.9	27	27.5
Solar Absorption	%	.75	.75	-	.7
Emmitance	%	.9	.9	-	.9
Exterior Finish	-	-	Brick Veneer	-	Brick Veneer
Construction	-	-	Wood Framed	-	Wood Framed
Basement Wall					
R- Value	hr ft² F⁰/Btu	0	.62	0	.6
Insulation	yes/no	-	No	-	No
Construction	-				
Exterior Roof					
R- Value	hr ft² F⁰/Btu	49	50.2	70	70.7
Emittance	%	.75	.75	-	.75
Solar Absorption	%	.9	.9	-	.9
Exterior Finish	-	-	Asphault	-	Asphault
Interior Floors					
R- Value	hr ft² F⁰/Btu	13	13	13	13
Construction	-	-	Wood Framed	-	Wood Framed
Interior Walls					
R- Value	hr ft² F⁰/Btu	0	.62	0	.62
Construction	-	-	Wood Framed	-	Wood Framed
Slab					
R- Value	hr ft² F⁰/Btu	0	0	0	0
Insulation	-	no	no	-	no
Construction	-		.8" Conc		.8" Conc
Glazing					
U-Value	hr ft² F⁰/Btu	.35	.35	.18	.18
SHGC	-	.25	.24	.3	.3
tvis		-	.6	.6	.6
Ratio		15% of FA	15% of FA	15% of FA	15% of FA
Infiltration					
ACH50	ACH/hr	3	3	.6	.6
ACH4	ACH/hr	-	.15	.03	..03
Envelope Area	m³/s/m²	-	.000154	-	.000031
HVAC					
Template	-	ACCA Man S	VRF + DOAS	<10W/m² peak	VRF + DOAS
COP	-	-	3.33	-	3.33
EER	(Btu/hr)/W	-	11.36	-	11.36
SEER	(Btu/hr)/W	14	13.3*	-	13.3*
Cooling Set-point	C	-	23	-	25
Ventilation	l/s	-	10	-	10
Heat Recovery Efficiency	%	-	-	yes	70 Sensible
DOAS	yes/no	-	yes	-	yes
DCV	yes/no	-	no	-	no

Table 6. Miami IECC and Passive House model parameters

Miami, FL
Reference and Model Parameters

Parameter	Units	IECC Referenced	Modeled	Passive House Referenced	Modeled
Exterior Wall					
R-Value	hr ft² F⁰/Btu	13	14.4	27	27.5
Solar Absorption	%	.75	.75	-	.75
Emmitance	%	.9	.9	-	.9
Exterior Finish	-	-	Stucco	-	Stucco
Construction	-	-	Wood Framed	-	Wood Framed
Basement Wall					
R- Value	hr ft² F⁰/Btu	0	.62	0	.6
Insulation	yes/no	-	No	-	No
Construction	-				
Exterior Roof					
R- Value	hr ft² F⁰/Btu	30	31.1	60	60.25
Emittance	%	.9	.9	-	.9
Solar Absorption	%	.75	.75	-	.75
Exterior Finish	-	-	Asphault	-	Asphault
Interior Floors					
R- Value	hr ft² F⁰/Btu	13	13	13	13
Construction	-	-	Wood Framed	-	Wood Framed
Interior Walls					
R- Value	hr ft² F⁰/Btu	0	.62	0	.62
Construction	-	-	Wood Framed	-	Wood Framed
Slab					
R- Value	hr ft² F⁰/Btu	0	.78	0	.78
Insulation	-	-	no	-	no
Construction	-		.8" Conc		.8" Conc
Glazing					
U-Value	hr ft² F⁰/Btu	-	.5	.18	.5
SHGC	-	.25	.25	.25	.25
tvis		.6	.6	..06	.6
Ratio		15% of FA	15% of FA	15% of FA	15% of FA
Infiltration					
ACH50	ACH/hr	7	7		.6
ACH4	ACH/hr	-	.35		.03
Envelope Area	m³/s/m²	-	.000287		.000025
HVAC					
Template	-	ACCA Man S	VRF + DOAS	<10W/m² peak	VRF + DOAS
COP	-	-	3.46	-	3.46
EER	(Btu/hr)/W	-	11.80	-	11.80
SEER	(Btu/hr)/W	14	14.07*	-	14.07*
Cooling Set-point	C	-	23	-	25
Ventilation	l/s	-	10	-	10
Heat Recovery Efficiency	%	-	-	yes	70 Sensible
DOAS	yes/no	-	yes	-	yes
DCV	yes/no	-	no	-	no

Table 7 DC IECC and Passive House model parameters

DC

Reference and Model Parameters

Parameter	Units	IECC Referenced	Modeled	Passive House Referenced	Modeled
Exterior Wall					
R-Value	hr ft² F⁰/Btu	20	22.2	51	51.5
Solar Absorption	%	.75	.75	-	.75
Emmitance	%	.9	.9	-	.9
Exterior Finish	-	-	Hardie Board	-	Hardie Board
Construction	-	-	Wood Framed	-	Wood Framed
Basement Wall					
R- Value	hr ft² F⁰/Btu	13	13.9	13	14.5
Insulation	yes/no	yes	yes	-	No
Construction	-				
Exterior Roof					
R- Value	hr ft² F⁰/Btu	49	50.5	80	80
Emittance	%	.9	.9	-	.9
Solar Absorption	%	.75	.75	-	.75
Exterior Finish	-	-	Asphalt	-	Asphalt
Interior Floors					
R- Value	hr ft² F⁰/Btu	13	13	13	14.8
Construction	-	-	Wood Framed	-	Wood Framed
Interior Walls					
R- Value	hr ft² F⁰/Btu	0	.62	0	.62
Construction	-	-	Wood Framed	-	Wood Framed
Slab					
R- Value	hr ft² F⁰/Btu	10	11	20	14.5
Insulation	-	yes	yes	-	yes
Construction	-		.8" Conc		.8" Conc
Glazing					
U-Value	hr ft² F⁰/Btu	.32	.32	.15	.15
SHGC	-	.55	.4	.4	.4
tvis		.6	.6	.6	.6
Ratio		15% of FA	15% of FA	15% of FA	15% of FA
Infiltration					
ACH50	ACH/hr	3	3		.6
ACH4	ACH/hr	-	.15		.03
Envelope Area	m³/s/m²	-	.000122		.000024
HVAC					
Template	-	ACCA Man S	VRF + DOAS	<10W/m² peak	VRF + DOAS
COP	-	-	3.36	-	3.36
EER	(Btu/hr)/W	-	11.46	-	11.46
SEER	(Btu/hr)/W	14	13.47*	-	13.47*
Cooling Set-point	C	-	23	-	25
Ventilation	l/s	-	10	-	10
Heat Recovery Efficiency	%	-	-	yes	70 Sensible
DOAS	yes/no	-	yes	-	yes
DCV	yes/no	-	no	-	no

While Passive House Standards have guidelines regarding power densities and efficiencies, to simplify the model and because model simulation period is relatively brief (168 hours), the decision was made to keep model loads constant. However, for the Passive House Standards, the peak cooling load limit of 10W/m² was enforced.

Model Loads
Costant Across All Models

Parameter	Units	Value		Parameter	Watts	* #	* Frac	= Use (W)
Occupancy				**Occupancy**				
People	#	3.5		Desktop PC	200	1	0.5	**100**
Occupant Density	occ/m²	.2		Television	100	2	0.2	**40**
Activity	W	120		Video Game	50	1	0.1	**5**
Lighting				Music Speakers	50	1	0.2	**10**
Power Density	W/m²	5		Internet	10	1	1	**10**
Radiant Fraction	-	.6		Laptop	30	3	0.2	**18**
Visible Fraction	-	.2		Tablet	15	3	0.2	**9**
Electic Equipment				Smartphone	4	4	0.2	**3.2**
Total Watts	W	1345		Fans (Ceiling)	55	5	0.2	**55**
Power Density	-	~7.1		Microwave	1500	1	0.01	**15**
Radiant Fraction	-	.5		Fridge	350	2	1	**600**
Gas Equipment				Freezer	100	1	1	**100**
Watts per Area	W/m²	5.5		Washing Machine	500	1	0.02	**10**
Radiant Fraction	-	.2		Dryer	2000	1	0.04	**80**
Hot Water				Dishwasher	500	1	0.05	**25**
Flow per Area	W/m²	.12		Range	2500	1	0.1	**250**
Target Temp	C	.6		Vacuum	750	1	0.02	**15**
Sensible Fraction	-	.5					Total:	*1345W*

Model Schedules
*Heat/Cool Set-points are Constant
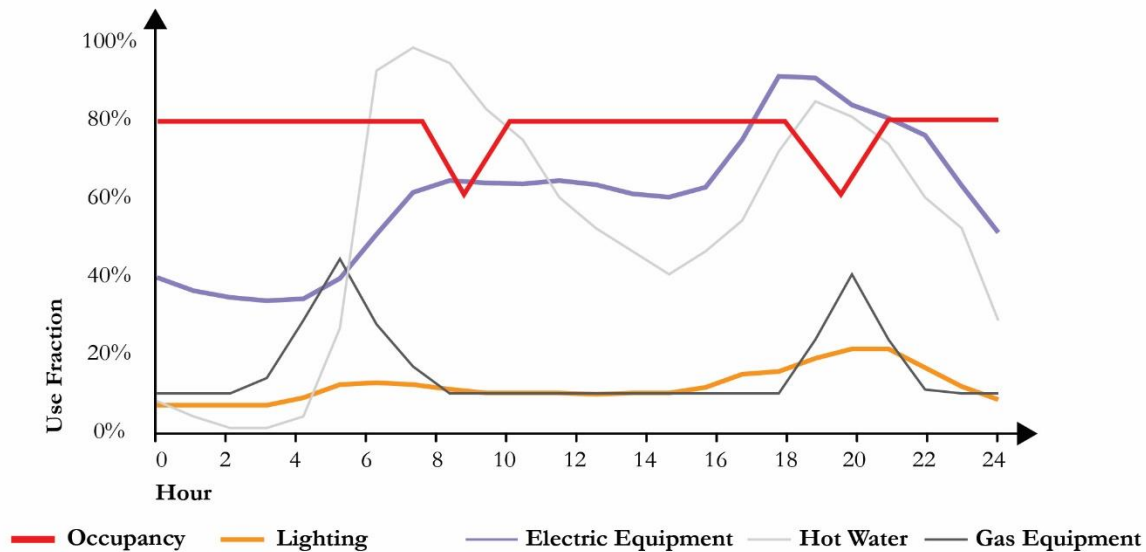
Figure 13. Model loads and model schedules

3.4.4. Honeybee and EnergyPlus

Airflow Network

For all simulations, the EnergyPlus Airflow Network was applied for a more accurate representation of interior temperatures during both "Grid-On" and "Grid-Off" Scenarios. The Airflow Network is especially useful when modeling airflow through multiple zones with natural ventilation.[77] Honeybee modeling converts all objects related to airflow into Airflow Network objects. Infiltration for the Airflow Network was calculated with an interior/exterior delta pressure of 4 Pa. The results from Airflow Network provide a more accurate interior temperature, particularly important in the "Grid-Off" scenario and enables a more nuanced understanding of air flow through the house which can be visualized as point-in-time vectors at each ventilated window.

Ground Temperatures

Ground temperatures have long been a tricky aspect of energy modeling. It is widely documented that one should not use temperature provided by the EPW for many reasons: EPW ground temperatures represent undisturbed ground and EPW ground temperatures do not account for heat flux through slabs or adjacent walls from conditioned zones. The rule of thumb says to use a ground temperature that is 2 degrees Celsius less than the zone's conditioned temperature.[78] For small buildings, though, this approach is also ultimately too simplified, especially for our purposes with interest in basement temperatures. Thus, a more nuanced ground temperature value was calculated through the EnergyPlus Ground Heat Transfer Auxiliary Program. Further ground modeling methods are presented in Chapter 4. Here, the Basement Pre-Program and the Slab Pre-Program are used to calculate ground temperatures using the historic EPW data for each location using the reference IECC slab or basement characteristics. In all cases the EnergyPlus sample IDF files were modified to reflect the modeled building characteristics. Each program provides a set of temperatures at different locations on basement walls and slabs. For slabs, the "TAverage[C]" temperature was used. For basements, the "MonthlyTSurfWallUpper[C]" was used. These values were applied to the model as a string through the Honeybee "ModeltoOSM" component. Ground temperatures used for each location can be found in Table 8. See Chapter 4 for more on ground modeling methods.

Table 8. Ground Temperatures During Simulation Period

	DC	MI	ATX	PHO
Temp (ºC)	24.59	23.3	24.47	22.37

---

[77] Lixing Gu, "Airflow Network Modeling In EnergyPlus," *Building Simulation*, 2007, 11.

[78] Drury B. Crawley et al., "EnergyPlus: Energy Simulation Program," *ASHRAE Journal* 42 (2000): 49–56.

HVAC Efficiency

It goes without saying that the efficiency of the HVAC system used in energy simulation has a high impact on resulting energy use output. In this case, the HVAC system used is an OpenStudio template that includes a Variable Refrigerant Flow (VRF) with Dedicated Outdoor Air System (DOAS) which may commonly be seen as VRF with DOAS. These systems are widely considered to be state of the art in residential cooling. A diagram of such a system may be seen in Figure 14 . Among other things, such as efficiency curves, a simple characteristic of HVAC systems that captures efficiency is the coefficient of performance (COP). The COP is a unitless ratio determined by Equation 1:

$$COP = \frac{|Q_W|}{W}$$
(1)

where Q_W is useful heat in Watts removed from the cooling system and W is the energy used to remove such heat in Watts. The energy efficiency ratio (EER) is linearly related to COP and is commonly used when referring specifically to cooling systems (Equation 2).

$$EER = 3.412 * COP$$
(2)

The EER is calculated similarly to COP (Equation 3):

$$EER = \frac{|Q_{BTU}|}{W}$$
(3)

where Q_{BTU} is useful heat in BTUs removed from the cooling system in BTUs and W is the energy used to remove such heat in Watts. The resulting units are BTU/W-hrs.

Both COP and EER are point-in-time measurements and range greatly based on operating conditions and system constraints. For this reason, the US government standards for cooling equipment are given in a Seasonal Energy Efficiency Ratio (SEER). As of January 1, 2015, the SEER requirement in the United States is 14, and in 2023 will be raised to 15[79]. The SEER captures a seasonal efficiency for cooling equipment which has the effect of de-emphasizing point-in-time efficiency ratings and taking a more holistic approach to efficiency. A simplified calculation for SEER is the total heat removed in BTUs divided by the total energy used over the entire season (Equation 4).

$$SEER = \frac{Total\ Heat\ Removed\ Over\ Season\ (BTUs)}{Total\ Energy\ Used\ Over\ Season\ (Watt\ hours)}$$
(4)

As SEER is a seasonal rating, it does not easily map to COP or EER. There are some back-of-the-envelope calculations that poorly approximate EER from SEER and vice versa. In our EnergyPlus model, the inputs for cooling equipment efficiency are through heating and cooling coil COPs. To determine the appropriate input COP, simulations were run with increasing COPs during an appropriate cooling period until the appropriate SEER was reached. The American National Standards Institute (ANSI) provides benchmark cooling hours per climate zone: Zone 1 = 2400hrs (Miami), Zone 2 = 1800hrs (Phoenix and Austin), and Zone 4 = 800hrs (DC/Baltimore). For Zone 1, a time period between June 20th and August 31st was used. For Zone 2, a time

---

[79] "2017-05-26 Energy Conservation Program: Energy Conservation Standards for Residential Central Air Conditioners and Heat Pumps; Confirmation of Effective Date and Compliance Date for Direct Final Rule.," Pub. L. No. EERE-2014-BT-STD-0048-0200, 82FR24211 10 CFR Part 430 24211 (2017), https://www.regulations.gov/document/EERE-2014-BT-STD-0048-0200.

period between June 20th and August 10th was used, and for Zone 4, a time period between July 1st and August 1st was used. Equation 5 gives the calculation method used to determine the resulting SEER from ANSI. [80]

$$SEER = \frac{\sum_{j=1}^{8} \frac{q\,(T_j)}{N_j}}{\sum_{j=1}^{8} \frac{e\,(T_j)}{N_j}} \qquad (5)$$

where $q\,(T_j)$ is the heat removed in BTUs and $e\,(T_j)$ is the energy in Watts used for cooling in j temperature bins where j is the bin number. N_j is the fraction of total hours from each temperature bin (T_j). There are eight temperature bins, 5 degrees Fahrenheit wide, beginning at the center 67.5F. Bins (j), temperature bins (T_j), bin centers, and hour fractions (N_j) are shown in Table 9.

Through this trial-and-error process, the COPs were determined such that the VRF with DOAS system met or slightly exceeded the US standard of SEER 14 while only varying by one significant figure (Table 10). The EnergyPlus outputs used to probe cooling provided an energy use to determine the COP were "Cooling Coil Total Cooling Rate" (W), and "Facility Total HVAC Electricity Demand Rate" (W). Cooling Coil Total Cooling Rate was converted to BTU-hrs. by using a multiplier of 3.4121.

Table 9. Binned temperature values used to calculate SEER

Bins (j)	Temperature Bins (T_j) (F)	Temperature Bins (T_j) (ºC)	Bin Center Temp (ºF) [ºC]	Fraction of Total Hours (N_j)
1	$65 \leq t < 70$	$18.3 \leq t < 21.1$	67.5 [19.7]	0.214
2	$70 \leq t < 75$	$21.1 \leq t < 23.8$	72.5 [22.5]	0.231
3	$75 \leq t < 80$	$23.8 \leq t < 26.6$	77.5 [25.2]	0.216
4	$80 \leq t < 85$	$26.6 \leq t < 29.4$	82.5 [28]	0.161
5	$85 \leq t < 90$	$29.4 \leq t < 32.2$	87.5 [30.8]	0.104
6	$90 \leq t < 95$	$32.2 \leq t < 35$	92.5 [33.6]	0.052
7	$95 \leq t < 100$	$35 \leq t < 37.7$	97.5 [36.3]	0.018
8	$100 \leq t < 105$	$37.7 \leq t < 40.5$	102.5 [39.1]	0.004

---

[80] AHRI, "2017 Standard for Performance Rating of Unitary Air- Conditioning & Air-Source Heat Pump Equipment" (ANSI and AHRI, 2017).

Table 10. Input COP and resulting SEER in each location over climate zone cooling season

Location	Input COPs for VRF and DOAS Cooling Coils	Resulting SEER (BTUs/W-hr)	Cooling Season Length (hr)
DC	7.4	14.06	800
Miami	4.9	14.15	2400
Austin	5.4	14.05	1800
Phoenix	6.3	14.03	1800

Air Source VRF Heat Pump

Refrigerant Lines

Zone

Return Air

Supply Air

VRF Terminal Unit

Thermometer

Fresh Air

Heat/Cool Recovery

Cooling/Heating Coils

Fan

Exhaust Air
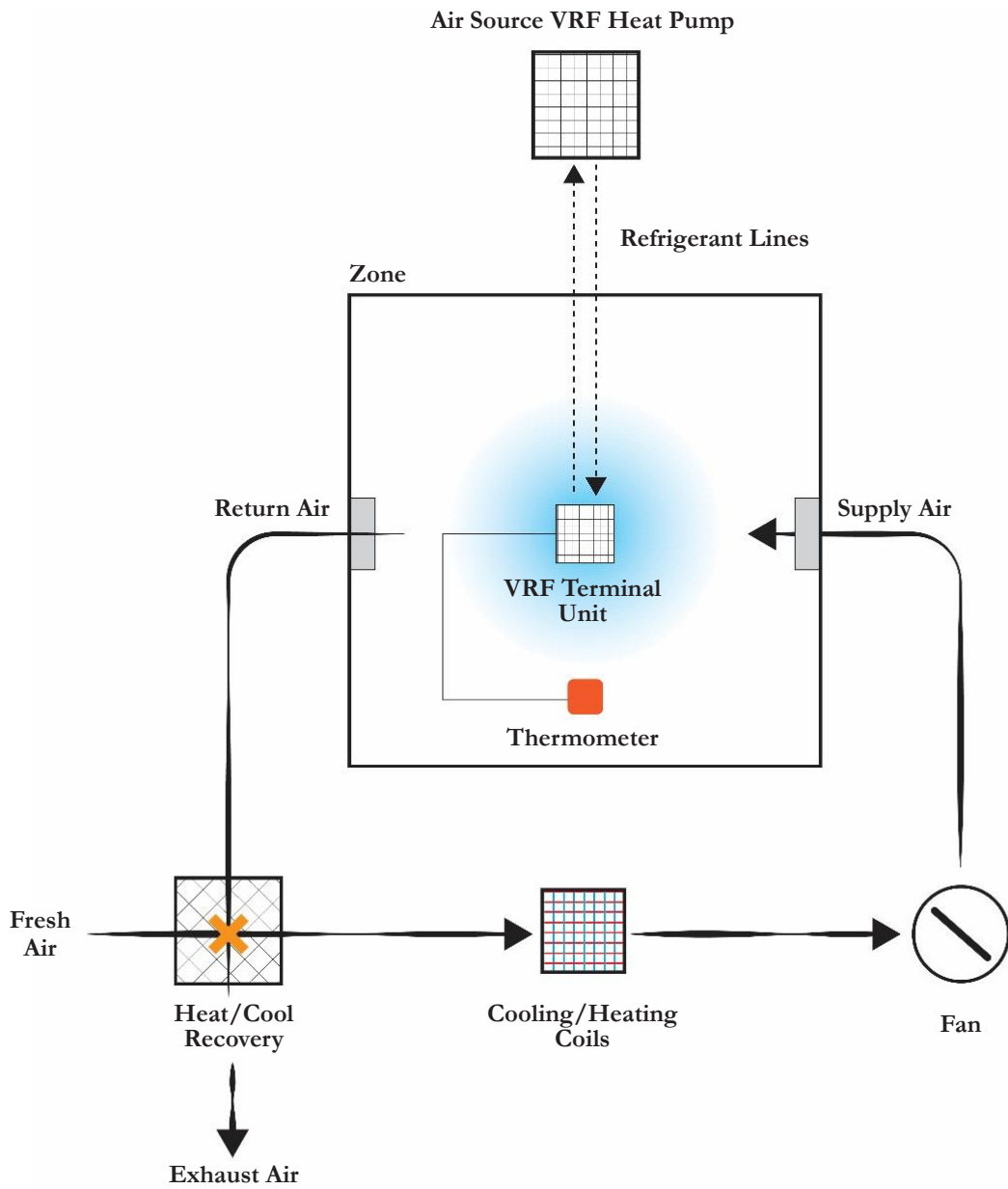
Figure 14. VRF and DOAS System Diagram

3.4.5. Passive Survivability Criteria

The ability for a building to maintain safe temperatures in extraneous circumstances ensures the health and wellbeing of occupants. Many organizations have produced research and guidelines that address passive survivability. LEED's passive survivability credit provides 2 options and several pathways towards creating passive resilience in buildings. Option 1 has 3 paths: path 1 uses psychrometry wherein thresholds of either Heat Index or WBGT temperature are maintained; path 2 uses a cooling degree day Standard Effective Temperature (SET) threshold; and path 3 uses Passive House certification with the inclusion of operable windows as qualifying characteristics for suitable passive survivability.[81] The LEED heat index threshold is "extreme caution" during the hot season. The CIBSE TM59:2017 *Design Methodology for Assessment of Overheating Risk in Homes* in the UK has two criteria for homes, one for homes that are primarily naturally ventilated, and one for homes that are primarily mechanically ventilated. For naturally ventilated homes, an operative temperature should not exceed 26 ºC between 10pm and 7am in bedrooms for more than 1% of the year. For mechanically ventilated homes, an operative temperature should not exceed 26 ºC for more than 3% of occupied hours.[82]

The criteria used in this thesis are two heat index thresholds: caution and extreme caution. Equation 6 shows the Heat Index calculation method for the heat index chart (Figure 15).[83] Note that no adjustments were used in the calculation of heat index.

$$\text{Heat Index} = C_1 + C_2*T + C_3*RH - C_4*T*RH - C_5*T^2 - C_6*RH^2 + C_7*T^2*RH + \tag{6}$$

$$C_8*T*RH^2 - C_9*T^2*RH^2$$

Where: T = ambient dry bulb temperature (ºF), RH = relative humidity (%), $C_1 = 42.379$, $C_2 = 2.04901523$, $C_3 = 10.14333127$, $C_4 = .22475541$, $C_5 = .00683783$, $C_6 = .05481717$, $C_7 = .00122874$, $C_8 = .00085282$, $C_9 = .00000199$

The metric established in this thesis is heat hazard hours (HHH) and defines the total hours above a heat index threshold. The first threshold is 28, "caution" (HHH28) and the second threshold is 32, "extreme caution" (HHH32). In the simulation week (168 days), 40 hours are spent with power-on and 128 are spent with power off.

---

[81] "Passive Survivability and Back-up Power During Disruptions | U.S. Green Building Council," accessed March 8, 2022, https://www.usgbc.org/credits/new-construction-core-and-shell-schools-new-construction-retail-new-construction-data-48.

[82] *Design Methodology for the Assessment of Overheating Risk in Homes: CIBSE TM59.*, 2017.

[83] Lans P Rothfusz, "The Heat Index 'Equation' (or, More Than You Ever Wanted to Know About Heat Index)," 1990, 2.

Temperature (Celsius)

Relative Humidity (%)	27	28	29	30	31	32	33	34	35	36	37	38	39	40	41	42	43
40	27	28	29	30	31	32	34	35	37	39	41	43	46	48	51	54	57
45	27	28	29	30	32	33	35	37	39	41	43	46	48	51	54	57	
50	27	28	30	31	33	34	36	38	41	43	46	49	51	55	58		
55	28	29	30	32	34	36	38	40	43	46	48	52	54	59			
60	28	29	31	33	35	37	40	42	46	48	51	55	58				
65	28	30	32	34	36	39	41	44	48	51	54	59					
70	29	31	33	35	38	40	43	47	51	54	58						
75	29	31	34	36	39	42	46	49	54	58							
80	30	32	35	38	41	44	48	52	58								
85	30	33	36	39	43	47	51	52									
90	31	34	37	41	45	49	54										
95	31	35	38	42	47	51	54										
100	32	36	39	44	49	54											

Caution	Extreme Caution	Danger	Extreme Danger

Figure 15. Heat Index Chart [84]

---

[84] NOAA US Department of Commerce, "Heat Index Chart" (NOAA's National Weather Service), accessed May 13, 2022, https://www.weather.gov/ffc/hichart.

Thermal Sensation	Heat Index	Standard Effective Temperature	Effective Temperature	Wet Bulb Global Temperature
Frosty				
Very Cold			<1	
Cold			1-9	
Cool			9-17	
No Stress		<17	17-21	<18
Warm	27-32	17-30	21-23	18-24
Hot	32-41	30-34	23-27	24-18
Very Hot	41-54	>34	>27	28-30
Sweltering	>54			>30

Figure 16. Thermal metric comparison [85]

---

[85] Krzysztof Blazejczyk et al., "Comparison of UTCI to Selected Thermal Indices," *International Journal of Biometeorology* 56, no. 3 (May 2012): 515–35, https://doi.org/10.1007/s00484-011-0453-2.

Section 3.5. Future Weather

3.5.1. Simulation Framework
Simulation Set 1

There are several models for morphing weather files, and each has unique implications on building modeling. Simulation Set 1 compares morphed weather data in two US locations: Phoenix, AZ (2B) as a representative hot/dry climate and Miami, FL (1A) as a representative hot/wet climate. The motivation for this set of simulations is to compare different morphed weather data scenarios on a building during heat waves and to locate the files morphed using HadAM3 A2 which are used in Simulation Sets 2 and 3. The model is run during the representative hot week in a grid-on (power available) scenario to determine peak loads and a grid-off (power outage) scenario where power is cut on hour 40 of the 168 hour simulation from which point the building is considered "free-running" to determine passive survivability (see 3.3.3). Natural ventilation is used in this scenario and follows the "adjacent" natural ventilation scheme defined in Simulation Set 2. Simulation Set 1 uses a single-family home modeled to the latest locally adopted IECC (1.3.3) Figure 17 shows the simulation matrix for Set 1. The metrics used to compare morphed weather data are peak cooling energy (Wh/m²), total cooling energy (Wh/m²), and heat hazard hours (HHH28 and HHH32)

Grid-on
Power available for entire 168 hour simulation

Grid-off
Power available for the first 40 hours

Figure 17. Simulation Matrix for Set 1

3.5.2. Results

Figure 18 shows the relative humidity and dry bulb temperatures from each morphed weather scenario during one day during the hot week. Peak cooling energy demand during the hot week for each of the 10 weather scenarios are shown in Figure 19 and Figure 20. Total cooling energy from each of the 10 weather scenarios are shown in Figure 21 and Figure 22. As the data show, the peak cooling energy (PCE) and total cooling energy (TCE) for 2020 A2 is most like 2049 RCP 4.5. 2050 A2 is most like 2075 RCP 8.5, and 2050 A2 is most like 2099 RCP 8.5. The 2080 A2 is an outlier in terms of total energy in both cases. This can be observed in **Error! R eference source not found.** and Figure 24, which show cooling energy use over a three-day period at the beginning of the hot week. These results show a greater separation between climate scenarios in Miami than in Phoenix, likely a product of relative humidity in each location.

When considering heat hazard hours during a power outage, the data shows 2080 A2 as an outlier in both Phoenix and Miami. Similarly, in Miami, 2050 A2 shows a much higher number of HHH32 than any of the files morphed under an RCP scenario. The marginal increase between Miami's 2050 and 2080 A2 scenario is also notable (Figure 25 and Figure 26). More detailed heat index time charts are shown below in Figure 27 and Figure 28.
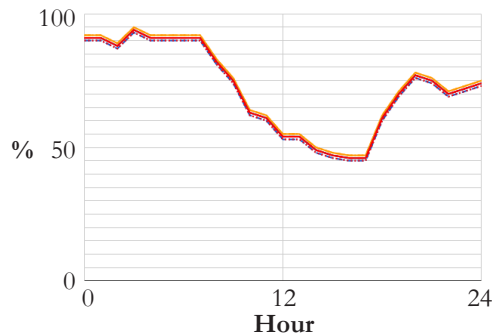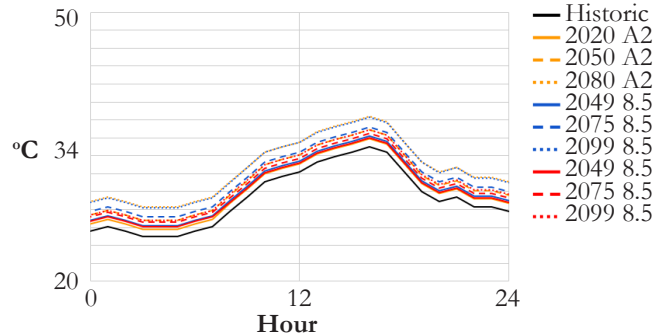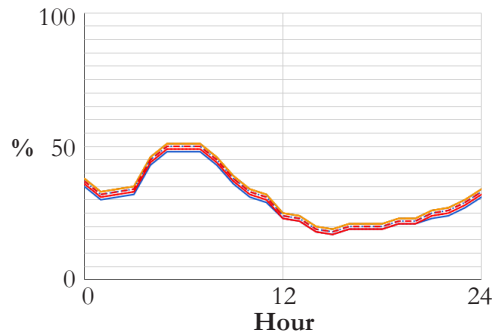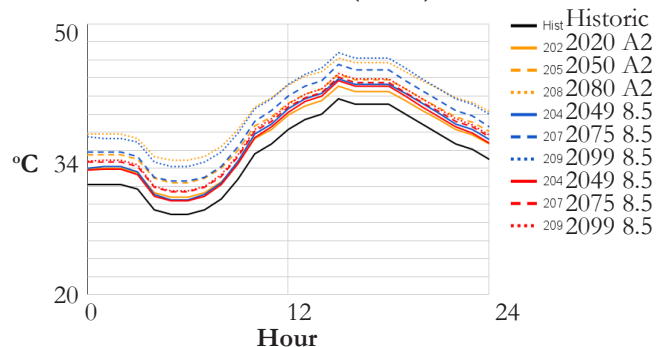
Figure 18. Relative humidity (%) and dry bulb temperature (°C) over one day during the simulated hot week in Miami and Phoenix weather scenarios

Miami Peak Cooling Energy
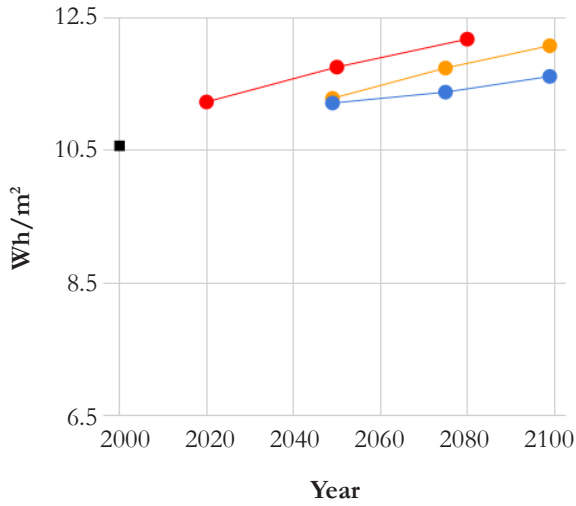
Figure 19. Miami Peak Cooling Energy

Phoenix Peak Cooling Energy
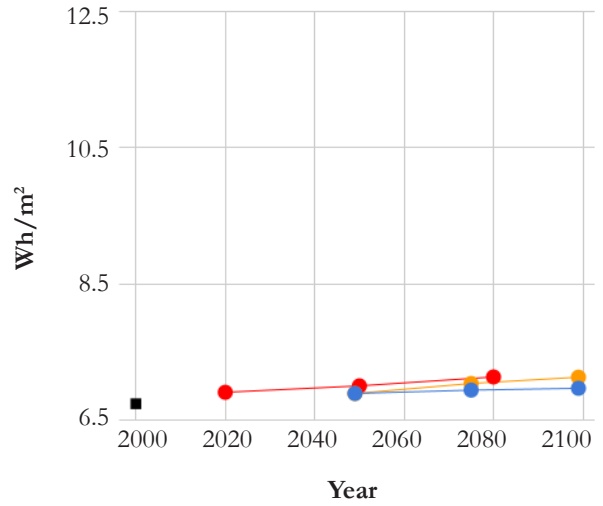
Figure 20. Phoenix Peak Cooling Energy

Miami Total Cooling Energy
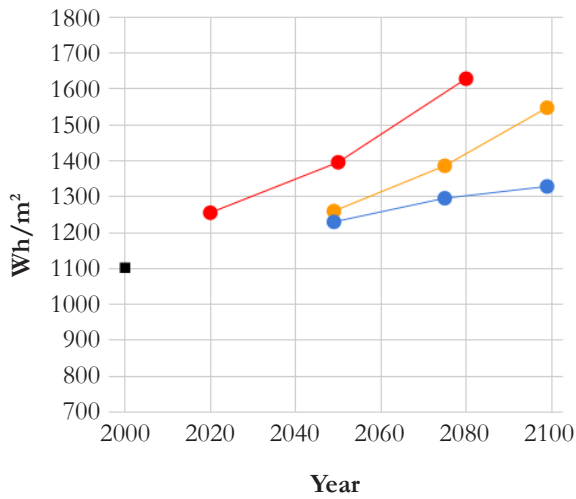
Figure 21. Miami Total Cooling Energy

Phoenix Total Cooling Energy
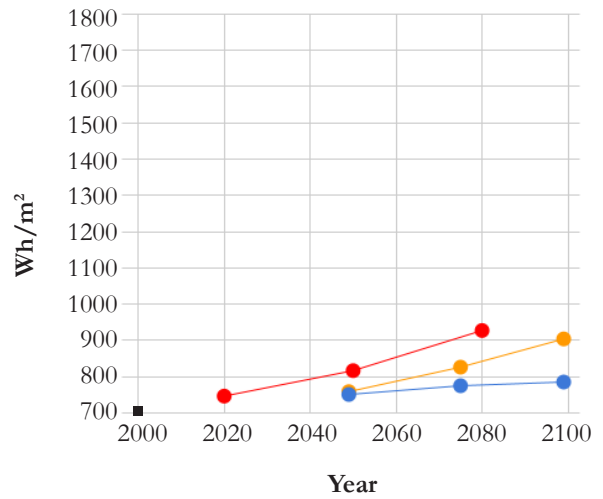
Figure 22. Miami Total Cooling Energy

■ Present ● A2 ● RCP 8.5 ● RCP 4.5

Miami Cooling Energy
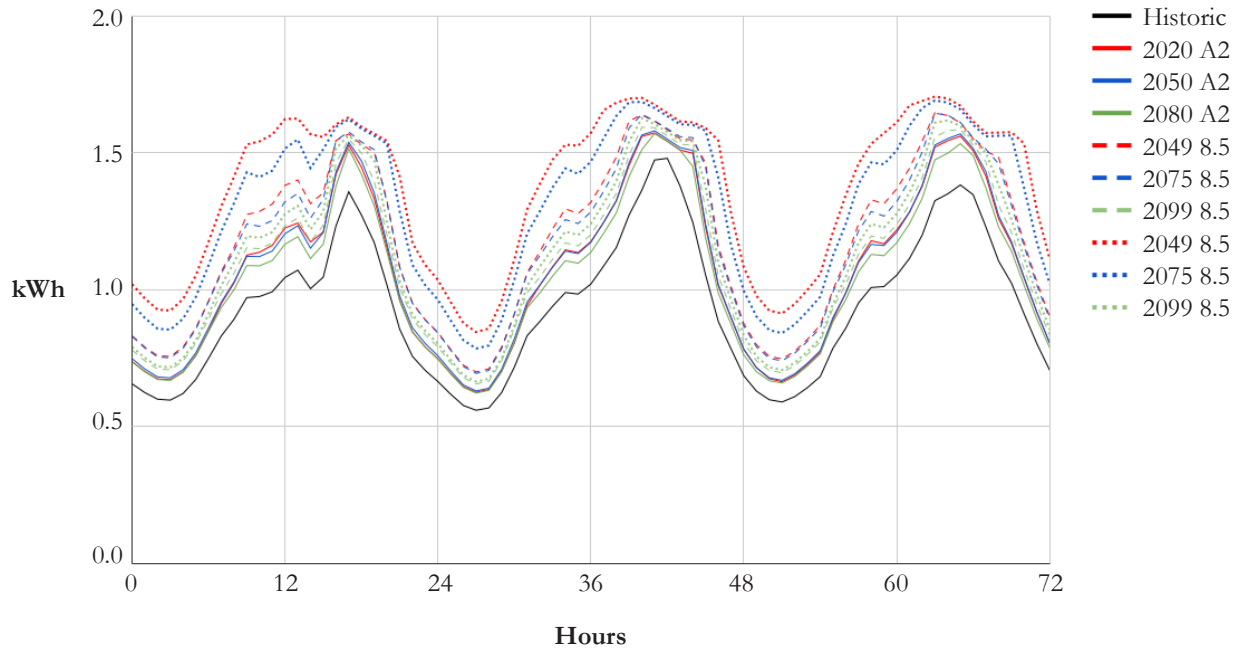
Figure 23. Cooling energy in Miami over three days during the simulated hot week

Phoenix Cooling Energy
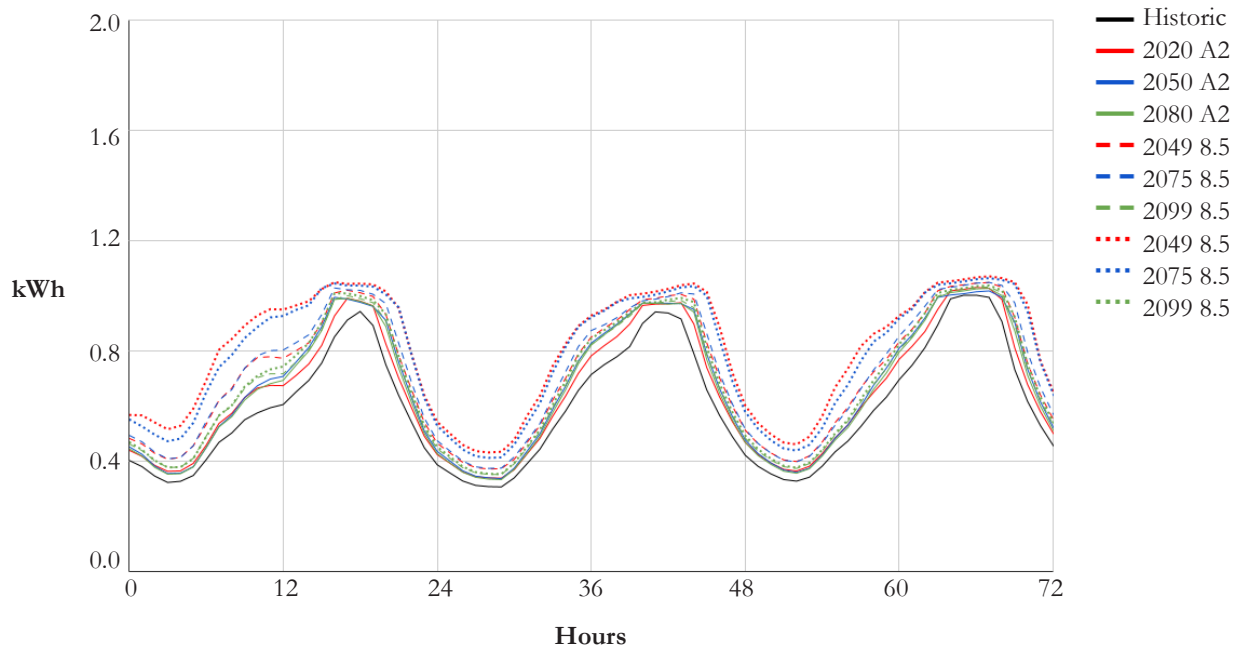
Figure 24. Cooling energy in Phoenix over three days during the simulated hot week

Miami Heat Hazard Hours

Phoenix Heat Hazard Hours
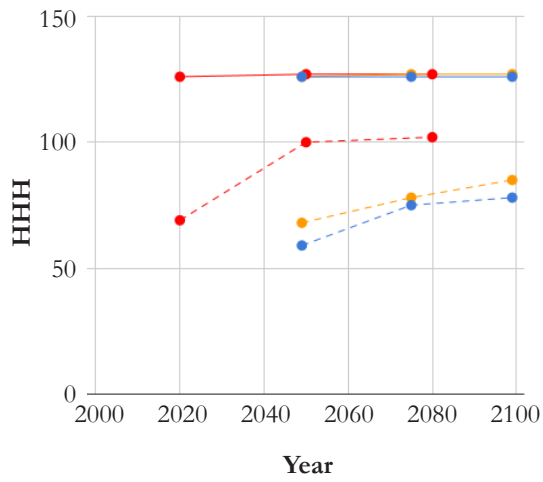
Figure 25. Heat Hazard Hours in Miami
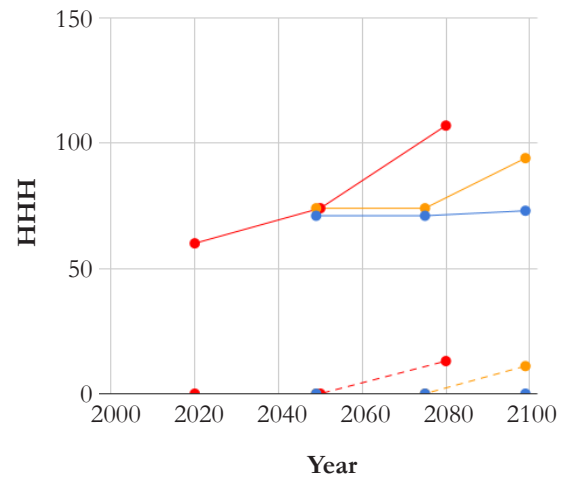
Figure 26. Heat Hazard Hours in Phoenix

■ Present ● A2 ● RCP 8.5 ● RCP 4.5

Solid line = HHH28, Dashed line = HHH32

Miami Heat Index
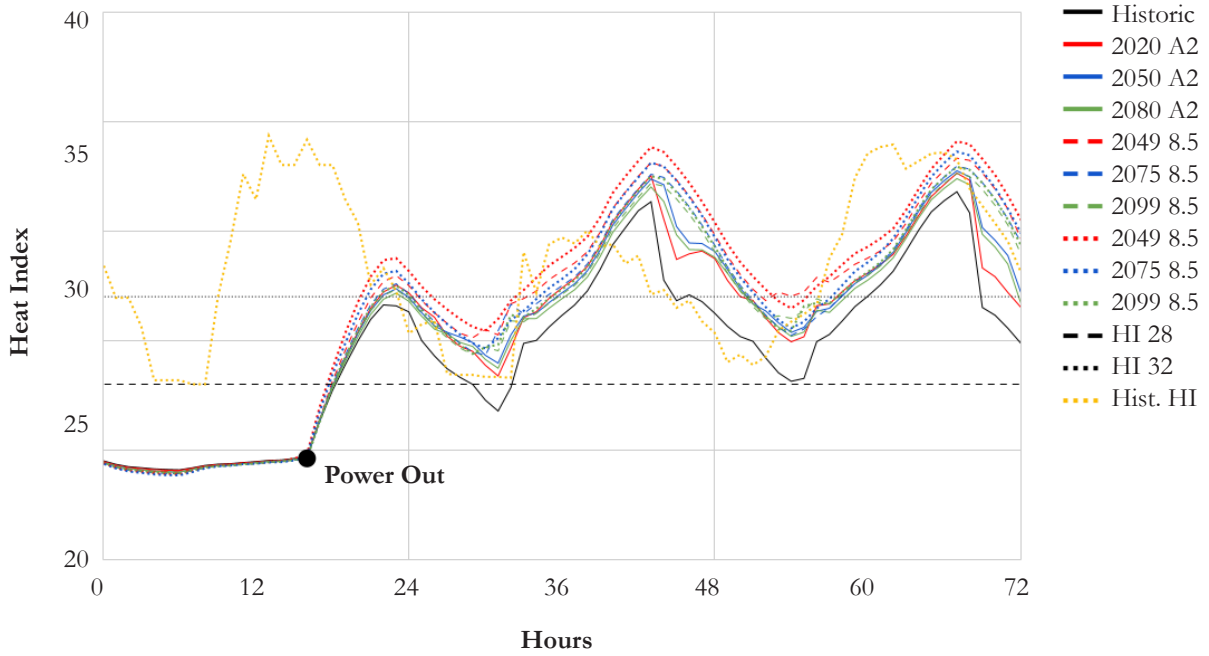
Figure 27. Internal heat index in Miami over three days during the simulated hot week

Phoenix Heat Index
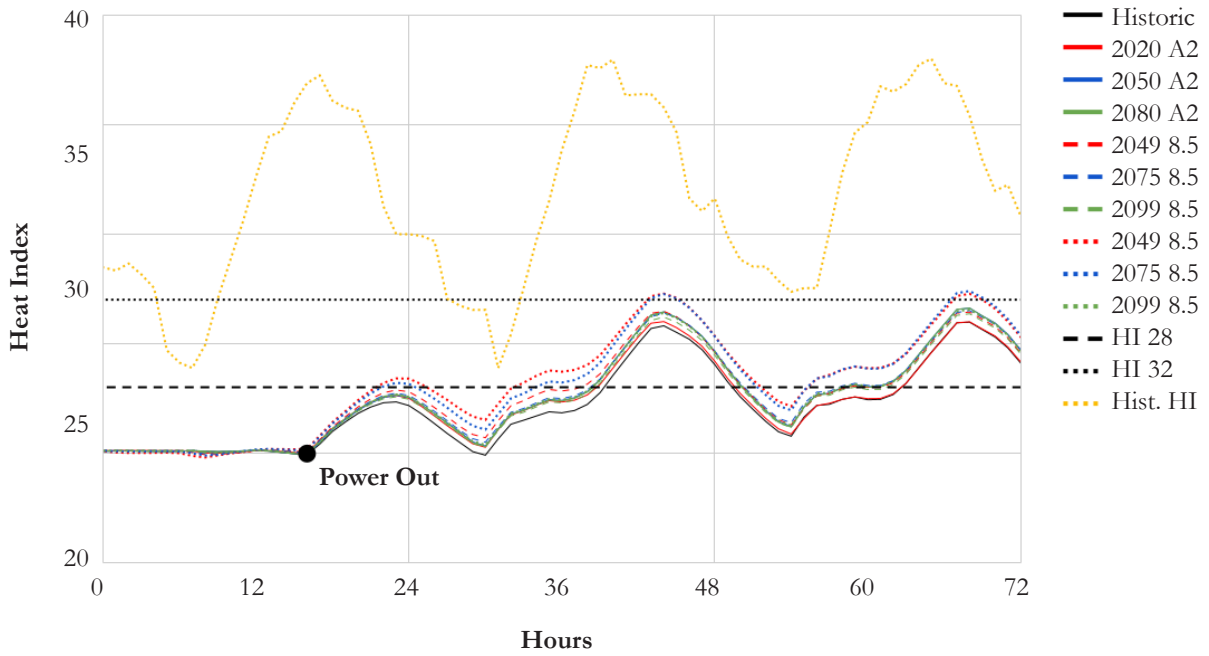
Figure 28. Internal heat index in Phoenix over three days during the simulated hot week

3.5.3. Discussion

Locating weather results among a set of morphed weather data provides important insights into question of resilience in an uncertain future. What is shown in the future weather comparison is ultimately insightful because it represents a translation of how multiple future weather scenarios effect a building function in grid-on and grid-off configurations. It is one thing to understand and compare the projected warming associated with each emission and warming scenarios, but another to be able to be able to locate those pathways with concern for peak and total energy as well as vulnerability in buildings with a degree of confidence. A key takeaway is that the 2080 A2 scenario that was morphed with CCWorldWeatherGen represents the most extreme increase in temperatures, which translates to consistently higher total cooling energy consumption. Peak cooling energy, however, has clearer parallels between weather scenarios where A2 represents similar increases to RCP 8.5 but 30 years later. A2's closest relationship with RCP 4.5 pathway is between the 2020 A2 and the 2049 RCP 4.5. The 2099 RCP 4.5 scenario also shares a similar peak cooling energy increase with 2050 A2 scenarios, though there is a larger discrepancy when it comes to total energy.

The most notable observation that can be made of the grid-off scenarios matches that of energy use; the 2080 A2 scenario is an outlier. Generally, both RCP scenarios track closely regarding heat hazard hours. A likely explanation for this is the reduction in nighttime energy valley minima that CCWorldWeatherGen outputs compared to WeatherShift's methods and can be seen in Figure 18.

Section 3.6. Natural Ventilation

3.6.1. Simulation Framework

Ventilation is an essential aspect of regulating building occupant comfort when power is unavailable. Simulation Set 2 compares the effectiveness of four natural ventilation strategies with two different operable window area characteristics in reducing internal temperatures for IECC and Passive House models in four locations, Phoenix, AZ (2B), Austin, TX (2A), Miami, FL (1A), DC/Baltimore, MD (4A). The models were only run under historic weather conditions. Natural Ventilation is available only during the grid off scenario and is triggered using a dynamic schedule where outdoor DBT is one degree Celsius above the interior temperature. In this case, preliminary testing showed that it was beneficial to begin natural ventilation sooner, rather than waiting for the outdoor temperature to be cooler than indoors. The metrics used to determine efficacy of each scenario are heat hazard hours (HHH28 and HHH32) (1.3.6). Simulation Set 2 simulates seven natural ventilation scenarios shown in Figure 29, Table 11 and Figure 30 with the intention of assessing the impact of natural ventilation scenarios during a power outage.

	Location	
Building Characteristics	**IECC**	**Passive House**
Weather Data	**Historic**	**Historic**
No Natural Ventilation		
Single Side (Op Area 50%)		
Single Side (Op Area 100%)		
Opposite (Op Area 50%)		
Adjacent (Op Area 50%)		
Adjacent (Op Area 100%)		
Multi-Direction (Op Area 50%)		
Multi-Direction (Op Area 100%)		
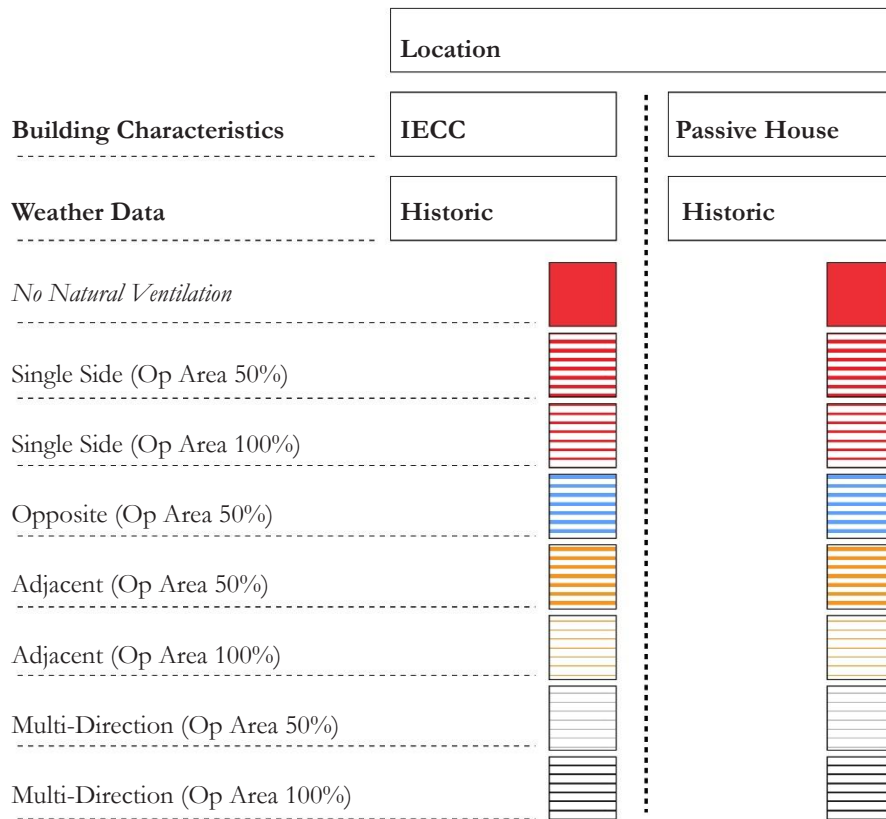
Figure 29. Simulation Matrix for Set 2

Table 11. Ventilation Scenario Details

	Ventilation Scenario	Operable Window Area (%)	Ventilation Type
A	Single Sided 1	50%	Operable window(s), 1 wall
B	Single Sided 2	100%	Operable window(s), 1 wall
C	Opposite	50%	Operable window(s), 1 wall, opposite door
D	Adjacent 1	50%	Operable window(s), 2 perp. walls
E	Adjacent 2	100%	Operable window(s), 2 perp. walls
F	Multi-Direction 1	50%	Operable window(s), 2 perp. walls, opposite door
G	Multi-Direction 2	100%	Operable window(s), 2 perp. walls, opposite door
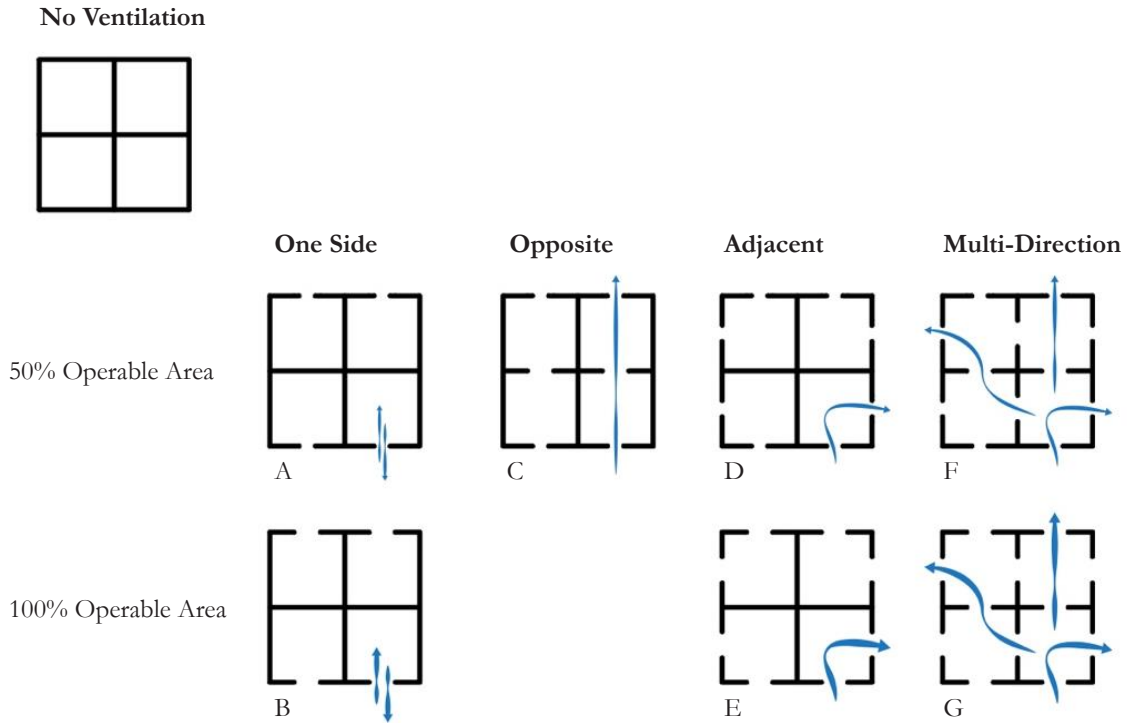
Figure 30. Ventilation Scenarios

3.6.2. Results

Results for natural ventilation are shown in two sets of time series heat index charts for each location. Each set has one heat index chart for the IECC model and one for the Passive House model. Additionally, the table for each result includes HHH28 and HHH32 for each ventilation strategy. Figure 31 shows the extreme interior heat indexes which can occur with no natural ventilation. The impact of natural ventilation is writ large. However, significant improvements are only seen where the temperature delta between outdoor and indoor is not so large that the zone temperature never has the opportunity for natural ventilation to take effect. Results from Phoenix and Miami (Figure 34, Figure 35, Table 14, Figure 38, Figure 39, Table 16) exemplify this, where the indoor zone temperature remains consistently cooler than outdoors, and so no natural ventilation occurs. It is also clear from all simulation results that the multi-directional ventilation scenario with all doors and windows open in all zones of the house performs the best. Further, a 100% operable area also performs better than windows with 50% operable area. In Miami and Phoenix, the Passive House model improves the interior heat index conditions, making them much safer even without any natural ventilation. In DC and Austin (Figure 32, Figure 33, Table 13, Figure 36, Figure 37, Table 15) the Passive House model exacerbates the interior heat index conditions, an important finding that illustrates a tension between energy efficiency and resilience.

No Natural Ventilation Power Outage
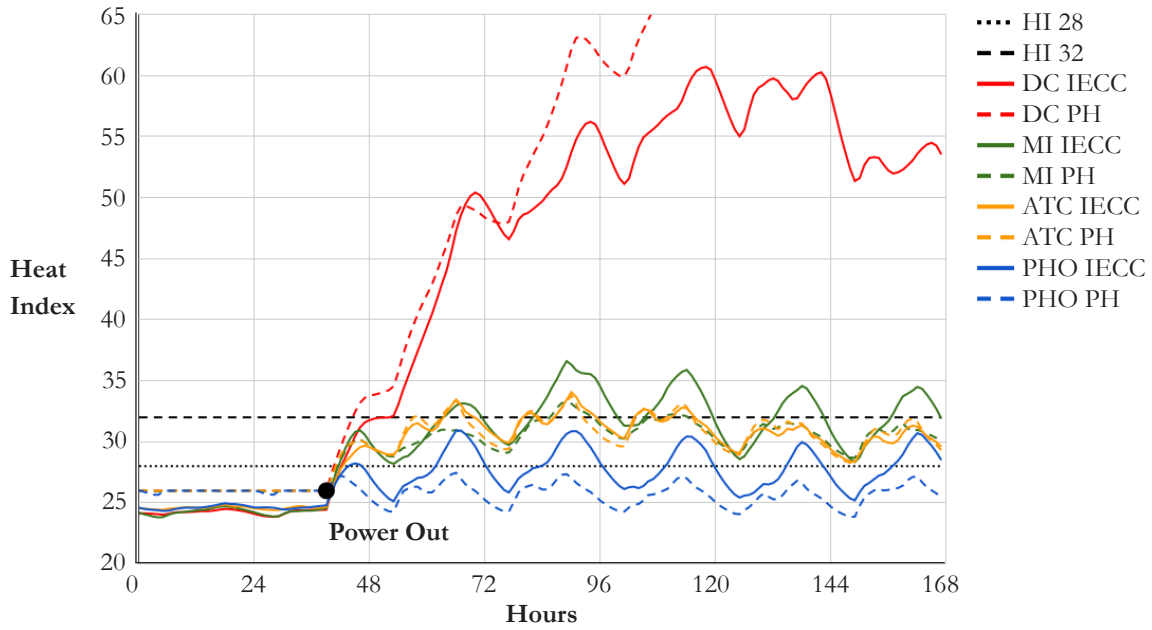
Figure 31. Interior heat index with no natural ventilation available

Table 12. HHH28 | 32 with no natural ventilation in IECC and Passive House during a power outage

	DC	MI	ATX	PHO
IECC	127 | **115**	126 | **60**	125 | **27**	56 | **0**
PH	127 | **123**	126 | **14**	127 | **26**	0 | **0**

DC Ventilation Strategies (IECC)
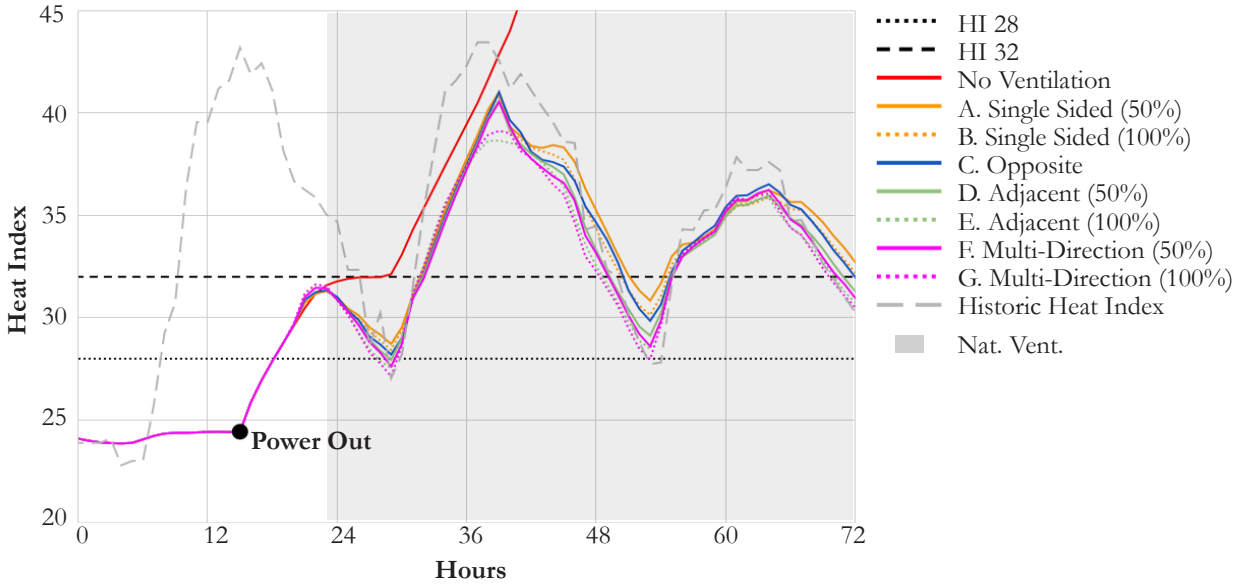
Figure 32. DC IECC natural ventilation results in heat index (°C)

DC Ventilation Strategies (PH)
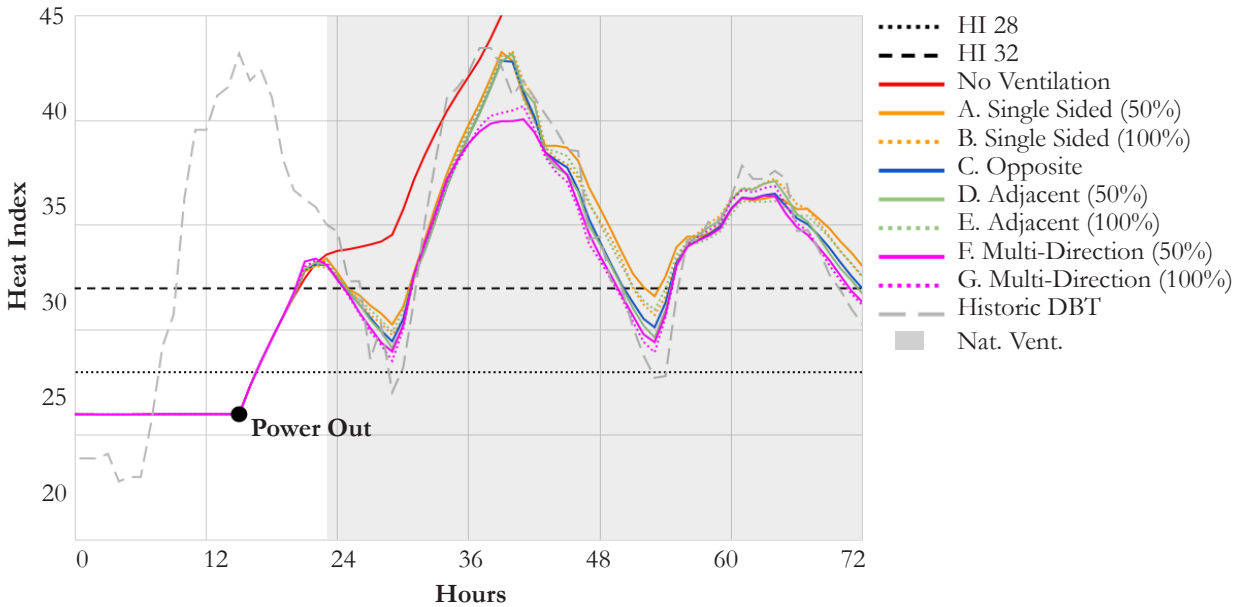
Figure 33. DC Passive House natural ventilation results in heat index (°C)

Table 13. HHH28 | 32 in DC IECC and Passive House models under ventilation scenarios A-G.

	A	B	C	D	E	F	G
IECC	119 | **78**	117 | **72**	118 | **75**	114 | **64**	113 | **61**	115 | **61**	111 | **59**
PH	122 | **87**	121 | **82**	121 | **82**	120 | **77**	118 | **69**	120 | **74**	118 | **70**

Miami Ventilation Strategies (IECC)
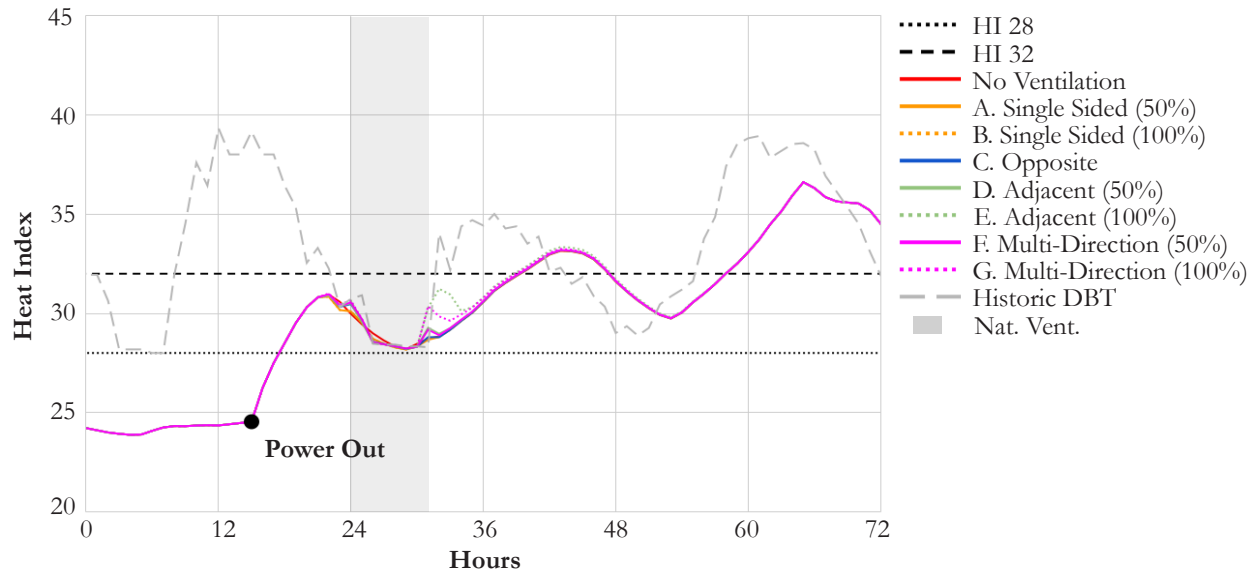
Figure 34. Miami IECC natural ventilation results in heat index (°C)

Miami Ventilation Strategies (PH)
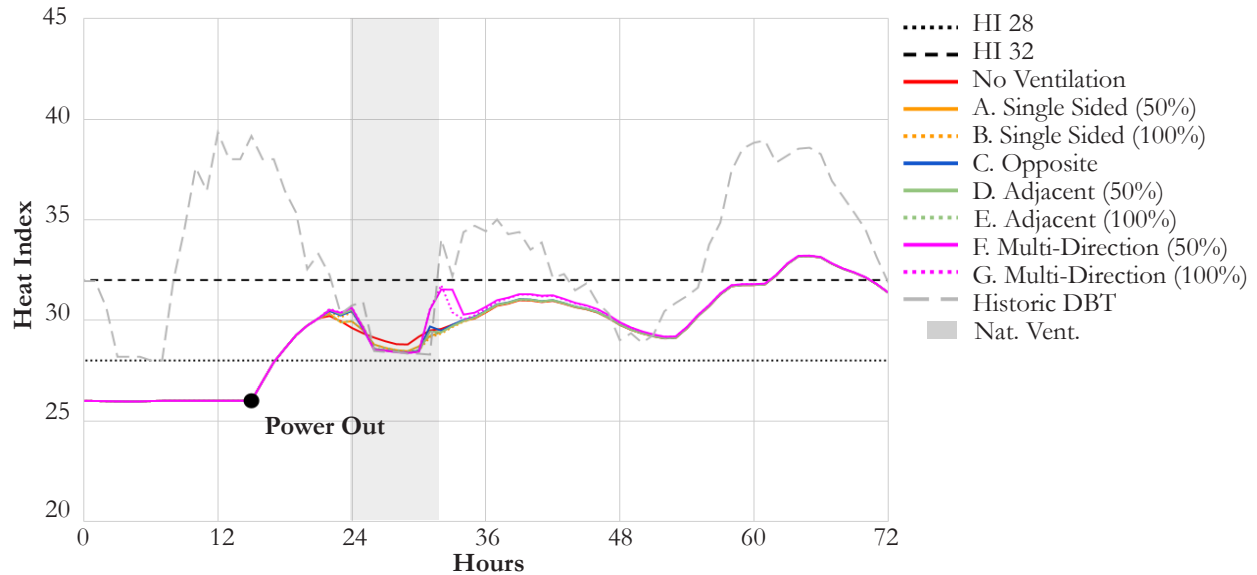
Figure 35. Miami Passive House natural ventilation results in heat index (°C)

Table 14. HHH28 | 32 in Mami IECC and Passive House models under ventilation scenarios A-G.

	A	B	C	D	E	F	G
IECC	125 | **49**	125 | **48**	125 | **49**	124 | **48**	124 | **48**	124 | **48**	124 | **49**
PH	126 | **15**	126 | **14**	126 | **14**	126 | **14**	124 | **19**	126 | **14**	124 | **22**

Austin Ventilation Strategies (IECC)
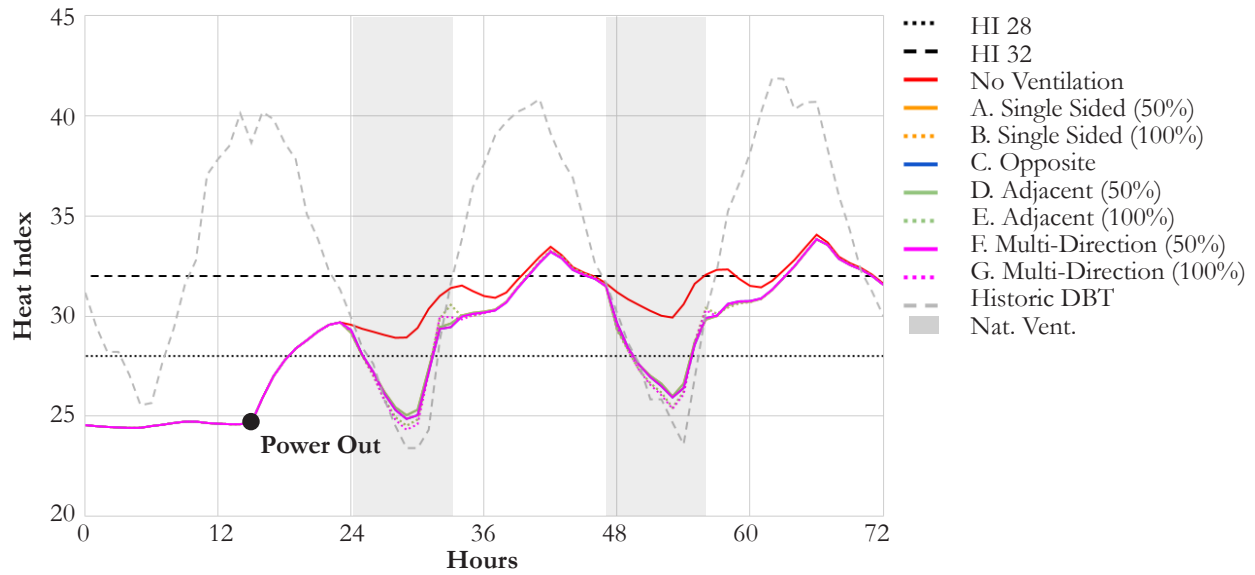
Figure 36. Austin IECC natural ventilation results in heat index (°C)

Austin Ventilation Strategies (PH)
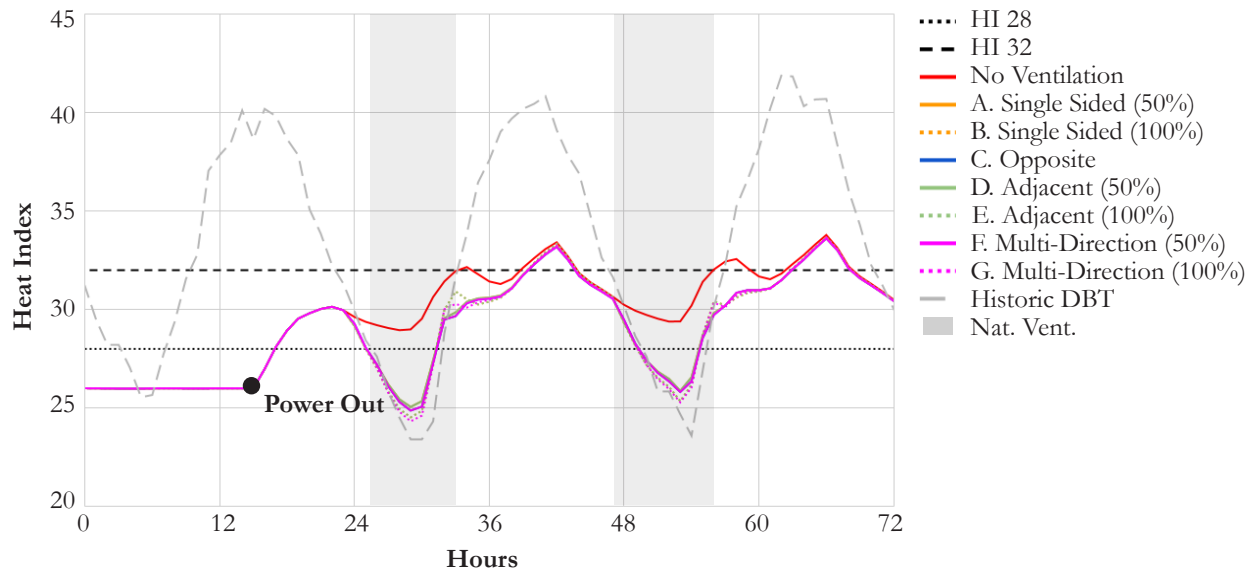
Figure 37. Austin Passive House natural ventilation results in heat index (°C)

Table 15. HHH28 | 32 in Austin IECC and Passive House models under ventilation scenarios A-G.

	A	B	C	D	E	F	G
IECC	80 | **15**	78 | 26	80 | **15**	80 | **15**	78 | **26**	80 | 15	79 | **23**
PH	82 | **13**	80 | **23**	82 | **13**	82 | **13**	80 | **23**	82 | **13**	80 | **21**

Phoenix Ventilation Strategies (IECC)
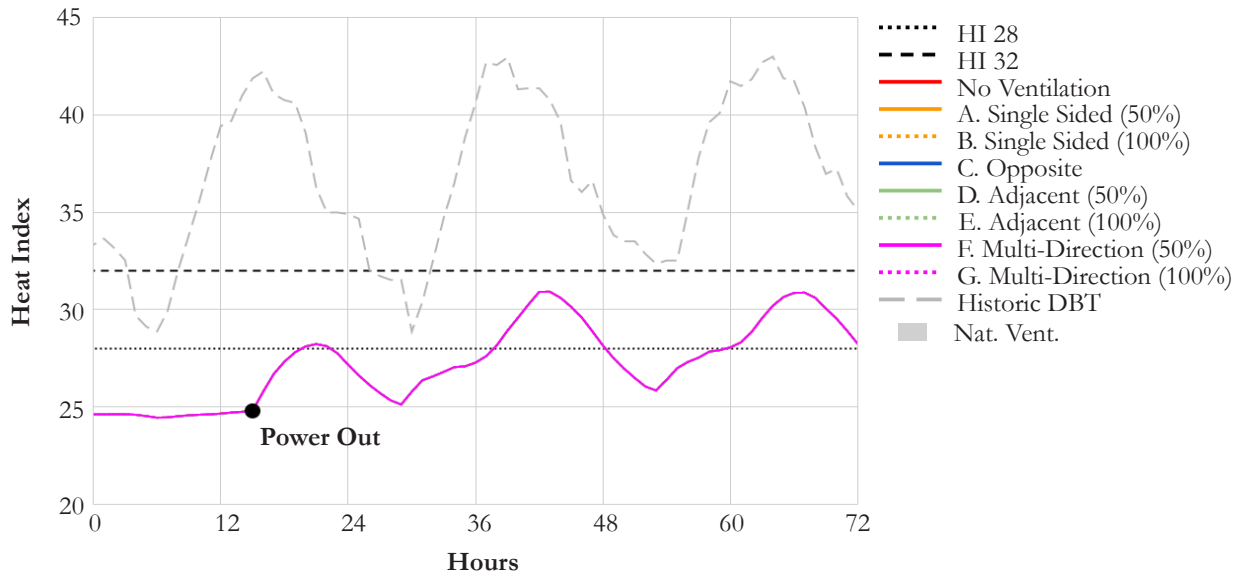
Figure 38. Phoenix IECC natural ventilation results in heat index (oC)

Phoenix Ventilation Strategies (PH)
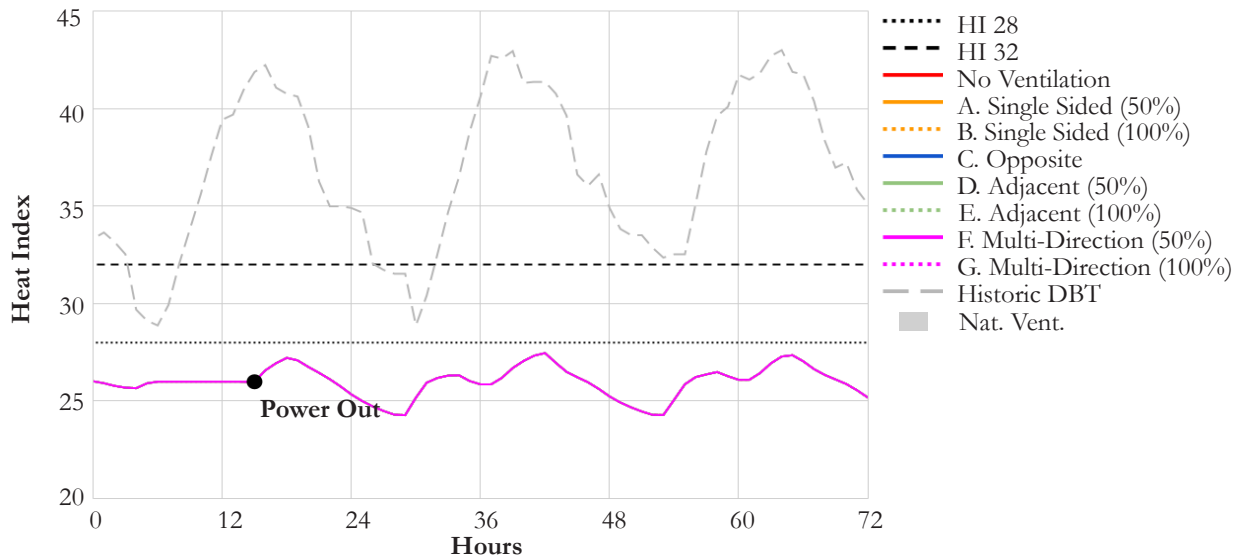
Figure 39. Phoenix Passive House natural ventilation results in heat index (oC)

Table 16. HHH28 | 32 in Phoenix IECC and Passive House models under ventilation scenarios A-G.

	A	B	C	D	E	F	G
IECC	56 | 0	56 | 0	56 | 0	56 | 0	56 | 0	56 | 0	56 | 0
PH	0 | 0	0 | 0	0 | 0	0 | 0	0 | 0	0 | 0	0 | 0

3.6.3. Discussion

Natural ventilation is an essential element of resilience in extreme heat scenarios, made clear by the dramatic improvements seen in the presence of any natural ventilation versus none as can be seen in Figure 32, Figure 33, Figure 36, and Figure 37. The efficacy of natural ventilation is highly dependent on weather conditions, however. In Miami and Phoenix, outdoor dry bulb temperatures were generally too high for natural ventilation to be activated. When natural ventilation was available, a fully open building, characterized by the ventilation scenarios F and G or "multi-directional", generally outperform all other scenarios in reducing heat hazard hours. A larger operable window fraction, resulting in a greater mass flow rate, also reliably improved given strategy. Strategy "D", adjacent ventilation (windows at ᵒ90) performed better than strategy "C", opposite or cross-ventilation. The likely explanation for this is that hot air is forced to exhaust thought adjacent zones in strategy "C" where strategy "D" exhausts hot air directly to the outdoors.

Section 3.7. Heat Vulnerability

3.7.1. Simulation Framework

The simulation framework for determining heat vulnerability is to use two single family housing models, one modeled to IECC standard, the other to Passive House standard in each of the four climate zones. All scenarios are then run during the representative hot week during the year under four climate scenarios: a historic EPW file and three morphed weather files using CCWWG: 2020 A2, 2050 A2, and 2080 A2 (see 3.3.2). Each simulation is run under a grid-on (power available) scenario to determine peak loads and a grid-off (power outage) scenario where power is cut on hour 40 of the 168-hour simulation from which point the building is considered "free-running". Hour 40 is where the assessment of passive survivability begins (see 3.3.3). The "D" natural ventilation scheme from Set 2 is used in this simulation set. The metrics used to compare morphed weather data are peak cooling energy (Wh/m²), total cooling energy (Wh/m²), and heat hazard hours (HHH28 and HHH32). Figure 40 shows the simulation matrix for Set 3.
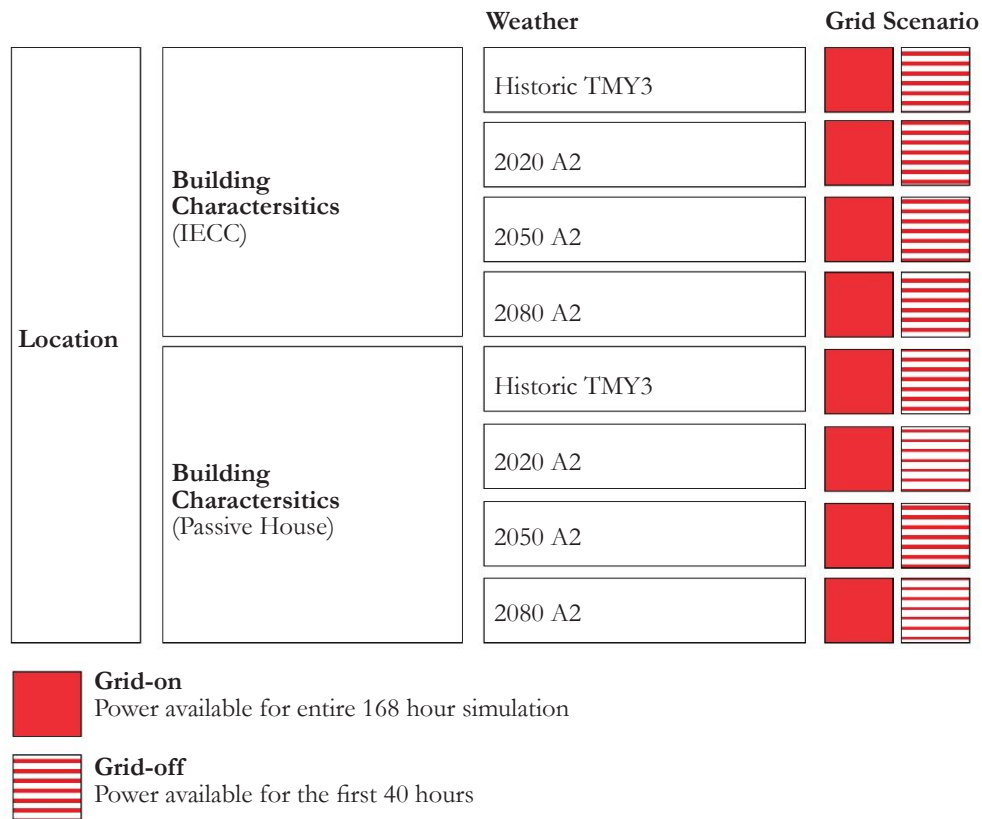
Figure 40. Simulation Matrix for Simulation Set 3

3.7.2. Grid-on Results

Energy results from the simulation set 3 "Grid-on" scenarios are given in: 1) peak cooling energy per m², 2) total cooling energy per m², and 3) time series energy plots. Further results are found in comparative tables. Figure 41 shows the distribution of total energy use over the simulated hot week for each model type, future weather scenario, and location, Phoenix, AZ, Austin, TX, Miami, FL, and Baltimore/DC, MD. Figure 42 shows peak energy demand for each scenario. Both Figure 41 and Figure 42 are normalized to building floor area. Figure 43, Figure 44, Figure 45, and Figure 46, show time series plots of cooling energy (kWhs) over the simulated hot week. The most significant peak and total cooling energy reductions between the IECC and PH models are found in Phoenix (Table 23, Table 24).

An important result is that relative to the IECC model, the Passive House model's total cooling energy percent reduction increases through time, meaning that the Passive House improves in performance relative to IECC performance in total cooling energy used under increased warming. In general, peak cooling energy percent change from IECC to Passive House models either stays the same or slightly decreases with future weather. DC and Miami exemplify this, where in DC, the Passive House achieves a 41% peak cooling energy reduction from the IECC model with historic weather but decreases to a 36% reduction in peak cooling energy in 2080 (Table 18). In Miami, a peak cooling energy reduction of 41% from the IECC to PH models in historic weather reduced to 36% in 2080 (Table 20).

Of note across all cities is that the energy valleys in time series energy plots show that valleys become less defined and peaks "shrug" their shoulders (Figure 43, Figure 44, Figure 45, Figure 46). This increase in local energy valley minima, along with a narrowed nighttime valley are the source of most of the total energy increase over the hot week. This is important in relation to peak cooling energy increases which increase by an average of ~10% across models from historic to 2080 weather where the total cooling energy increases by an average of ~42% across models.

DC Peak Cooling Energy
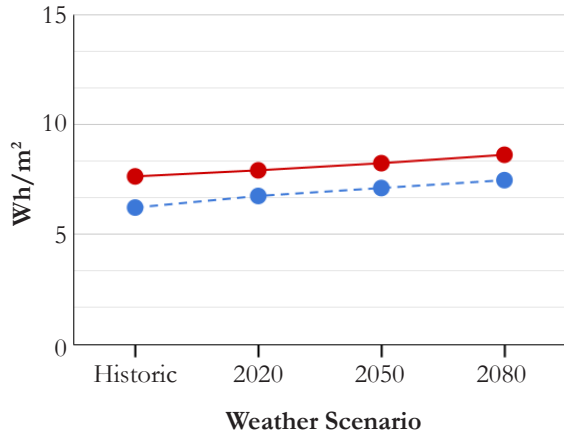
Miami Peak Cooling Energy
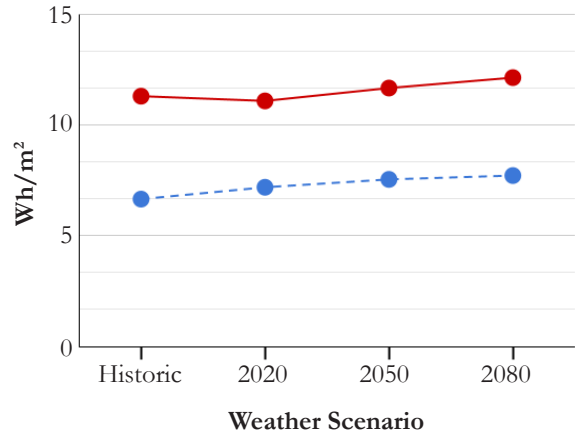
Austin Peak Cooling Energy
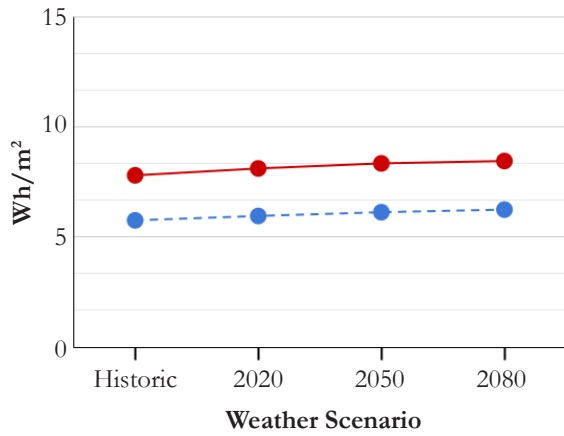
Phoenix Peak Cooling Energy
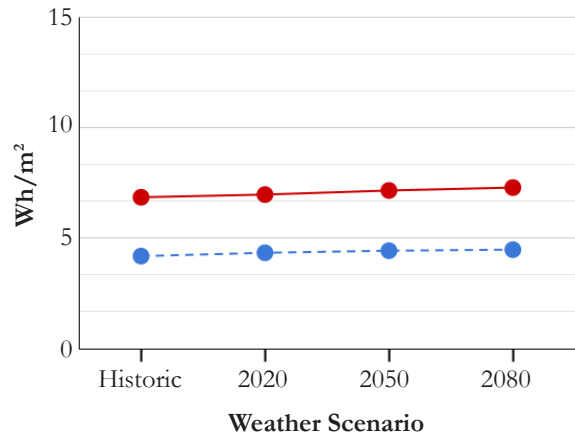
● IECC ● Passive House

Figure 41. Peak cooling energy (Wh/m²) from each location and climate scenario
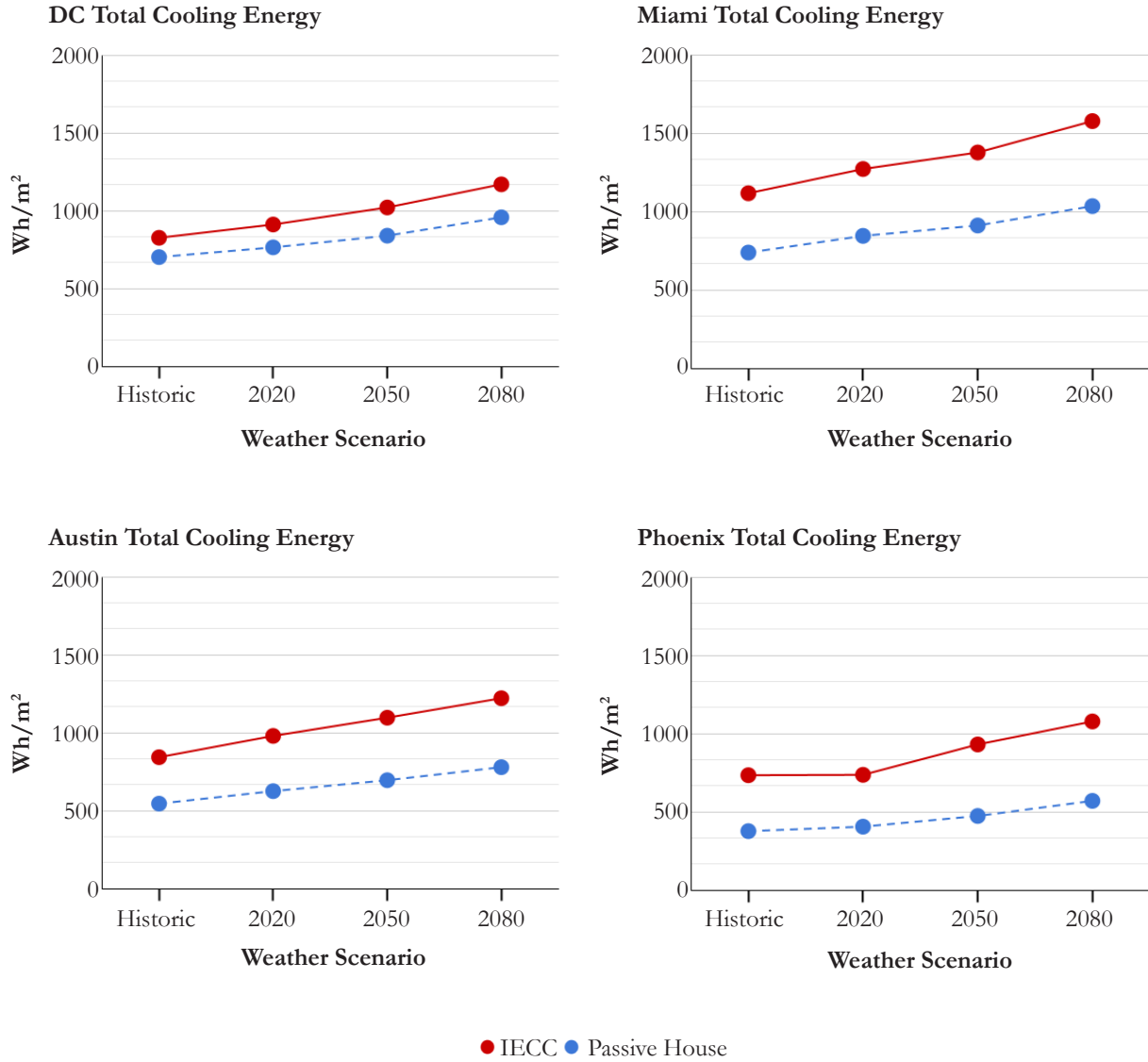
Figure 42. Total cooling energy (Wh/m²) from each location and climate scenario

DC Cooling Energy
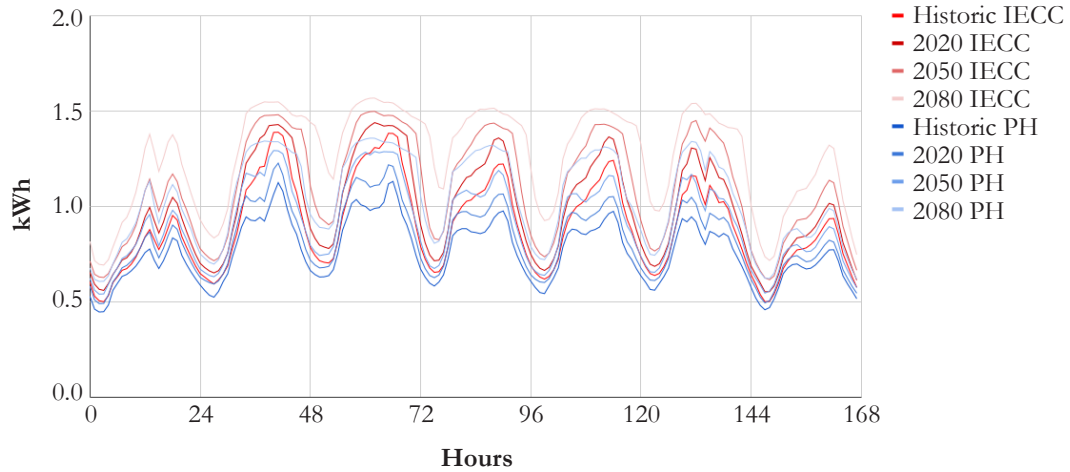
Figure 43. DC cooling energy for IECC and PH models during simulated hot week

Table 17. DC total cooling energy results

	Historic	2020	2050	2080
IECC (Wh/m²)	826	911	1020	1169
PH (Wh/m²)	702	764	839	957
% change from IECC to PH	-15%	-16%	-17.5%	-18%
IECC change from IECC historic	-	10%	23%	41%
PH change from PH historic	-	8%	19%	36%

Table 18. DC peak cooling energy results

	Historic	2020	2050	2080
IECC (Wh/m²)	7.79	7.91	8.23	8.62
PH (Wh/m²)	6.22	6.74	7.11	7.46
Change from IECC to PH	-18%	-14%	-%13	-13%
IECC change from IECC historic	-	3%	7%	13%
PH change from PH historic	-	8%	14%	20%

Miami Cooling Energy
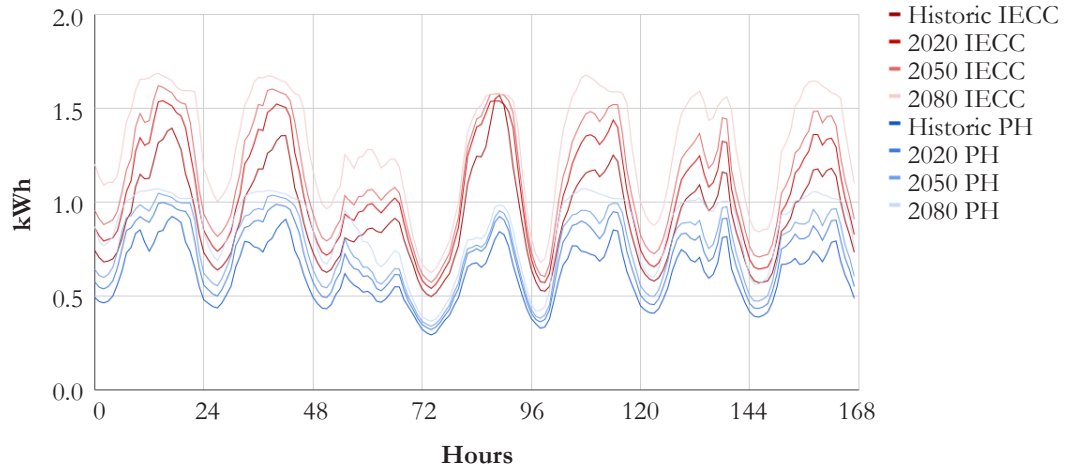
Figure 44. Miami cooling energy for IECC and PH models during simulated hot week

Table 19. Miami total cooling energy results and comparison

	Historic	2020	2050	2080
IECC (Wh/m²)	1116	1271	1376	1576
PH (Wh/m²)	738	844	911	1034
Change from IECC to PH	-33%	-33%	-33%	-34%
IECC change from IECC historic	-	13%	23%	41%
PH change from PH historic	-	14%	23%	40%

Table 20. Miami peak cooling energy results and comparison

	Historic	2020	2050	2080
IECC (Wh/m²)	11.29	11.08	11.66	12.13
PH (Wh/m²)	6.65	7.18	7.54	7.71
Change from IECC to PH	-41%	-35%	-35%	-36%
IECC change from IECC historic	-	-1.7%	3%	7%
PH change from PH historic	-	8%	13%	15%

Austin Cooling Energy
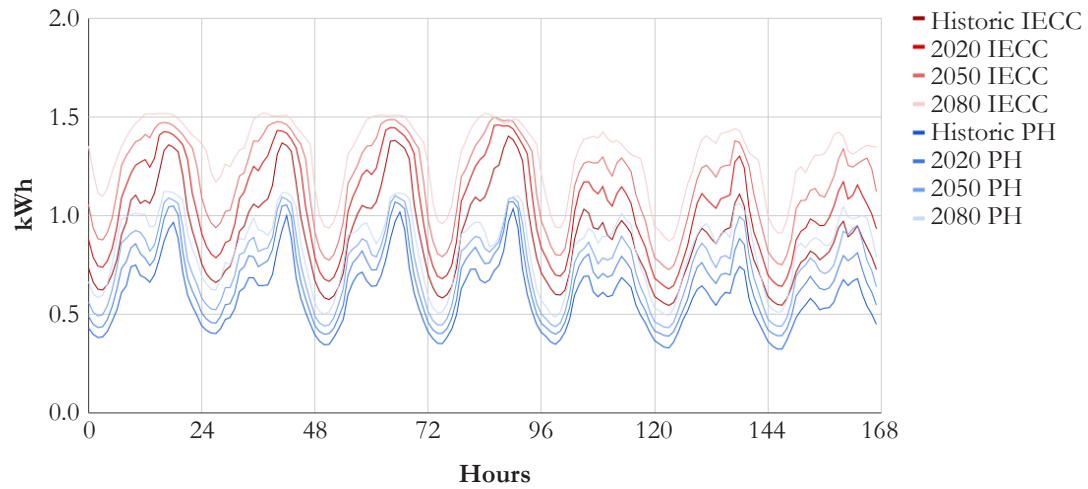
Figure 45. Austin cooling energy for IECC and PH models during simulated hot week.

Table 21. Austin total cooling energy results and comparison

	Historic	2020	2050	2080
IECC (Wh/m²)	842	979	1095	1220
PH (Wh/m²)	544	624	694	778
% change from IECC to PH	-34%	-36%	-36%	-36%
IECC change from IECC historic	-	16%	30%	44%
PH change from PH historic	-	14%	27%	43%

Table 22. DC peak cooling energy results

	Historic	2020	2050	2080
IECC (Wh/m²)	7.79	8.11	8.34	8.44
PH (Wh/m²)	5.75	5.95	6.12	6.24
Change from IECC to PH	-26%	-26%	-26%	-26%
IECC change from IECC historic	-	4%	7%	8%
PH change from PH historic	-	3%	6%	8%

Phoenix Cooling Energy
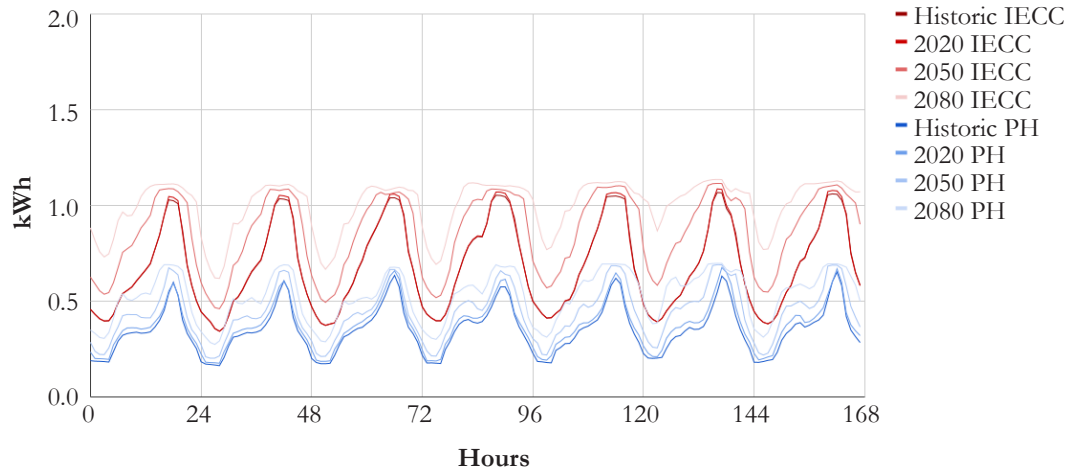
Figure 46. Phoenix cooling energy for IECC and PH models during simulated hot week

Table 23. Phoenix total cooling energy results and comparison

	Historic	2020	2050	2080
IECC (Wh/m²)	734	736	930	1077
PH (Wh/m²)	376	405	473	570
Change from IECC to PH	-48%	-44%	-49%	-47%
IECC Change from IECC historic	-	0.2%	26%	46%
PH Change from PH historic	-	7%	25%	50%

Table 24. Phoenix peak cooling energy results and comparison

	Historic	2020	2050	2080
IECC (Wh/m²)	6.84	6.97	7.15	7.28
PH (Wh/m²)	4.19	4.33	4.43	4.48
Change from IECC to PH	-38%	-37%	-38%	-38%
IECC change from IECC historic	-	2%	5%	6%
PH change from PH historic	-	3%	5%	7%

3.7.3. Grid-off Results

"Grid-off" scenario results are given in: 1) HHH28 and HHH32, and 2) time series heat index plots. Power outage scenarios produce a diverse set of results across the four sample cities captured in Figure 47, Figure 48, Figure 49, and Figure 50. These figures deconstruct the average internal zone temperatures and relative humidifies in each model location. In DC (Figure 47) because zone air temperatures are consistently within a degree of the outdoor dry bulb temperature, natural ventilation is consistently used, and so temperatures and relative humidity track the outdoor conditions. In Miami (Figure 48) natural ventilation is rarely used because the outdoor dry bulb temperature is consistently greater than the zone air temperature. As a result, zone relative humidity increases due to the lack of ventilation. The plot showing relative humidity highlights the passive house's airtightness where the internal relative humidity does not fluctuate as much as the IECC model worse air tightness. In Austin (Figure 49) outdoor temperatures drop at night to be less than the zone air temperature which triggers natural ventilation which can be observed in the small temperature valleys and more extreme relative humidity fluctuations. In Phoenix (Figure 50) dry bulb temperatures are consistently significantly higher than the zone temperatures so no natural ventilation is used. These results show the variation of zone conditions and behavior based on the outdoor conditions.

Figure 51 shows heat index threshold results from each location and weather scenario. In DC, Miami, and Austin by 2050, the IECC model has over 70% HHH32 and 98% HHH28 (Table 25, Table 26, Table 27). In DC, Table 25 and Figure 52, the Passive House model produces worse interior conditions than the IECC model. Models in Phoenix perform significantly better than the others with 86% HHH28 and 14% HHH32 in the 2080 IECC model and only 5% HHH28 and no HHH32 in the 2080 Passive House model (Figure 55 and Table 28). Models in Miami and Austin perform similarly where house form and weather conditions are similar although in Miami the Passive House model consistently performs better than the IECC model whereas the Passive House model and the IECC models perform similarly in historic and 2020 weather. The models diverge in 2050 and 2080 where Passive House performs increasingly better than IECC (Figure 48).
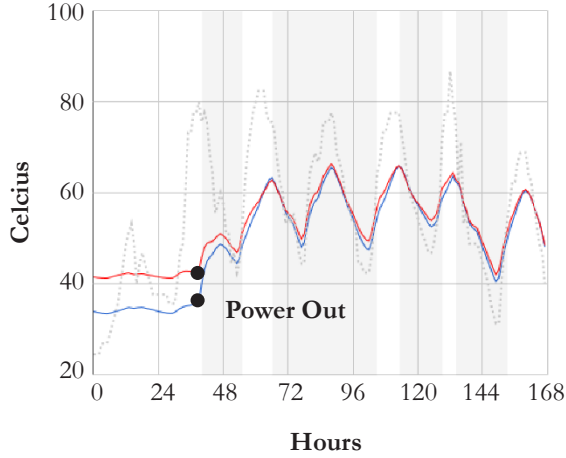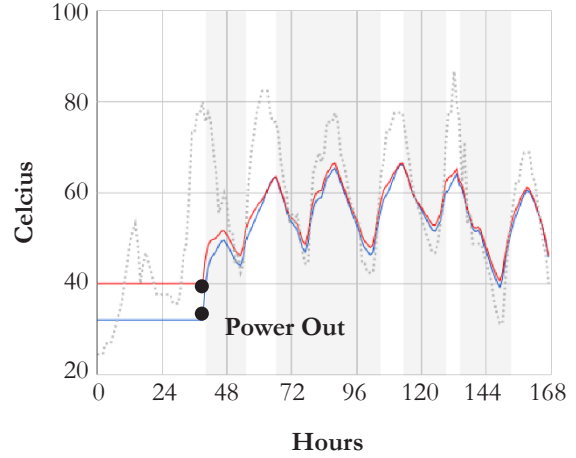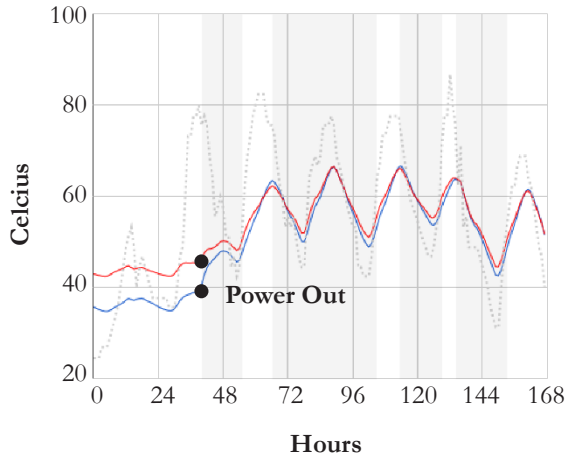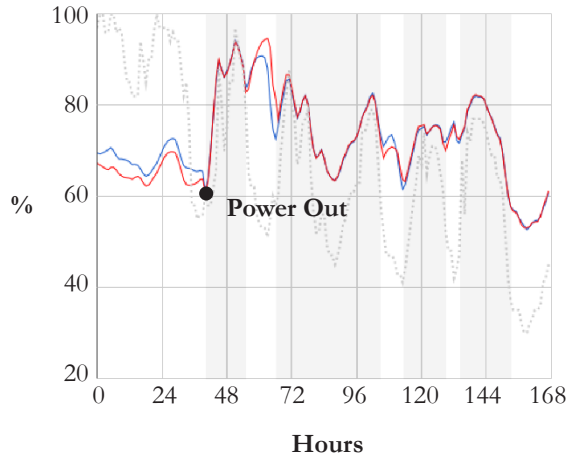
Figure 47. Passive House and IECC average zone conditions during power outage under historic weather conditions in the DC model

Miami House Internal Conditions
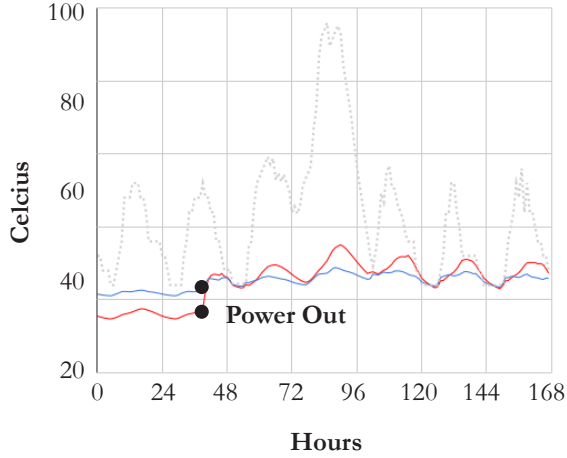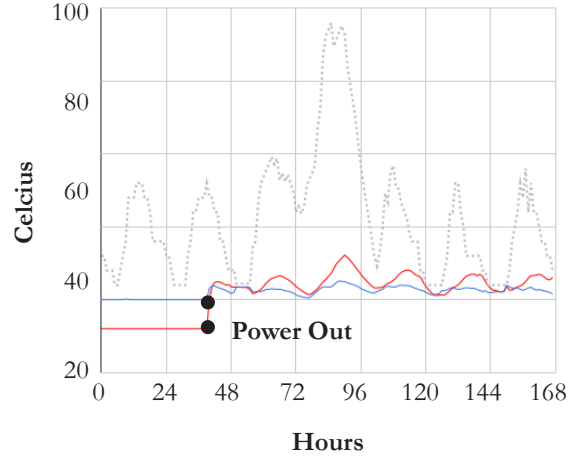
Operative Temperature

Air Temperature

Mean Radiant Temperature
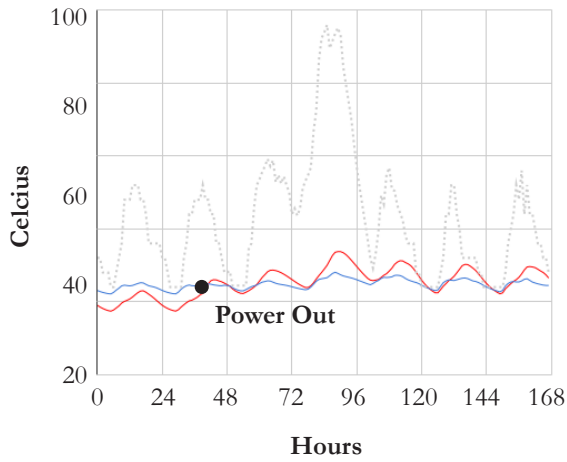
Relative Humidity
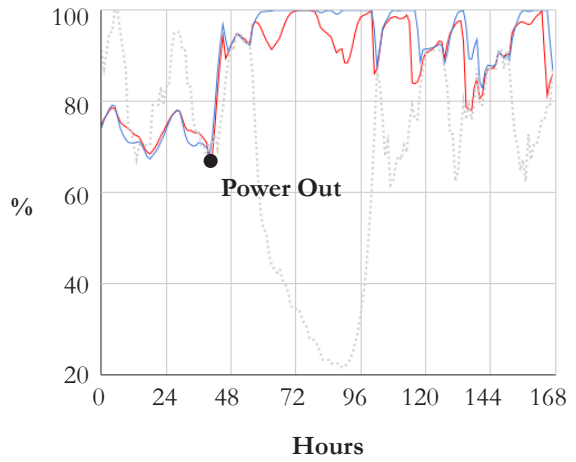
IECC — Passive House — Historic Weather — Natural Ventilation

Figure 48. Passive House and IECC average zone conditions during power outage under historic weather conditions in the Miami model
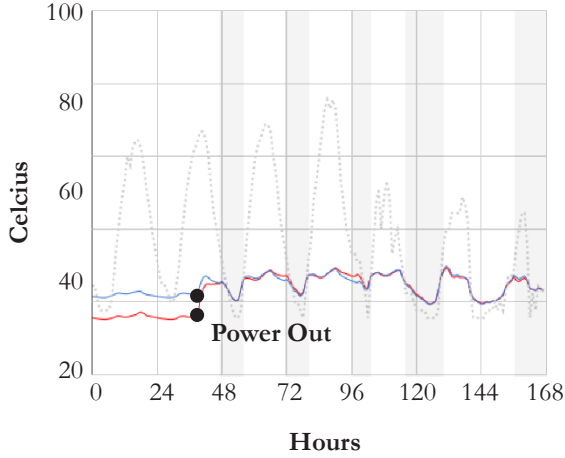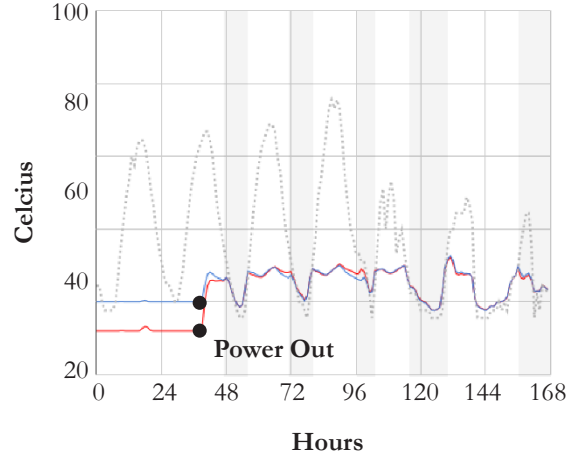
Operative Temperature

Air Temperature

Mean Radiant Temperature
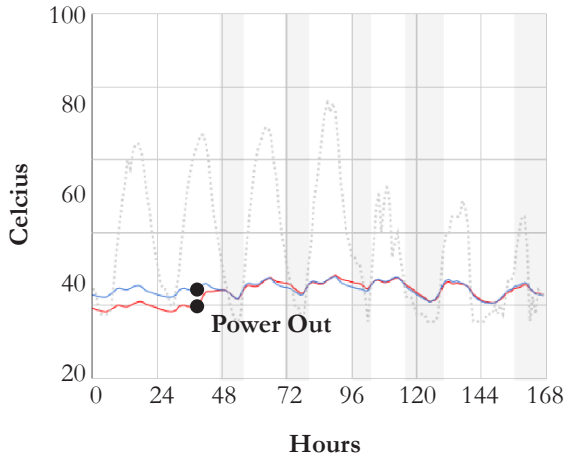
Relative Humidity
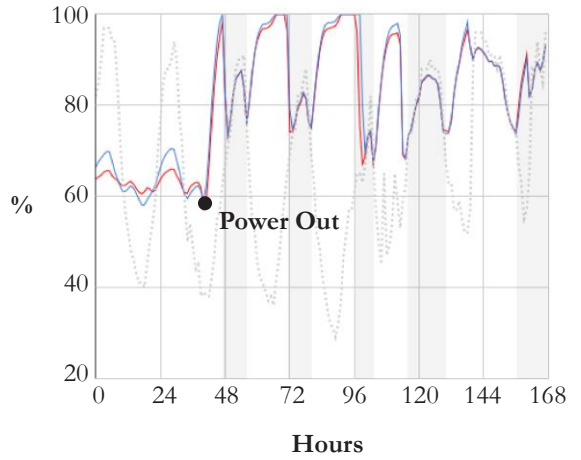
Figure 49. Passive House and IECC average zone conditions during power outage under historic weather conditions in the Austin model.

Phoenix House Internal Conditions
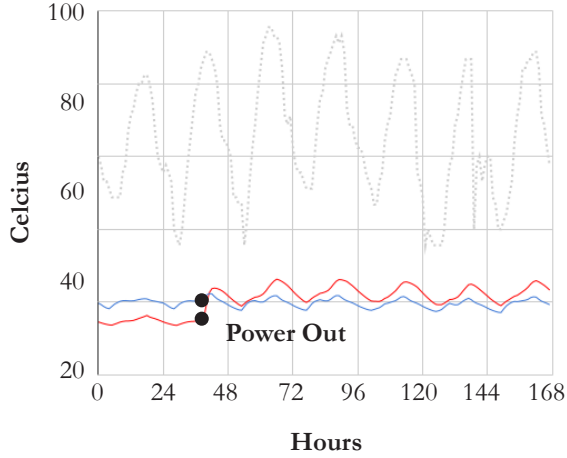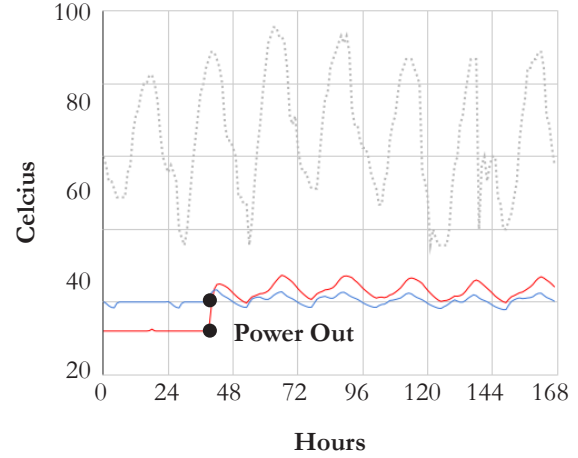
Operative Temperature

Air Temperature

Mean Radiant Temperature
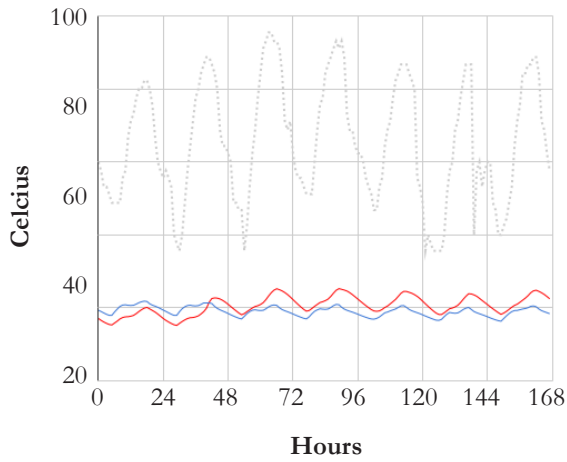
Relative Humidity
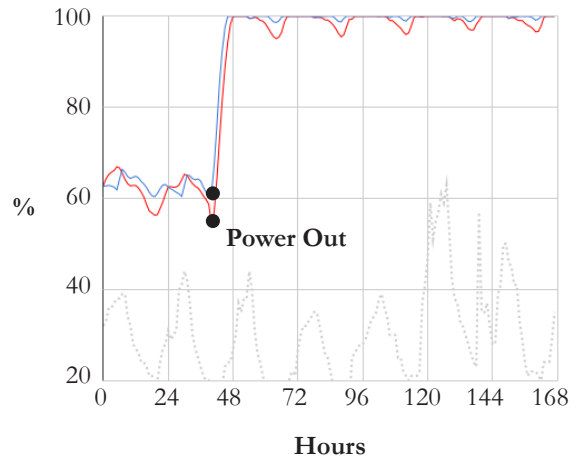
IECC — Passive House — Historic Weather — Natural Ventilation

Figure 50. Passive House and IECC average zone conditions during power outage under historic weather conditions in the Phoenix model
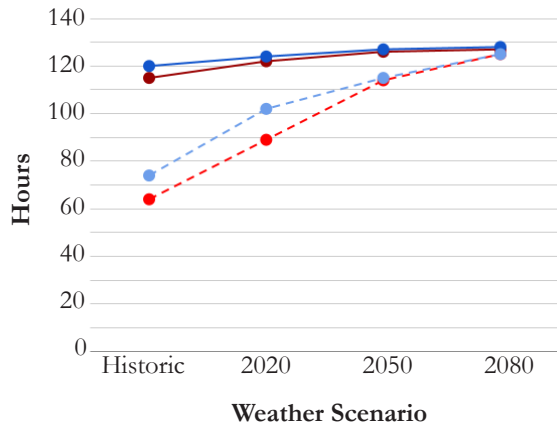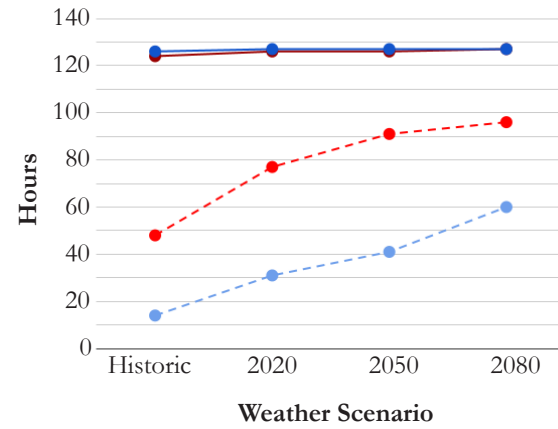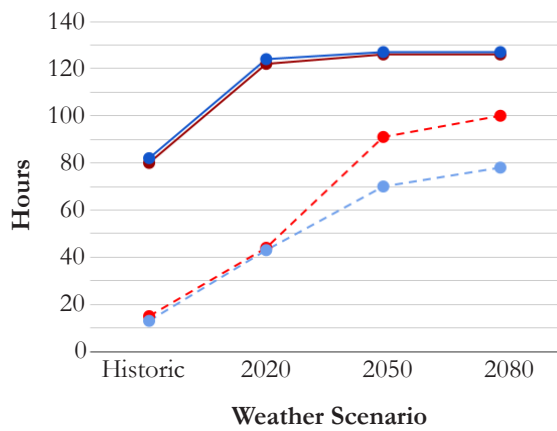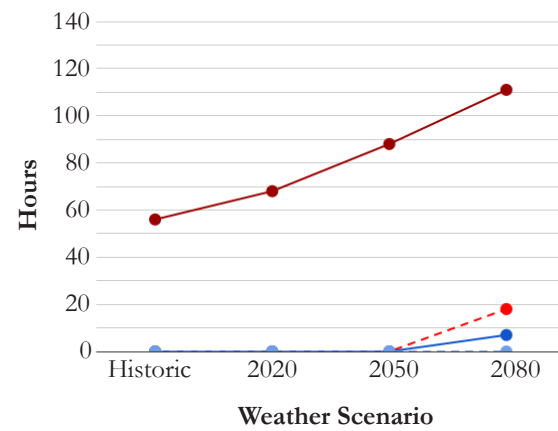
Figure 51. Heat hazard hours in DC, Miami, Austin, and Phoenix for IECC and Passive House models

IECC and Passive House Grid-Off, DC
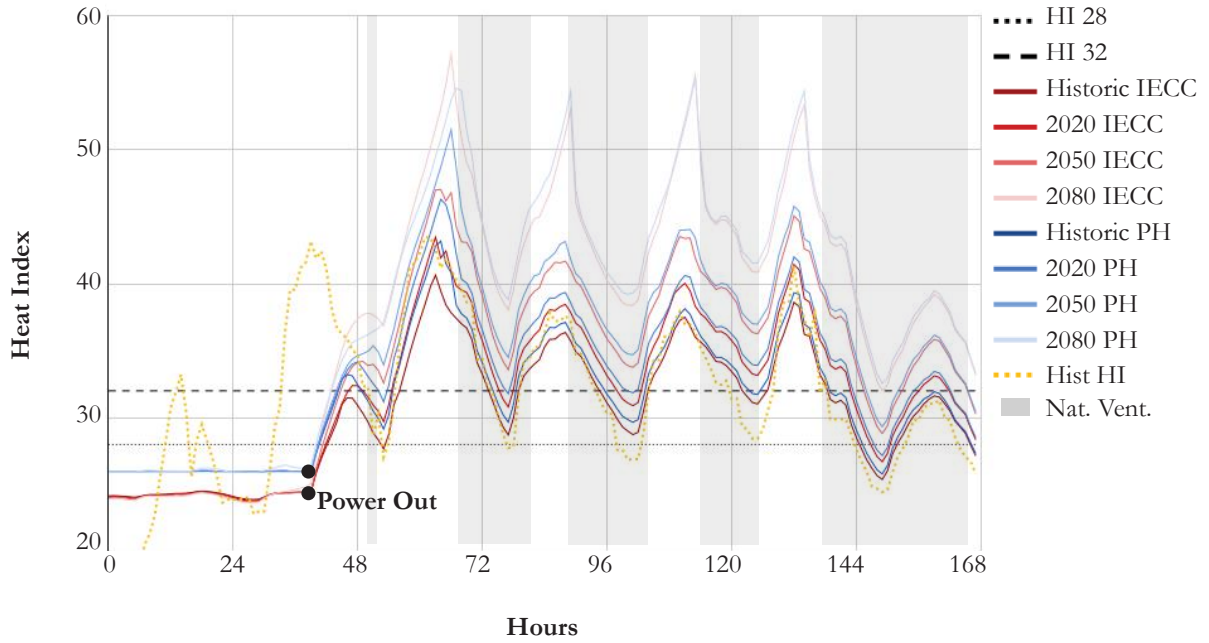
Figure 52. Heat Index time series plot of IECC and Passive House models during grid-off scenario in DC

Table 25. Heat Hazard Hours of IECC and Passive House models during grid off scenario in DC. Results given in number of hours over heat index threshold and percent of hours above threshold.

		Historic (# | %)	**2020 (**# | %)	**2050 (**# | %)	**2080 (**# | %)
IECC	HHH28	115 | 89%	122 | 95%	126 | 98%	127 | 99%
	HHH32	64 | 50%	89 | 69%	114 | 89%	125 | 97%
PH	HHH28	120 | 93%	124 | 96%	127 | 99%	128 | 100%
	HHH32	74 | 57%	102 | 79%	115 | 89%	125 | 97%

IECC and Passive House Grid-Off, Miami
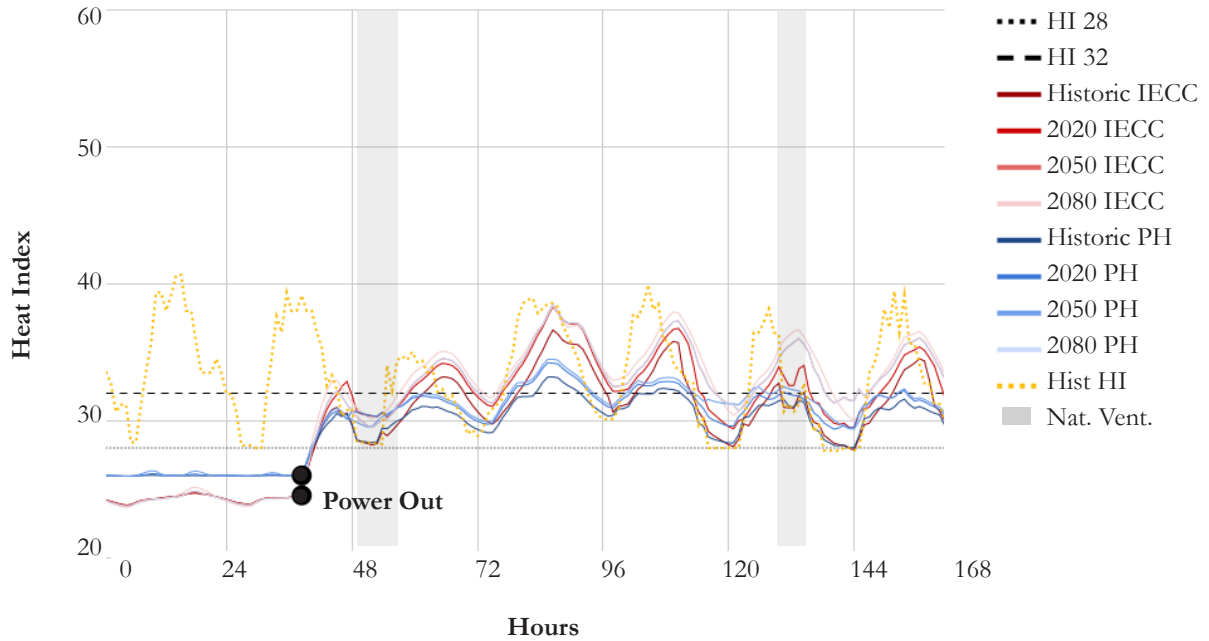
Figure 53. Heat Index time series plot of IECC and Passive House grid off scenario in Miami

Table 26. Heat Hazard Hours of IECC and Passive House models during grid off scenario in Miami. Results given in number of hours over heat index threshold and percent of hours above threshold.

		Historic (# | %)	2020 (# | %)	2050 (# | %)	2080 (# | %)
IECC	HHH28	124 | 96%	126 | 98%	126 | 98%	127 | 99%
	HHH32	48 | 37%	77 | 60%	91 | 71%	96 | 75%
PH	HHH28	126 | 98%	127 | 99%	127 | 99%	127 | 99%
	HHH32	14 | 10%	31 | 24%	41 | 32%	60 | 46%

IECC and Passive House Grid-Off, Austin
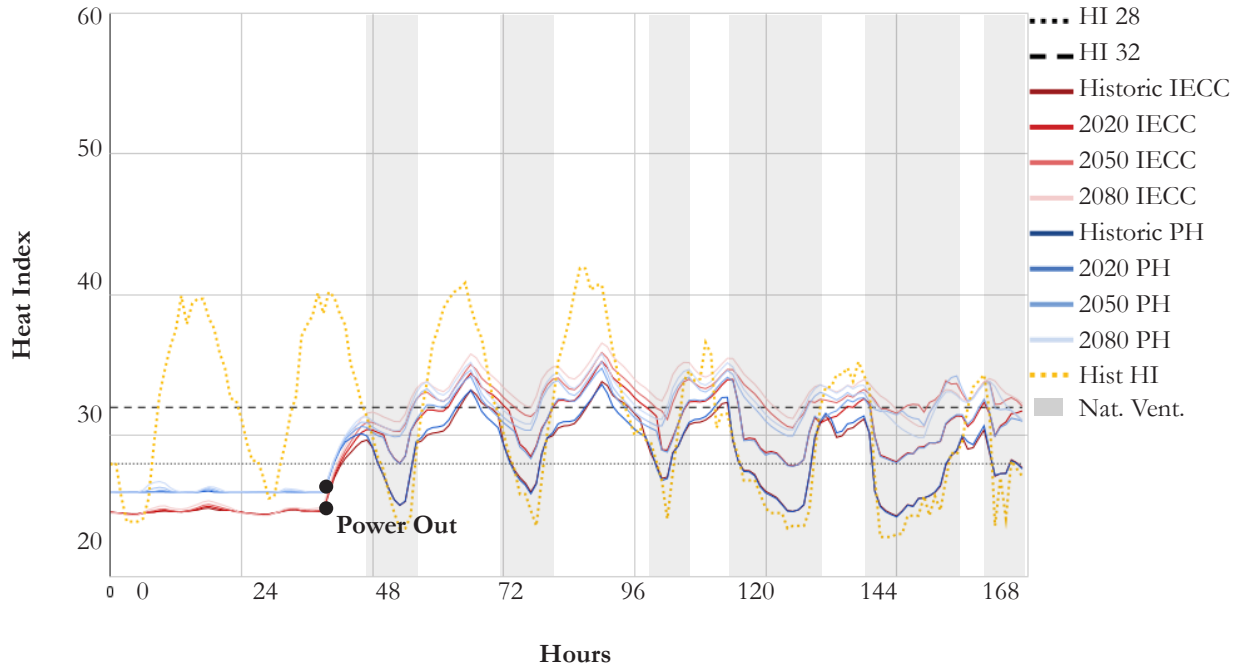
Figure 54. Heat Index time series plot of IECC and Passive House grid off scenario in Austin

Table 27. Heat Hazard Hours of IECC and Passive House models during grid off scenario in Austin. Results given in number of hours over heat index threshold and percent of hours above threshold.

		Historic (# | %)	**2020** (# | %)	**2050** (# | %)	**2080** (# | %)
IECC	HHH28	80 | 65%	122 | 95%	126 | 98%	126 | 98%
	HHH32	15 | 14%	44 | 35%	91 | 71%	100 | 80%
PH	HHH28	82 | 66%	124 | 97%	127 | 99%	127 | 99%
	HHH32	13| 14%	43 | 36%	70 | 55%	78 | 61%

IECC and Passive House Grid-Off, Phoenix
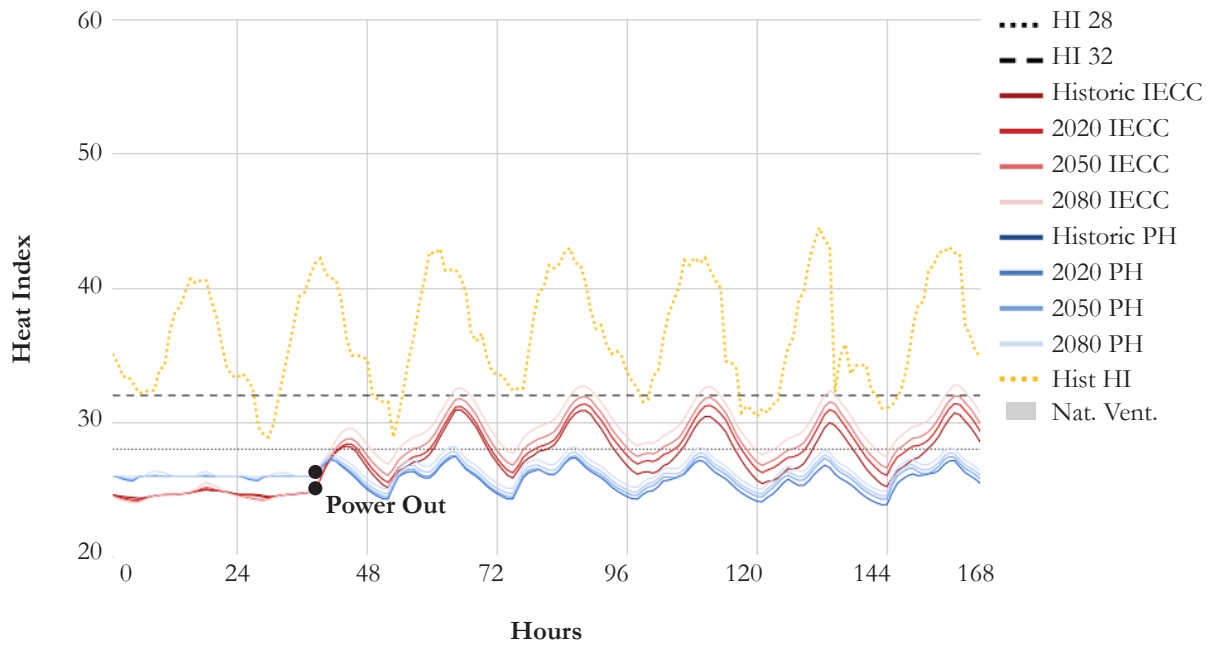
Figure 55. Heat Index time series plot of IECC and Passive House grid off scenario in Phoenix

Table 28. Heat Hazard Hours of IECC and Passive House models during grid off scenario in Phoenix. Results given in number of hours over heat index threshold and percent of hours above threshold.

		Historic (# | %)	2020 (# | %)	2050 (# | %)	2080 (# | %)
IECC	HHH28	56 | 43%	68 | 53%	88 | 69%	111 | 86%
	HHH32	0 | 0%	0 | 0%	0 | 0%	18 | 14%
PH	HHH28	0 | 0%	0 | 0%	0 | 0%	0 | 5%
	HHH32	0 | 0%	0 | 0%	0 | 0%	0 | 0%

3.7.4. Discussion

An unexpected finding from these results is that the peak cooling energy increase across weather scenarios is not more than 20% from the historic weather data. This is important as it relates to grid stability and peak energy demand. The largest peak increase occurs in the DC Passive House model of 20% from the historic value although it performs much better (13%) than its IECC counterpart. In a nutshell, this is good news for heat resilience. A peak increase of not more than 20% in a little over half a century under worst case conditions seems to be manageable from the position of energy supply. Conversely, the average total cooling demand increase over a hot week of ~40% has significant cost implications for building occupants caused by increased peaks and increased demand for cooling energy during traditional off-peak nighttime hours. Total cooling energy increases have notable impacts on a decarbonized grid that may partially rely on solar production to meet demands. This is also important when broadening the perspective of resilience to include socioeconomic insecurity wherein a 20-40% increase in an energy bill for a potentially already housing burdened family or person has other serious implications on wellbeing and health.

One of the main causes for the difference in performance across locations and IECC and Passive House Standard is that, in the case where the Passive House model performed worse than the IECC model slab insulation, was present. The three models that performed better had little resistance between slabs and the ground and are essentially ground coupled. As a result of Phoenix, Austin, and Miami's slabs being uninsulated, much fewer heat hazard hours are observed compared to DC. Regardless of slab insulation, the only model that successfully reduced all hazard hours is the Phoenix Passive House, meaning that all other models contain risk and vulnerability during an extreme heat event.

Section 3.8. Conclusion

In this chapter, four weather scenarios that are used for later simulations (HadCM3 A2) were located in a broader context of two other future emission scenarios (RPC 4.5 and 8.5). The A2 scenario has been shown to be the worst-case scenario of the three. Yet, each morphed weather year has a demonstrable relation to other warming scenarios across time. This is established both through comparing peak and total cooling energy in an archetypal home as well as comparing heat hazard hours in a power outage scenario in two locations and climate zones, Phoenix and Miami. Ultimately, this provides a low-resolution proxy to map vulnerability across climate projections and gives a sense of the possibilities of future climate extremes.

This chapter also establishes that natural ventilation is an essential component in creating passively survivable conditions in homes. It demonstrates that the larger the operable area of windows, the greater reduction in heat hazard hours due to increased air flow. Various configurations of natural ventilation can be effective, but some form of cross or adjacent ventilation is shown to have the greatest cooling effect during nighttime temperature swings. This establishes a baseline of building operation during a heatwave necessary to improve internal conditions.

In terms of heat vulnerability, this chapter shows that future weather does not have an outsized effect on peak cooling energy demand for model homes built to the latest IECC or Passive House standards which does not increase more than 20% across models. However, future weather does increase total cooling energy required to maintain interior comfort by ~40%. As such, a potential resiliency impact does not implicate significant new strain on the grid but does bring socio-economic resilience into focus where increased cooling energy leads to significantly higher cooling costs during warmer futures and extreme events. Passive House standards make a significant dent in reducing peak and total energy. However, depending on the ground construction, Passive House potentially worsens passive survivability where passive houses, under conventional wisdom, insulate their slabs such the ground cannot act as a heat sink. Further, natural ventilation during a power outage is not an adequate strategy for creating passive survivability in both house models. These conclusions highlight a tension in the thesis between energy efficiency, resilience, and passive survivability. In the case of Passive House, conceptualized in heating dominant climates and adapted for cooling dominated climates, laudable logics that privilege energy use reduction, at times can exacerbate extreme conditions and negatively impact passive survivability.

Chapter 4
Ground Coupling and Simulation Methods

Chapter 4. Ground Coupling and Simulation Methods

Section 4.1. Chapter Summary

This chapter addresses key aspects and challenges of modeling ground coupled buildings in EnergyPlus. In this chapter:

1. An overview of fundamental EnergyPlus heat transfer concepts and objects is presented
2. A survey of ground modeling methods is conducted
3. Each surveyed method is tested and compared for major differences and application drawbacks
4. A simple fit-to-data ground temperature equation is defined and tested against a THERM model compared with the methods tested in 3.

Section 4.2. Motivation

Chapter 3 revealed a significant difference between the DC models and the models from Austin, Phoenix, and Miami. In the case of DC, the Passive House model performed only marginally better during the grid on scenario and worse than the IECC model in a power outage scenario. The archetypal DC model has a notably different building form than the other three; a two-story home with a conditioned basement. Additionally, each model uses unique constructions. After some exploratory sensitivity testing, slab and basement insulation revealed themselves to be the most significant factors in both active and passive performance during the hot week across models. In simple terms, a single-family home's relationship with the ground has an outsized impact on performance during an extreme heat event. An example of this can be observed in the Figure 56, which provides a motivating example of the Austin, TX models with three different slab insulation values. As was briefly mentioned in 3.4.4, accurately accounting for ground temperatures and ground heat transfer in energy simulations is extremely important, especially for smaller buildings. As such, this chapter explores the effects of slab and basement constructions on cooling energy, annual space conditioning EUI, and passive resilience in single family homes. Firstly, a survey of available ground modeling methods in EnergyPlus is conducted. Secondly, a set of energy and grid-off scenarios is presented. Thirdly, a fit-to-data method of basement outside ground temperatures is defined. The greatest limitation of this method comparison is that no real-world data are available to compare these methods against. With this limitation in mind, two questions are addressed: 1) What are the key differences between simulation methods and 2) when modeling free running buildings, or buildings undergoing a power outage, which method should be used for modeling heat transfer in ground coupled buildings.
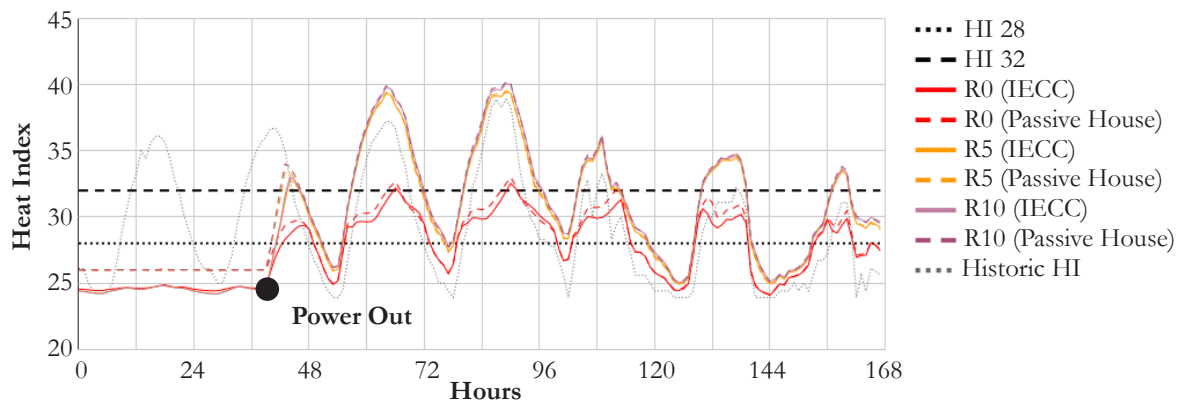
Figure 56. A motivating heat index plot that gives an example of passive performance during a power outage in the Austin, TX models from Chapter 3 with three different slab insulation scenarios.

Section 4.3. Ground Heat Transfer Methods

The introduction of the EnergyPlus Auxiliary Programs documentation recommends using "the Slab or Basement program described in this section to calculate custom monthly average ground temperatures. This is especially important for residential applications and very small buildings." It further goes on to state that "if one of these ground temperature preprocessors is not used, for typical commercial buildings in the USA, a reasonable default value is 2oC less than the average indoor space temperature."[86] EnergyPlus documentation goes on to acknowledge the challenge of ground heat transfer in full building energy simulation as a result of two main constraints: 1) the time scale of ground temperature (on the order of months and years) versus the time scale of building energy simulation on the order of hours and 2) the increased dimensionality of ground heat transfer in either two dimensions where heat travels through a section of the building and ground, or three dimensionally where heat flows in all directions. When EnergyPlus performs a heat balance calculation it solves a one-dimensional (1-D) heat transfer problem where surfaces and exterior boundary conditions are constant temperatures across the surface, or "isothermal" in EnergyPlus lingo. Four of the five methods (all but Kiva) tested below use a method of creating a "separation plane" that defines an outside boundary condition similar to the process used to perform a one-dimensional heat transfer calculation in other locations in the model.

Ground heat transfer methods further explicated in this chapter:

1. Rule of thumb
2. Auxiliary programs
3. FC factor method
4. Ground Domain
5. Kiva ground heat transfer
6. Novel fit-to-data basement ground temperatures

Methods 1 – 5 are well-documented in either the EnergyPlus Engineering Reference or the Auxiliary Program reference that accompanies EnergyPlus software. [87] [88] Method 6 is developed in this chapter as an approximation method for use in ground coupled basements of regular sizes.

---

[86] "Energy Plus Version 9.6.0 Documentation, Engineering Reference" (U.S. Department of Energy, September 23, 2021).
[87] "Engineering Reference."
[88] "Energy Plus Version 9.6.0 Documentation, Auxiliary Programs" (U.S. Department of Energy, September 23, 2021).

Section 4.4. Key EnergyPlus Heat Transfer Equations and Objects for Common Ground Modeling Practice

The EnergyPlus 1-D ground heat transfer process is designed to slot into the methods of 1-D heat transfer that are used on all other constructions in EnergyPlus. While the below equations are available in the EnergyPlus Engineering Reference, they are relevant to communicating the fundamentals of how EnergyPlus performs its 1-D heat transfer calculations and how ground relationships are accounted for.

4.4.1. Construction Conduction

For conduction through walls, EnergyPlus uses a lot of clever math which results in a time series solution to a linear equation by Stephenson and Mitalas in 1967 with the basic form

$$q''_{ko}(t) = \sum_{j=0}^{\infty} X_j T_{o,t-j\delta} - \sum_{j=0}^{\infty} Y_j T_{o,t-j\delta} \tag{7}$$

where the q term is the outside heat flux, X and Y are response factors, T_o is the outside temperature and T_i is the inside temperature.[89] To negotiate the fact of the above equation needing infinite terms to converge on a solution to the linear equation, constant coefficient terms called conduction transfer functions (CTF) are introduced which are unique to each EnergyPlus construction.

The heat flux solution then takes the forms

$$q''_{ki}(t) = -Z_o T_{i,t} - \sum_{j=1}^{nz} Z_j T_{i,t-j\delta} + Y_o T_{o,t} + \sum_{j=1}^{nz} Y_j T_{o,t-j\delta} + \sum_{j=1}^{nq} \Phi_j q''_{ki,t-j\delta} \tag{8}$$

$$q''_{ko}(t) = -Y_o T_{i,t} - \sum_{j=1}^{nz} Y_j T_{i,t-j\delta} + X_o T_{o,t} + \sum_{j=1}^{nz} X_j T_{o,t-j\delta} + \sum_{j=1}^{nq} \Phi_j q''_{ko,t-j\delta} \tag{9}$$

Where X_j = Outside coefficient (j = 0,1…nz) , Y_j = Cross coefficient (j = 0,1…nz), Z_j = Inside coefficient (j = 0,1…nz), Φ_j = Flux coefficient (j = 1,2…nz), T_i is the inside face temperature, T_o is the outside face, q''_{ko} is the conduction heat flux on outside face, and q''_{ki} is the conduction heat flux on the inside face.[90]

In 1987, John Seem's PhD thesis developed the use of the state space method to solve the linear equations which avoids using a Laplace transformation of the generic form:[91]

$$\frac{d[x]}{dt} = [A][x] + [B][u] \tag{10}$$

$$[y] = [C][x] + [D][u]$$

[89] D G Stephenson, "Room Thermal Response Factors," *ASHRAE* 73, no. 1 (1967): 15.
[90] Ipseng Iu and D E Fisher, "Application of Conduction Transfer Functions and Periodic Response Factors in Cooling Load Calculation Procedures," *ASHRAE Transactions*, 2004, 14.
[91] John Seem E., "Modeling of Heat Transfer in Buildings" (PhD, Madison, University of Wisconsin, 1987)..

EnergyPlus then uses a finite difference algorithm to solve the system which more specifically takes the form:

$$\frac{d\begin{bmatrix} T_1 \\ \vdots \\ T_n \end{bmatrix}}{dt} = [A]\begin{bmatrix} T_1 \\ \vdots \\ T_n \end{bmatrix} + [B]\begin{bmatrix} T_{inside} \\ T_{outside} \end{bmatrix} \tag{11}$$

$$\begin{bmatrix} q''_{inside} \\ q''_{outside} \end{bmatrix} = [C]\begin{bmatrix} T_1 \\ \vdots \\ T_n \end{bmatrix} + [D]\begin{bmatrix} T_{inside} \\ T_{outside} \end{bmatrix}$$

Where n is the number of steps on the finite difference mesh, T_n are difference temperatures at each mesh point n, and $T_{outside}$ and T_{inside} are temperatures inside and outside the wall. As such, this model can be represented as a resistance-capacitance model shown in Seem's thesis generalized as a set of ODEs with n mesh points:[92]

$$C\frac{d[T_1]}{dt} = h[A](T_{outside} - T_1) + \frac{T_2 - T_1}{R}$$

$$C\frac{d[T_n]}{dt} = h[A](T_{inside} - T_n) + \frac{T_{n-1} - T_n}{R} \tag{12}$$

$$q''_{inside} = h(T_{inside} - T_2)$$
$$q''_{outside} = h(T_1 - T_{outside})$$

Or in matrix form:

$$\begin{bmatrix} \dfrac{d[T_1]}{dt} \\ \vdots \\ \dfrac{d[T_n]}{dt} \end{bmatrix} = \begin{bmatrix} A & B & 0 & \cdots & 0 \\ B & A & 0 & \cdots & 0 \\ 0 & \ddots & \ddots & \ddots & \vdots \\ \vdots & \ddots & \ddots & \ddots & 0 \\ 0 & \cdots & 0 & B & A \end{bmatrix}\begin{bmatrix} T_1 \\ \vdots \\ T_n \end{bmatrix} + \begin{bmatrix} \dfrac{hA}{C} & 0 & \cdots & 0 \\ 0 & \ddots & \ddots & \vdots \\ \vdots & \ddots & \ddots & 0 \\ 0 & \cdots & 0 & \dfrac{hA}{C} \end{bmatrix}\begin{bmatrix} T_{outside} \\ T_1 \\ \vdots \\ T_n \\ T_{inside} \end{bmatrix}$$

$$\tag{13}$$

$$\begin{bmatrix} q''_{outside} \\ q''_1 \\ \vdots \\ q''_n \\ q''_{outside} \end{bmatrix} = \begin{bmatrix} 0 & \cdots & \cdots & 0 & -h \\ \vdots & & & -h & 0 \\ \vdots & & & & \vdots \\ 0 & -h & & & \vdots \\ h & 0 & \cdots & \cdots & 0 \end{bmatrix}\begin{bmatrix} T_1 \\ \vdots \\ T_n \end{bmatrix} + \begin{bmatrix} 0 & \cdots & \cdots & 0 & h \\ \vdots & & & h & 0 \\ \vdots & & & & \vdots \\ 0 & h & & & \vdots \\ -h & 0 & \cdots & \cdots & 0 \end{bmatrix}\begin{bmatrix} T_{outside} \\ T_1 \\ \vdots \\ T_n \\ T_{inside} \end{bmatrix}$$

$$A = \frac{-1}{RC} - \frac{hA}{C}, B = \frac{1}{RC}$$

---

[92] Seem.

Where thermal resistance $= R = \frac{L}{kA}$ and thermal capacitance $= C = \frac{\rho cLA}{2}$, L = wall length, k = wall thermal conductivity, A = area, ρ = density, c = specific heat, and h = convection coefficient. A diagram of such system is shown in Figure 57.[93]
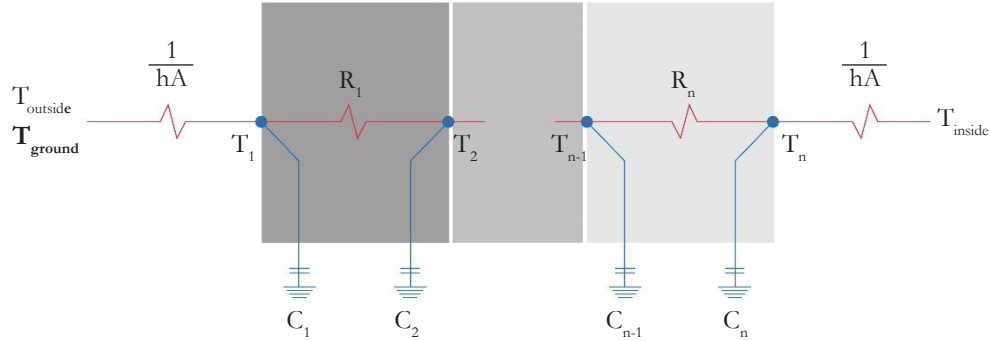
Figure 57. Resistance capacitance finite difference diagram of heat transfer through multilayered wall adapted from Seem's 2 node R-C circuit diagram[94]

4.4.2. Inside and Outside Surface Heat Balance

The EnergyPlus outside surface heat balance is simple in that it amounts to four terms that account for environmental energy exchange.

For outside heat balance:

$$q''_{solar} + q''_{longwave} + q''_{conv} - \boldsymbol{q''_{ko}} = 0 \tag{14}$$

Where *solar* = short wavelength radiation heat flux from the sun, *longwave* = longwave radiation flux from environment, *conv* = convective flux from environment, and **ko** = conduction heat flux into the wall.

For inside heat balance:

$$q''_{surface\ longwave} + q''_{short\ wave} + q''_{equip\ longwave} + \boldsymbol{q''_{ki}} + q''_{solar} + q''_{conv} = 0 \tag{15}$$

Where *surface longwave* = surface longwave radiant exchange with zone surfaces, *short wave* = net shortwave radiation from zone lighting, *equip longwave* = long wave radiation from zone equipment, **ki** = conduction flux through wall, *solar* = absorbed solar radiation flux, *conv* = convective flux from zone

Heat flux from conduction through wall in 14 and 15 (q''_{ko} and q''_{ki}) are bolded to reference the heat flux determined by 7-13.[95] A diagram of the heat flux equations is shown in Figure 58.

[93] Iu and Fisher, "Application of Conduction Transfer Functions and Periodic Response Factors in Cooling Load Calculation Procedures."
[94] Seem, "Modeling of Heat Transfer in Buildings."
[95] "Engineering Reference."
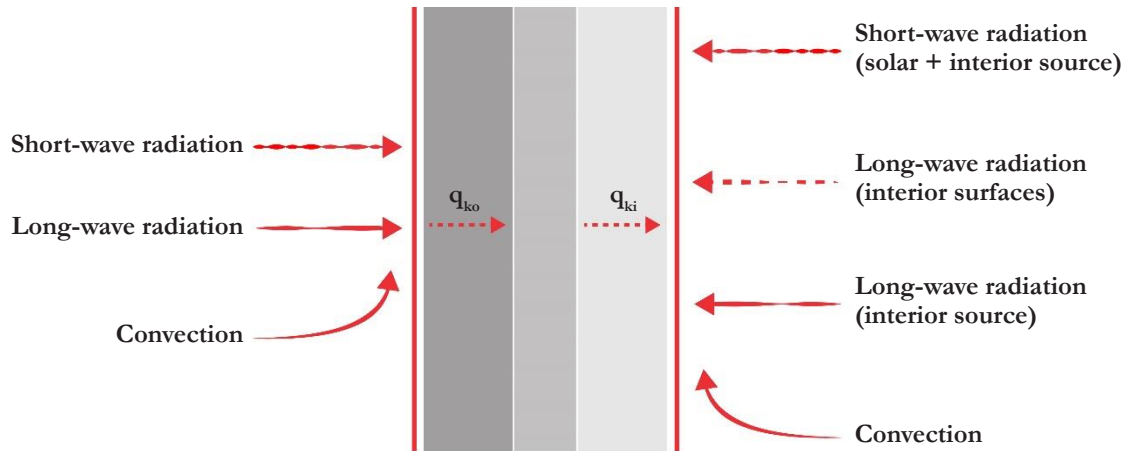
Figure 58. Outside and inside heat balance diagram adapted from EnergyPlus Engineering Reference[96]

4.4.3. Energy Plus Object Surface Property: Other Side Coefficients

Inside and outside surface heat balance equation terms account for multiple heat fluxes, which of course contributes to its accuracy and robustness. One mechanism for controlling the $T_{outside}$ or T_{ground} referenced in Figure 58 is through setting the properties of the outside temperature of either the air, which then accounts for convective and radiative fluxes, or of the temperature of the surface itself, which ignores convective and radiative fluxes. The temperature of either the air or surface described by the other side coefficient is:

$$T = C2 * C3 * C4 * T_{outdoor\,db} + C5 * T_{ground} + C6 + W_{speed} * T_{outdoor\,db} + C7 \\ * T_{zone+} C8 * T_{past} \tag{16}$$

Where:

        C2 = Sin variation of constant temp
        C3 = Constant temperature
        C4 = External dry bulb temperature
        C5 = Ground temperature coefficient
        C6 = Wind speed coefficient
        C7 = Zone air temperature coefficient
        C8 = Previous other side temperature coefficient

---

[96] "Engineering Reference."

4.4.4. Energy Plus Object Building Surface: Detailed

A second EnergyPlus object that allows for the control of a building surface's relationship with the ground is the Building Surface: Detailed object. Of particular relevance are the input fields:

Outside Boundary Condition – Specifies the boundary condition of the surface

Outside Boundary Condition Object – Specifies the Other Side Coefficients object (4.4.3)

Sun Exposure – Specifies if the surface receives solar gains

Wind Exposure – Specifies if the surface is exposed to the wind. No wind exposure sets the convection coefficient to the ASHRAE simple convection coefficients found in Appendix B4 of ASHRAE Standard 111-2008[97]

4.4.5. Energy Plus Object Site: Ground Temperature: Building Surface

As one of the simplest means of inputting the surface ground temperature, the object "Site:GroundTemperature:BuildingSurface" is used. This is a simple object that contains 12 values for the ground temperature during each month of the year. It is called when surfaces from the surface object in 4.4.4 uses the "Outside Boundary Condition" of "Ground". This object, or a variation of it, will be referenced by multiple methods in section 4.5.
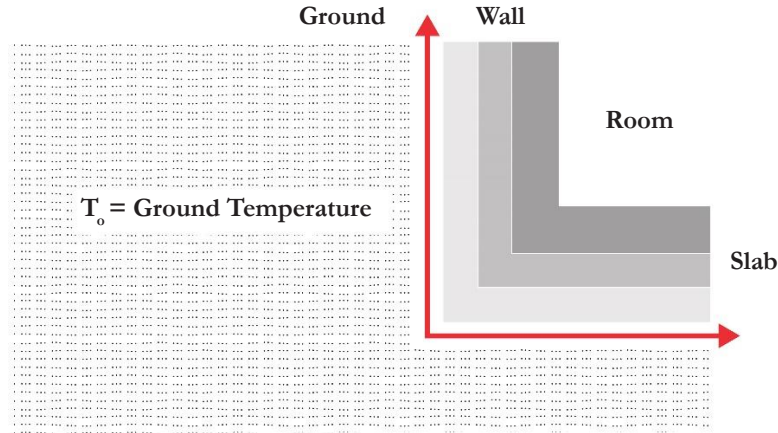
Figure 59. Ground temperature: building surface diagram shows a constant ground temperature the building surface regardless of depth or surface orientation

---

[97] Roger Richardson, "Measurement, Testing, Adjusting, and Balancing of Building HVAC Systems" (ASHRAE, 2017), https://ashrae.iwrapper.com/ASHRAE_PREVIEW_ONLY_STANDARDS/STD_111_2008_RA_2017.

4.4.6. Section Summary

Section 4.4 presents a set of objects and equations that are fundamentally relevant to the most common ground heat transfer modeling method used in EnergyPlus. In simple terms:

- At its heart, EnergyPlus calculates heat transfer through a building construction using a 1-D conduction transfer function (Equation 13 and Figure 57) that uses a heat flux equation to determine the temperatures inside and outside that construction (Equation 14 and 15, Figure 58). This makes simulating ground heat transfer, a 3-D heat transfer problem, a difficult problem.
- In order to be able to model building surfaces that are coupled with the ground, the most simplified methods use a 1-D heat transfer equation and specify the surface $T_{outside}$ value for the ground temperature (Equations 7-13).
- There are multiple ways of modeling ground heat exchange. The most straight forward interfaces simply with the EnergyPlus 1-D CTF and use rules of thumb to determine ground temperatures, though there are several methods that produce more nuance which are further detailed in Section 4.5.

<u>**Section 4.5. Ground Simulation Methods**</u>

This section gives a short overview of the origin, conceptual differences, and implementation in EnergyPlus via Honeybee of several ground modeling methods. Table 29 provides a high-level snapshot of each method.

Table 29. Ground heat transfer methods and their respective timestep's, ground temperature or heat transfer calculation methods, and heat transfer from ground in whole building simulation.

Method	Timestep Resolution	Heat Transfer (Ground)	Heat Transfer (Building)
EnergyPlus Default	Monthly	-	1-D
Rule of Thumb	Monthly	-	1-D
Auxiliary Programs	Monthly	3-D	1-D
FC Factor	Monthly	-	1-D
Ground Domain	Hourly	2-D	1-D
Kiva	Hourly	2-D	2-D

4.5.1. Energy Plus Default

Characteristics:
- **Time resolution:** Monthly
- **Heat Transfer:** 1-D CTF

The default ground temperature for each month of the year if no custom ground temperatures are provided is 18 °C as the outside boundary temperature on all surfaces with a ground boundary condition.

Implementation:
> The "Site:GroundTemperature:BuildingSurface" is used to input monthly ground temperature of 18 °C into the Honeybee model.

4.5.2. Rule of Thumb

Characteristics:
- **Time resolution:** Monthly
- **Heat Transfer:** 1-D CTF

The rule of thumb provided by EnergyPlus comes without reference. The rule says to use the Zone Temperature – 2 °C. In this case, more nuance is given between heating and cooling season, yet still assumes a constant heat loss throughout the year and on all surfaces.

Implementation:
> The "Site:GroundTemperature:BuildingSurface" is used to input monthly ground temperatures equal to the monthly set-point - 2 °C.

4.5.3. Auxiliary Programs in EnergyPlus

Characteristics:
- **Time resolution:** Monthly
- **Heat Transfer:**
    - 3-D finite difference ground temp calculation
    - 1-D CTF in building energy simulation

Two auxiliary programs are of particular interest in this thesis: the slab and basement programs. Both programs operate in a similar manner and the process of implementation is similar. The method is defined by a three-dimensional heat conduction boundary value equation defined by Bahnfleth in 1989 which outlines models for four fundamental boundary conditions: earth coupled surfaces, far-field boundaries, deep ground, and the ground surface. Bahnfleth further defines a finite difference solution to the admittedly rather ugly, yet efficacious formulation that is the meat and potatoes of both the slab and basement programs. Of note is the level of environmental detail included in this calculation wherein an EPW is supplied, as are soil properties, and a few building properties such as building height, area to perimeter ratio, slab thickness, monthly average zone temperatures, and both vertical and horizontal slab insulation details.

Slab Program
The slab program provides a set of ground temperatures at the slab perimeter, core, and the average. The program also provides a set of IDF objects which may be included in a building IDF. The most important objects are an example "Other Side Coefficient" object and monthly ground temperature schedules.

Implementation:
> Resulting slab program IDF objects may be smoothly integrated into building IDF files, however, this thesis simplifies the implementation by using the $T_{average}$ slab outputs and applying them using the "Site:GroundTemperature:BuildingSurface" object. One reason for this simplification is that the building IDF zoning does readily break down into "perimeter" and "core" constituent parts.

Basement Program
The basement program operates conceptually the same with some added nuance in building material inputs and surrounding conditions. Thermal properties are assigned to the foundation, slab, ceiling, gravel, insulation and the wooden rim joist. Gravel below and beside the slab is also accounted for. Similar to the slab, some simple building characteristics are supplied namely building footprint area to perimeter ratio, basement depth, and monthly zone temperatures.

Implementation:
> In chapter 3, a simplified implementation similar to the implementation of the slab program can be used, where wall and slab temperatures are applied to building surfaces using "Site:GroundTemperature:BuildingSurface". This is a simplified approach and does not capture the nuance provided by the basement program. As such, a second method applies monthly temperature schedules via Other Side Coefficients to the slab and walls respectively.

4.5.4. FC Factor Method

Characteristics:
- **Time resolution:** Monthly
- **Heat Transfer:** 1-D CTF

The FC factor method is curious, and originates from a need to simply model buildings to be able to easily input thresholds mandated by standards like ASHRAE. Effectively, the method replaces below grade walls and slabs with a representative construction of a certain C and F factor equivalent to a .15m concrete layer and a no-mass layer generic construction. These factors assigned to the abstracted constructions can be referenced in the latest ASHRAE Standard 90.1 Appendices A4.2 and A6.3.[98] Another unique aspect of the FC factor method is that it models steady state heat transfer through a total wall area in Watts and inputs ground temperatures through effectively the same means as the "Site:GroundTemperature:BuildingSurface" object. The ground temperatures used, however, are simply the monthly mean dry-bulb temperatures delayed by 3 months.

$$T_{ground,i} = T_{monthly\ db\ mean,i-3}$$

17

Where i = a given month

Implementation:

The implementation of the FC factor Method is simple. All ground coupled wall and slab constructions are replaced for their C and F factors, respectively and their boundary conditions are set to reference the FC Factor ground temperature object. After the initial building IDF is written, the necessary objects are modified and simulated.

4.5.5. Ground Domain

Characteristics:
- **Time resolution:** Hourly
- **Heat Transfer:**
    - 2-D implicit finite difference over the ground domain
    - 1-D CTF at wall surface

The Ground Domain finite difference algorithm essentially conducts a 2-D heat transfer calculation over a 2-D ground boundary field that provides detailed temperatures over a specified mesh at the building surface where a CTF calculates heat transfer through the wall.[99] Cell weights are defined by Pinel and Beausoleil-Morrison 2012. Ground domain temperatures are given by Kusada and Achenbach as default, but any ground temperature algorithm may be used that is included in the EnergyPlus software.[100] Slab and basement methods are included in EnergyPlus and use existing building construction, though non-uniform insulation scenarios over slabs and basement walls are possible.

---

[98] Matt Wilburn, "ANSI/ASHRAE/IES Standard 90.1-2019," 2019, 368.
[99] Patrice Pinel and Ian Beausoleil-Morrison, "Coupling Soil Heat and Mass Transfer Models to Foundations in Whole-Building Simulation Packages," 2012, 14.
[100] T Kusuda and Paul R Achenbach, "Earth Temperature and Thermal Diffusivity at Selected Stations in the United States," 1965, 236.

Implementation:

The Ground Domain IDF object contains the thermal characteristics of the surrounding soil as well as any insulation scenarios and building characteristics. The object also references the undisturbed ground temperature algorithm that is used. In our implantation, the Xing 2012 method is used.[101] After the initial building IDF is written, the necessary objects are modified and simulated.

Note: Due to the implicit finite difference method used in the Ground Domain objects, care should be taken to provide adequate simulation time prior to the time period of interest. This is particularly important when studying a limited simulation time frame like a heat wave. The best results come from running an annual simulation and bracketing results from the period of interest. This differs from other methods that uses EnergyPlus Other Side Coefficients.

4.5.6. Kiva

Characteristics:

- **Time resolution:** Hourly
- **Heat Transfer:** 2-D finite difference over ground, wall, and slab mesh

The Kiva foundation is the most recent addition to ground heat transfer modeling toolkit in EnergyPlus. Developed by Neal Kruis in his PhD thesis, the method uses a 2D finite difference method that utilizes EnergyPlus boundary conditions and simulation data to produce timestep foundation heat transfer calculations.[102] Kiva brought three significant advancements in ground modeling, the first is its novel 2D heat transfer that includes 2D transfer through below grade walls and slabs, effectively skirting the EnergyPlus 1D CTFs that other methods use. The second, in line with the 2D methods, Kiva accounts for a wider variety of slab and foundation shapes, particularly those with indicate concavity. Lastly, Kiva allows for very nuanced insulation locations that also consider EnergyPlus constructions.

Implementation:

The Kiva implementation in Honeybee is similar to the FC factor Method and Ground Domain methods wherein building IDF objects are edited to include Kiva objects. One small limitation is that Kiva generally required more unique objects, and makes it slightly more difficult to correctly implement, e.g. each slab zone needs a unique Kiva object. These additional steps are not prohibitive, however.

Note: Similar to the Ground Domain objects, Kiva's finite difference algorithm is best served by a longer simulation period.

---

[101] Lu Xing, "Estimations of Undistrubed Ground Temperatures Using Numerical and Analytical Modeling" (2010).
[102] Neal Kruis and Moncef Krarti, "Three-Dimensional Accuracy with Two-Dimensional Computation Speed: Using the Kiva™ Numerical Framework to Improve Foundation Heat Transfer Calculations," *Journal of Building Performance Simulation* 10, no. 2 (March 4, 2017): 161–82, https://doi.org/10.1080/19401493.2016.1211177.

Section 4.6. Ground Modeling Comparison

In this section, the ground simulation methods outlined above will be compared and deployed in order to compare their simulation results for a single-family home during a heat wave in grid-on and grid-off scenarios. In conjunction with comparing methods, ground insulation scenarios will be compared with the goal of understanding the strengths and limitations of each method.

4.6.1. Methodology and Simulation Plan

Two models will be compared, a slab-on grade house, and a house with a basement. Additionally, two locations will be tested, Phoenix, AZ and Austin, TX. These two in order to simplify the simulation and ultimately make these results more comparable, the same single-family building form will be used. Building construction remains constant across model. The constructions used will be the Phoenix, AZ IECC constructions and loads (Table 4 in Chapter 3)

Methods for simulation:
1. Energy Plus Default (4.5.1)
2. Rule of thumb (4.5.2)
3. Auxiliary programs (4.5.3)
4. FC factor method (4.5.4)
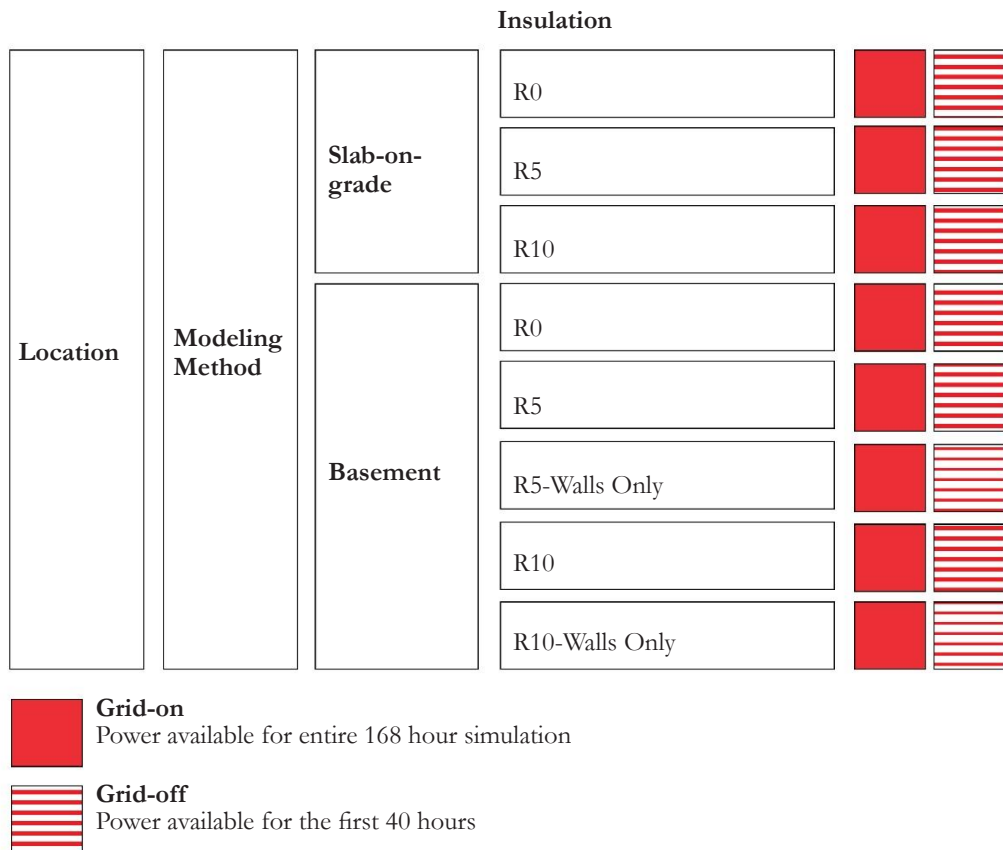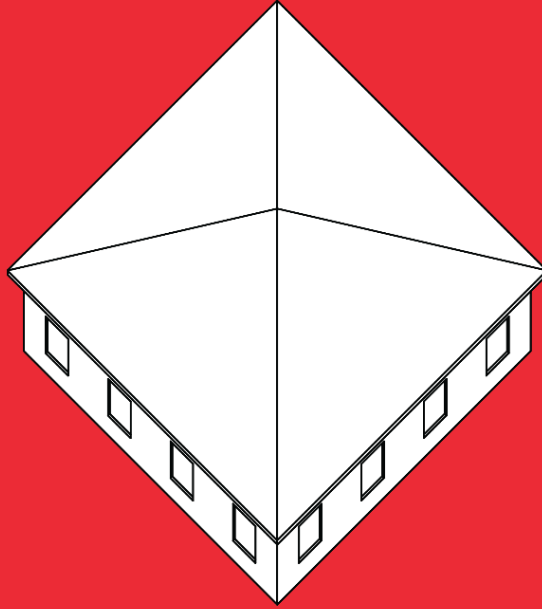5. Ground Domain (4.5.5)
6. Kiva ground heat transfer (4.5.6)

Figure 60. Simulation diagram for ground modeling methods.

117

Slab-on-grade
160 m^2
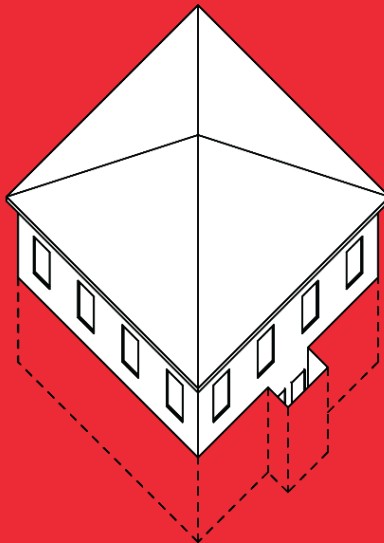4 zones

Basement
160 m^2
8 zones

Figure 61.Two models used for ground methods simulations

4.6.2. Results

The primary findings presented in this study show that ground simulation methods provide significantly varied results when simulating small ground coupled buildings. However, as construction R-values increase, methods produce increasingly similar results in both grid- and grid-off scenarios.

Results here are found in two categories: 1) slab-on-grade, and 2) basements. These categories are again presented in two sets: 1) grid-on, cooling energy plots and annual heating/cooling EUI charts and 2) grid-off, shown in heat index plots.

Slabs

Slab-on-grade cooling energy results vary widely with no slab insulation. Nearly a kWh separates the peaks in Phoenix with R0 insulation seen in Figure 62, albeit the default ground temperature is an extreme case. The same is true of Austin in Figure 66. As slab R-value increases, all methods become much more closely related (Figure 63, Figure 67). Importantly, Kiva method and Ground Domain, both of which use a 2-D finite difference hourly timestep, appear lockstep in their energy peaks until Ground Domain separates from Kiva in deeper valleys (Figure 62, Figure 66 Similarly, methods that use "Other Side Coefficients" produce comparable peaks, varying primarily in their amplitude.

Heating and cooling EUI in both cases captures the difference in space heating energy over a longer time period (Figure 64, Figure 65, Figure 68, Figure 69) Kiva method produces the greatest cooling loads when no insulation is present but is overtaken by Ground Domain with R10 insulation below the slab. The auxiliary programs with no insulation in both cases produced results that are notably lower than Kiva and Ground Domain. In Phoenix, a 30% difference between the auxiliary slab program and Kiva; in Austin, a 43% difference.

In a grid-off scenario, the alignment of method results is starkly apparent with greater wall R-values (Figure 71, Figure 73). This is a result of the internal zone temperatures reaching the point where natural ventilation activates which leads to zone conditions being less influenced by ground temperatures and more by the outdoor conditions.

Basements

Basement results mirror those from slab simulations. With four of the house's zones on the floor above the basement effectively decoupled from the ground, energy and heat index plots do not converge on each other in the same way that slab methods do (Figure 76, Figure 80, Figure 87, Figure 89). It is true that more similar results are seen with higher R-values (Figure 76, Figure 80). In scenarios with R0 slab insulation and R10 wall insulation, peaks are notably reducing primarily the default, rule of thumb, and auxiliary slab program methods (Figure 77, Figure 81).

EUIs across the board are higher than those that are slab on grade, despite being the same conditioned area. This is due to the upper, or ground floor, being decoupled from the ground. (Figure 82, Figure 83, Figure 84, Figure 85). Similar relationships that are observed in slab methods are seen in the EUIs of the basement house.

Grid-off scenarios in the basement model provide similar results to the slab methods (Figure 86, Figure 87, Figure 88, Figure 89). However, heat index plots do not distinguish between upper and lower basement zones in the interest of legibility. This difference is further explored in later chapters!

Slab Results

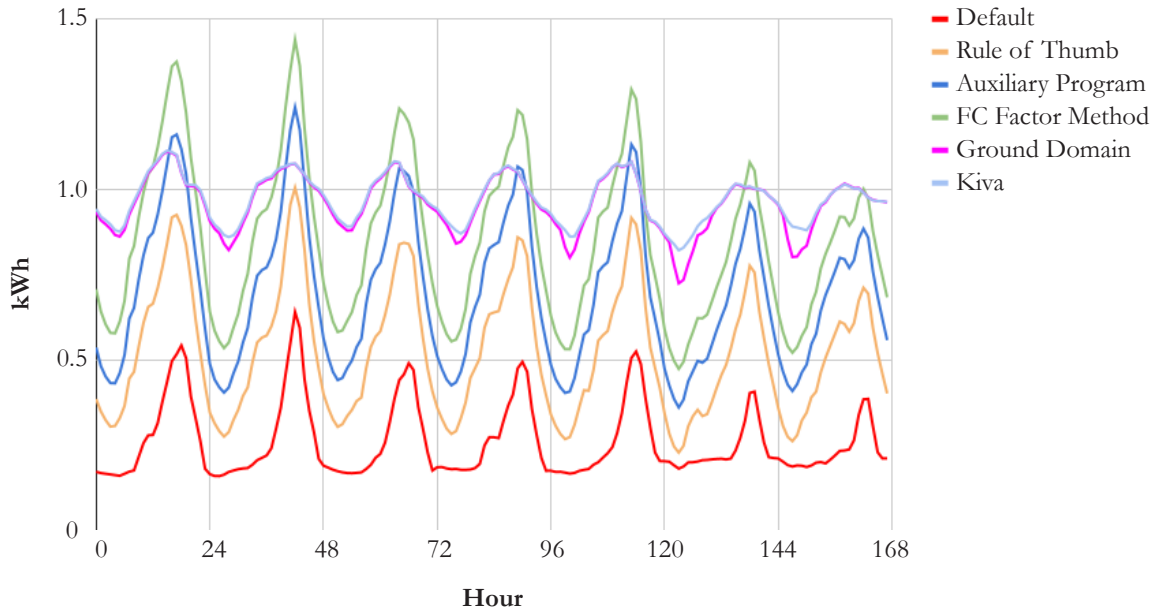### R0 Insulation Cooling Energy, Phoenix

Figure 62. Cooling energy from single story home in Phoenix with R0 insulation beneath the slab

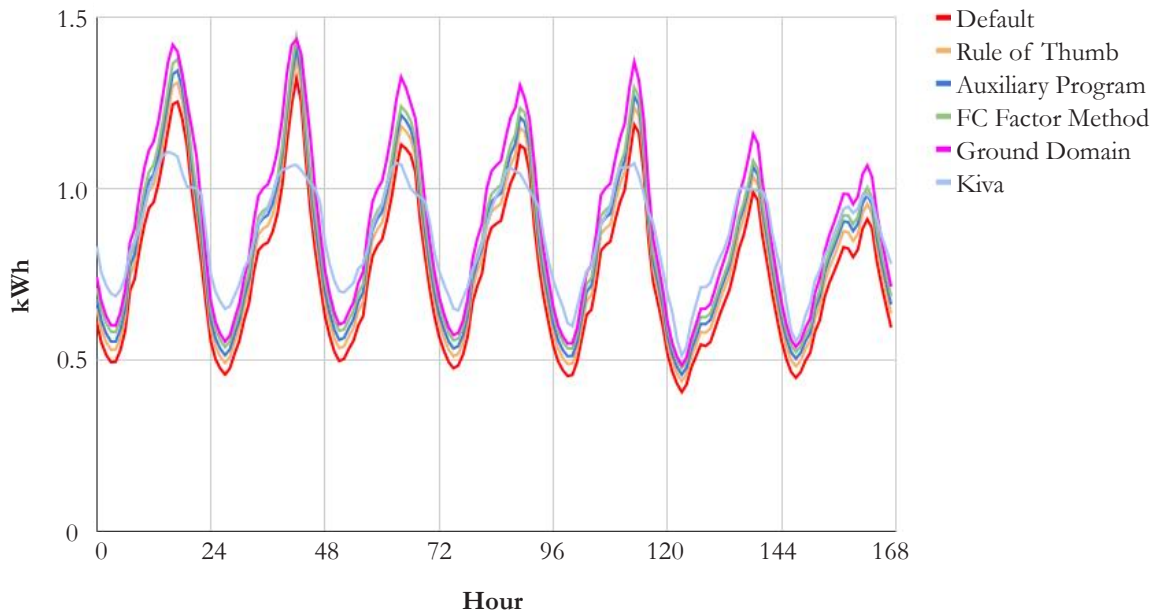### R10 Insulation Cooling Energy, Phoenix

Figure 63. Cooling energy from single story home in Phoenix with R10 insulation beneath the slab

R0 Insulation Heat/Cool EUI, Phoenix

Figure 64. Annual heat and cool EUI from modeling methods for a single-story Phoenix home with R0 insulation beneath the slab

R10 Insulation Heat/Cool EUI, Phoenix

Figure 65. Annual heat and cool EUI from modeling methods for a single-story Phoenix home with R10 insulation beneath the slab

R0 Insulation Cooling Energy, Phoenix

Figure 66. Cooling energy from single story home in Austin with R0 insulation beneath the slab

R10 Insulation Cooling Energy, Phoenix
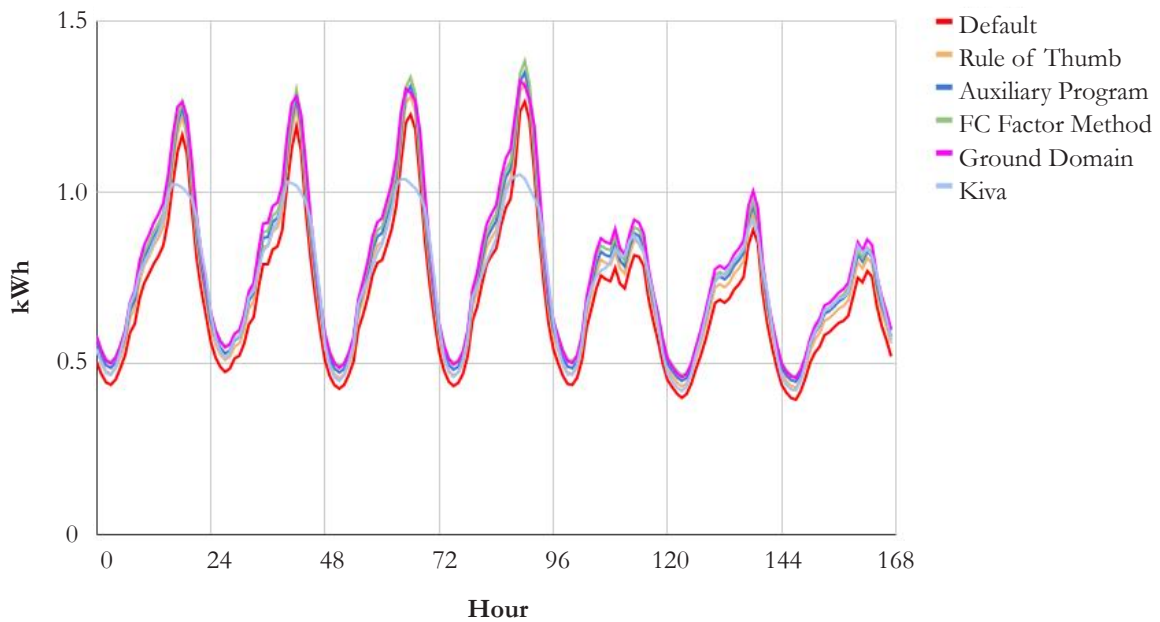
Figure 67. Cooling energy from single story home in Austin with R10 insulation beneath the slab

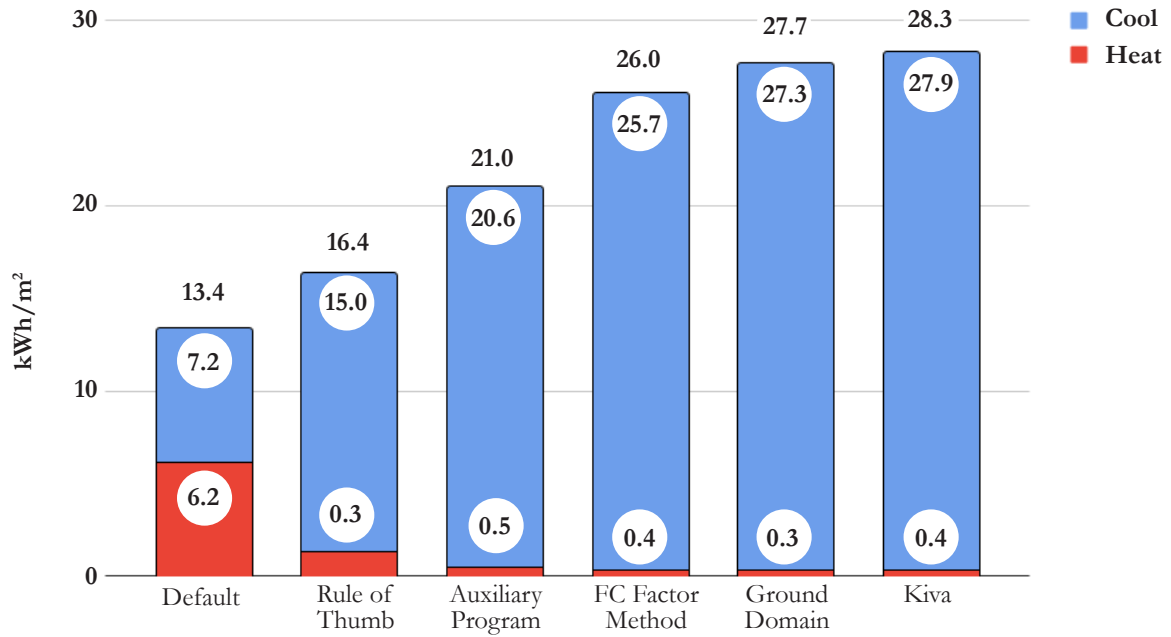**R0 Insulation Heat/Cool EUI, Phoenix**
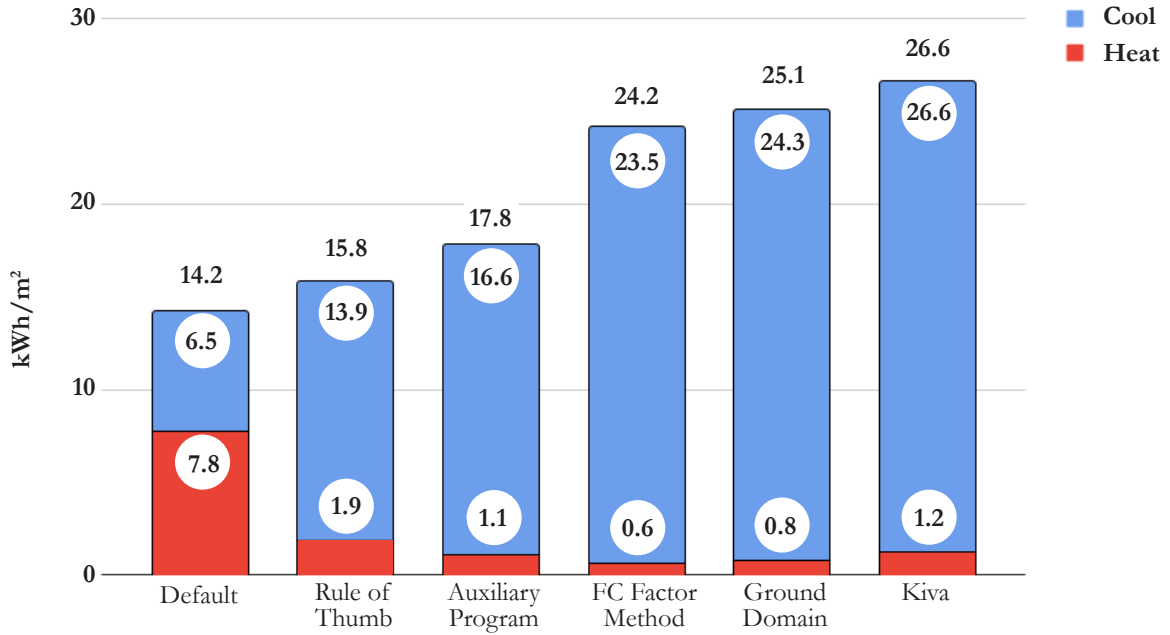
Figure 68. Annual heat and cool EUI from modeling methods for a single-story Austin home with R0 insulation beneath the slab
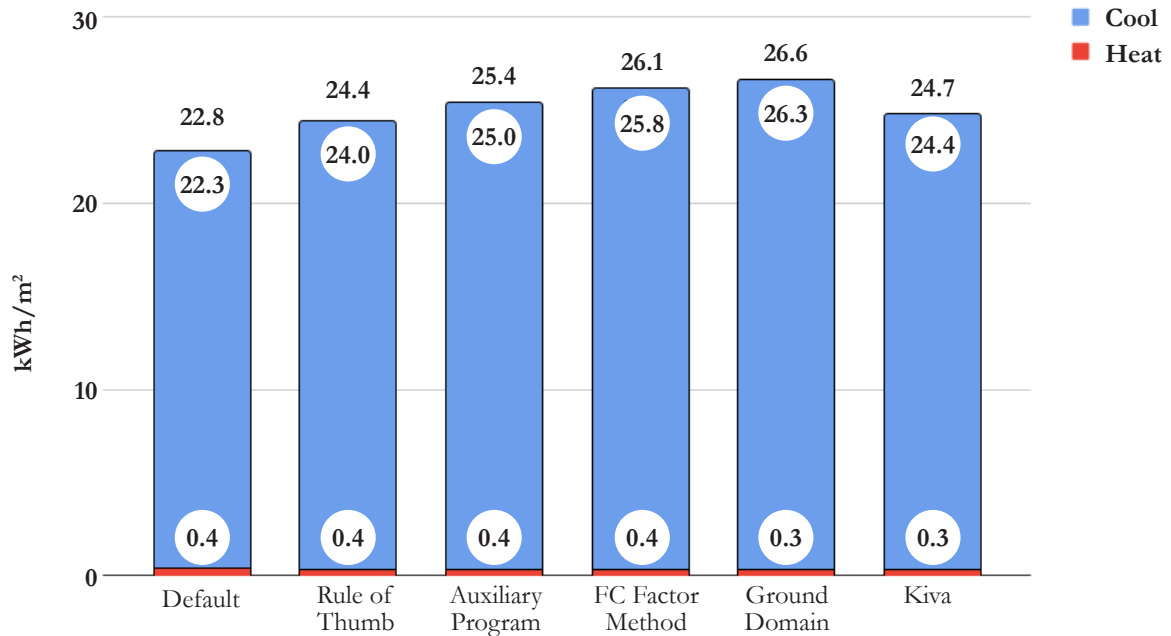
R10 Insulation Heat/Cool EUI, Phoenix
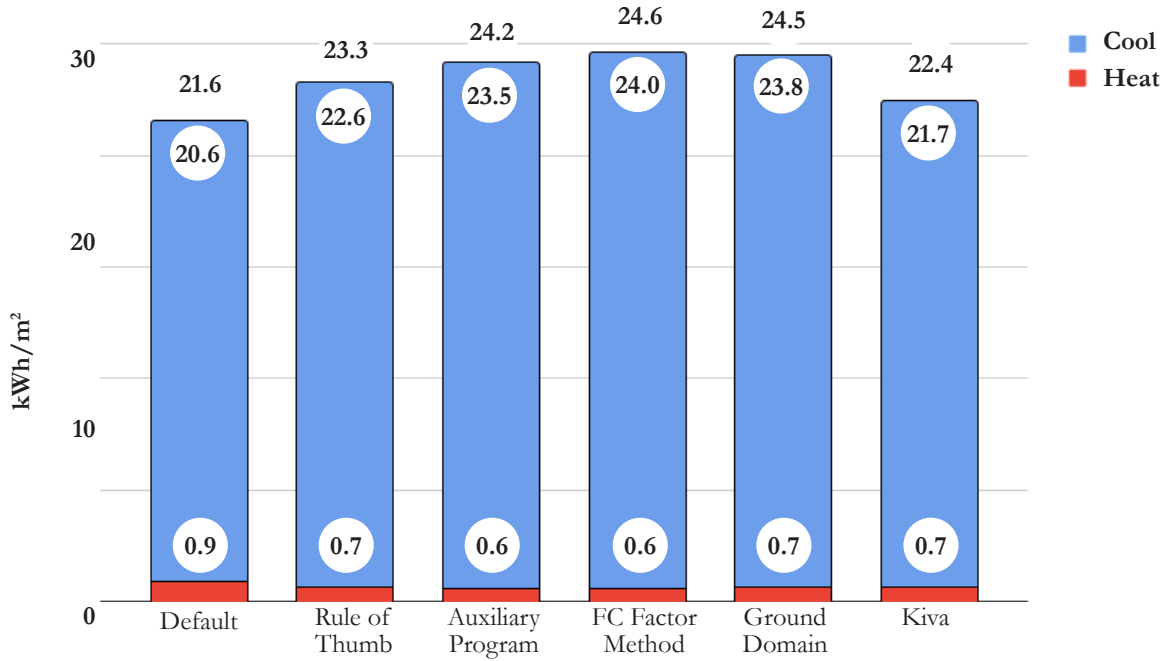
Figure 69. Annual heat and cool EUI from modeling methods for a single-story Austin home with R10 insulation beneath the slab

R0 Insulation Heat Index, Phoenix
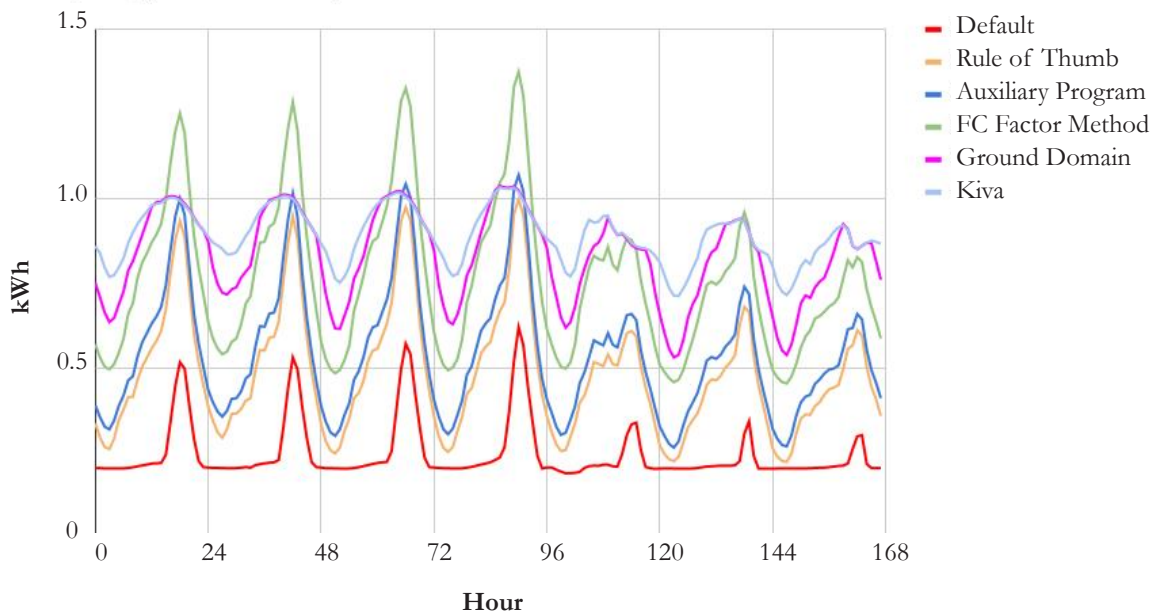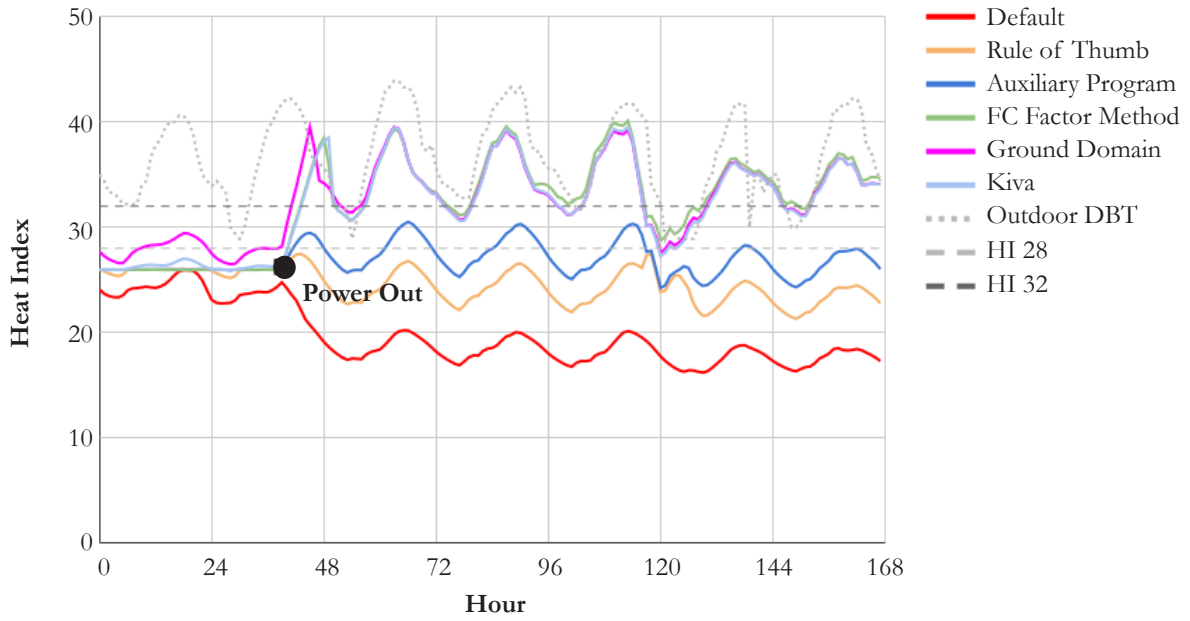

Figure 70. Heat index from single story home in Austin with R0 insulation beneath the slab

R10 Insulation Heat Index, Phoenix
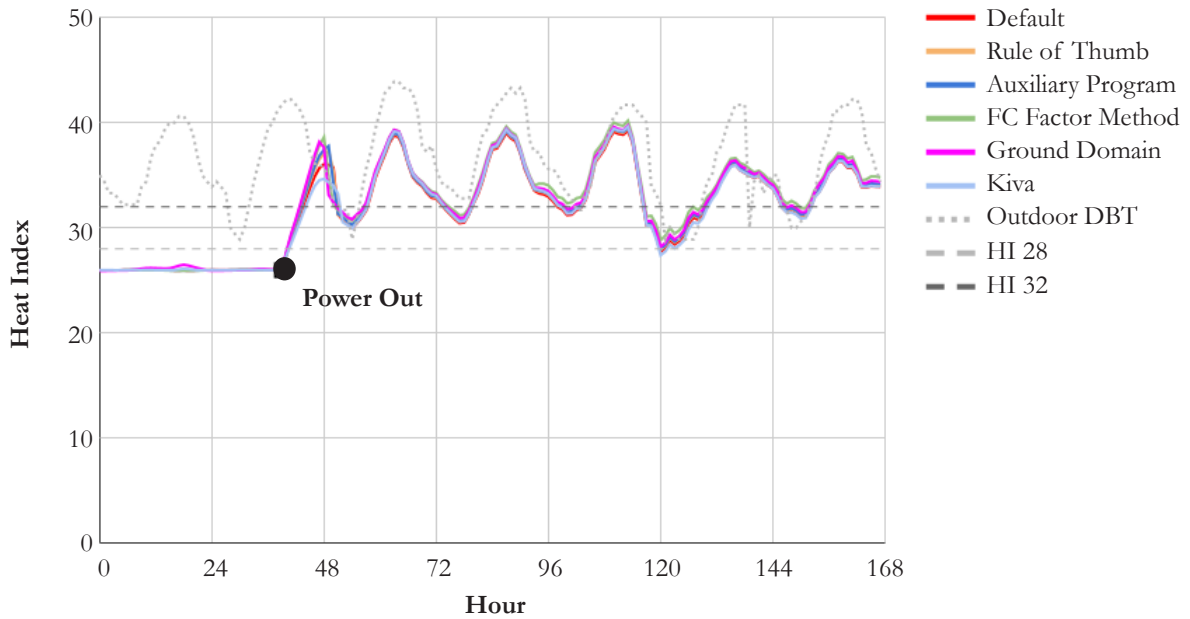
Figure 71. Heat index from single story home in Austin with R10 insulation beneath the slab

124

R0 Insulation Heat Index, Austin
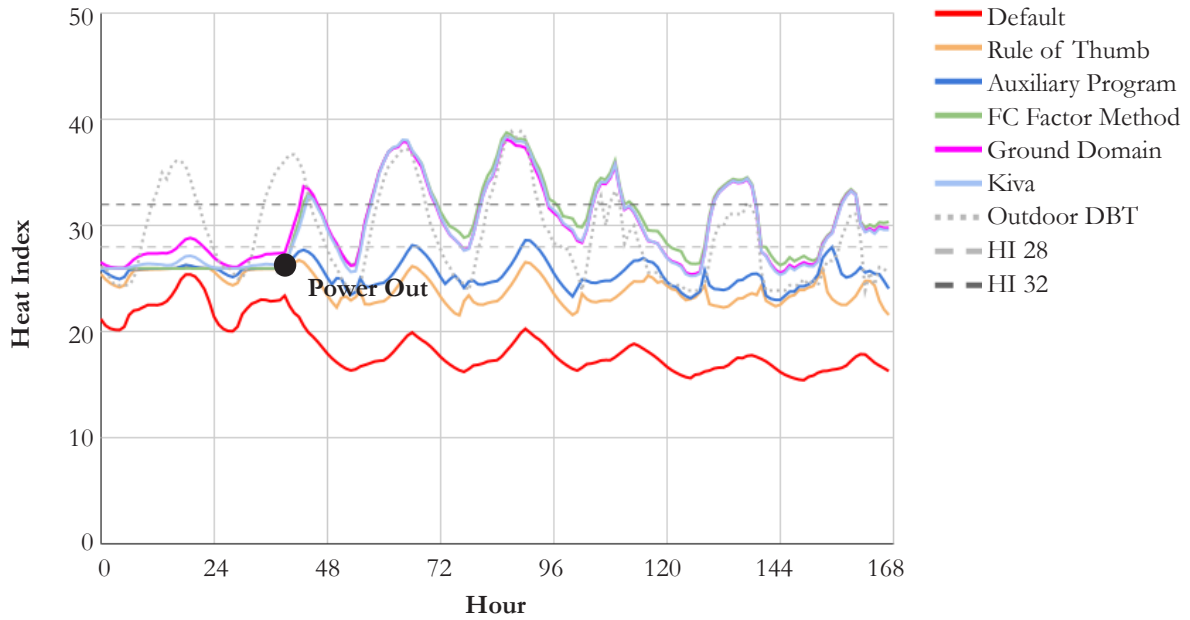
Figure 72. Heat index from single story home in Phoenix with R0 insulation beneath the slab

R10 Insulation Heat Index, Austin
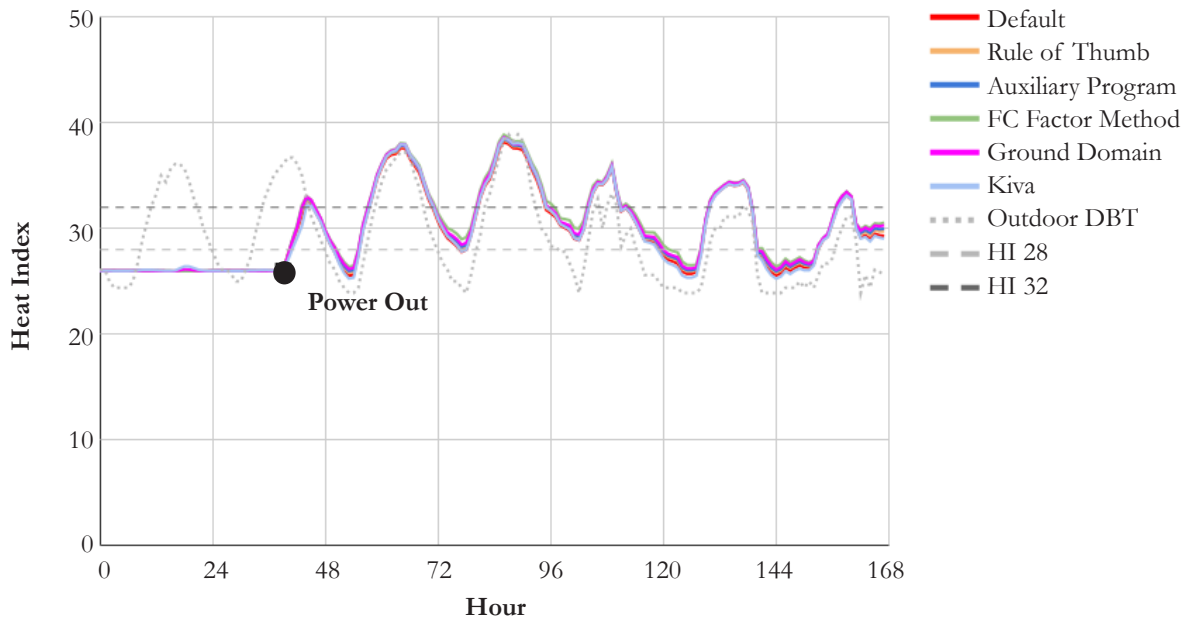
Figure 73. Heat index from single story home in Phoenix with R10 insulation beneath the slab

Basement Results

R0 Insulation Cooling Energy, Phoenix

Figure 74. Cooling energy from a home with a basement in Phoenix with R0 insulation beneath the slab or outside basement walls

R5 Insulation Cooling Energy, Phoenix

Figure 75. Cooling energy from a home with a basement in Phoenix with R5 insulation beneath the slab and outside basement walls

R10 Insulation Cooling Energy, Phoenix

Figure 76. Cooling energy from a home with a basement in Phoenix with R10 insulation beneath the slab and outside basement walls

R0 Slab Insulation/R10 Basement Wall Insulation Cooling Energy, Phoenix
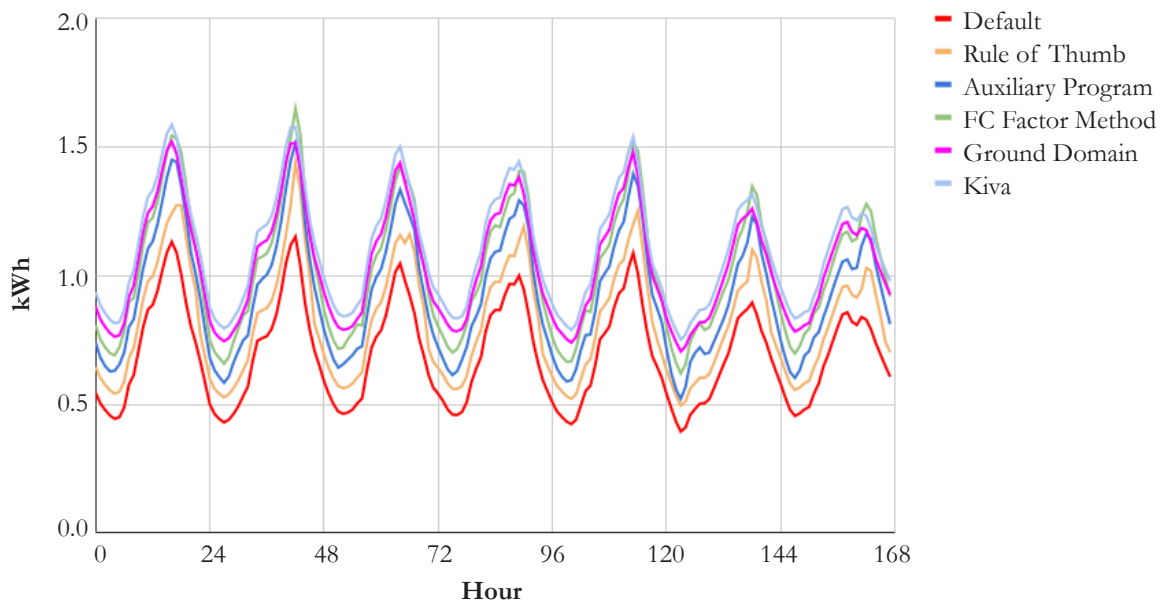
Figure 77. Cooling energy from a home with a basement in Phoenix with R10 basement wall insulation and R0 slab insulation

R0 Insulation Cooling Energy, Austin

Figure 78. Cooling energy from a home with a basement in Austin with R0 insulation beneath the slab and outside basement walls

R5 Insulation Cooling Energy, Austin

Figure 79. Cooling energy from a home with a basement in Austin with R10 insulation beneath the slab and outside basement walls

R10 Insulation Cooling Energy, Austin

Figure 80. Cooling energy from a home with a basement in Austin with R0 insulation beneath the slab or outside basement walls

R0 Slab Insulation/R10 Basement Wall Insulation Cooling Energy, Austin
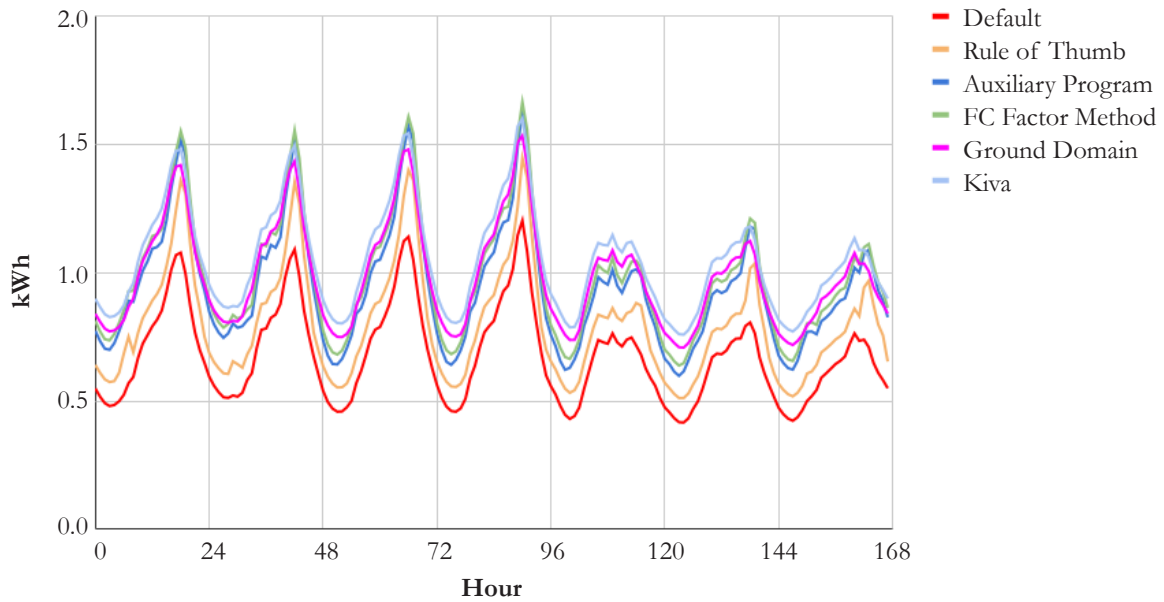
Figure 81. Cooling energy from a home with a basement in Austin with R10 basement wall insulation and R0 slab insulation

R0 Insulation Heat/Cool EUI, Phoenix
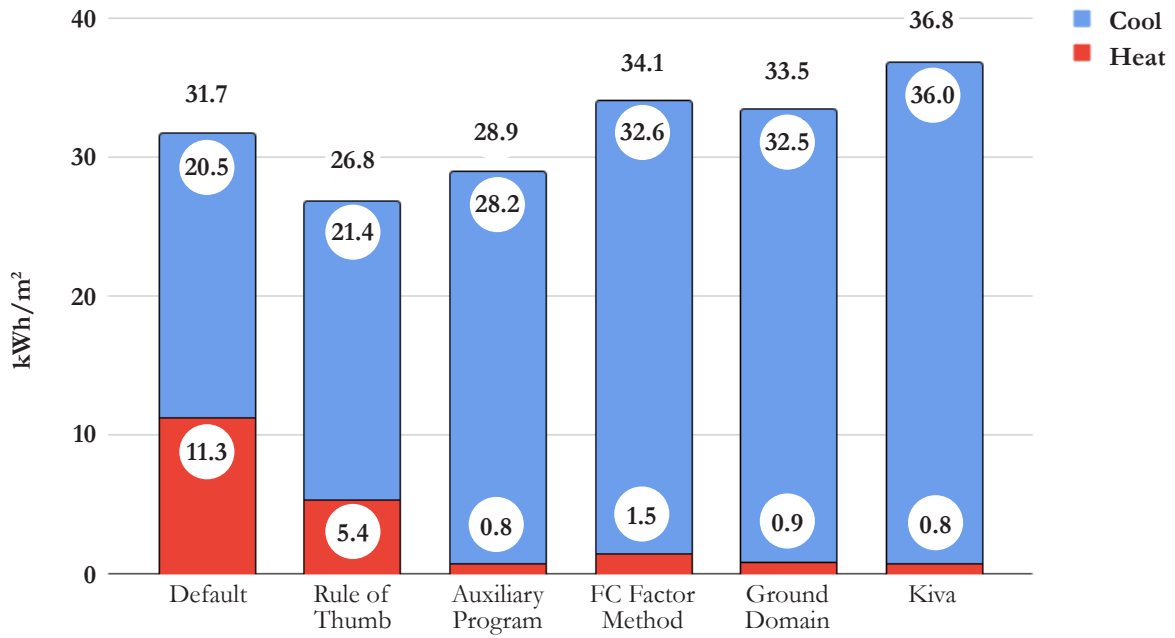
Figure 82. Annual heat and cool EUI from modeling methods for a home with a basement in Phoenix home with R0 insulation beneath the slab and outside the basement walls.

R0 Insulation Heat/Cool EUI, Phoenix
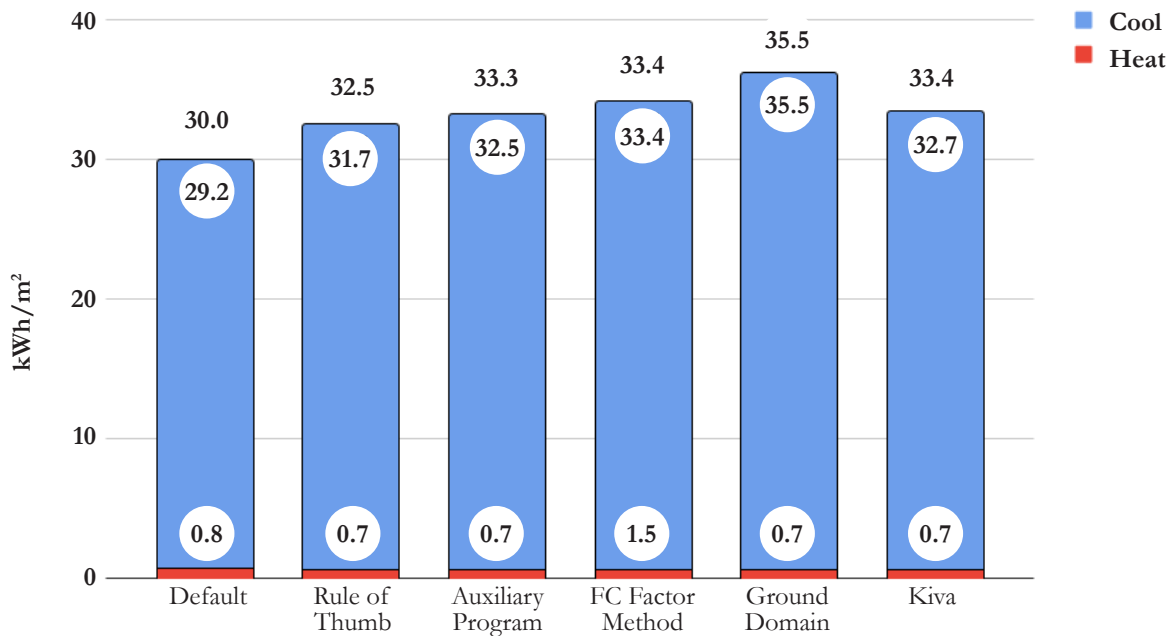
Figure 83. Annual heat and cool EUI from modeling methods for a home with a basement in Phoenix home with R10 insulation beneath the slab and outside the basement walls.
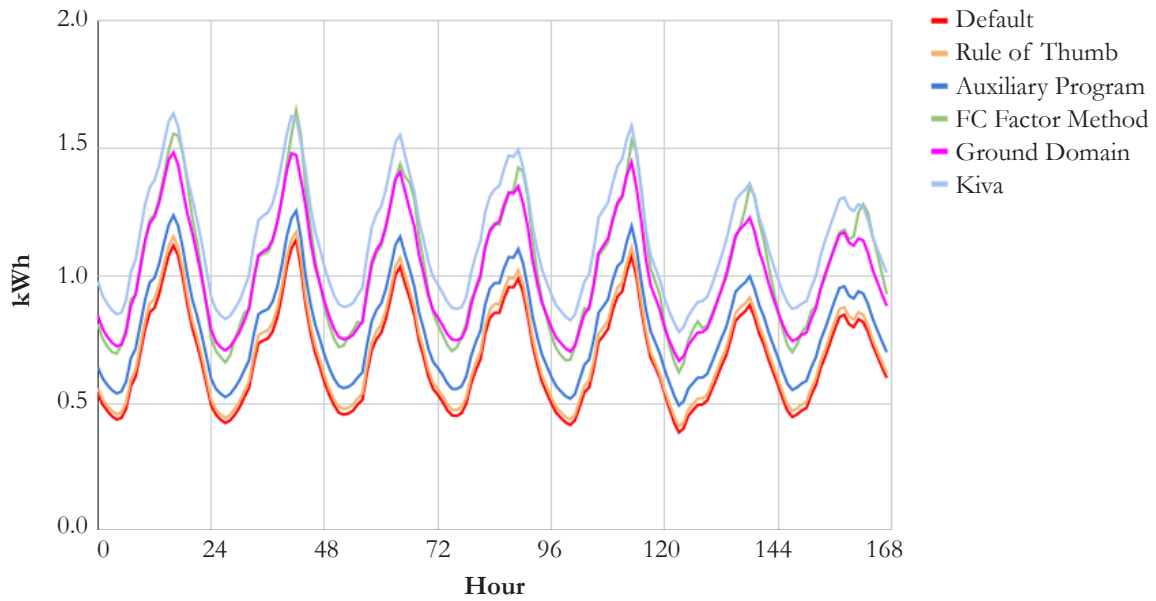
R0 Insulation Heat/Cool EUI, Austin
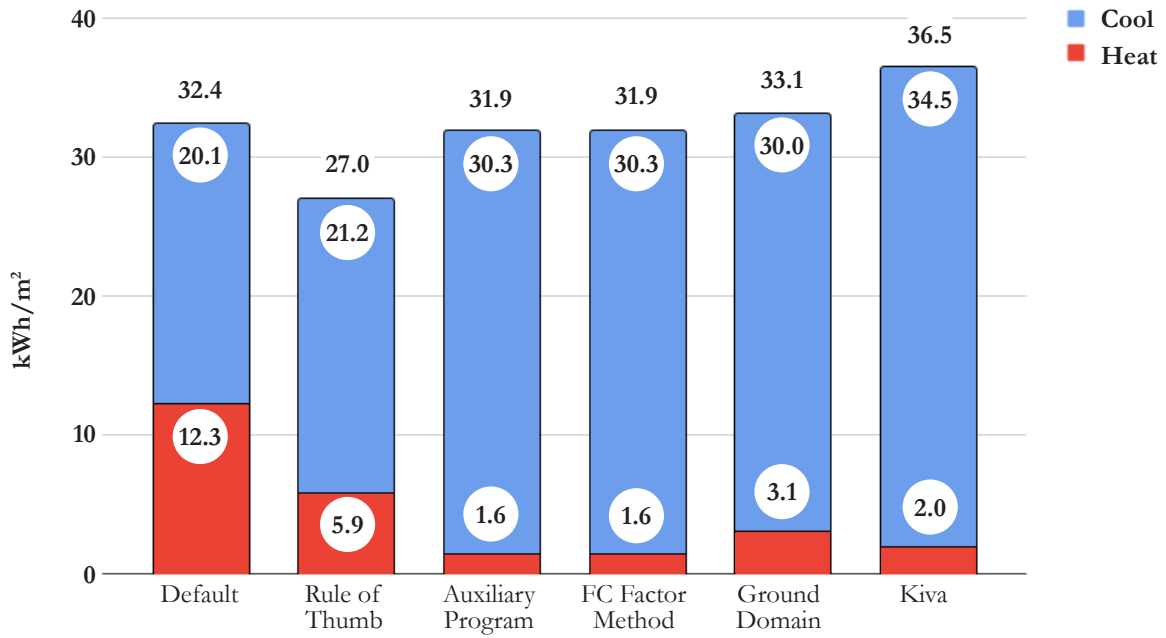
Figure 84. Cooling energy from a home with a basement in Phoenix with R0 insulation beneath the slab or outside basement walls

R0 Insulation Heat/Cool EUI, Austin
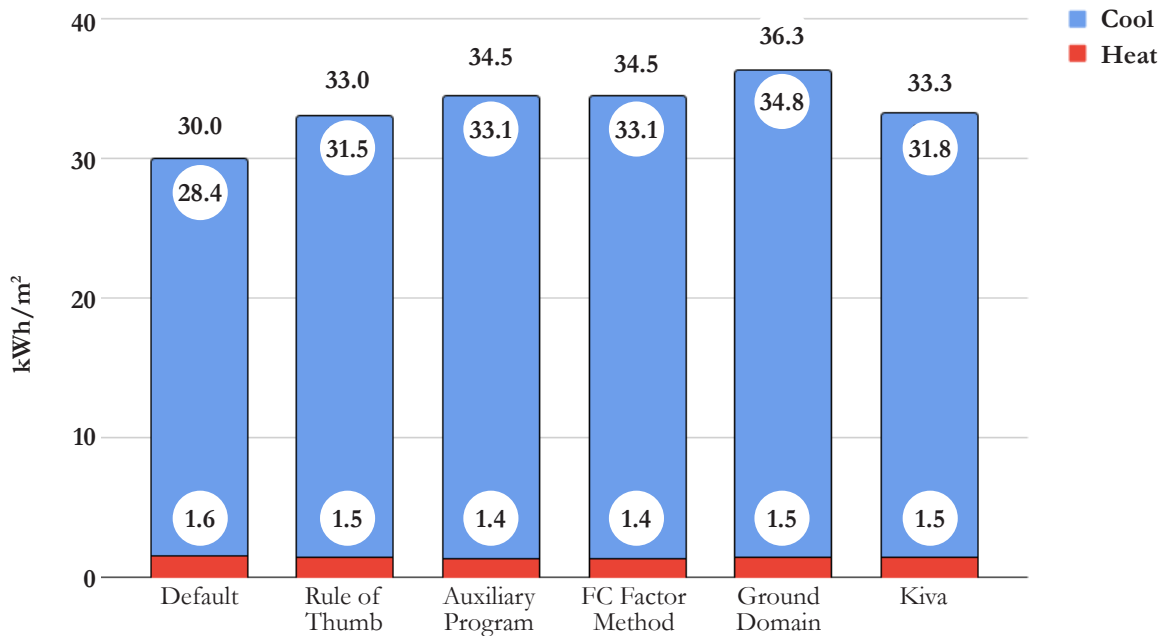
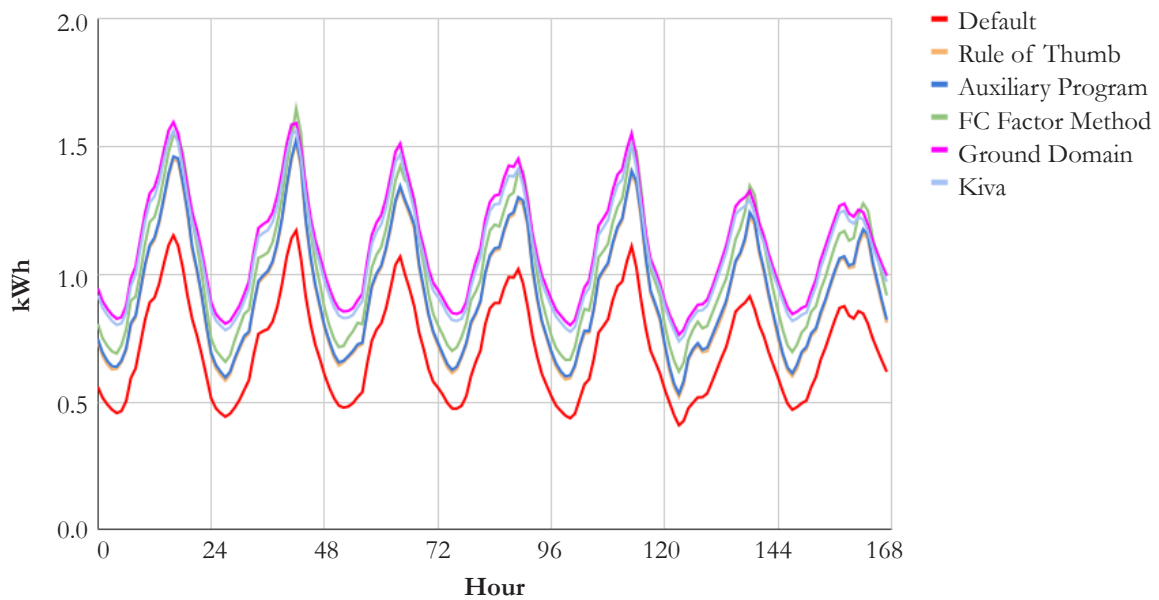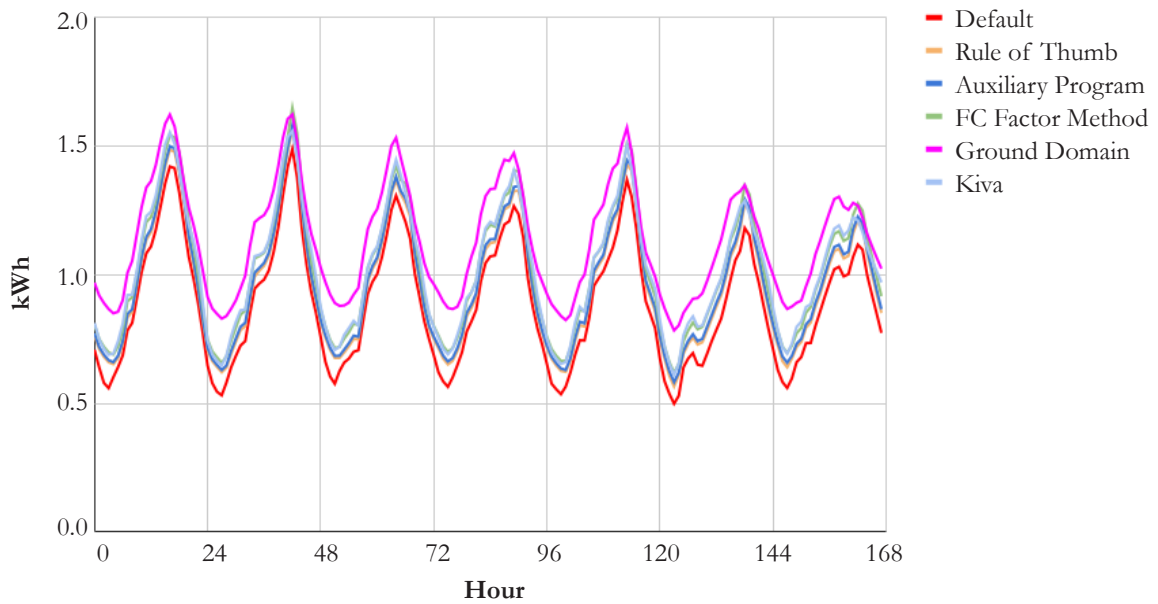*Figure 85. Cooling energy from a home with a basement in Phoenix with R10 insulation beneath the slab or outside basement walls*

R0 Insulation Heat Index, Phoenix
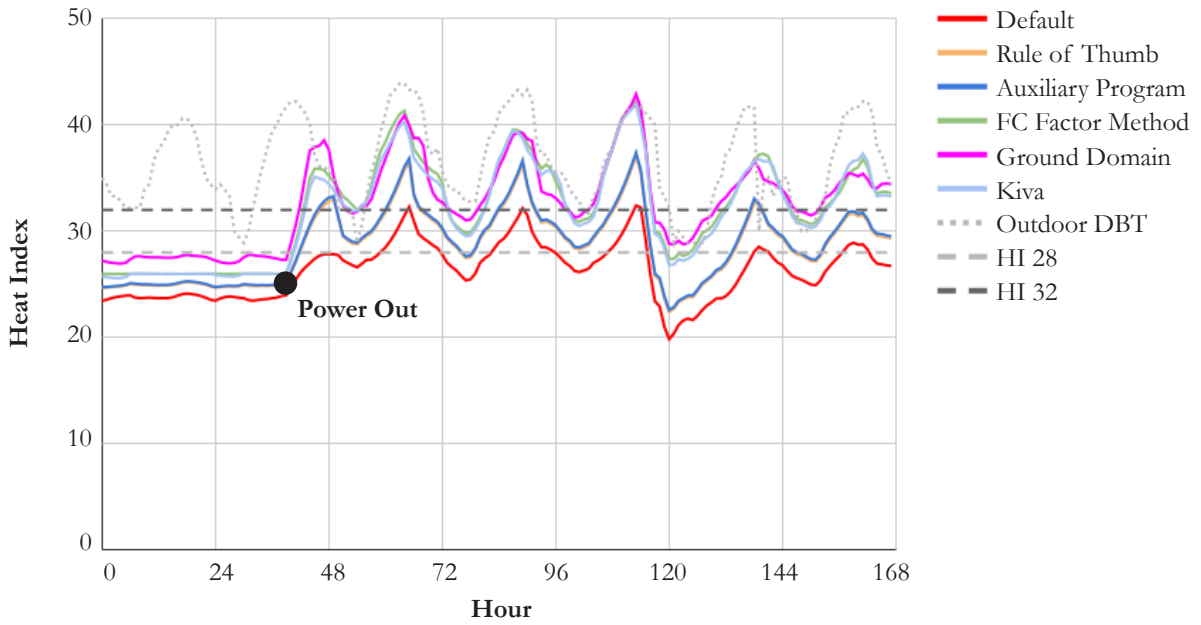
Figure 86. Heat index home with a basement in Phoenix with R0 insulation beneath the slab and outside basement walls

R10 Insulation Heat Index, Phoenix
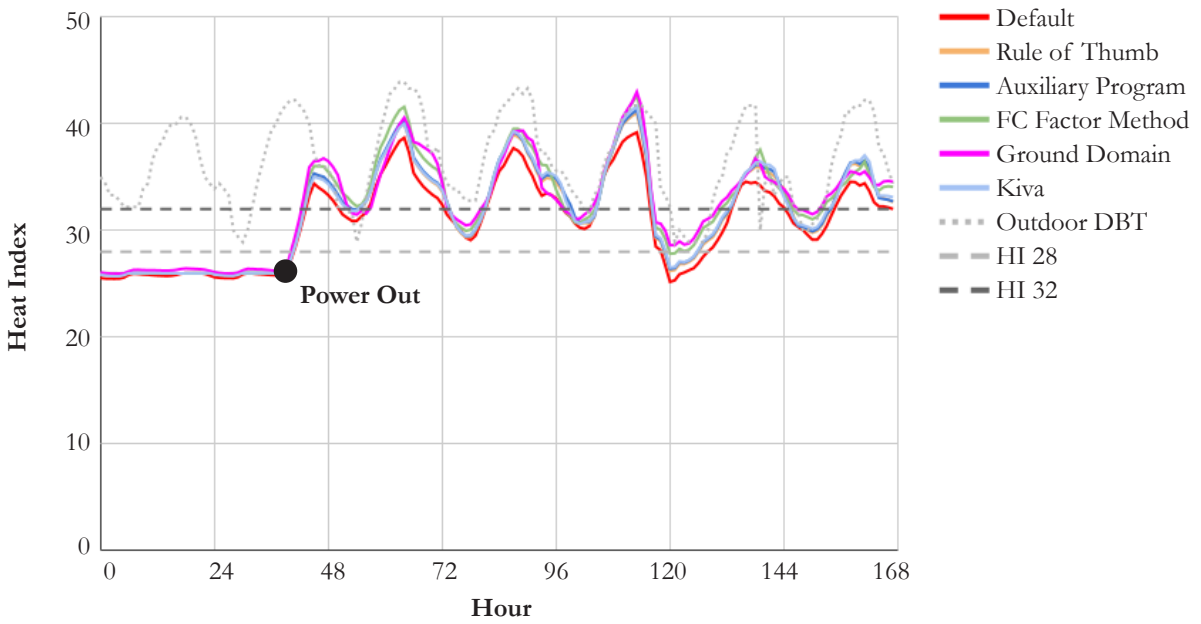
Figure 87. Heat index home with a basement in Phoenix with R10 insulation beneath the slab and outside basement walls

R0 Insulation Heat Index, Austin
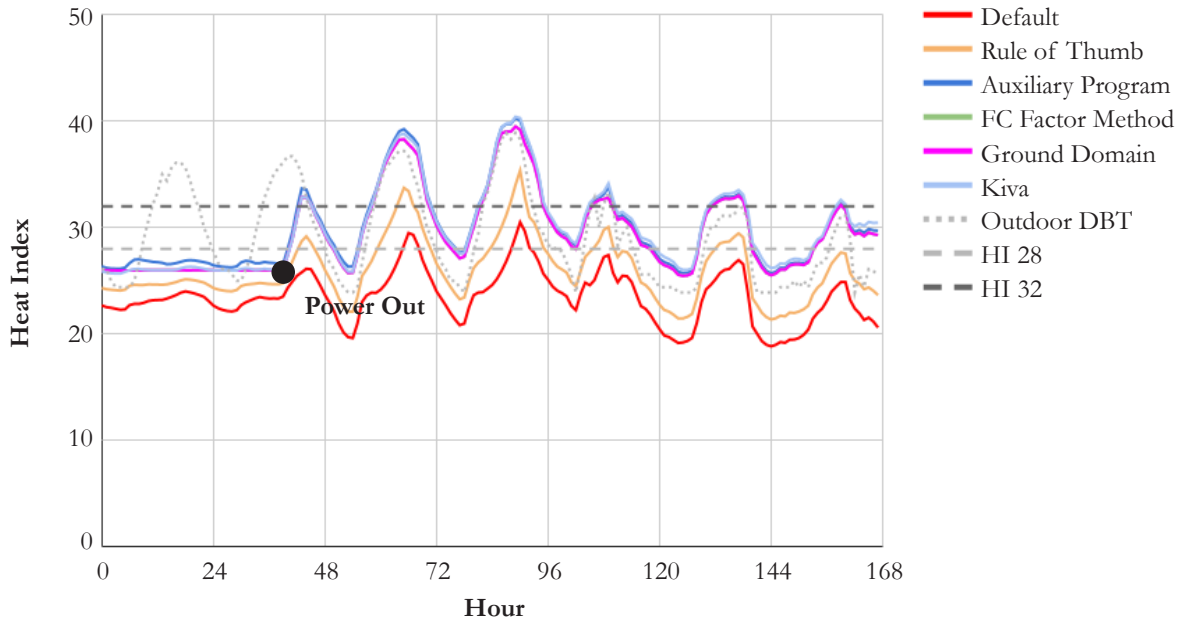
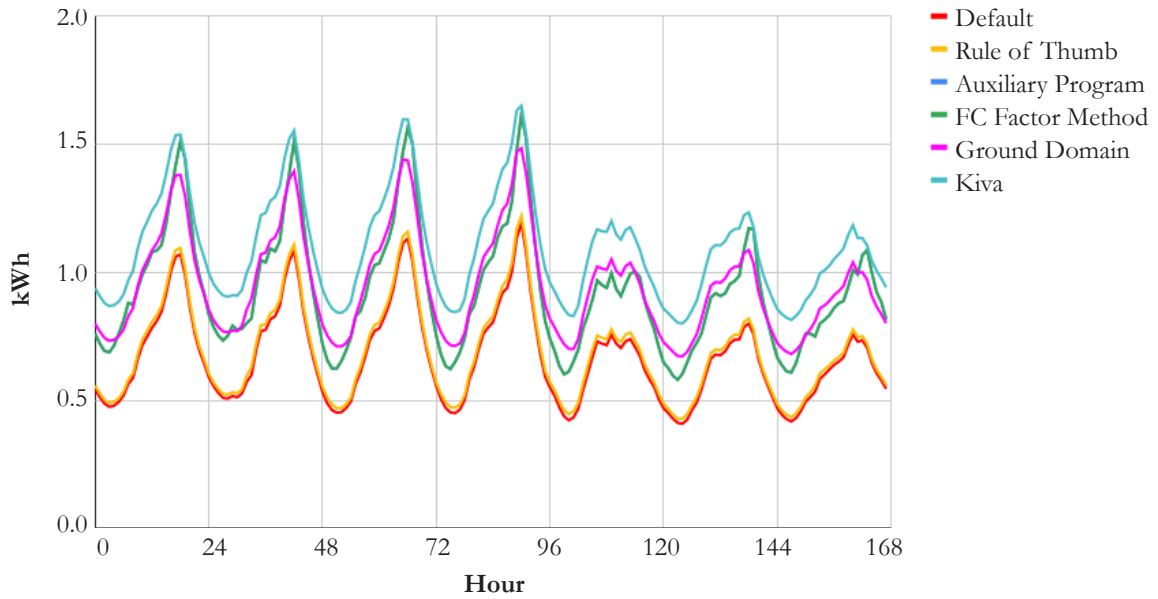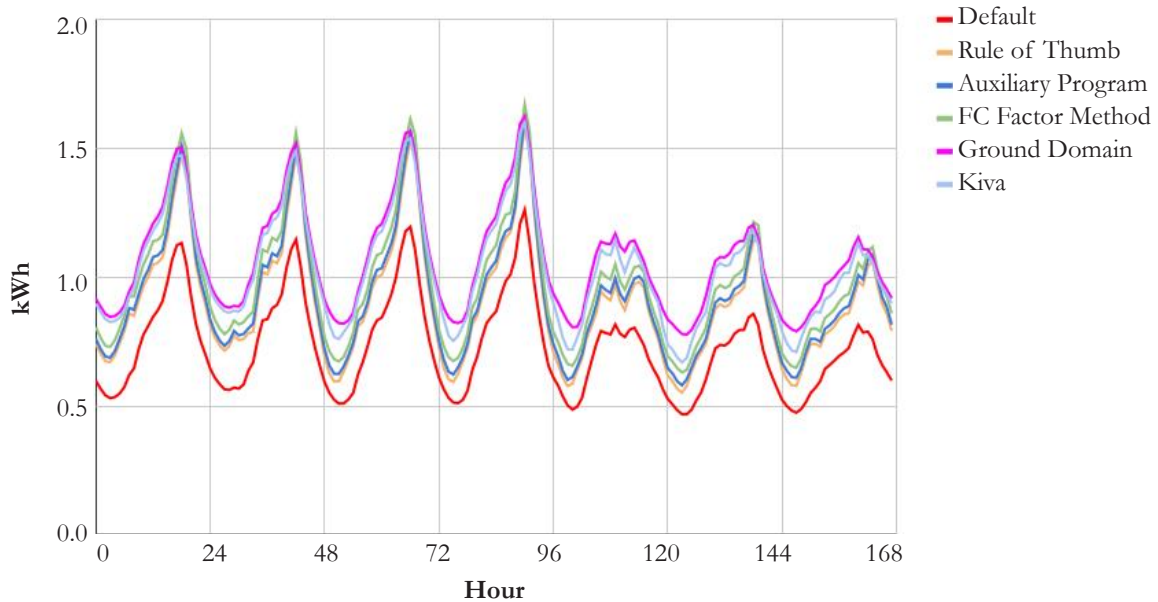*Figure 88. Heat index home with a basement in Austin with R0 insulation beneath the slab and outside basement walls*
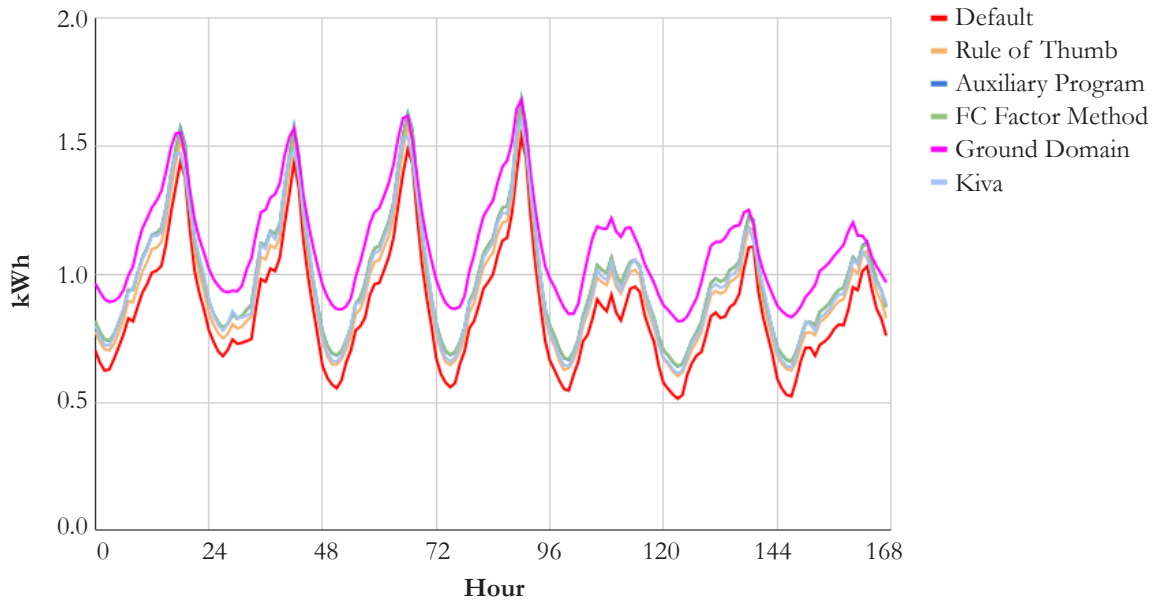
R10 Insulation Heat Index, Austin
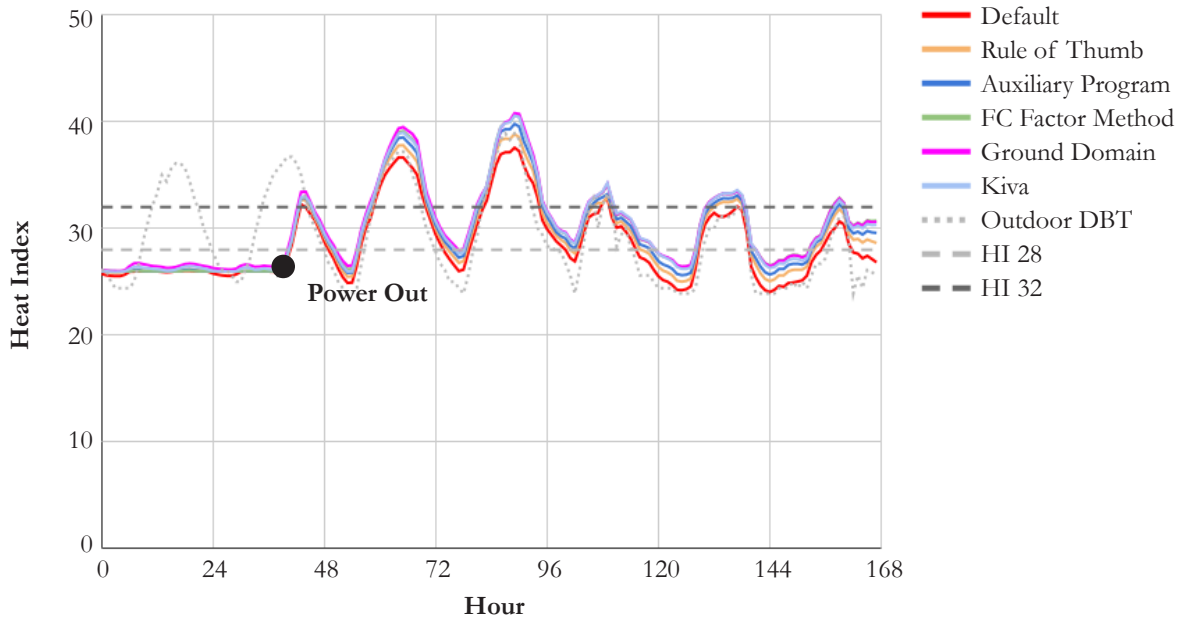
Figure 89. Heat index home with a basement in Austin with R10 insulation beneath the slab and outside basement walls

4.6.3. Discussion

After being bombarded with charts that all look mostly the same, a question of value arises. The outcomes of this exercise reveal the remarkable difference yielded from available ground modeling methods in building energy simulations that have interest in ground coupling. As was mentioned at the beginning of this section, no data are available to validate these results under extreme heat conditions which makes pointing to one of the methods and saying, "you're it!" a bit challenging. It is easy to say that the default and rule of thumb are not suitable for achieving nuanced results. The auxiliary program results are comparable with Ground Domain and FC factor method, despite being on the lower end of cooling energy demand. A potential issue with the auxiliary method that may bring pause is its results during grid-off scenarios. Figure 70 and Figure 72 show that zone heat indices do not increase over the course of the power outage without natural ventilation. While it is possible, and zone temperatures do rise and fall, it may not be the most suitable for evaluating passive survivability. Kiva and Ground Domain, despite some unexpected anomalies in the R0 slab models (Figure 62, Figure 66) where peaks and valleys appear truncated compared to other methods, deliver otherwise convincing grid-off results. It's important to note though, that during grid-off scenarios, overheating occurs almost immediately. The fact that Ground Domain, Kiva, and FC factor generally agree in both grid-on and grid-off scenarios leads to an emerging preference for either Kiva or Ground Domain methods as the preferred modeling method. FC factor method yields results largely in agreement with Kiva and Ground Domain, though the construction simplification, while suitable for certain applications, is less ideal in this context.

Section 4.7. Fit-To-Data Ground Temperature Calculation

While all of the methods in 4.6 have their own strong suits in terms of accuracy or ease of application, I have found myself left for want of **a simple approximation of ground temperatures beside an uninsulated basement**. As such, this section presents a study in the development of an equation (or simplified surrogate, if you like) which quickly provides an approximate set of monthly "Other Side Coefficients" constant temperatures to be implemented in EnergyPlus via "Site:GroundTemperature:BuildingSurface". The equation uses only the average interior set-point ($T_{zone\ avg}$) and the average soil surface temperature (T_{mean}) as defined by Derradji and Aiche (2014). The following steps were used to develop this equation:

1. Use THERM, an LBNL 2D heat transfer program, to model basement, walls, and ground field.[103]
2. Probe and average temperatures on wall-ground boundary condition (T_{wall}) from 5 places in the US.
3. Use a combination of weighted averages of T_{zone} and T_{mean} and correction terms to approximate outside temperatures found using THERM.
4. Validate against THERM data.
5. Validate against ground EnergyPlus modeling methods from sections 4.5 and 4.6.

This process involves some testing and back and forth comparison to arrive at an equation that provides an approximation. Its output is rough; however, it does give numbers in a similar range as higher accuracy methods without needing to run an auxiliary program or define a basement in more detail through Kiva or Ground Domain. Results are shown in 4.7.4 and 4.7.5.

4.7.1. THERM model

Sparing the details, THERM uses finite element analysis to numerically solve a heat balance equation which determines temperatures and heat fluxes through building materials from specified boundary conditions. The THERM model used here is unconventional (the program is usually used in wall section and fenestration modeling), but should, in theory, produce results that are suitable for this approximation. The model uses three boundary conditions: 1) a zone boundary condition set to 23 ℃ (T_{zone}), 2) a ground surface temperature boundary condition ($T_{surface}$), and 3) a shallow ground, 10m), boundary conditions ($T_{shallow}$). Geometry and boundary conditions are shown in Figure 90. Material characteristics are shown in Table 30 and boundary condition characteristics are shown in Table 31.

The equation used to calculate temperatures at different ground depths for each of the boundary conditions is shown in Equation 17:[104]

$$T(z,t) = T_m - A_s \cdot exp\left[-z\left(\frac{\pi}{365\alpha_s}\right)^{1/2}\right] cos\left\{\frac{2\pi}{365}\left[t - t_0 - \frac{z}{2}\left(\frac{365}{\pi\alpha_s}\right)^{1/2}\right]\right\} \qquad (17)$$

Where z is depth, t is the day of the year, T_m is the average ground surface temperature, A_s is the amplitude of soil surface temperature variation, and t_0 is the phase constant of soil surface.

---

[103] Robin Mitchell, "THERM 7 / WINDOW 7 NFRC Simulation Manual" (National Fenestration Rating Council, July 2017).

[104] Mohamed Derradji and Messaoud Aiche, "Modeling the Soil Surface Temperature for Natural Cooling of Buildings in Hot Climates," *Procedia Computer Science*, The 5th International Conference on Ambient Systems, Networks and Technologies (ANT-2014), the 4th International Conference on Sustainable Energy Information Technology (SEIT-2014), 32 (January 1, 2014): 615–21, https://doi.org/10.1016/j.procs.2014.05.468.
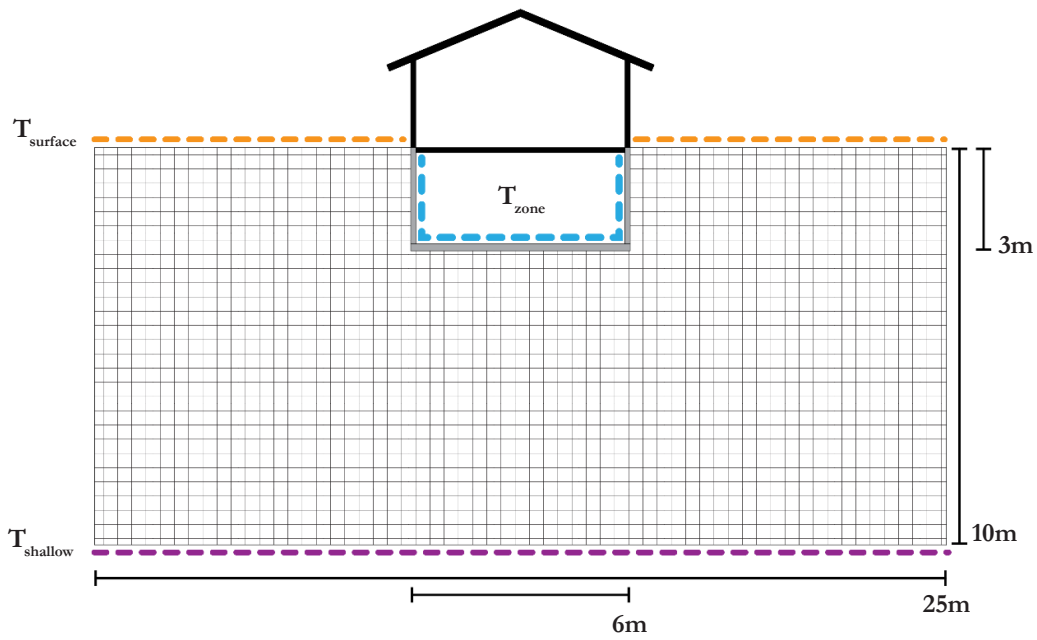
Figure 90. THERM model geometry and boundary conditions.

Table 30. THERM material characteristics

	Conductivity (W/mK)	Emissivity	Absorptivity
Concrete Walls and Slab	1.5	.9	.5
Ground	.75	.9	.7

Table 31. THERM boundary condition characteristics

	Temperature (°C)	Film Coefficient (W/m²K)
Zone (T_{zone})	23	10
Ground Surface ($T_{surface}$)	$T(0,t)$	20
Shallow Ground ($T_{shallow}$)	$T(10,t)$	0

4.7.2. Probing Outside Wall Condition

In order to gather a range of outside temperatures, five total locations were simulated. The four usual suspects: Phoenix, Austin, Miami, DC, as well as a fifth in Chicago. Figure 91 shows a diagram of probed locations and Figure 92 -Figure 96 show the temperature gradients of thermal exchanges between T_{zone} , $T_{surface}$, and $T_{shallow}$ over the course of the year. Values from T_{probe} are simply averaged and are labeled as T_{THERM} in Figure 97- Figure 101.
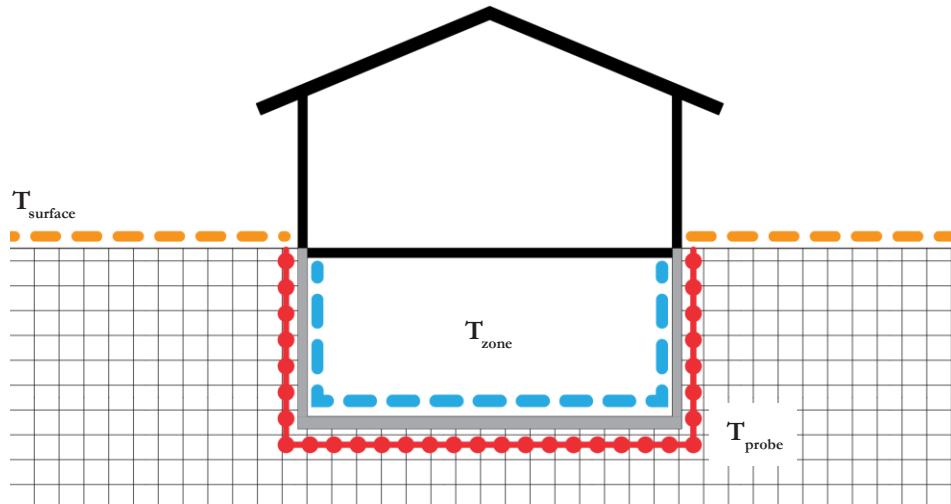
Figure 91. Diagram of probed temperature points outside of the basement walls.
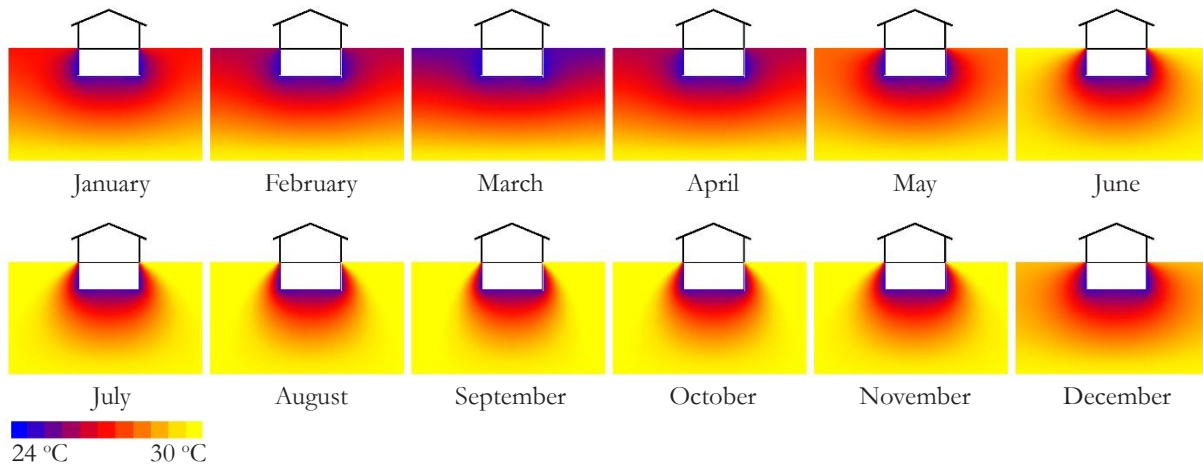
Figure 92. Ground temperature gradients in Phoenix for each month of the year.
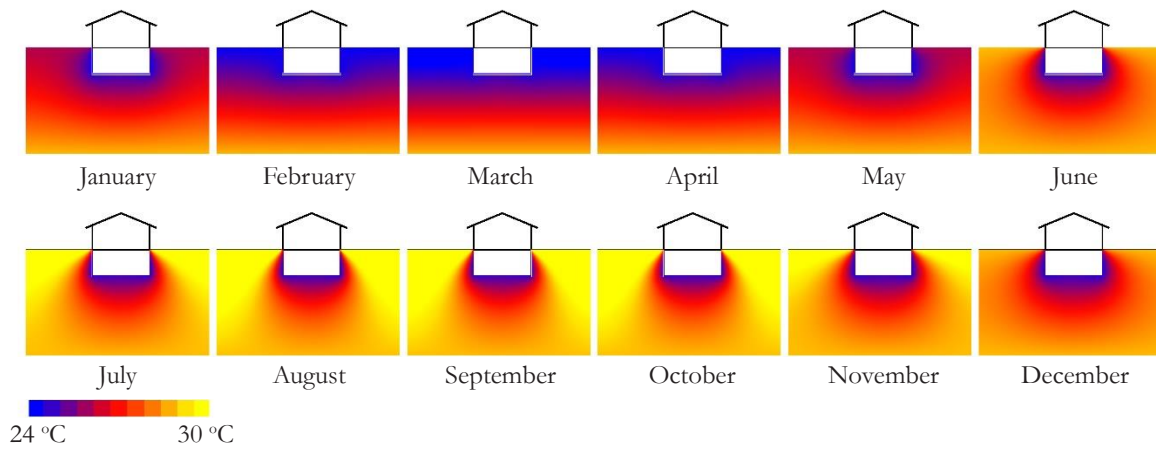
Figure 93. Ground temperature gradients in Miami for each month of the year.
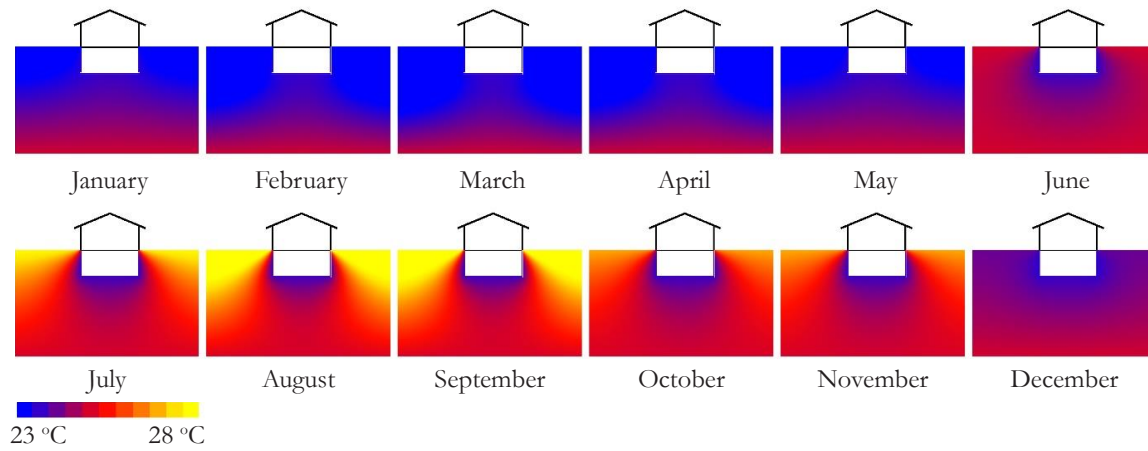
Figure 94. Ground temperature gradients in Austin for each month of the year.

January   February   March   April   May   June

July   August   September   October   November   December

17 ºC   22 ºC
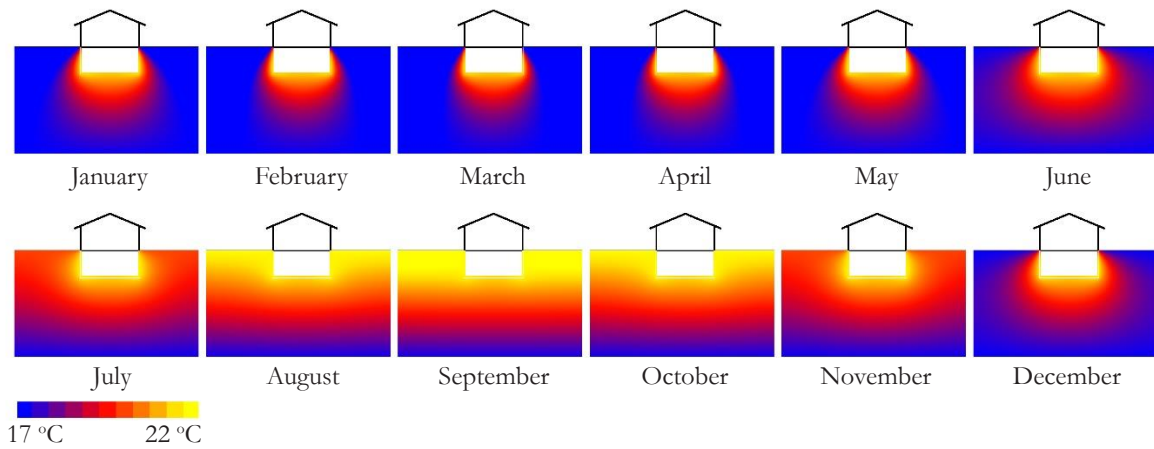
Figure 95. Ground temperature gradients in DC for each month of the year.

January   February   March   April   May   June

July   August   September   October   November   December

12 ºC   22 ºC
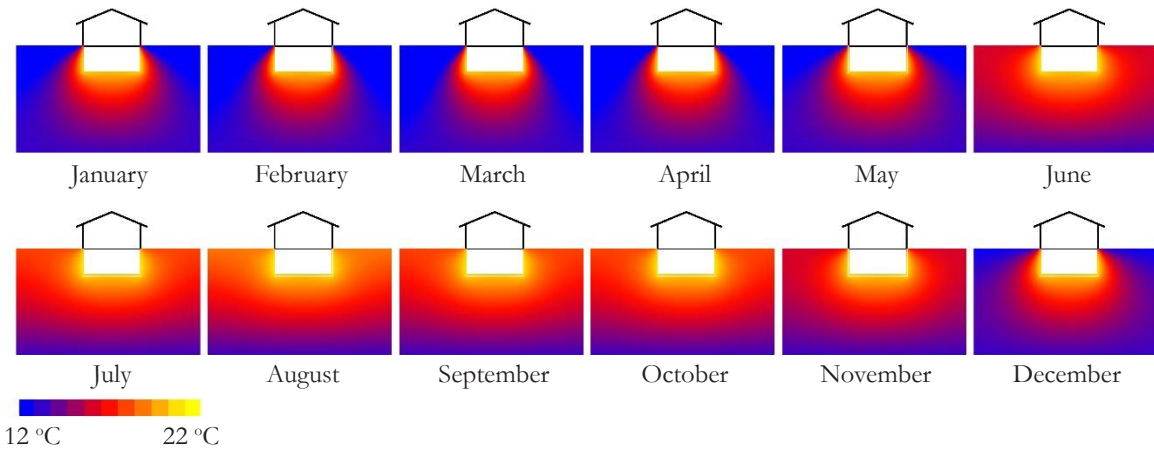
Figure 96. Ground temperature gradients in Chicago for each month of the year.

4.7.3. Equation Formulation

Below, $T_{zone\ avg}$ is the notation for the zone's average annual temperature (°C) and T_{mean} is the notation for average soil surface temperature (°C). In this case, $T_{zone\ avg}$ is assumed to be 23 °C. We begin with the average soil surface temperature (T_{mean}). Equations 18 shows the formulations necessary for this calculation:[105]

$$T_{mean} = \frac{1}{h_e}[h_r T_{ma} - \varepsilon \cdot \varDelta R + \beta \cdot S_m - 0.0168 \cdot h_s fb(1 - r_a)]$$

$$h_e = h_s(1 + 0.0168af) \tag{18}$$

$$h_r = h_s(1 + 0.0168a \cdot r_a \cdot f)$$

$$h_s = 5.7 + 3.8u$$

Where:

$a = 103\ Pa/°C$	Coefficient	
$b = 609\ Pa/°C$	Coefficient	
$f = .1$	Evaporation rate (faction)	
$r_a =$	Average annual relative humidity (%)	From EPW or STAT
$u=$	Average annual wind velocity (m/s)	From EPW or STAT
$T_{ma} =$	Average annual air temperature (°C)	From EPW or STAT
$\varepsilon = .92$	Ground surface	
$\varDelta R = 63$	Radiation constant (W/m²)	
$\beta = .92$	Solar absorption coefficient	
S_m	Average annual solar radiation (W/m²)	From EPW or STAT

We can now proceed with a weighted sum of T_{mean} and $T_{zone\ avg}$:

$$\bar{t} = \frac{T_{mean} + (3 * T_{zone\ avg})}{4} \tag{19}$$

Additionally, we include an amplitude term where i = month of the year (e.g. Jan = 1, Feb = 2, etc.):

$$T_{amp} = \frac{1}{4}\cos\left(\frac{3(i - 9)}{4\pi}\right) \tag{20}$$

Finally, a correction term:

$$c = \frac{|T_{mean} - T_{zoneavg}|}{8 * (T_{mean} - \bar{t})} \tag{21}$$

Where the final form is shown in Equation 22!

$$T_{outside} = \bar{t} + T_{amp} + c \tag{22}$$

---

[105] Barbara Larwa and Krzysztof Kupiec, "Heat Transfer in the Ground with a Horizontal Heat Exchanger Installed – Long-Term Thermal Effects," *Applied Thermal Engineering* 164 (January 5, 2020): 114539, https://doi.org/10.1016/j.applthermaleng.2019.114539.

4.7.4. Fit to THERM Output

Using only T_{mean} and $T_{zone\ avg}$, Equation 22 achieves an RMSE not greater than 0.25 °C for the five tested location's temperatures collected from THERM data. Results can be observed in Figure 97 -Figure 101. $T_{outside}$ is shown in black.

Phoenix Ground Outside Temperatures: THERM and Fitted
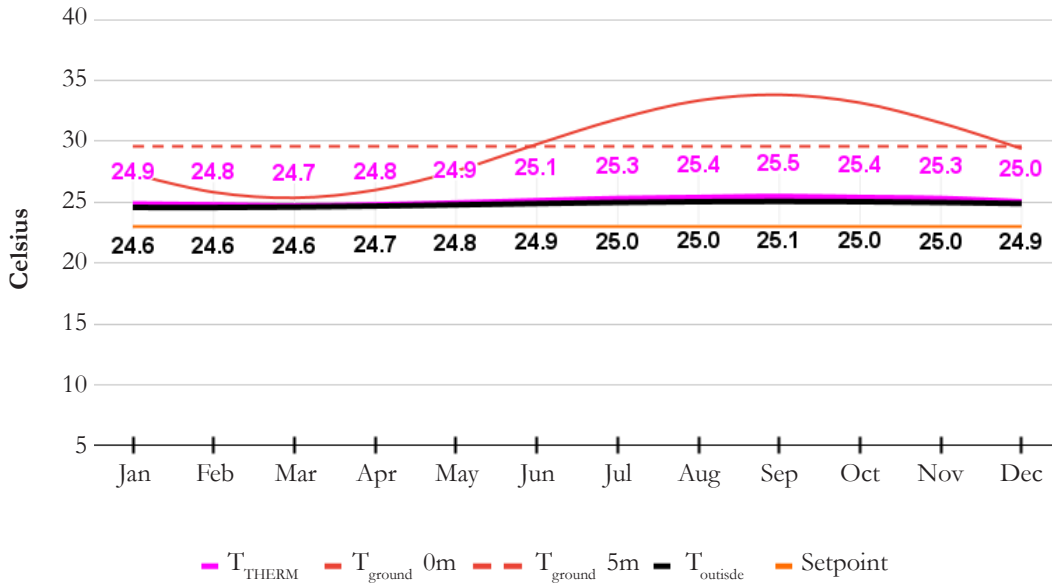
Figure 97. THERM and fitted outside ground temperatures for Phoenix. **RMSE from THERM data = 0.25 ($T_{m\ =}$ 29.59 °C)**

Austin Ground Outside Temperatures: THERM and Fitted
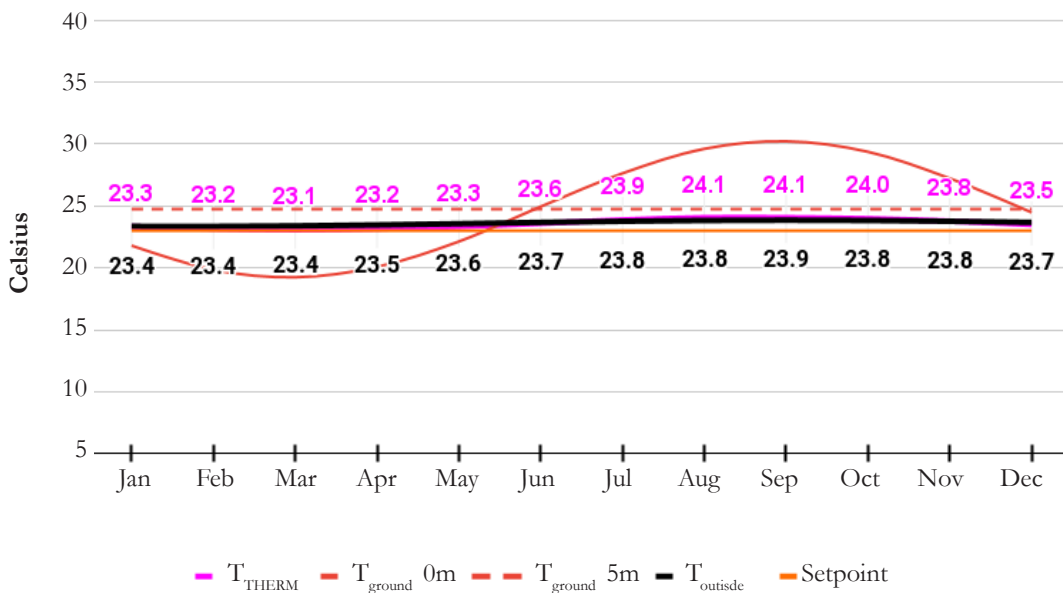
Figure 98. THERM and fitted outside ground temperatures for Austin. **RMSE from THERM data = 0.19 ($T_{m\ =}$ 24.74 °C)**

Miami Ground Outside Temperatures: THERM and Fitted
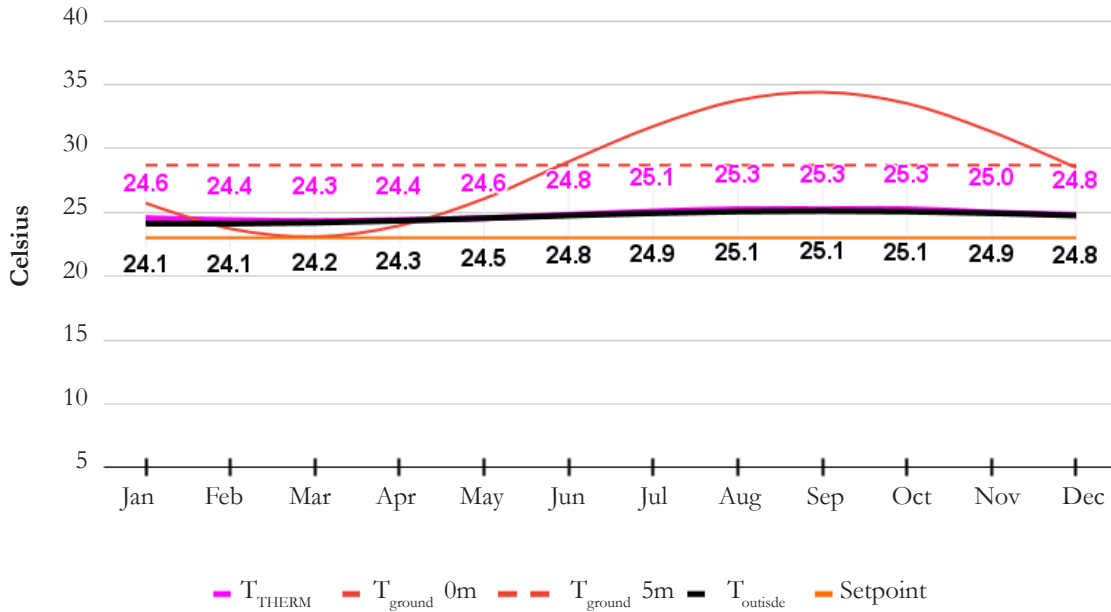
Figure 99. THERM and fitted outside ground temperatures for Miami. **RMSE from THERM data = 0.18 ($T_m = 29.59\,^oC$)**

DC Ground Outside Temperatures: THERM and Fitted
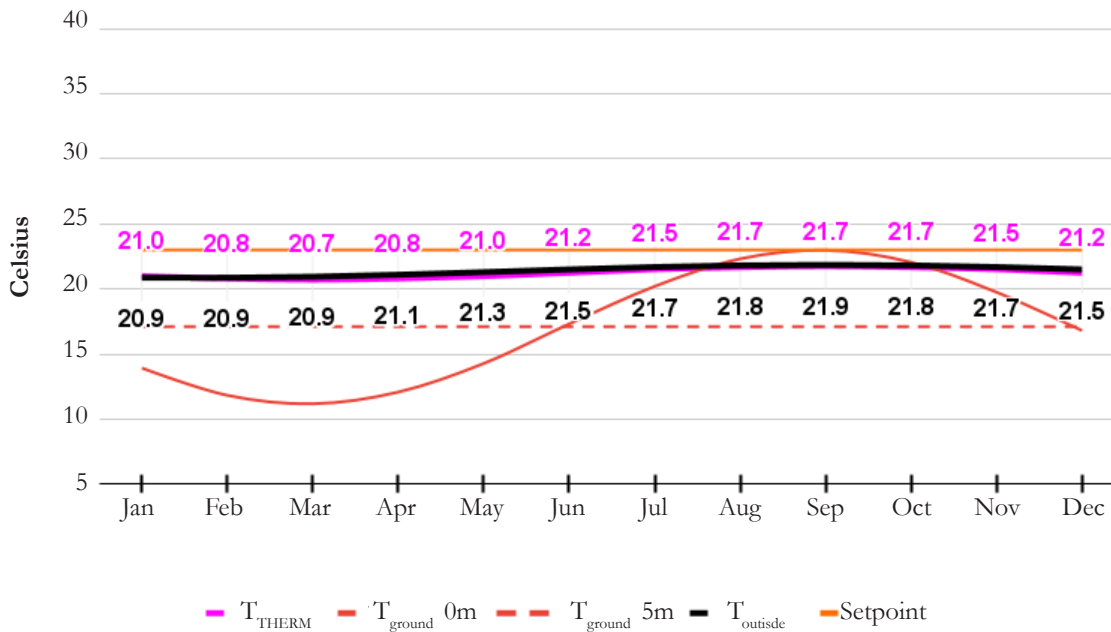
Figure 100. THERM and fitted outside ground temperatures for DC. **RMSE from THERM data = 0.20 ($T_m = 17.1\,^oC$)**

Phoenix Ground Outside Temperatures: THERM and Fitted
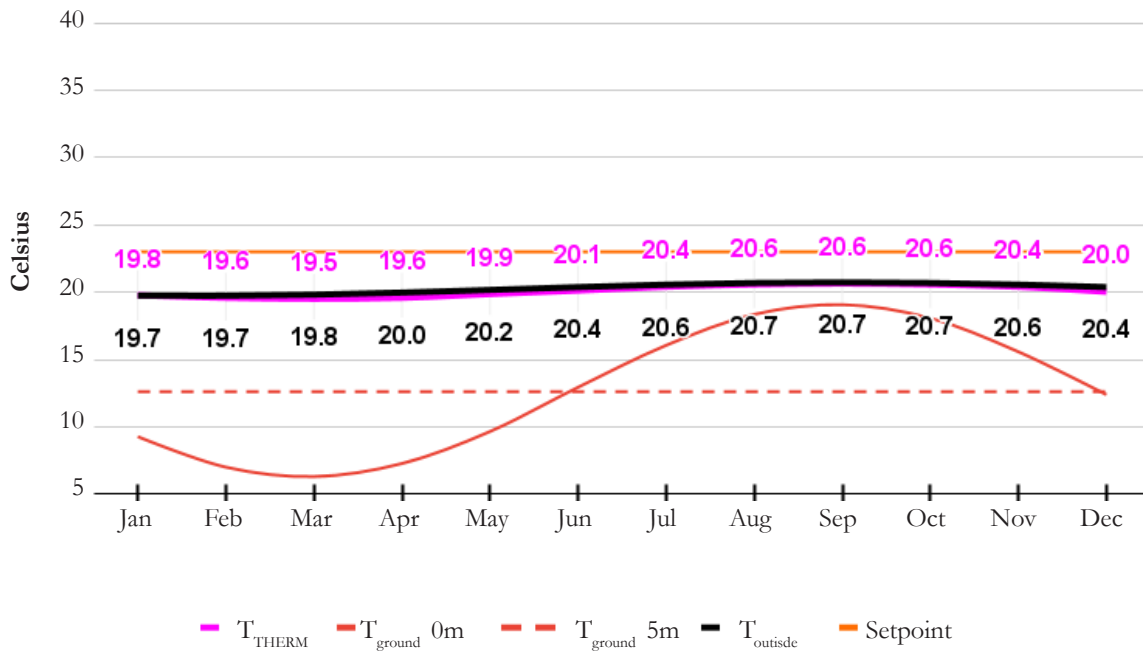
Figure 101. THERM and fitted outside ground temperatures for Phoenix. **RMSE from THERM data = 0.23 ($T_{m = }$ 12.6 ^{o}C)**

4.7.5. Validation Against EnergyPlus Energy and Heat Index Data

Ultimately, the objective of this exercise is to be able to use these twelve little numbers in a full building energy simulation. This subsection presents the use of such temperatures obtained through Equation 22 compared against results from other methods in a full building simulation. The assumed average annual setpoint in all cases is 23 °C.

Figure 102, Figure 103, Table 32 and Table 33, show results from Phoenix and Austin with their respective RMSEs. We assume that Kiva and Ground Domain methods are the preferred; a result of their hourly timestep and 2D finite difference methods. As such, Kiva and Ground Domain are the two methods that Equation 22 is compared against. In Phoenix, the Equation 22 method has an RMSE of 0.08 kWh from Kiva and the Ground Domain. In Austin, Kiva method has an RMSE of 0.14 kWh and an RMSE of 0.04 kWh for the Ground Domain method. The most closely related across the models is the Ground Domain RMSE.

R0 Basement Insulation Cooling Energy, Phoenix

Figure 102. Cooling energy results from $T_{outside}$ plotted against other simulation methods

Table 32. RMSE of three ground simulation methods, Phoenix (grid-on)

	Auxiliary Program	Ground Domain	Kiva
RMSE (kWh)	0.28	0.08	0.08

144

R10 Basement Insulation Cooling Energy, Austin
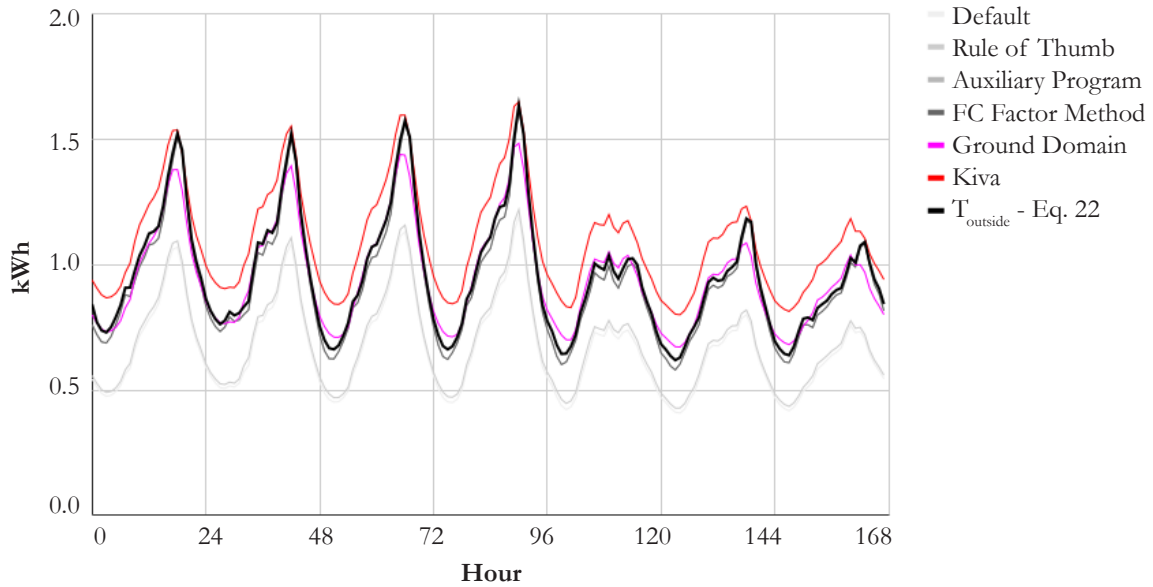
Figure 103. Cooling energy results from $T_{outside}$ plotted against other simulation methods

Table 33. RMSE of three ground simulation methods, Austin (grid-on)

	Auxiliary Program	Ground Domain	Kiva
RMSE (kWh)	.03	0.04	0.14

Using the same basement model, a weather file hot swap gives a sense of how other locations compare. The same week is used and all settings remain constant. Figure 104 shows the results from each week-long simulation with strong relationships to Kiva and Ground Domain cooling energy results.

R0 Basement Insulation Cooling Energy, Miami
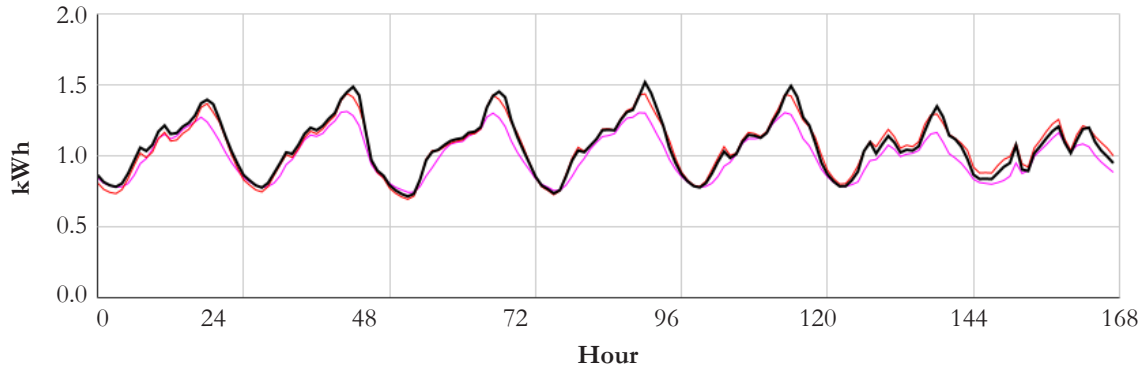
R0 Basement Insulation Cooling Energy, DC
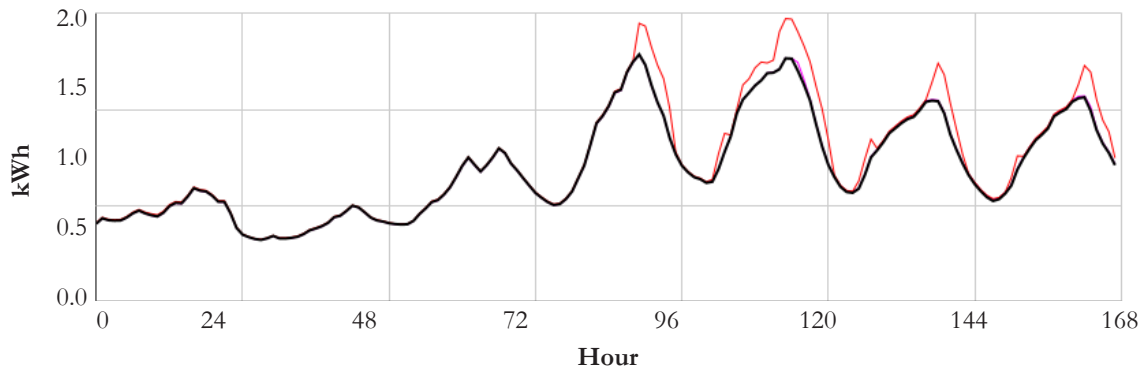
R0 Basement Insulation Cooling Energy, Chicago
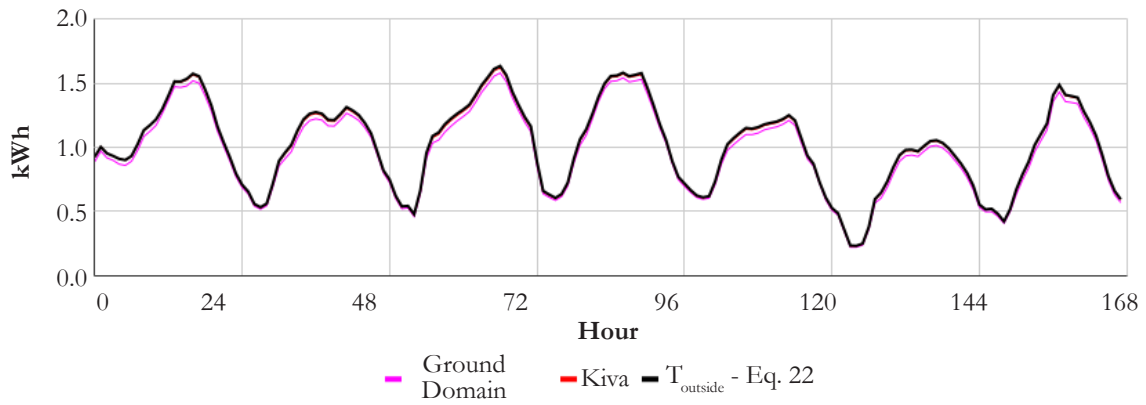
	Kiva RMSE (kWh)	**Ground Domain RMSE (kWh)**
Miami	0.03	0.08
DC	0.07	.005
Chicago	0.03	0.08

Figure 104. Miami, DC, and Chicago cooling energy comparison using Kiva, Ground Domain, and $T_{outside}$.

A grid-off scenario provides slightly more varied results, as is to be expected – grid-off scenarios generally show more pronounced discrepancies between methods, as does the basement model. RMSEs show a range of results with no clear relationship between methods (Table 34, Table 35, Figure 107). Plots, however, show the $T_{outside}$ method falling slightly below Kiva and Ground Domain in terms of heat index in hotter climates, (Phoenix, Austin, Miami) and slightly above in cooler climates (DC, and Chicago).

R0 Basement Insulation Heat Index, Phoenix
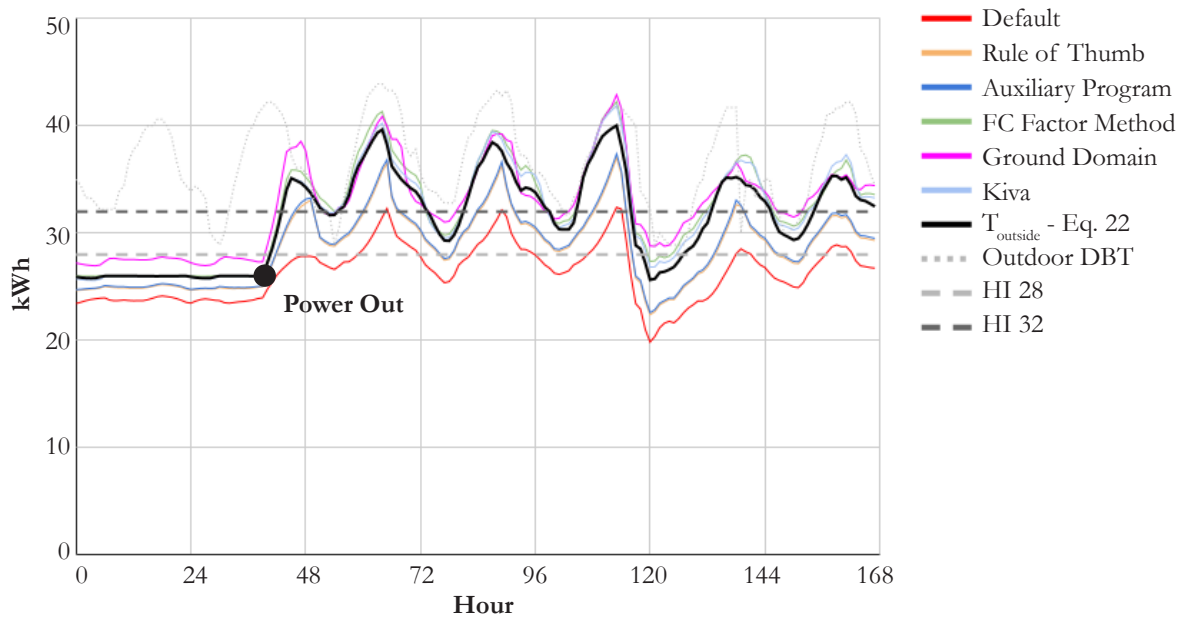
Figure 105. Heat Index results from $T_{outside}$ plotted against other simulation methods

Table 34. RMSE of three ground simulation methods, Phoenix (grid-off)

	Auxiliary Program	Ground Domain	Kiva
RMSE (Heat Index)	2.8	1.6	0.8

R0 Basement Insulation Heat Index, Austin

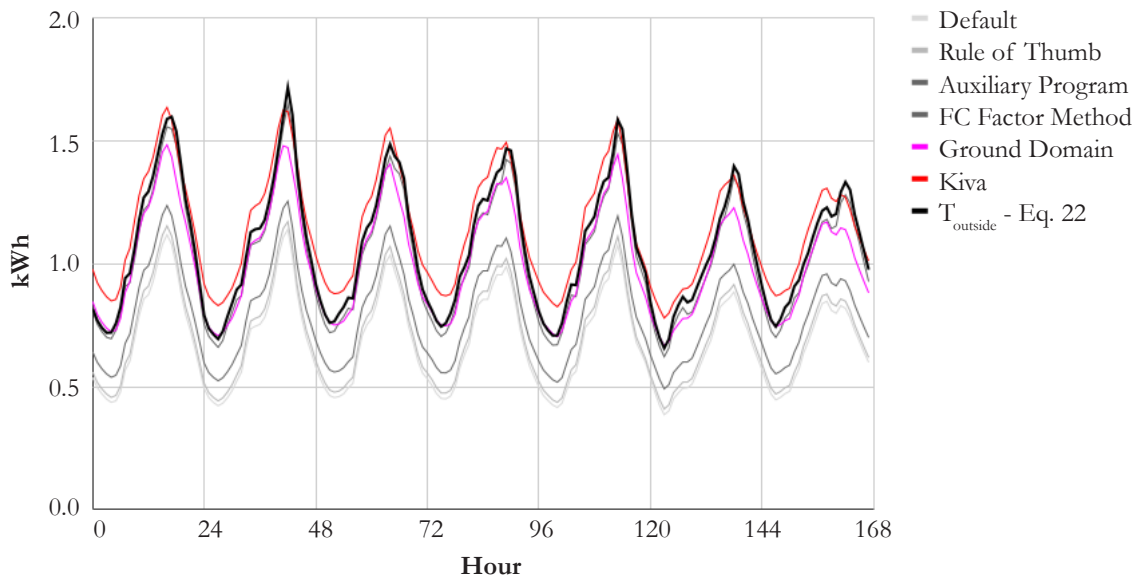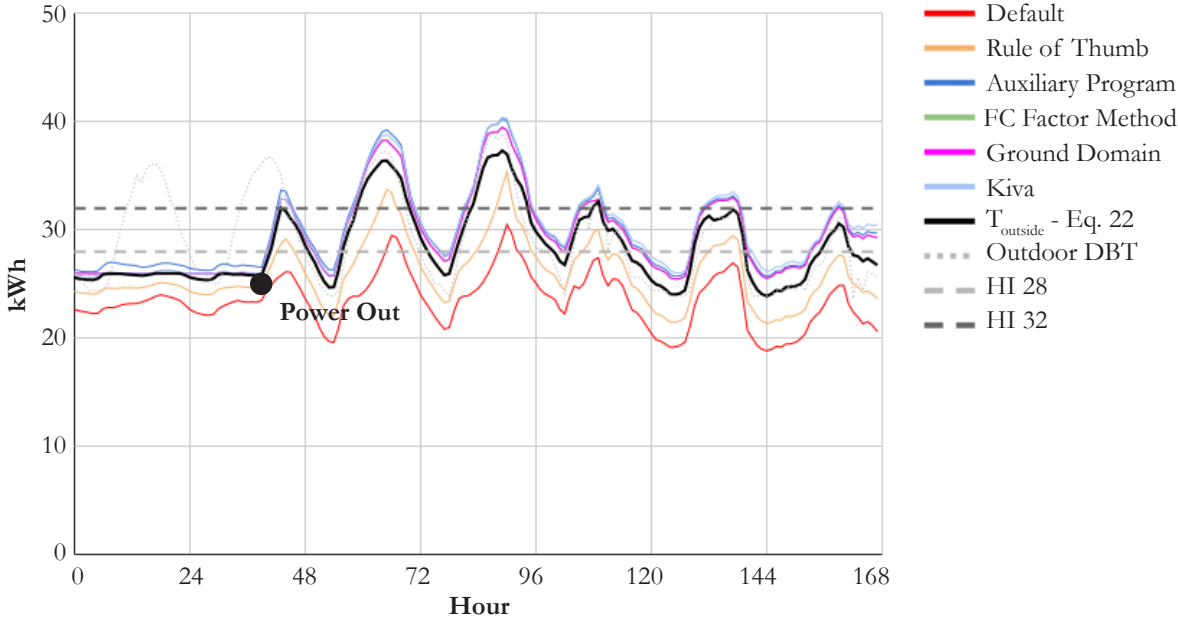*Figure 106. Heat Index results from T$_{outside}$ plotted against other simulation methods*

Table 35. RMSE of three ground simulation methods, Austin (grid-off)

	Auxiliary Program	Ground Domain	Kiva
RMSE (Heat Index)	1.6	1.2	1.7

R0 Basement Insulation Heat Index, Miami
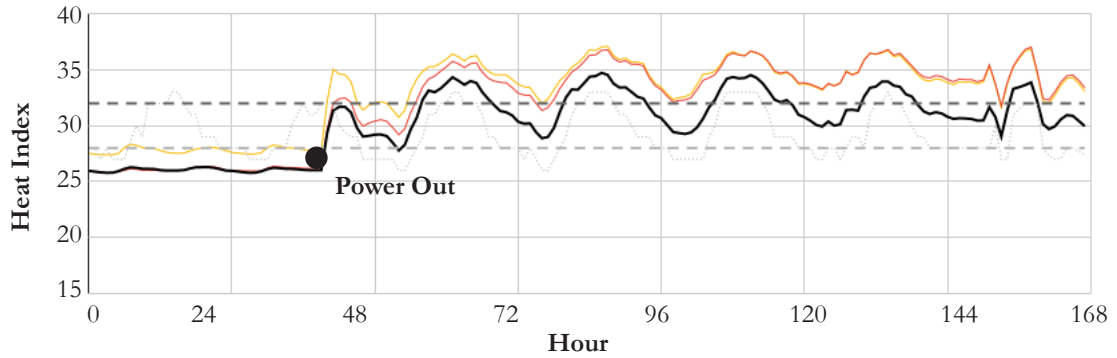
R0 Basement Insulation Heat Index, DC
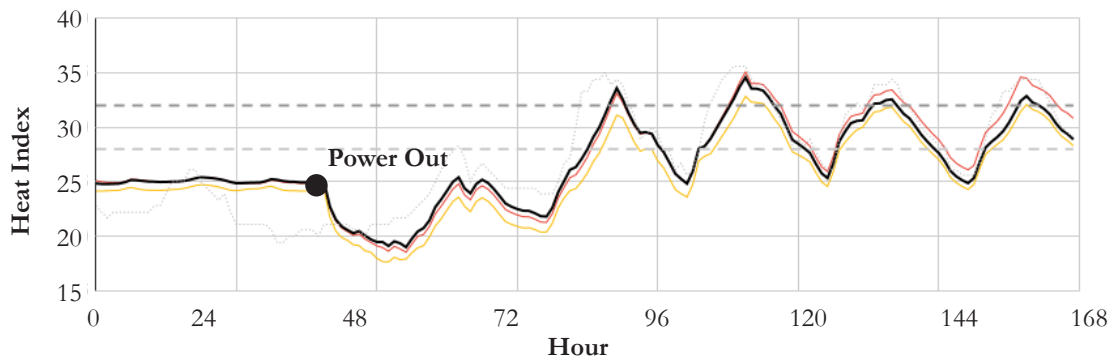
R0 Basement Insulation Heat Index, Chicago
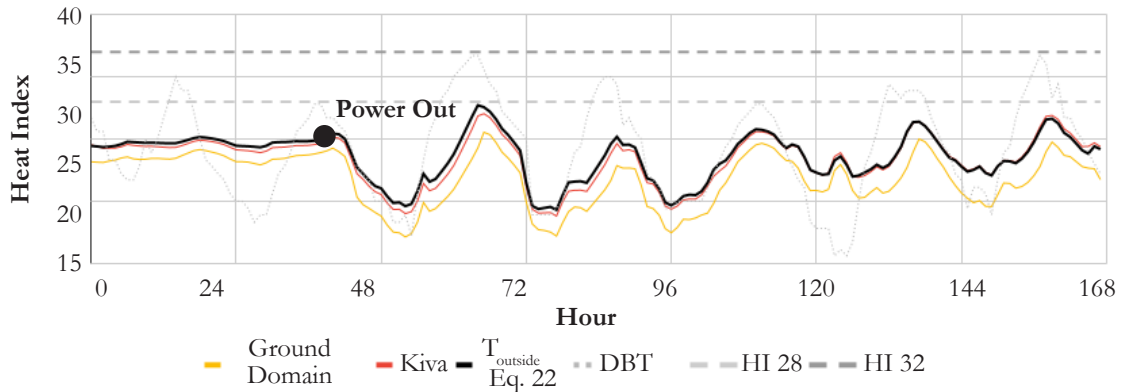
Figure 107. Miami, DC, and Chicago Heat Index comparison using Kiva, Ground Domain, and T$_{outside}$.

Table 36. RMSE of Equation 22 Power outage with respect to Kiva and Ground Domain

	Kiva RMSE (Heat Index)	Ground Domain RMSE (Heat Index)
Miami	2.2	2.6
DC	1.2	0.75
Chicago	0.4	1.9

149

Section 4.8. Conclusion

The effects of different ground modeling methods in ground coupled whole building energy simulations using EnergyPlus have been demonstrated in this chapter. Methods that require little definition on the part of the building modeler (default and rule of thumb) produce results that frequently outlie others which require more user input. A further method has been defined that uses the average zone setpoint and the annual soil surface mean temperature to obtain other side coefficients for ground coupled basements which requires little user input, one EnergyPlus object, and only the definition of "Ground" as another side coefficient in building surface modeling. Further work is needed to more thoroughly validate the method presented, particularly for more diverse geometries but on a simplified model, results show outcomes on par with higher accuracy methods and further contributes to the discussion in 4.3.6 where Kiva and Ground Domain were identified as the preferred ground coupled modeling method.

Page intentionally left blank

Chapter 5
Jerboa; a simulation toolset for advanced ground modeling in the Grasshopper environment

Chapter 5. Jerboa; a simulation toolset for advanced ground modeling in the Grasshopper environment

Section 5.1. Motivation

The previous chapter presented a broad selection of ground modeling methods. This brief chapter addresses a problem present in the application of these methods, and presents a toolset for the modeling community to use in more advanced ground modeling methods in the commonly used Grasshopper environment. Ground modeling through building energy modeling plugins in Grasshopper are fairly limited without leaving the Grasshopper environment and manually editing IDF or Open Studio files. This does not jive with a parametric mindset where fast iteration and model exploration is a key part of the designer's workflow. As such, a toolset is presented below as a set of Grasshopper user objects available for the wider modeling community on the plugin website Food4Rhino under the name "Jerboa". While modeling has been conducted using Honeybee from the Ladybug Tools suite, much of the outputted information can be easily included in the ground temperature field found in Climate Studio. The jerboa is a strange, hopping, desert dwelling rodent which seeks refuge from the desert heat in burrows, hence the origin of the name, plus, they are wicked cute. (Figure 108).

Download Link: https://www.food4rhino.com/en/app/jerboa
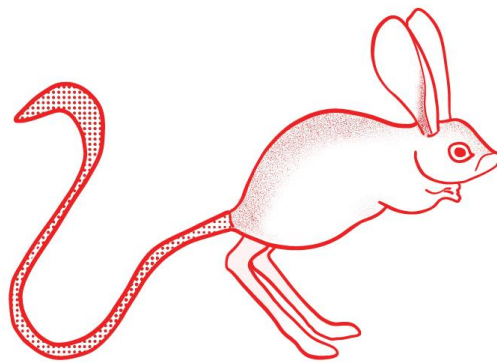
Figure 108. A drawing of a jerboa used as the icon for the Jerboa ground modeling toolkit

Section 5.2. Conceptual Workflow

Two generalized workflows are imagined in Jerboa. The first uses the "Add String" feature in Honeybee which allows for the addition of objects in an EnergyPlus IDF. The second, the one that perhaps has broader application beyond Honeybee, accepts an incoming IDF, which is already written and constructed. Necessary objects are then added and edited and written to a new IDF file ready for simulation with the new ground objects.

Workflow 1: Pre-Simulation Object Inclusion
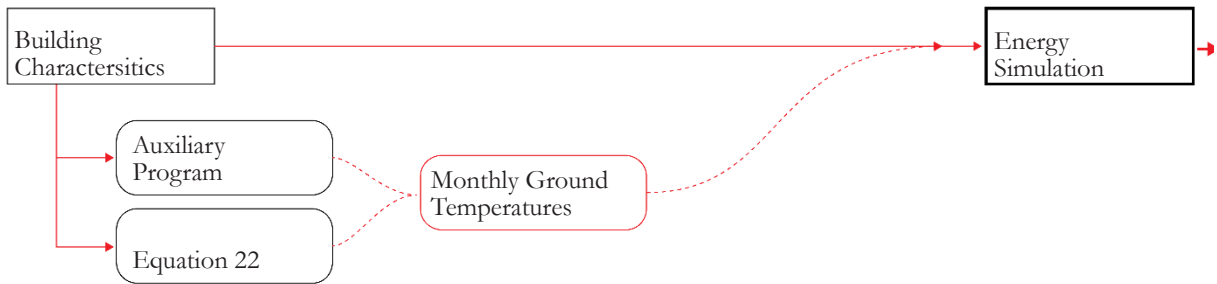
Figure 109. Diagram of Workflow 1 shows the inclusion of EnergyPlus Objects via Jerboa with the initial IDF creation.

Workflow 2: IDF Modification
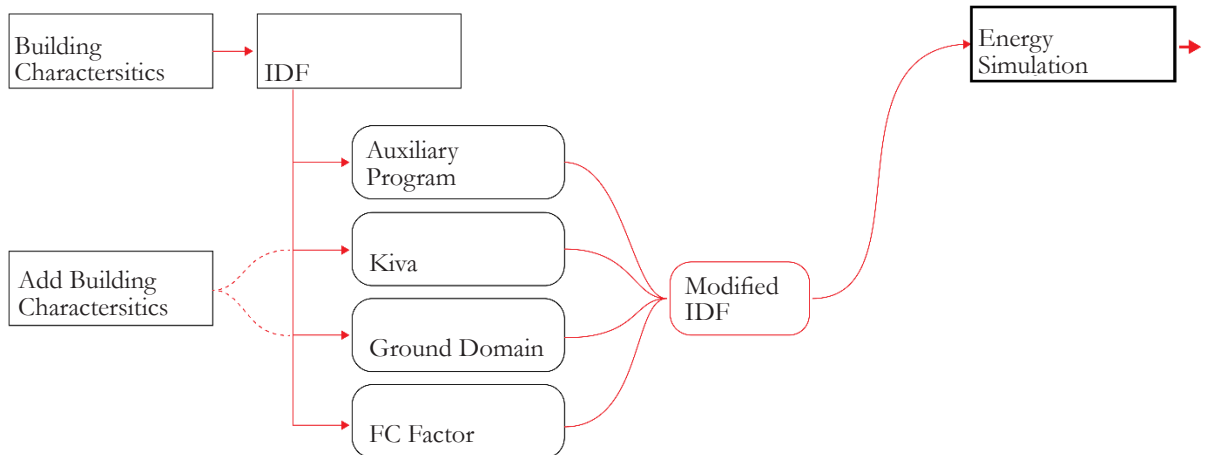
Figure 110. Diagram of Workflow 2 diagram shows the modification of an IDF by Jerboa that is subsequently simulated.

Section 5.3. Component Overview

This section provides an overview each collection of objects and their associated workflow. Refer to 4.5 for method details.

5.3.1. Auxiliary Programs
Slab – Workflow 1

Slab Material   **Building Characteristics**   **Run Slab Program**

Figure 111. Diagram of Slab Auxiliary program components

The slab auxiliary program comprises of three components and ultimately produces ground temperatures that are included in the IDF as outside boundary conditions.

Basement   - Workflow 1/Workflow 2

Basement Material   **Building Characteristics**   **Run Basement Program**   **Basement Program IDF Modifier**

Figure 112. Diagram of Basement program components

The basement auxiliary program is comprised of components that are similar to the slab program. These three produce ground temperatures that are included in the IDF. If using the fourth component, objects are not included in the IDF creation, instead an existing IDF is modified to include unique slab and floor schedules.

Section 5.4. FC Factor Method
Workflow 2

FC Factor Pre-Process   **FC Ground Temperatures**   **FC Factor Ground Modifier**
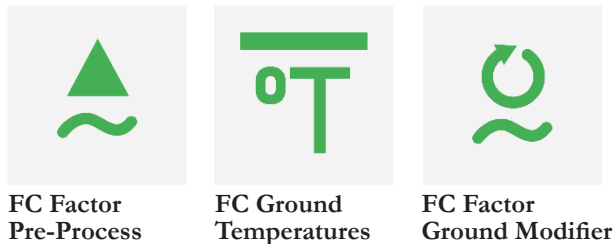
Figure 113. Diagram of FC factor Method components

FC Factor method uses three components to prepare slab and wall information, make the ground temperature object, and modify the existing IDF.

Section 5.5. Kiva
Workflow 2

| Kiva Pre-Process | Kiva Settings | Building Characteristics | Slab Perimeter Settings | Kiva IDF Modifier |
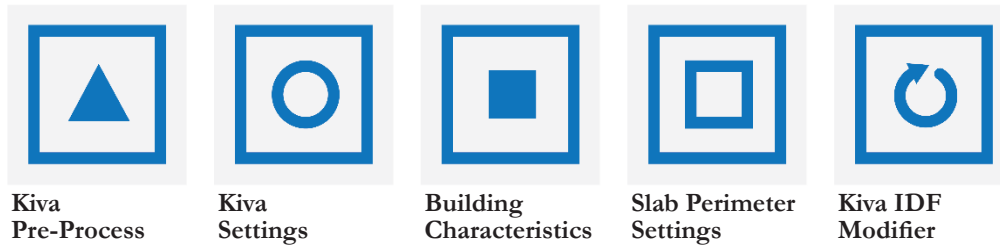
Figure 114.Diagram of Kiva method components

Kiva workflow is comprised of five components. The Kiva IDF Modifier edits and writes an existing IDF for simulation.

Section 5.6. Ground Domain
Workflow 2

| Xing Ground Temperatures | Slab Pre-Process | Slab IDF Modifier | Basement Pre-Process | Basement IDF Modifier |
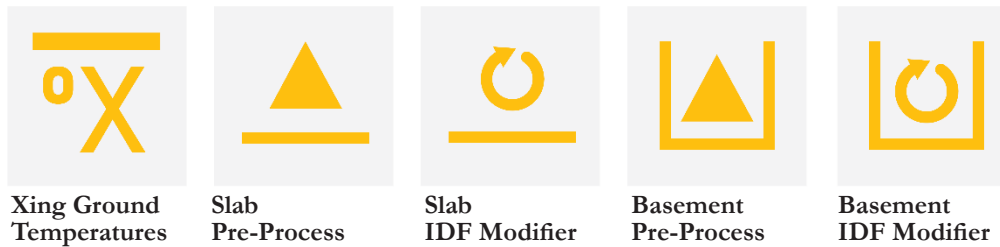
Figure 115. Diagram of Ground Domain components

The Ground Domain components contain both slab and basement objects which function similarly, with some varying options in building characteristics. The undisturbed ground temperature object uses the Xing ground model.[106]

Section 5.7. Jerboa Method
Workflow 1

| Analytic Ground Temp | Jerboa Method |
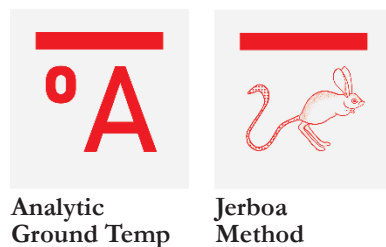
Figure 116. Diagram of Jerboa Method Components

The Jerboa Method uses two components, and is the name given to the method which uses Equation (22). Inputs are average zone temperature and average mean soil surface temperature which is provided by the Analytic Ground Temperatures component. Outputs are 12 ground temperatures supplied via Workflow 1.

---

[106] Xing, Lu. "Estimations of Undisturbed Ground Temperatures Using Numerical and Analytical Modeling," 2010.

Section 5.8. Utilities

Temperature Object Maker   EPW Looker   IDF Looker   Basement Program Copy
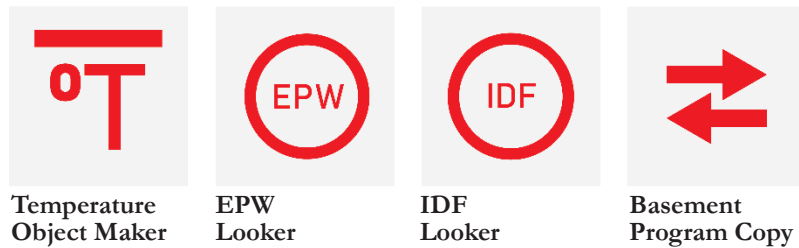
Figure 117. Diagram of utility components

Not terribly exciting, but the utility components provide some "nice-to-haves". "Temperature Object Maker" accepts temperature inputs for each month and outputs a ground temperature EnergyPlus object string.

EPW and IDF lookers both find their respective file types stored next to the Grasshopper file and provide them as paths for the purposes of simulation or modification.

A strange bug prevents the Basement program from running in EnergyPlus V9.6.0. Jerboa requires the installation of both EnergyPlus version 9.6.0 and 9.3.0. "Basement Program Copy" moves the required files from 9.3.0 to the correct location in 9.6.0.

Section 5.9. Documentation and Example Files

Jerboa documentation is provided in a PDF included with the ZIP download from Food4Rhino or in a live published Google Document. Example files are also included in the ZIP file from Food4Rhino.

Documentation Link: https://bit.ly/3v7s9ep

Section 5.10. Conclusion

The process of this tool creation was remarkably integral to getting a strong grasp on the methods available. The simulations and results from Chapter 4 relied on its creation, and are effectively an example of the outcomes produces by the user objects and Jerboa component family. In a sense, its development came from the want of a package that provided this capability, as well as documentation that provided the necessary knowledge to clearly apply each method.

Chapter 6
Strategies and Building Forms for Heat Resilience

Chapter 6. Strategies and Building Forms for Heat Resilience

Section 6.1. Motivation

Returning from our brief detour in chapters four and five that focused on ground modeling methods and toolset creation, the task at hand in chapter six returns to the question of heat resilience in US homes. Chapter three focused on the comparison between models that uses IECC building characteristics and Passive House building characteristics. In this case of Phoenix, AZ, the Passive House model produced much better results than the IECC model in cooling energy demand and in passive resilience. In Austin, however, the Passive House versus the IECC model did not perform as well as Phoenix in terms of reducing cooling energy demand and the two models performed comparably in terms of passive resilience. Phoenix, however, will be the focus of this chapter. The housing models simulated in chapters three and four were spatially symmetric and thus agnostic to orientation and function. This chapter maintains a similar attitude. While orientation is essential, production building on single family homes is not overly concerned with building orientation. As such, building orientation is not emphasized in this chapter. It is not a new idea that building form affects performance, or, further, that building form can be used as a means to improve interior conditions in hot climates. Plenty of contemporary examples exist, as do historical examples: Tunisian cave dwellings, Puebloan dwellings, and Islamic courtyard gardens, to name a few. As such, this chapter explores three building form strategies applied to the US low-rise, low-density context as a means to reduce cooling energy consumption and improve passive resilience. Below are the three strategies addressed in this chapter:

(1) **Ground Coupling** – Using the building's relationship to the ground through a basement

(2) **Party Walls and Unit Adjacency** – Creating building adjacencies to reduce energy demand and foster social resilience and create opportunities for more diverse housing

(3) **Thermal Nesting** – Creating thermal buffer zones and dedicated cool zones within a home.

A broad question in this chapter is if it is possible to achieve close to Passive House performance in cooling energy and passive survivability while using IECC constructions, infiltration, and systems (no heat recovery). Each strategy is accompanied by a house that demonstrates the concept in a speculative living scenario.

Section 6.2. Methodology

Model constructions, loads, and simulated hot week are consistent with Phoenix IECC characteristics (Table 1, Table 4, Figure 13). One simulation will be conducted using the Passive House characteristics on the base case to use as a benchmark. Additionally, as per our exploration of modeling methods, The Ground Domain method will be used. This will partially account for the variance in results if compared with Chapter 3, by the nature of the ground coupled variance detailed in Chapter 4. With a particular interest in future heat resilience in contemporary housing being built to days standards, the Phoenix 2050 A2 weather file will be used.

Section 6.3. Basements

6.3.1. Introduction

With a clearly defined interest in ground coupling as a means of both decreasing cooling energy demand and passive resilience, the first building form addressed in this chapter is the use of basements and below grade spatial arrangements that increase the building surface area coupled with the earth.

6.3.2. Depth and Daylight and Performance

One of the key questions in situating the main program and function of a house in the basement (bedrooms for example) is access to daylight and views. This section explores a number of building forms with different ground relationships, and views. Six scenarios are shown in Figure 118 and the following pages with passive and active performance numbers and figures, a continuous Daylight Autonomy (cDA300) annual heatmap and a visualization of an imagined below grade bedroom. Visualizations are shown looking west at 3 p.m. in late August. Cooling energy is shown in a plot and given in a number of kWhs/occupant over the course of the week; "option cooling energy" is the cooling energy of the basement form in question. In this case, we assume 4 occupants in the home. Heat index plots differentiate between the upper and lower zones of the house. The lower zone = zone 1 (Z1) and the upper zone = zone 2 (Z2). Natural ventilation uses only the exterior windows, not doors between zones.

1.

2.

3.

4.

5.

6.
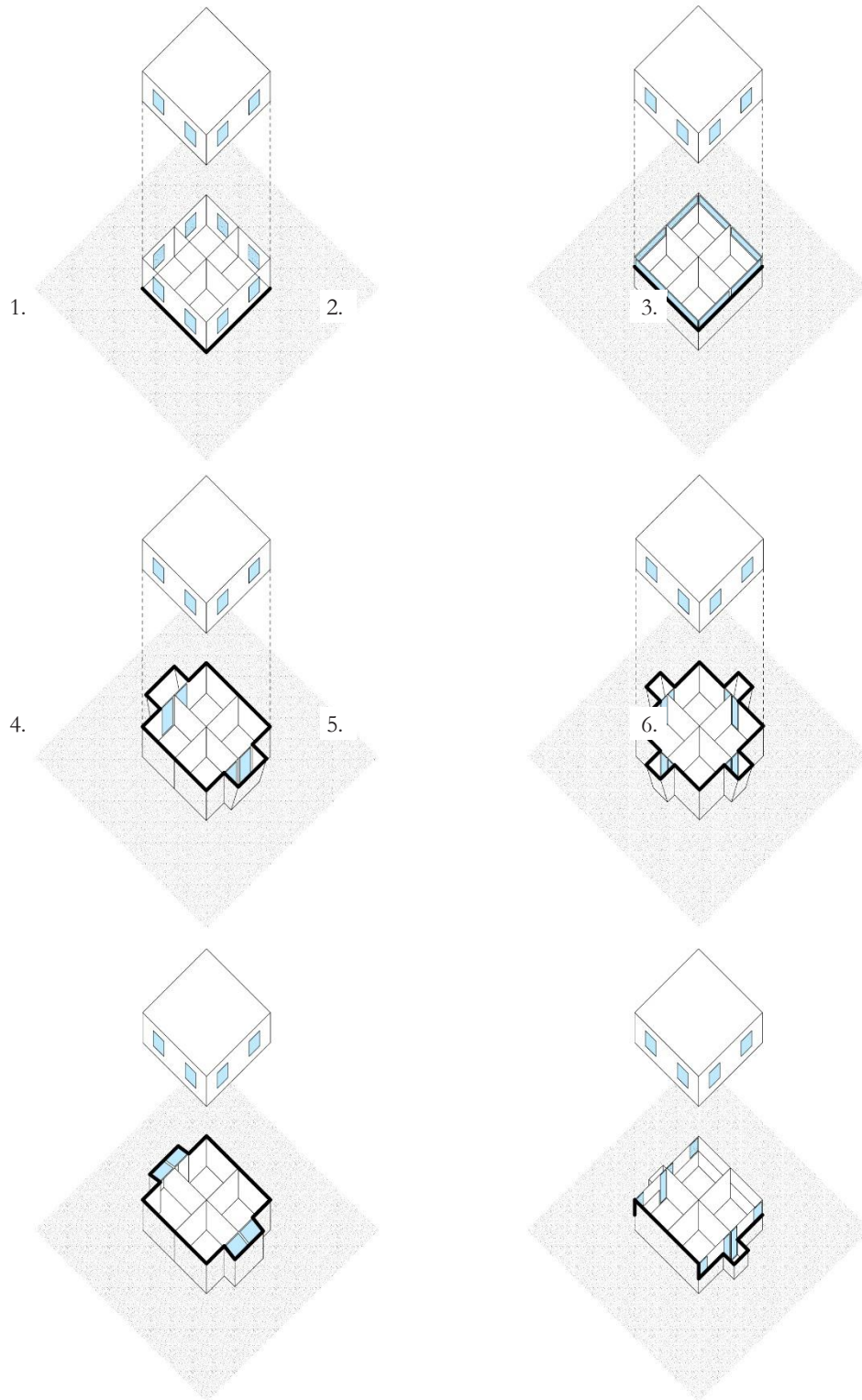
Figure 118. Basement scenarios shown and tested in the following pages

1. Baseline House

Basement Window Area: 18m²
Zone Average cDA: 46.1%

0%   50%
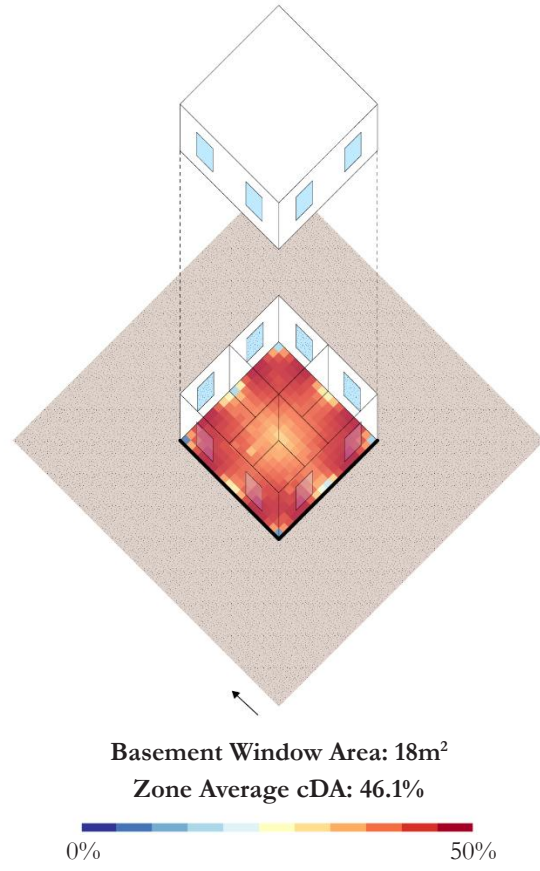
Figure 119. Baseline house diagram and visualization

Cooling Energy, Basement 1

Legend:
- Base Cooling IECC
- Base Cooling Passive House
- Basement 1
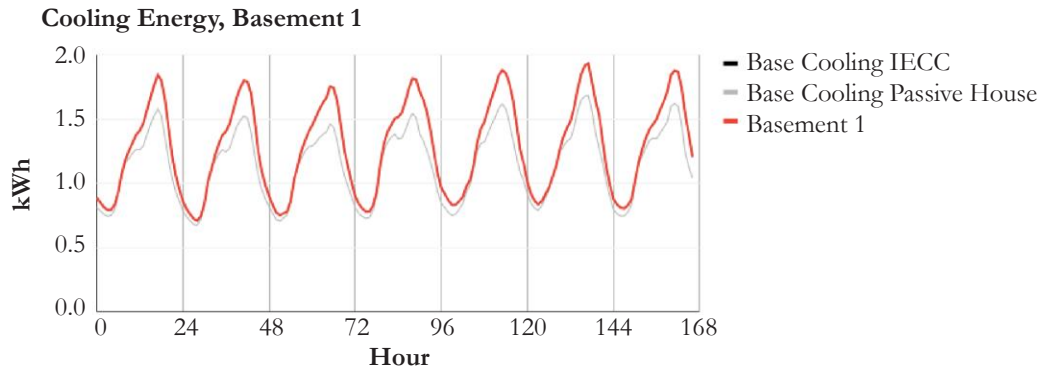
IECC cooling kWh/person : 53.7

Passive House cooling kWh/person : 47.9

Heat Index, Basement 1

Legend:
- Base IECC Zone 1
- Base IECC Zone 2
- Base PH Zone 1
- Base PH Zone 2
- Basement 1 Zone 1
- Basement 2 Zone 2
- HI 28
- HI 32
- Outdoor HI

Power Out
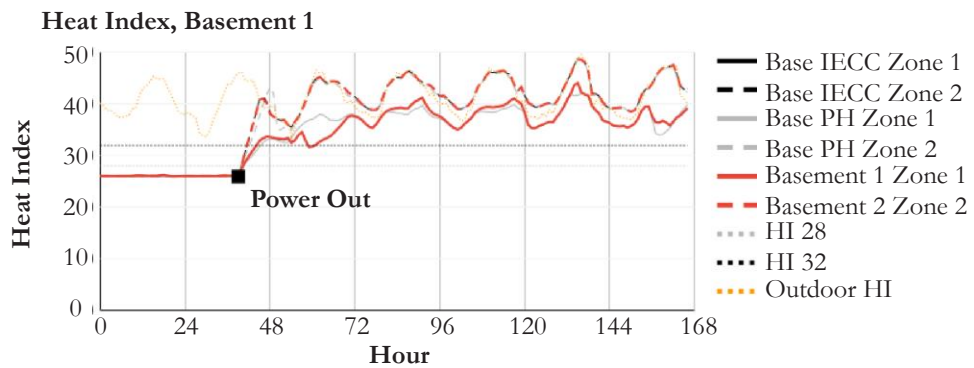
IECC HHH32: 121

Passive House HHH32: 121

Figure 120. Baseline house cooling energy and heat index hours

2. Clerestory

Basement Window Area: 23.5m²
Zone Average cDA: 46.6%

0%   50%
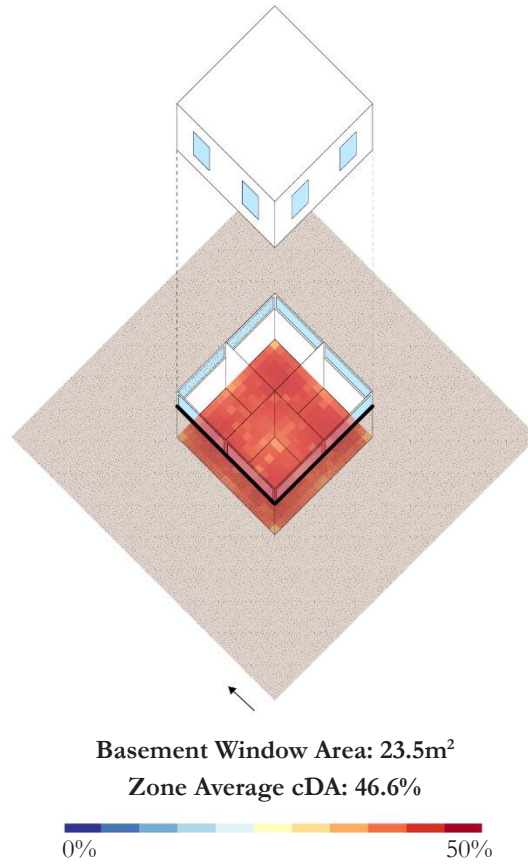
Figure 121. Basement 2 diagram with clerestory windows and interior visualization

Cooling Energy, Basement 2
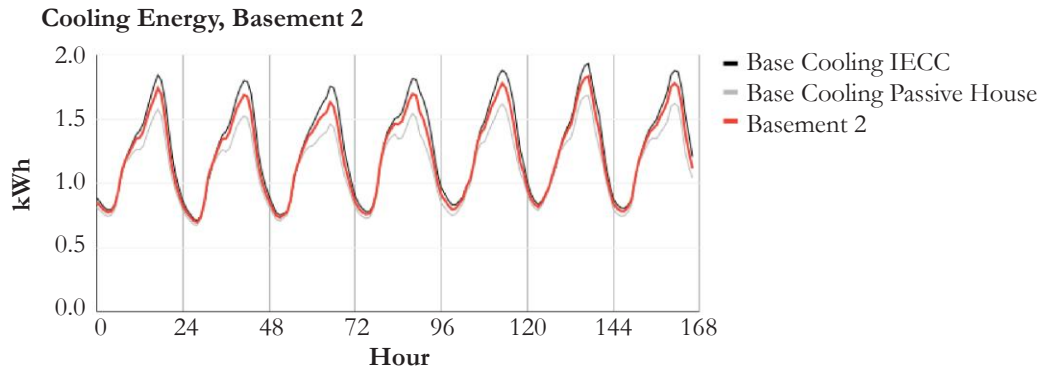
Cooling kWh/person : 51.3
Passive House cooling kWh/person : 47.9

Heat Index, Basement 2
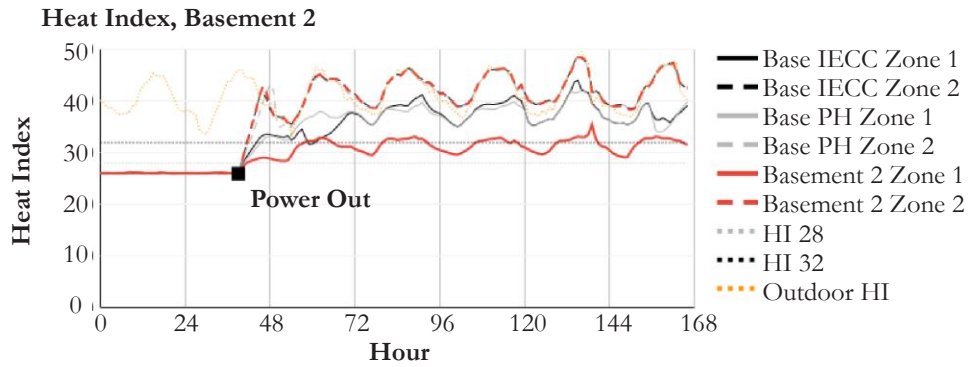
Basement HH28: 126
Basement HH32: 54

Figure 122. Basement 2 cooling energy and heat index hours

3. Canted Light-Wells (NS)

Basement Window Area: 16.3m²
Zone Average cDA: 24.9%

0%   50%
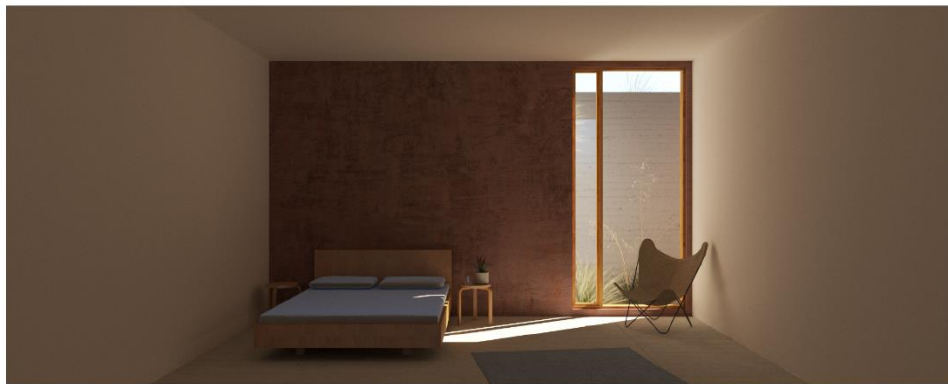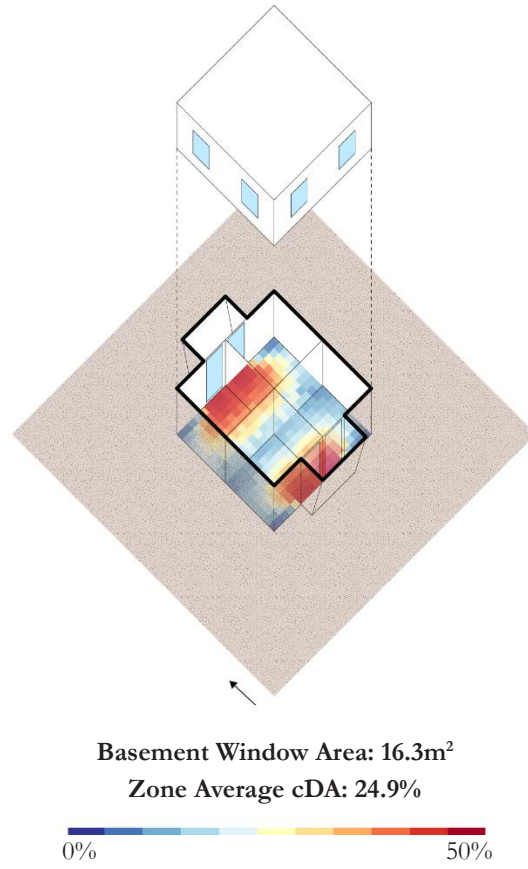
Figure 123. Basement 3 diagram with a light well and interior visualization

Cooling Energy, Basement 3

- Base Cooling IECC
- Base Cooling Passive House
- Basement 3
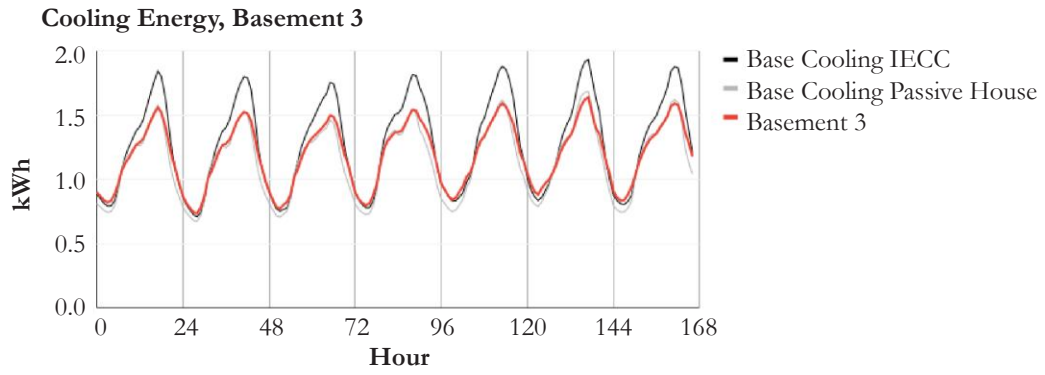
Cooling kWh/person : 48.9

Passive House cooling kWh/person : 47.9

Heat Index, Basement 3

- Base IECC Zone 1
- Base IECC Zone 2
- Base PH Zone 1
- Base PH Zone 2
- Basement 3 Zone 1
- Basement 3 Zone 2
- HI 28
- HI 32
- Outdoor HI

Power Out
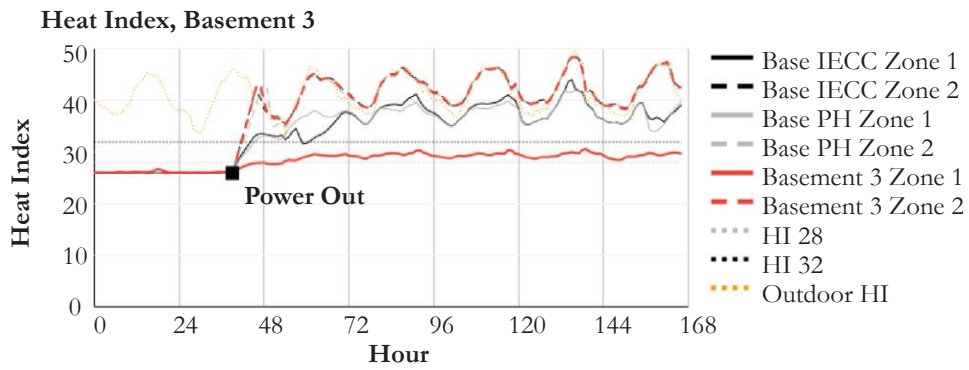
Basement HH28: 114
Basement HH32: 0

Figure 124 Basement 3 cooling energy and heat index hours

167

4. Canted Light-Wells

Basement Window Area: 18m²
Zone Average cDA: 24.0%

0%   50%
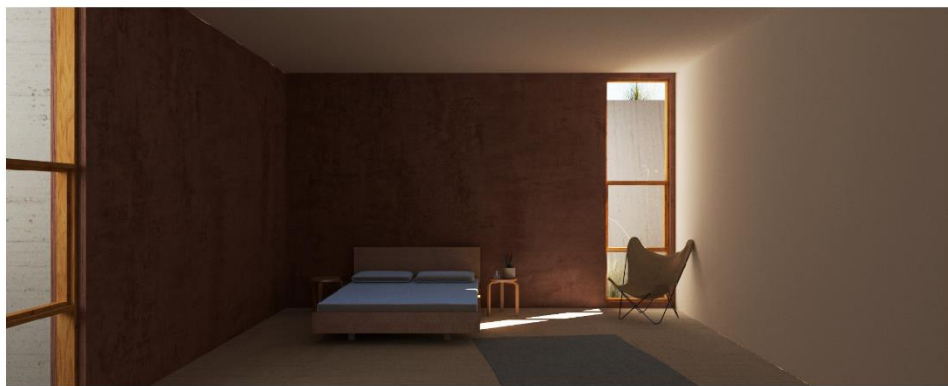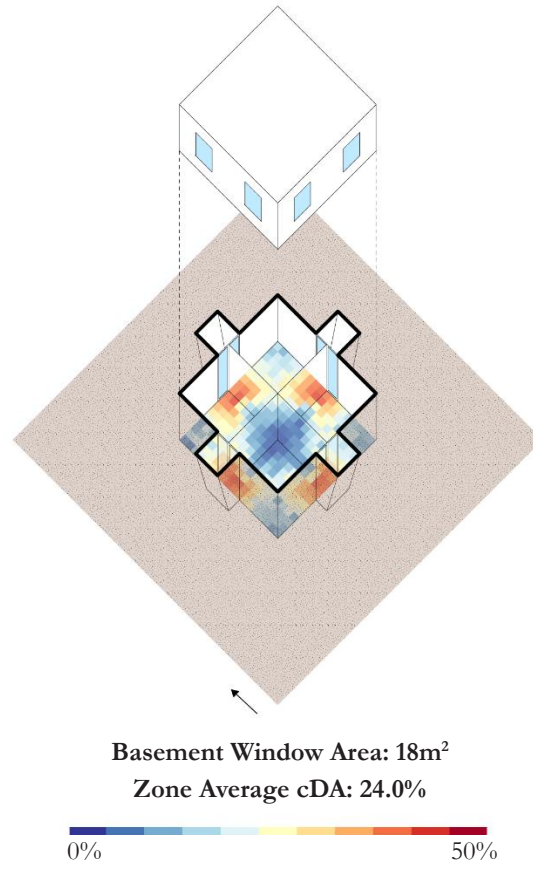
Figure 125 Basement 4 diagram with two light wells and interior visualization

Cooling Energy, Basement 4

Base Cooling IECC
Base Cooling Passive House
Basement 4
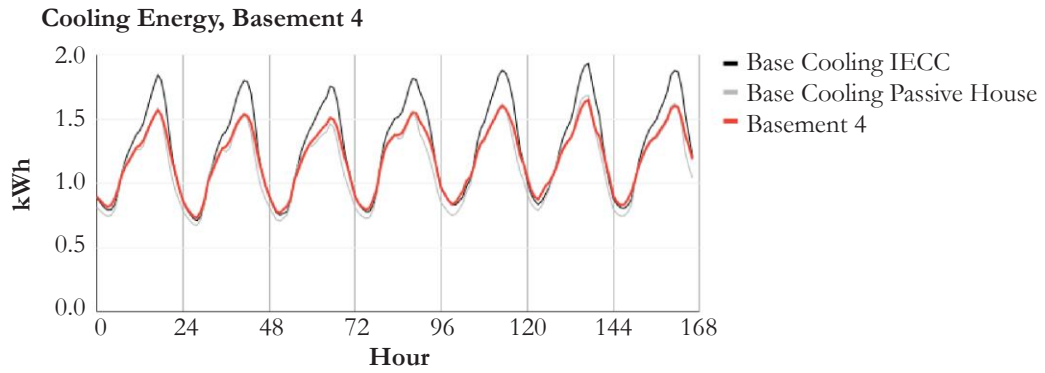
Cooling kWh/person : 50.1
Passive House cooling kWh/person : 47.9

Heat Index, Basement 4

Base IECC Zone 1
Base IECC Zone 2
Base PH Zone 1
Base PH Zone 2
Basement 4 Zone 1
Basement 4 Zone 2
HI 28
HI 32
Outdoor HI

Power Out
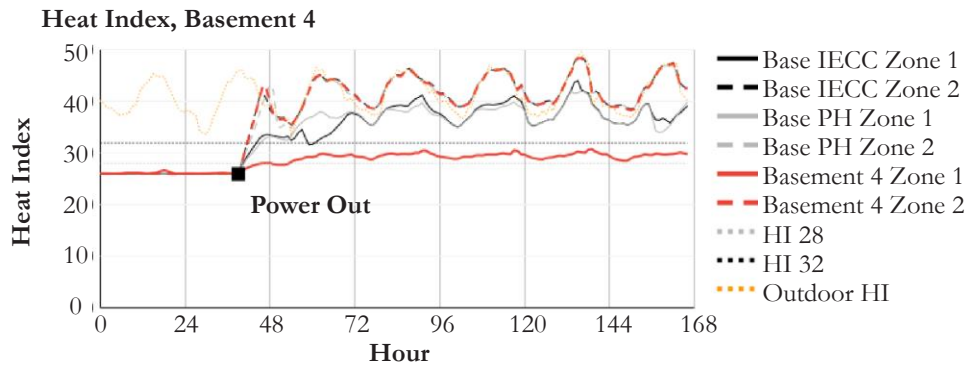
Basement HH28: 117
Basement HH32: 0

Figure 126. Basement 4 cooling energy and heat index hours

169

5. Skylights

Basement Window Area: 9.5m²
Zone Average cDA: 26.6%

0%   50%
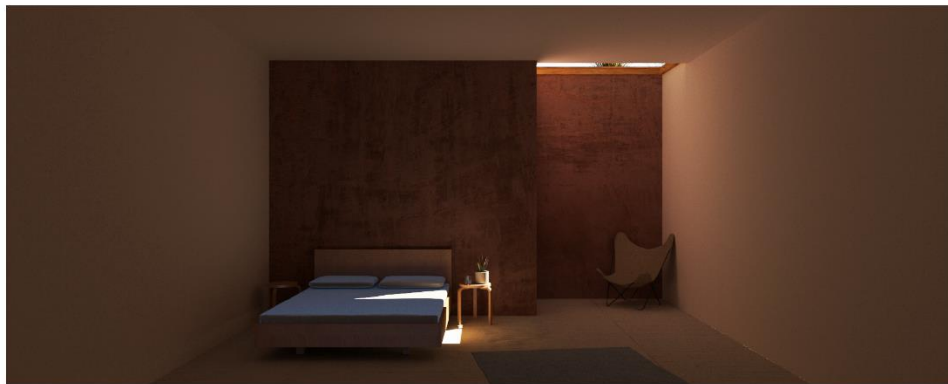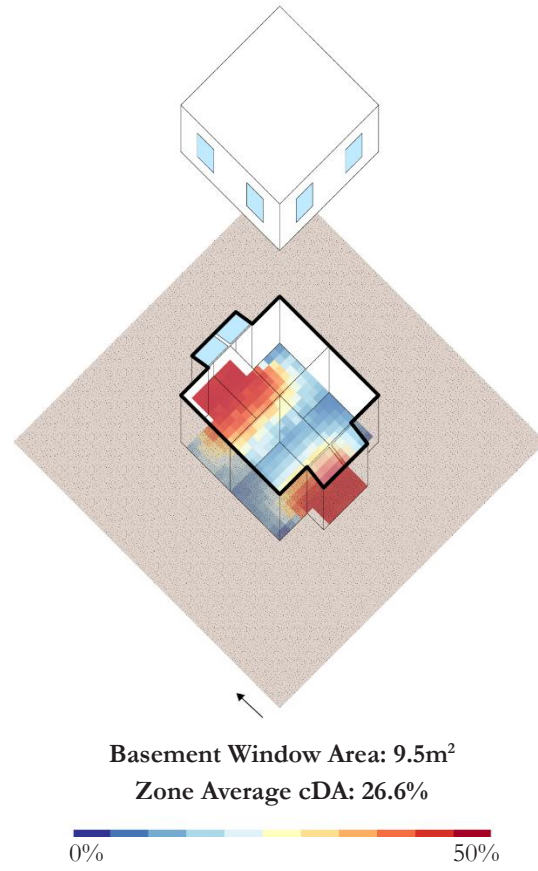
Figure 127. Basement 5 diagram with a skylight and interior visualization

Cooling Energy, Basement 5

Legend:
- Base Cooling IECC
- Base Cooling Passive House
- Basement 4

Y-axis: kWh (0.0 to 2.0)
X-axis: Hour (0 to 168)
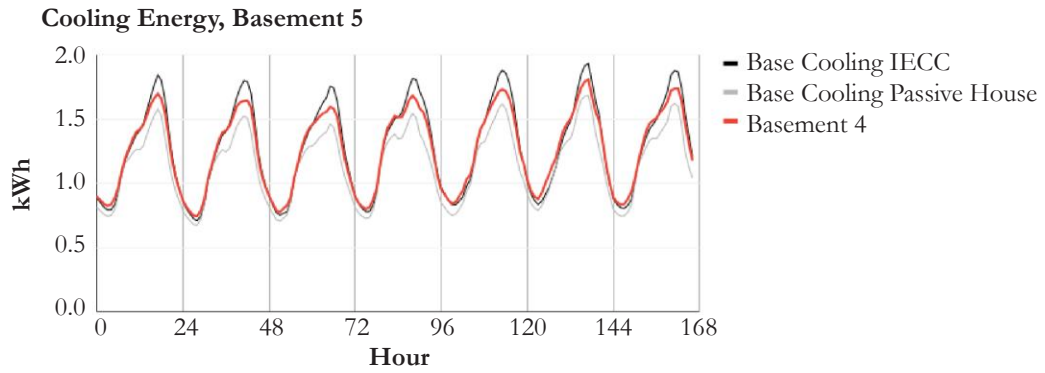
Cooling kWh/person : 52.9
Passive House cooling kWh/person : 47.9

Heat Index, Basement 5

Legend:
- Base IECC Zone 1
- Base IECC Zone 2
- Base PH Zone 1
- Base PH Zone 2
- Basement 5 Zone 1
- Basement 5 Zone 2
- HI 28
- HI 32
- Outdoor HI

Y-axis: Heat Index (0 to 50)
X-axis: Hour (0 to 168)

Power Out
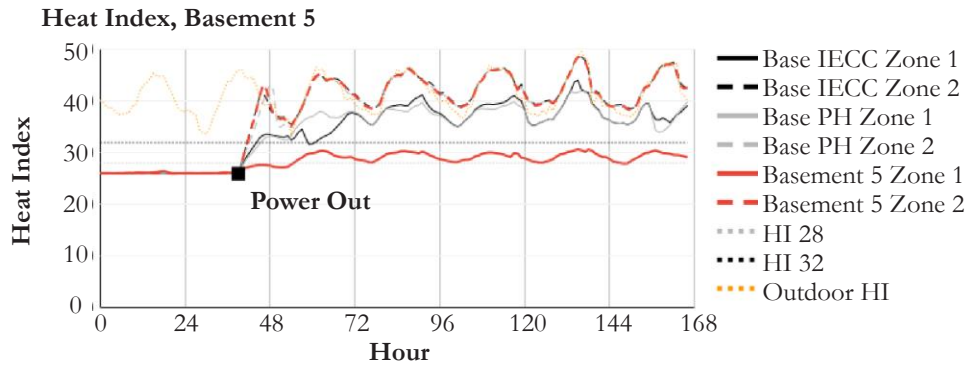
Basement HH28: 111
Basement HH32: 0

Figure 128. Basement 5 cooling energy and heat index hours

171

6. Almost Buried

Basement Window Area: 15m²
Zone Average cDA: 41.4%

0%   50%
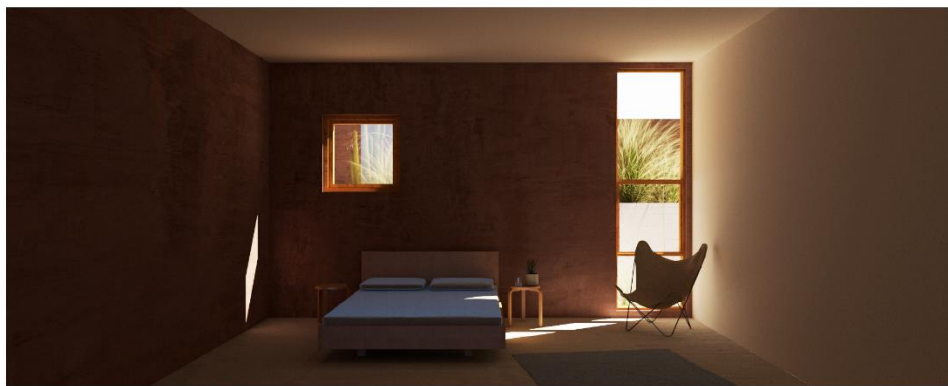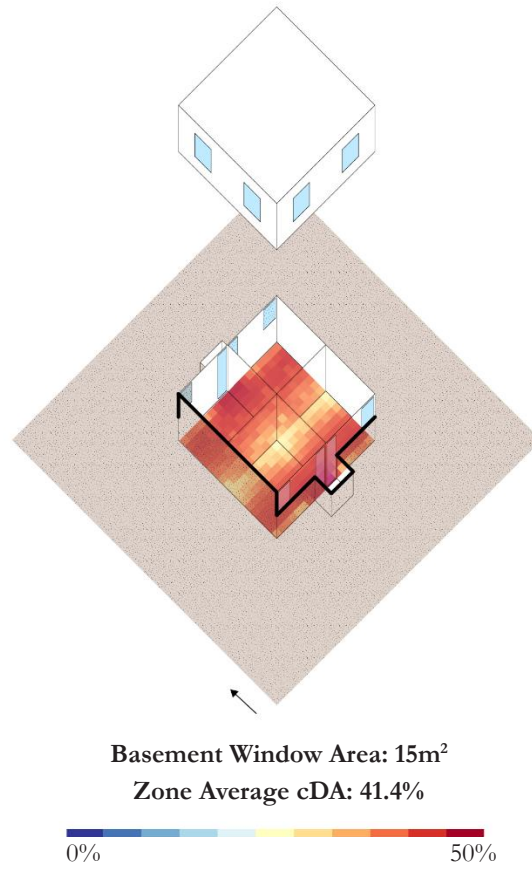
Figure 129. Basement 6 diagram with a small light well, high exterior window and visualization

Cooling Energy, Basement 5
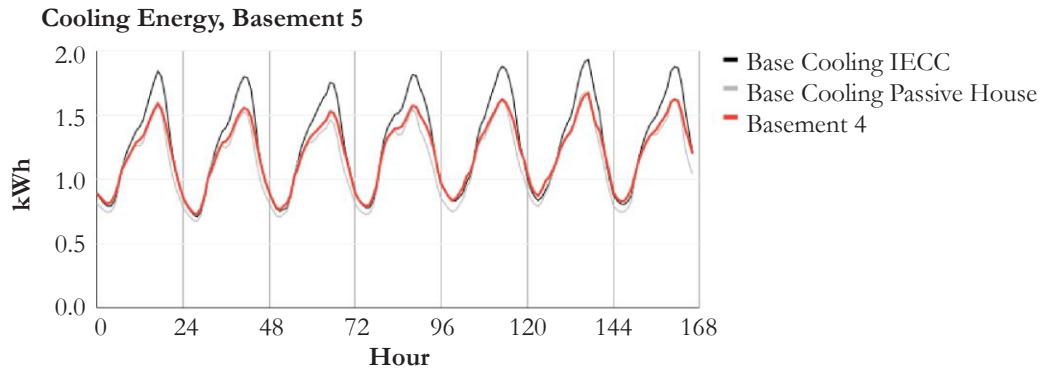
Cooling kWh/person : 50.4
Passive House cooling kWh/person : 47.9

Heat Index, Basement 5
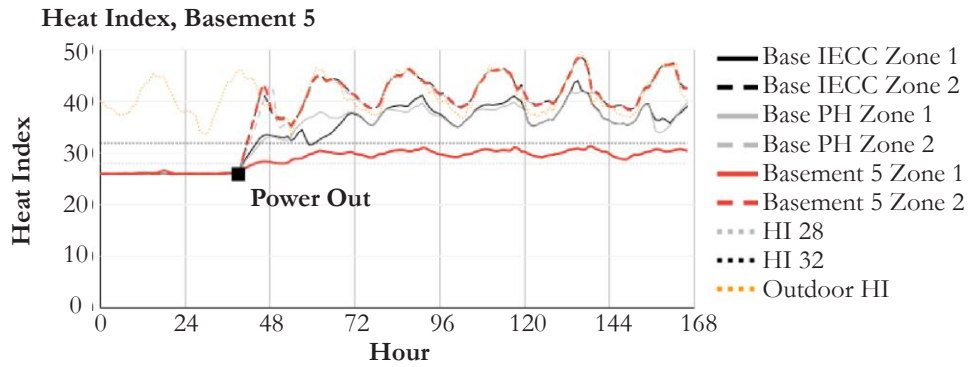
Basement HH28: 124
Basement HH32: 0

Figure 130. Basement 6 cooling energy and heat index hours

6.3.3. Resilient Function

Section 6.3.2 heat index plots distinguish between upper and lower zones. As can be seen in Figure 119 -Figure 130, in general, the lower zones perform significantly better in terms of passive resilience under a full power outage. One function of resilience that might be used is to increase the set point, or stop cooling the upper floors altogether, as a means of further reducing energy demand. The two scenarios shown below use the basement window scheme 3. The schemes are 1) raised set points which sets the upper floor to 28 °C and the lower floor to 23 °C and 2) Letting the upper floor free-run with windows open, and continue to cool the lower floor. Figure 131 shows the dramatic reduction in cooling energy demand deploying these two strategies. In scenarios shown below, Figure 131, it is assumed that the basement is fully occupied (four occupants) and the upper floor has not occupants.

Power Outage   N ↗

Hour: 40 (4pm)   64(4pm)   112(4pm)   136(4pm)

Upper Floor Off (Grid-on)

Hour: 40 (4pm)   64(4pm)   112(4pm)   136(4pm)

Heat Index

<18 °C   >40 °C

Cooling Energy Per Occupant as Percent Change from IECC Reference

Reference IECC House:	0%
Reference Passive House:	-10%
Basement 3:	-9%
Basement 3 Layered Setpoints:	-45%
Basement 3 Upper Off:	-63%
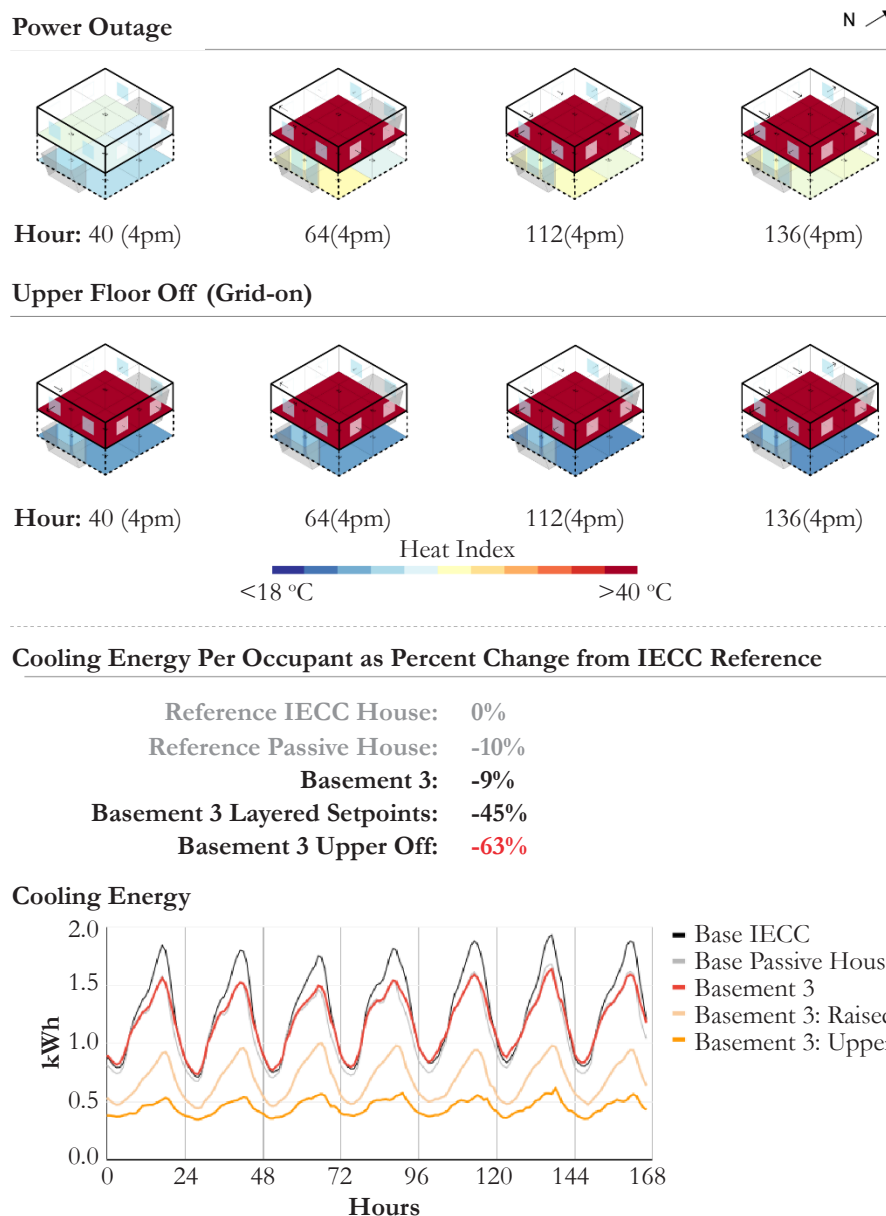
Cooling Energy

Figure 131. Zone heat indexes over the hot week are shown graphically. Cooling energy results for each resilience scenario are shown in percent reduction from reference IECC house and a cooling energy plot.

20m / ~65ft **30m / ~100 ft**
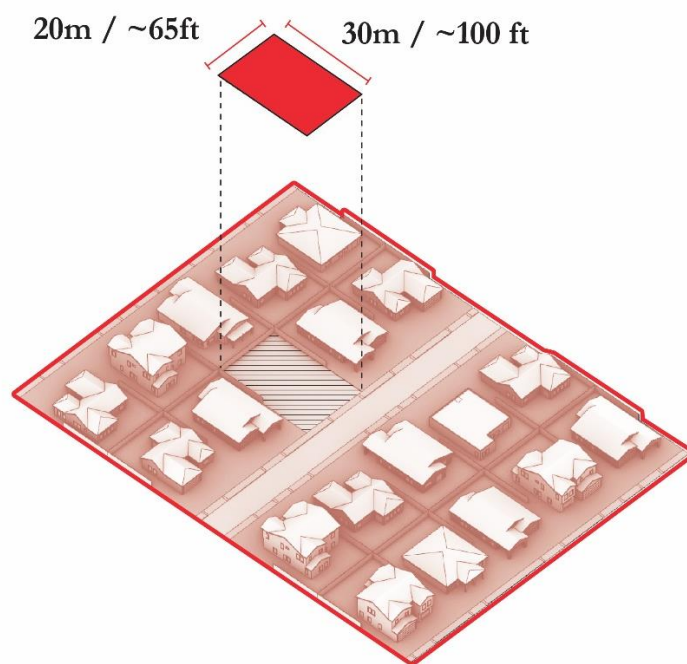
Figure 132. Houses in the following sections are tested on an archetypal urban site of 65' x 100'

6.3.4. Ground House
Occupancy: 4
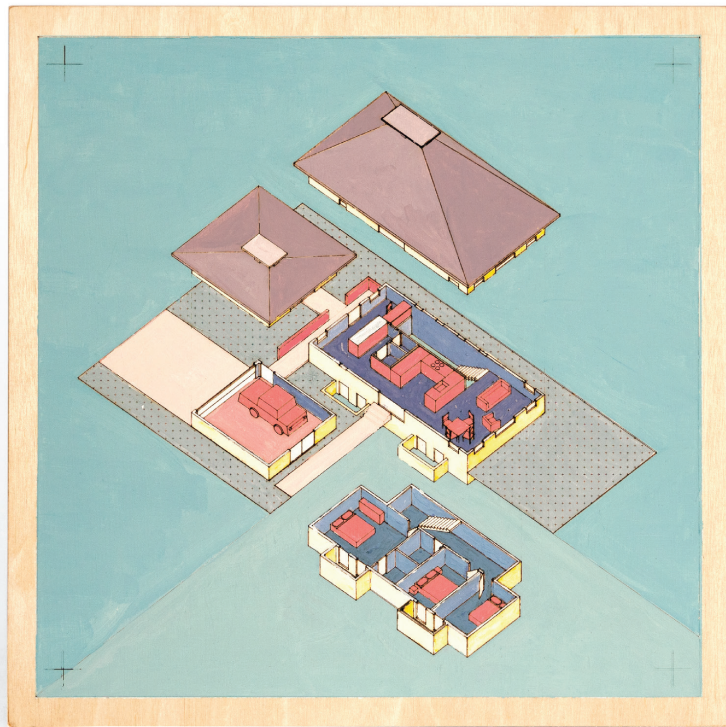
Ground House
Thermo-chromic paint on wood - 12"x12"
No heat applied

Figure 133. Ground House painting - normal conditions
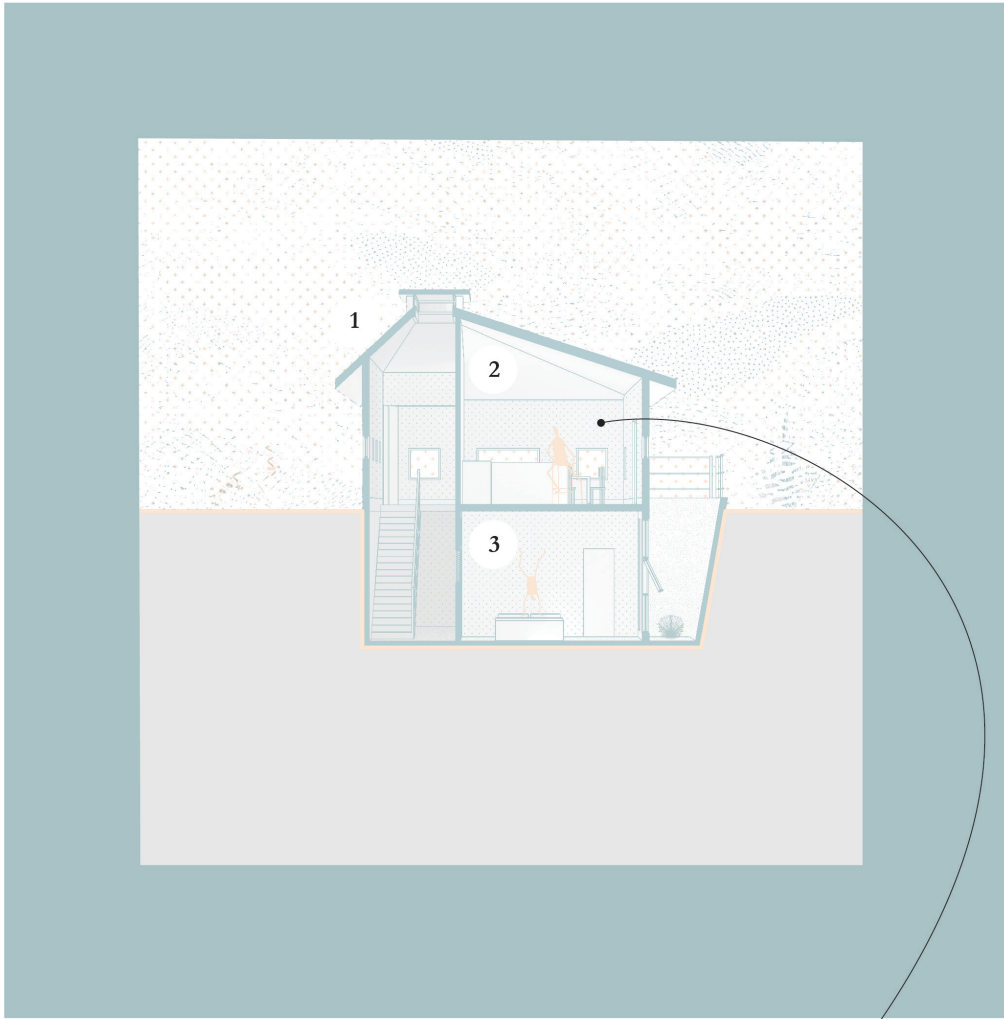
1. A suggestive chimney for buoyancy driven natural ventilation when appropriate
2. Open plan living upstairs
3. Bedrooms below grade

No heat wave

Figure 134. Ground House section perspective - normal conditions
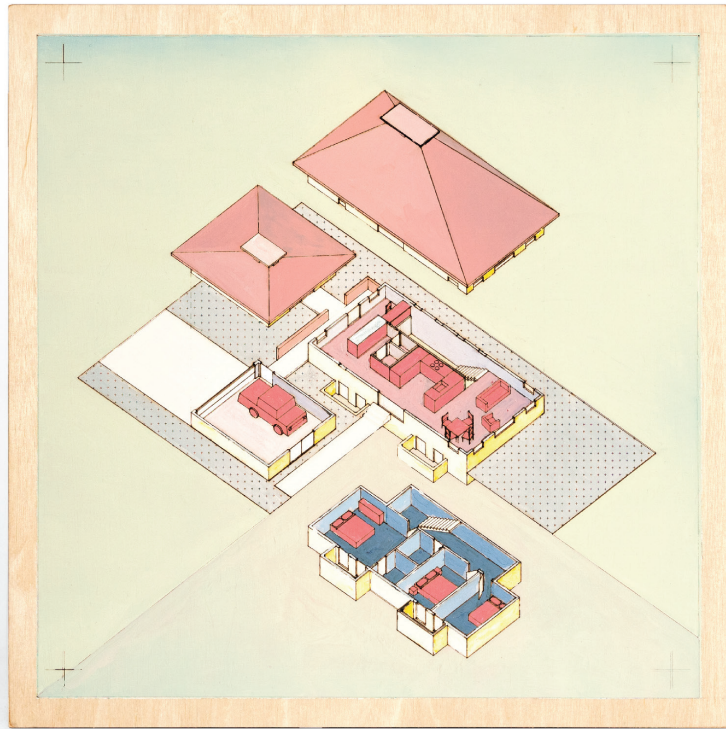
Ground House
Thermo-chromic paint on wood - 12"x12"
Heat applied

Figure 135. Ground House painting - heat wave

Close the stair door

Rest and sleep down below
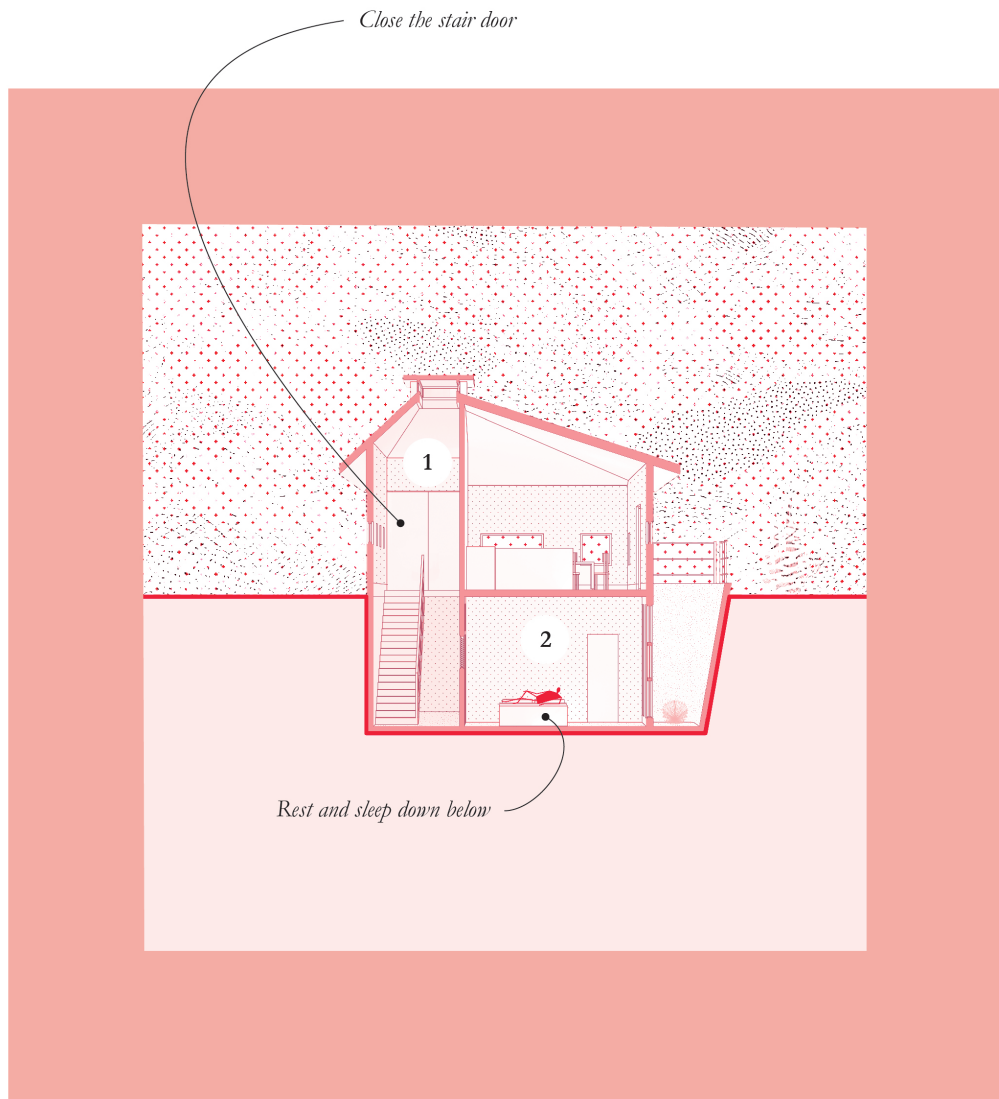
1. A door at the top of the stair defines flow path for warm air
2. Bedrooms remain cooler through the day and night

Figure 136. Ground house section perspective - heat wave

Cooling Energy, Ground House
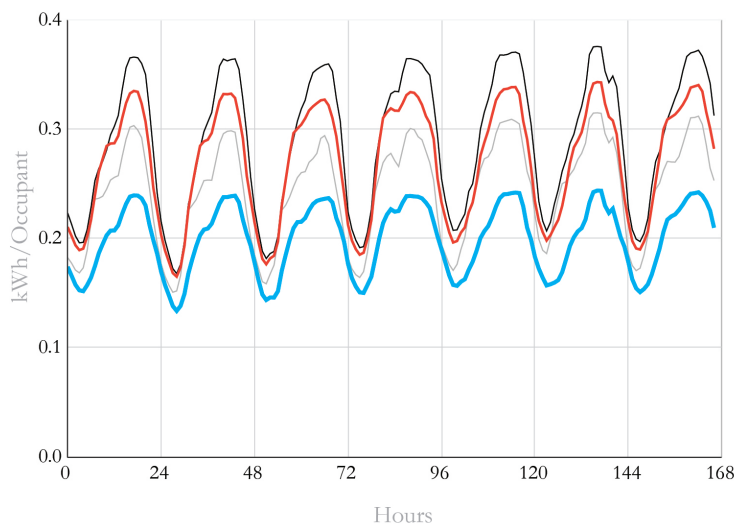
	Cooling Energy / Occupant	
— Base IECC	48.8 kWh	0%
— Base Passive House	40.1 kWh	-17.8 %
— **Ground House**	45.3 kWh	-7.1 %
— **Ground House (Upper Level Off)**	**33.6 kWh**	**-31.1 %**

Figure 137. Ground House hot week cooling energy plot

Heat Index, Ground House
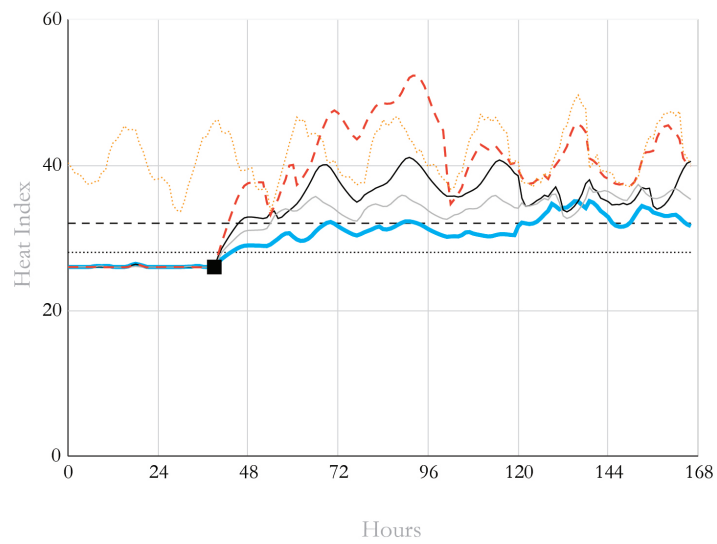
	Heat Hazard Hours >32
—— Base IECC	122
—— Base Passive House	114
— — Ground House (Upper Level)	125
—— Ground House (Lower Level)	44
- - - - Heat Index 28 °C	
— — Heat Index 32 °C	
- - - - Outdoor Heat Index	

Figure 138. Ground House power outage heat index plot

Section 6.4. Party Walls and Unit Adjacency

6.4.1. Introduction

Suburban density, resource intensity, and homogeneity is a well-defined and important problem. Austin and Phoenix are both cities that suffer from so-called urban sprawl as well as economic/racial segregation wherein efforts to densify and diversify are underway.[107] [108] [109] [110] As an attempt to address such an issue, this strategy has thoughts in creating a diversity of housing options in a single location, that range from something that might resemble a single family home, to a small one or two bedroom apartment whereby increasing density and ideally shifting occupant socio-economic diversity.

The second strategy explored is the use of housing attachment and unit aggregation as a means of decreasing cooling demand with an interest in simultaneously increasing social resilience through proximity and diversifying housing type. Figure 139 shows three scenarios where units are coupled and share a party wall and/or ceiling. The occupants in "Two of the Same" are 4 in each home, as such cooling energy is shared between eight occupants. In "Buddy Apartment – Side" and "Buddy Apartment - Below" the large house has an assumed occupancy of 4 and the apartment has an occupancy of 2 so cooling is shared between six occupants. In all schemes, larger houses are 150 m² and apartments are half of the size (75 m²). Additionally, natural ventilation only uses exterior windows with no ventilation through interior doors.

Two of the Same   **Buddy Apartment - Side**   **Buddy Apartment - Below**
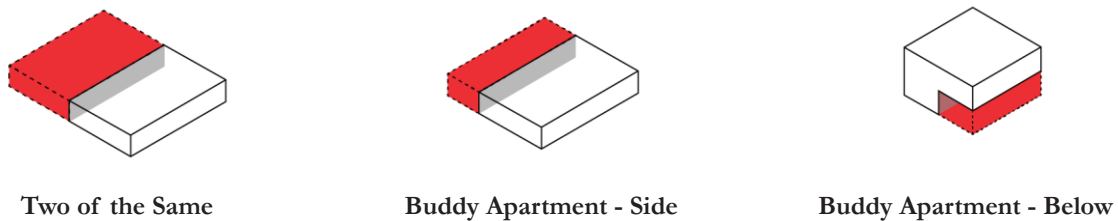
Figure 139. Three tested adjacency scenarios

[107] Helen Cole and Daniel Immergluck, "Reshaping Legacies of Green and Transit Justice through the Atlanta Beltline," in *The Green City and Social Injustice* (Routledge, 2021).

[108] Christopher Lukinbeal, Patricia L. Price, and Cayla Buell, "Rethinking 'Diversity' Through Analyzing Residential Segregation Among Hispanics in Phoenix, Miami, and Chicago," *The Professional Geographer* 64, no. 1 (February 1, 2012): 109–24, https://doi.org/10.1080/00330124.2011.583584.

[109] Eliot Tretter and Moulay Sounny-Slitine, "Austin Restricted: Progressiveism, Zoing, Private Racial Covenants, and the Segregated City" (Institute for Urban Policy Research and Analysis, 2012).

[110] Abigail York et al., "Zoning and Land Use: A Tale of Incompatibility and Environmental Injustice in Early Phoenix," *Journal of Urban Affairs* 36, no. 5 (December 1, 2014): 833–53, https://doi.org/10.1111/juaf.12076.

6.4.2. Performance Testing

Two of the Same

N ↗

Seperate

Together

Hour: 40 (4pm)   64(4pm)   112(4pm)   136(4pm)

Buddy Apartment - Side

Alone

Buddy

Hour: 40 (4pm)   64(4pm)   112(4pm)   136(4pm)

Buddy Apartment - Below

Alone

Buddy

Hour: 40 (4pm)   64(4pm)   112(4pm)   136(4pm)

Heat Index

<18 ºC   **>40 ºC**

Figure 140. Heat index in four party wall and multi-unit scenarios shown at four times during a power outage.

Heat Index: Two of the Same
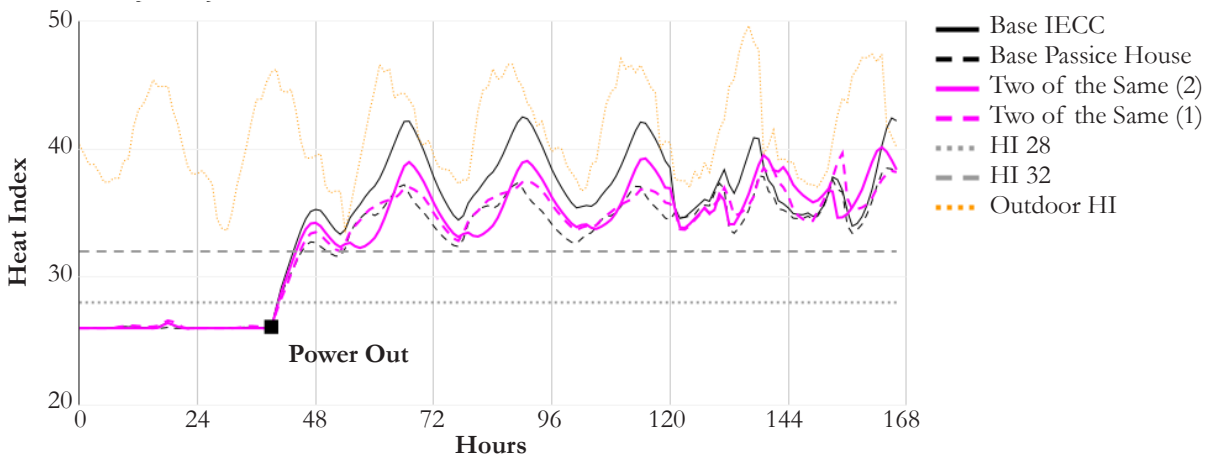
Heat Index: Buddy Apartment-Side
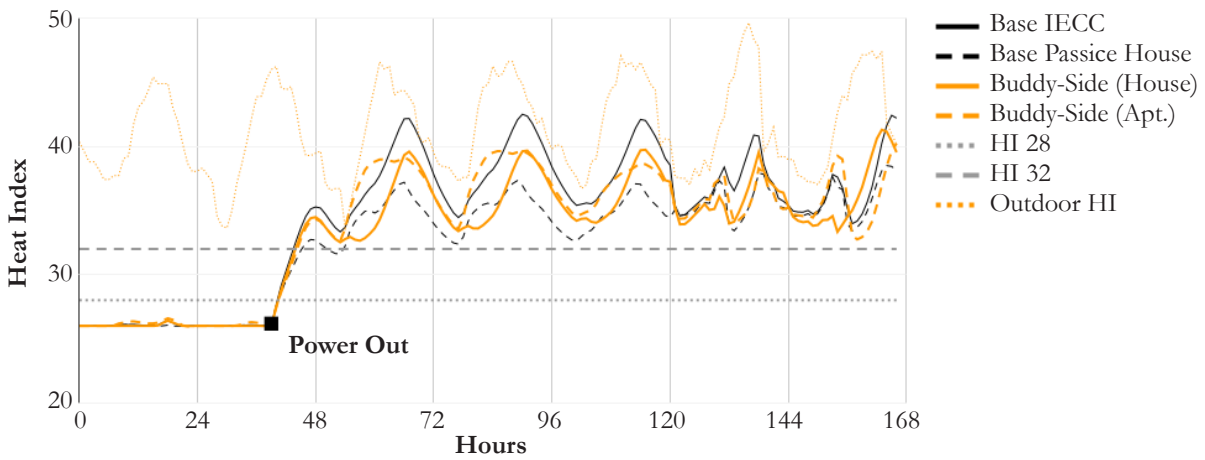
Heat Index: Buddy Apartment-Below
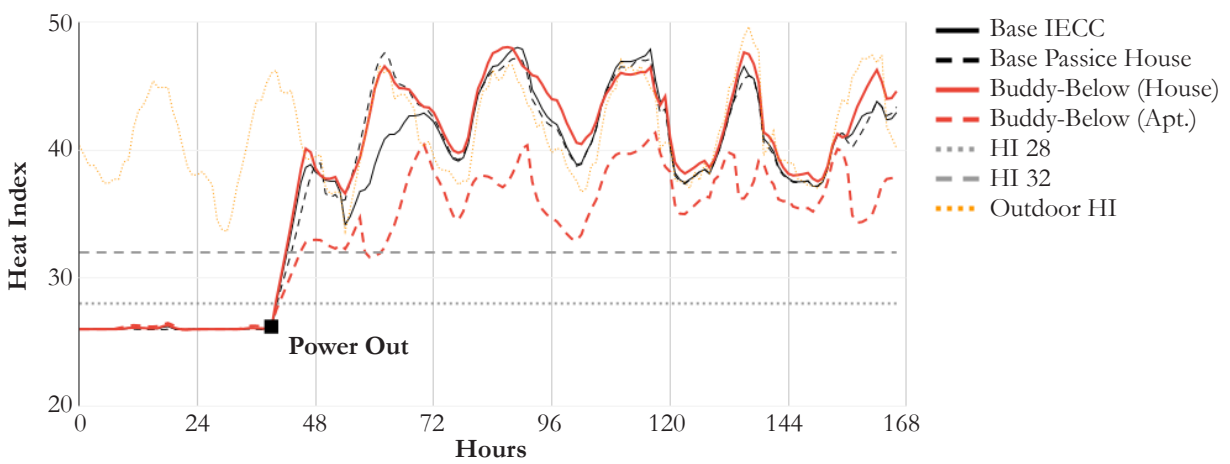
Figure 141. Heat index time plot of the three adjacency scenarios.

184

Cooling Energy Per Occupant as Percent Change from IECC Reference

	Two of the Same	Buddy-Side	Buddy-Below
Reference IECC House:	0%	0%	0%
Reference Passive House:	18%	18%	19%
Party Wall Scenario:	-5%	-5%	-19%

Figure 142.Cooling energy as a percentage of IECC reference for each party wall scenario.

Figure 140 - Figure 142 reveal an important insight in the aggregation and sharing of party walls; buildings with single story party walls do not ultimately decrease cooling magnificently, though 5 percent is not nothing. "Buddy Apartment – Below" manages to decrease cooling energy per head signif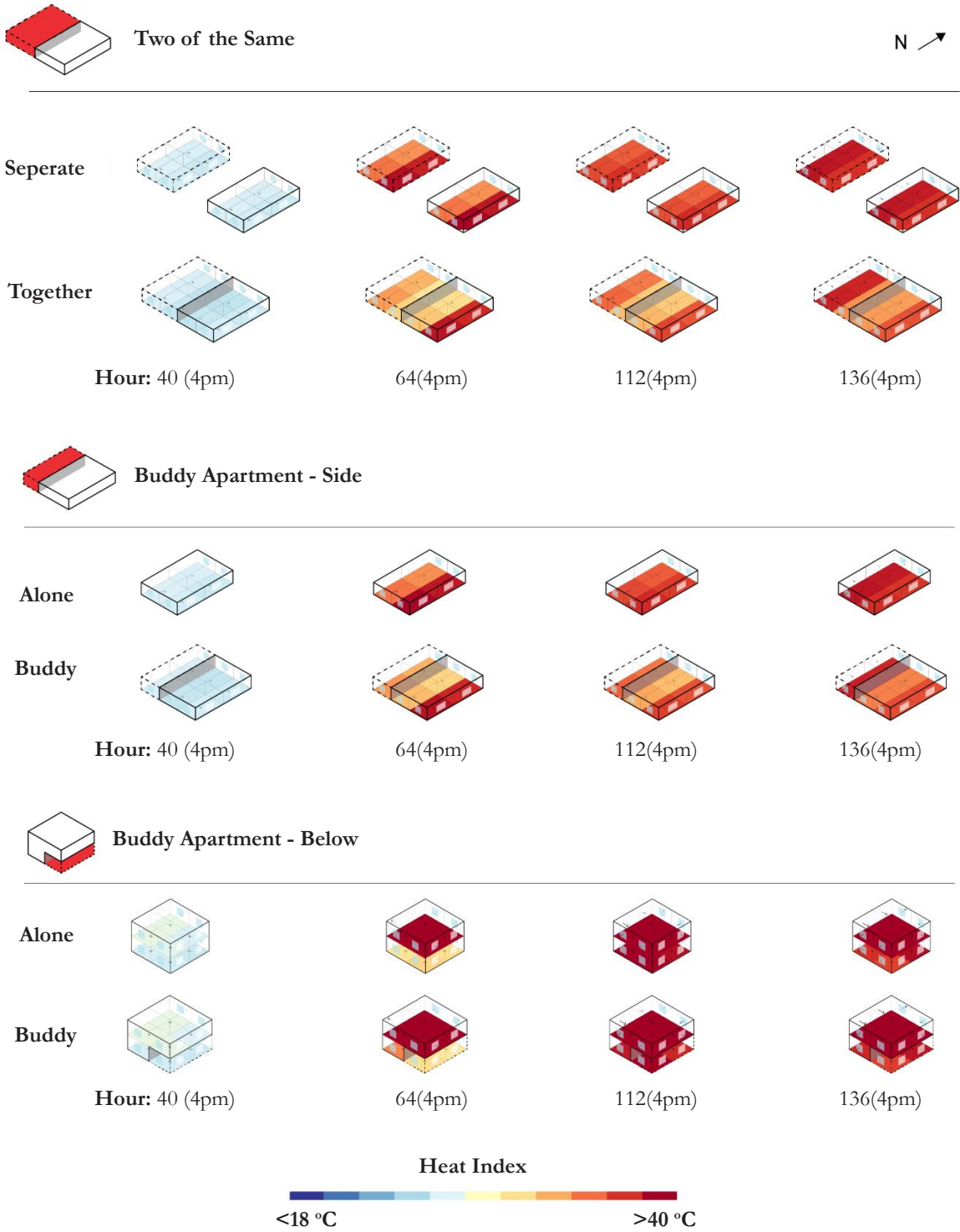icantly, however, Figure 141 shows that the house does not perform better, largely because the majority of the large house is on the upper floor. One reading of this is that while floor area remains the same, overall building volume is reduced in a two-story house compared to a single story with the same area. This combined with an increase in density (from four to six occupants results in cooling energy benefits. A two story shades the lower floor reducing solar exposure and benefits from ground coupling. The apartment of "Buddy Apartment – Below" stays cooler than the house, but still has the majority of its hours above HHH32. "Two of the Same" and "Buddy Apartment-Side" do reduce hazard hours through adjacency, but their heat hazard hours are still very high with most above HHH32. Figure 140 shows that many of the interior zones with less exposure to the outdoors remain cooler when they have a party wall, as well as showing that the lower floor remains cooler for longer in a grid-off scenario. An implication of this result is that if an apartment sits below the main house, it may have a reduced cooling demand, which aligns with the ethos of this experiment, which is to increase the diversity of housing stock in a given area.

Section 6.5. Shared House

Occupancy: 6
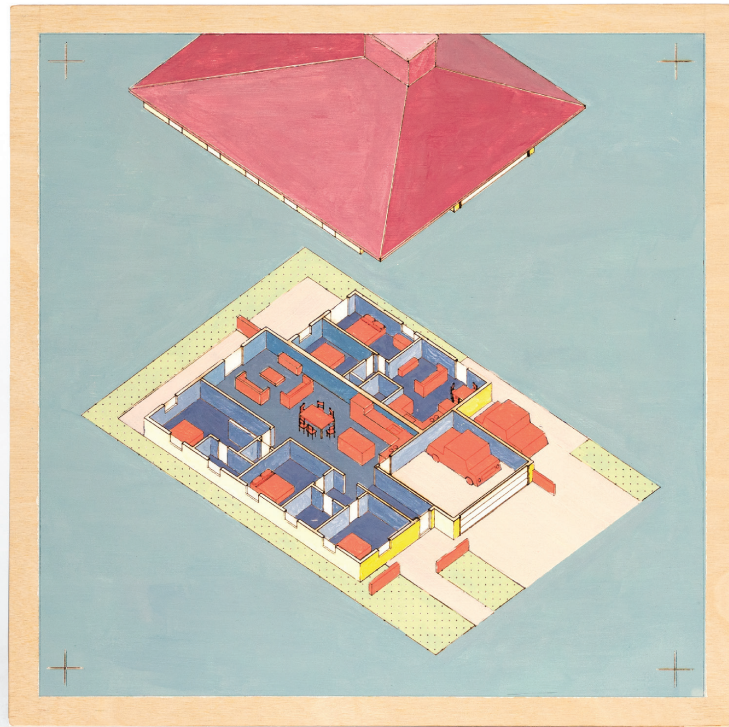
Share House
Thermo-chromic paint on wood - 12"x12"
No heat applied

Figure 143. Shared House painting - normal conditions

*A suggestively massive central wall divides
the larger house from a two bedroom side apartment*

1. Three bedroom house
2. Two or one bedroom apartment

Figure 144. Shared House section perspective - normal conditions
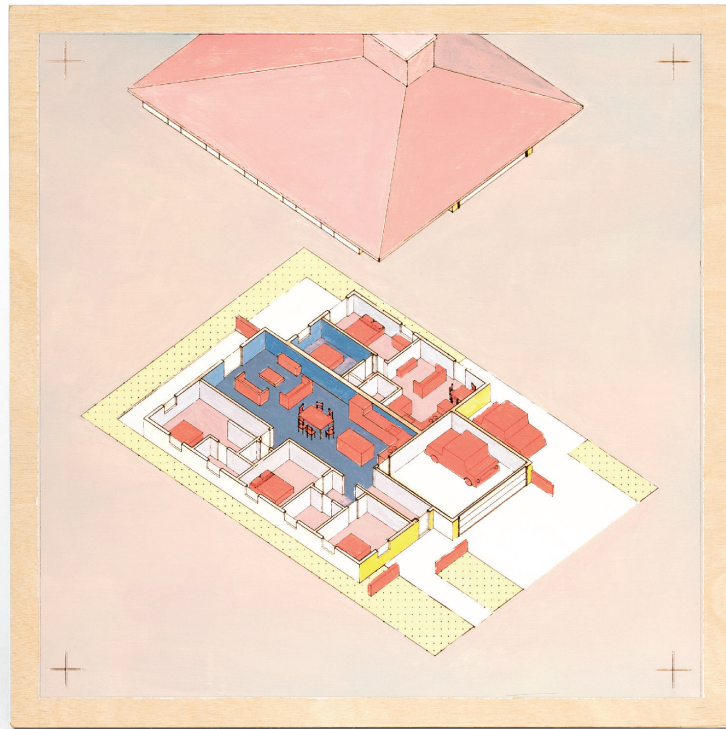
Share House
Thermo-chromic paint on wood - 12"x12"
Heat applied

Figure 145. Shared House painting - heat wave
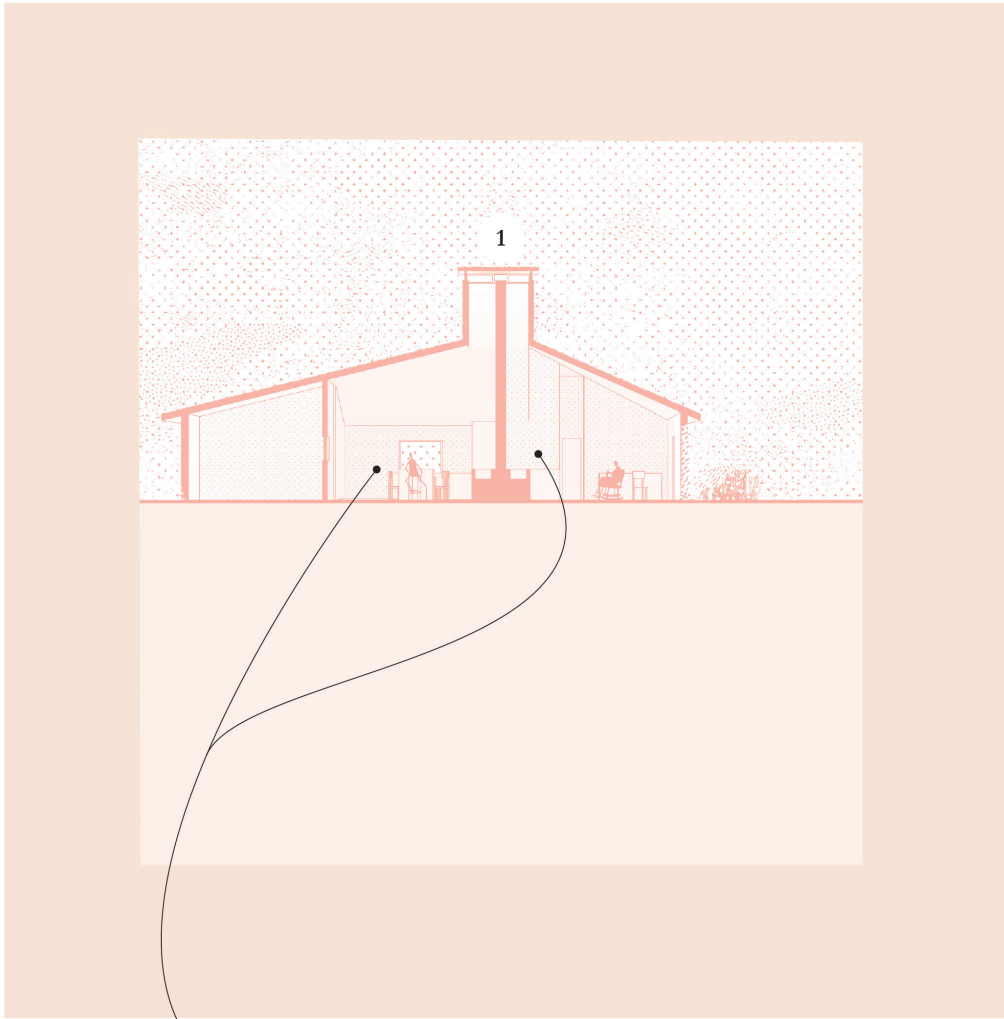
1. A suggestive ventilation chimney drives natural ventilation in each home when appropriate

*Zones on either side of the wall stay cool
during peak heat of the day*

Figure 146. Shared House section perspective - heat wave

Cooling Energy, Shared House
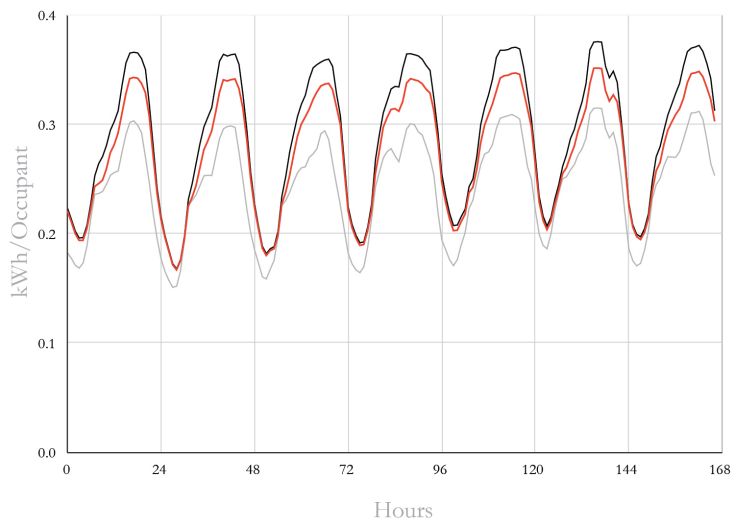
	Cooling Energy / Occupant	
■ Base IECC	48.8 kWh	0%
■ Base Passive House	40.1 kWh	-17.8 %
■ Shared House	45.6 kWh	-6.5%

Figure 147. Shared House hot week cooling energy plot

Heat Index, Shared House
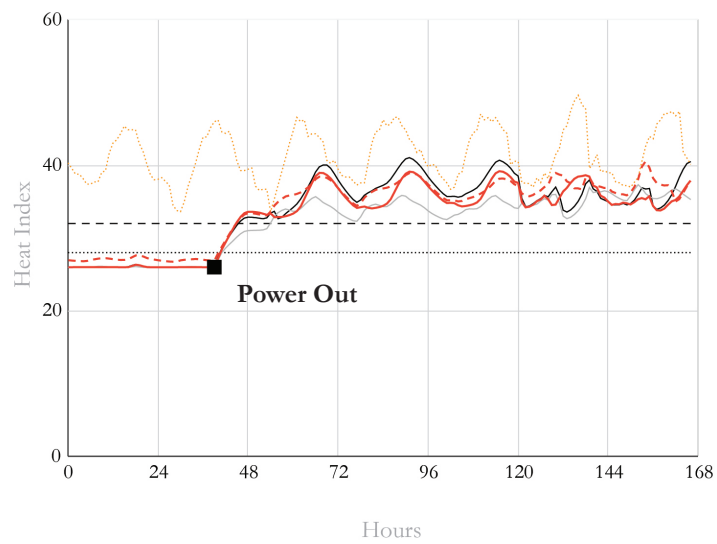
	Heat Hazard Hours >32
—— Base IECC	122
—— Base Passive House	114
- - **Small Apartment**	123
—— **Main House**	123
---- Heat Index 28 ℃	
– – Heat Index 32 ℃	
---- Outdoor Heat Index	

Figure 148. Shared House power outage heat index plot

Section 6.6. Zone Nesting

6.6.1. Introduction

A concept studied rigorously and also exercised in practice is the use of thermal gradients, buffer zones, and nests in buildings. [111] [112] Little research exists, however, on the use of this strategy as a resilience method. This strategy is tested for its application in heat resilience as a means of cooling one zone, or creating a cool zone in the event of a power outage. For this study, three nest sizes are tested and are decided as a fraction of floor area: 20m² (~1/8th), 40m² (~1/4th), and 80m² (~1/2). Two specific scenarios are of interest, the first is the application of targeted cooling, where one or two zones receive cooling, and the other zones free-run, similar to the resilience applications in 6.3. The comparison, then, is between cooling energy demand of a standard building layout and the nested zones (Figure 149). Importantly, though the focus of this strategy is on added resilience and passive survivability, zone reconfiguration does result in marginally different cooling demands with slightly higher peaks as can be seen in Figure 150. The tested scenarios are resilience scenarios. As such, the nest is assumed to have full occupancy of the house (four people) during cooling and during the power outage. Nest zones have doors which operate if the zones reach 5 ℃ of the outdoor dry bulb temperature. This never occurs in the simulations, because of the extremes found in the 2050 hot weather week.
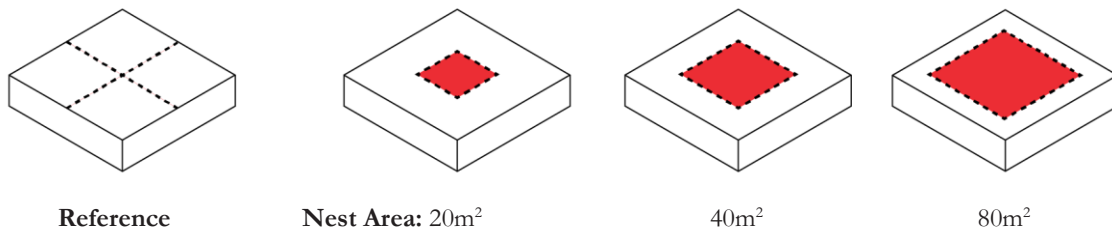
Figure 149. Reference zone layout and tested nest areas
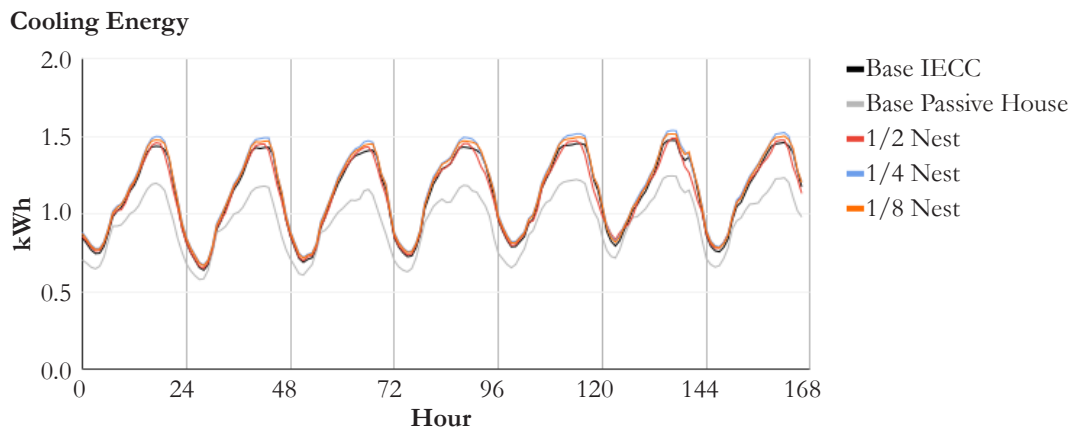
Figure 150. Nest scenario cooling

[111] Frank Suerich-Gulick, Anna Halepaska, and Salmaan Craig, "Cascading Temperature Demand: The Limits of Thermal Nesting in Naturally Ventilated Buildings," *Building and Environment* 208 (January 2022): 108607, https://doi.org/10.1016/j.buildenv.2021.108607.
[112] Lacaton & Vassal, *Transformation de 530 Logements*, 2017, Building, Bordeaux, France, 2017.

6.6.2. Targeted Cooling

Shown in Figure 151 is a targeted cooling scenario where the quarter nest is compared with a quarter of the reference house being cooled. Importantly, the quarter nest targeted cooling performs worse than the corner cooling, not with higher peaks, but greater total energy. This is likely a result of being surrounded by zones that are overheating and a small area with high occupancy. The eighth nest is included in the time plot in Figure 151 demonstrating that a further reduction is possible, yet a 4% decrease from corner cooling for half of the cool space does not make it viable.
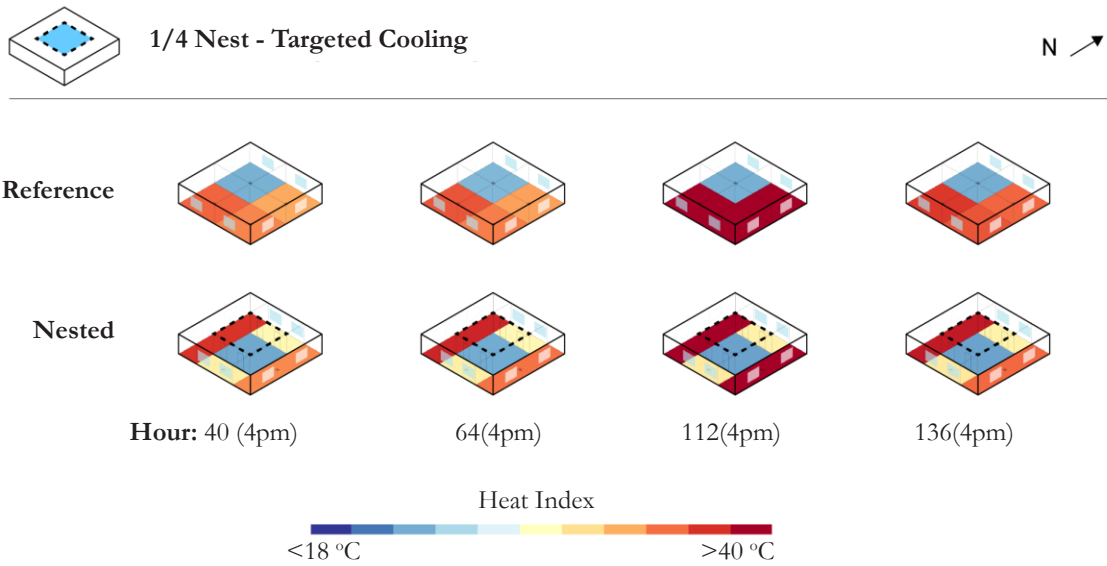
1/4 Nest - Targeted Cooling   N

Reference

Nested

Hour: 40 (4pm)   64(4pm)   112(4pm)   136(4pm)

Heat Index

<18 ºC   >40 ºC

Cooling Energy Per Occupant as Percent Change from IECC Reference

Reference IECC House:	0%
Reference Passive House:	-15%
Corner Cooling:	-51%
Quarter Nest Cooling:	-44%
Eighth Nest Cooling:	-55%

Cooling Energy
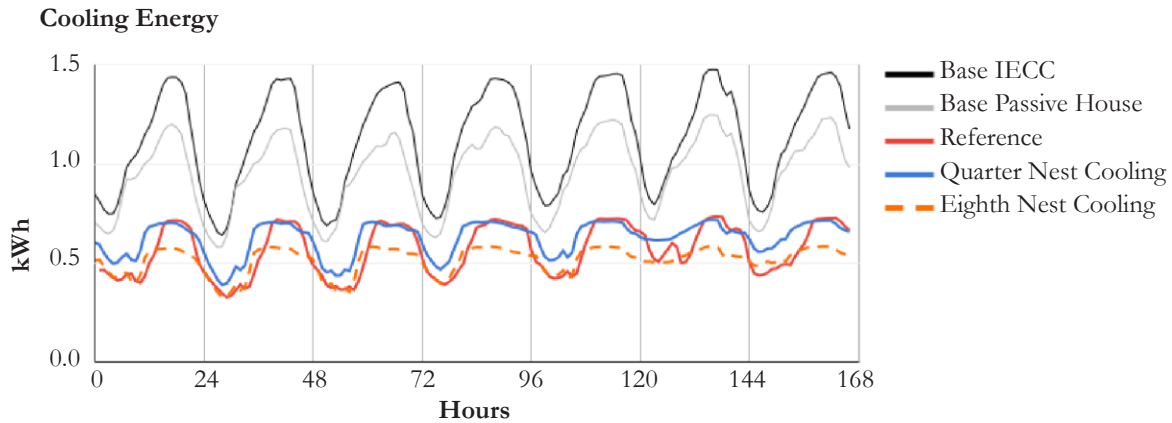
Figure 151. Quarter nest targeted cooling scenarios

193

In the half nest targeted cooling scenario, however, the half nest does perform more favorably than the half-cooled area, (Figure 152), likely a result of the reference building having twice as much exposed façade area than the corner cooling scenario in Figure 151. The half nest, with greater cooled area, does not reduce the cooling energy demand as much as the quarter nest which is to be expected. The bottom line is that being able to target and cool specific zones has a dramatic impact on cooling demand. The implications for the nesting strategy are not immediately obvious. Smaller nested rooms do not reduce cooling demand over simply targeting an existing room. Larger nested rooms with a narrower buffer reduce cooling demand when compared to the reference house.
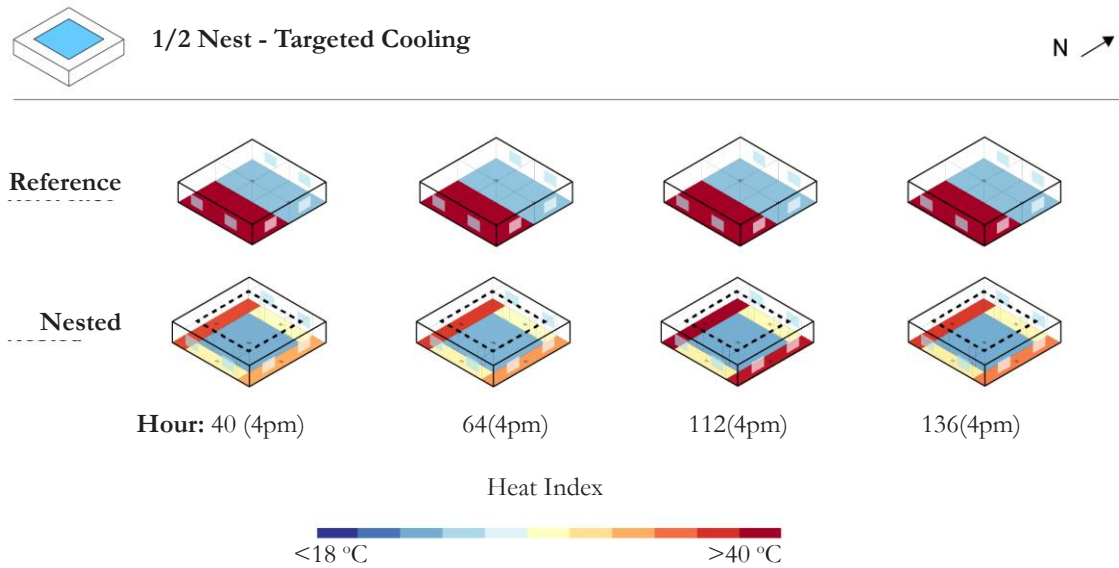
1/2 Nest - Targeted Cooling

Cooling Energy Per Occupant as Percent Change from IECC Reference

Reference IECC House:	0%
Reference Passive House:	-15%
Corner Cooling:	-30%
Quarter Nest Cooling:	-33%
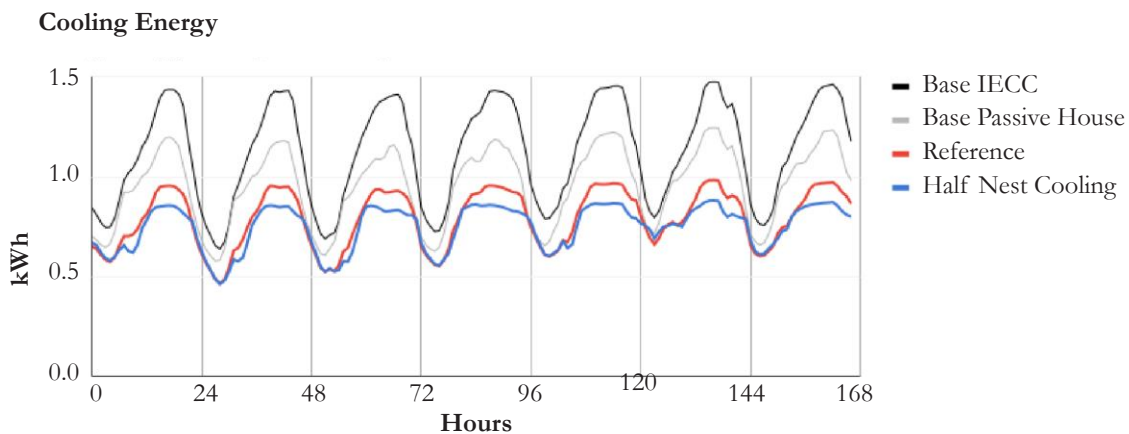
Cooling Energy

Figure 152. Half nest targeted cooling scenarios

6.6.3. Power Outage Resilience

While zone nesting shows some promise in reducing peak loads and reducing total energy demand if applied in the right circumstance, the main strength of zone nesting is in power outage resilience. As can be seen in Figure 153 - Figure 155, larger zones stay cooler as a result of more area per occupant in the nested zone. Visualizations are shown at 4pm on multiple days, which is generally the time that the outdoor heat index peaks. The nested zone does have a higher heat index than its buffer zones during a period of a few hours during the night. Half nest generally performs better in this case with its nest having a lower peak heat index than the quarter nest. It should be noted that all zones have the majority of their hours well above HHH32 and well into the heat index danger zone, though are still lower than the heat index outside.
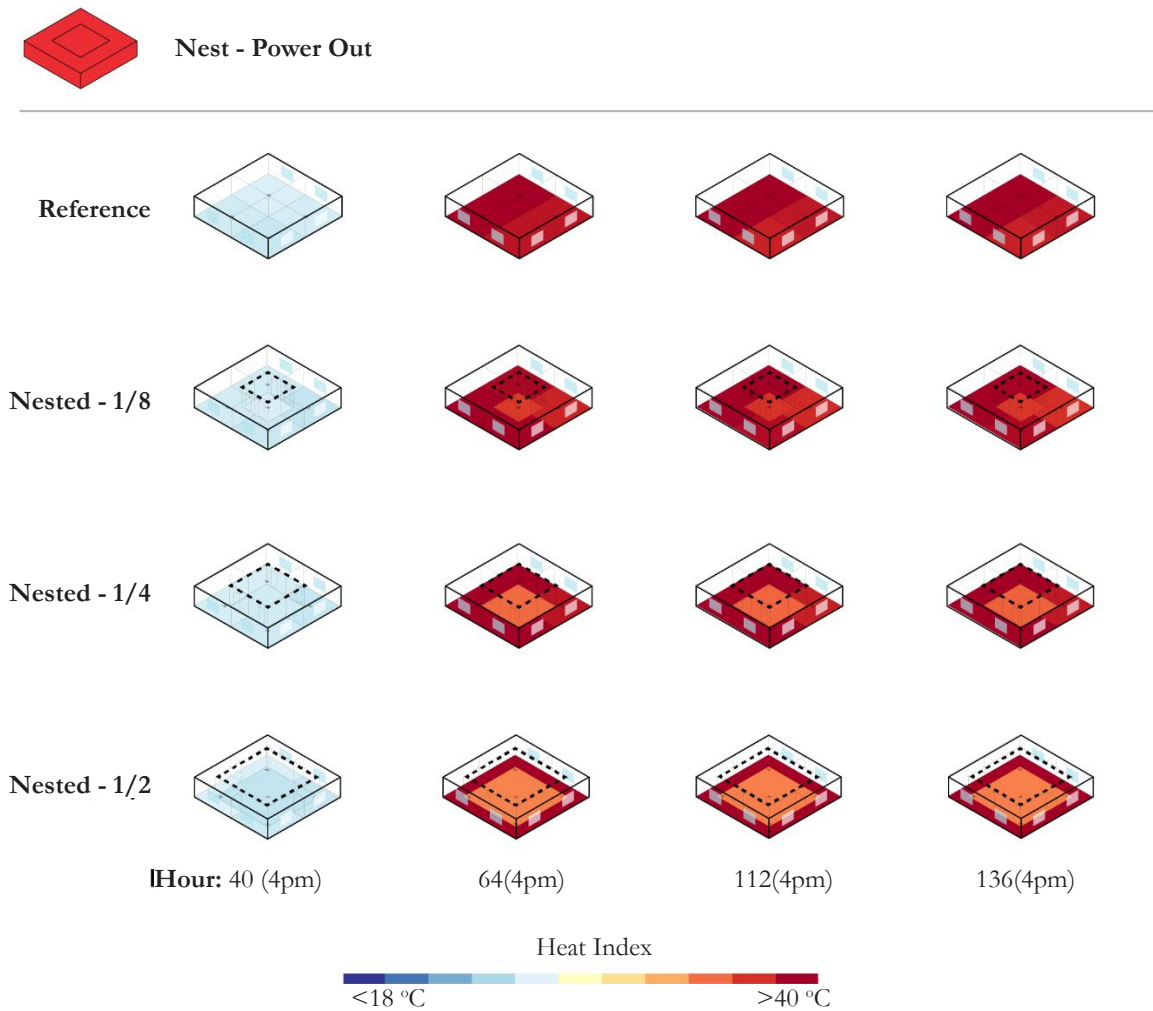
Figure 153. Point in time power outage representations of each nest scenario.

Cooling Energy, Quarter Nest
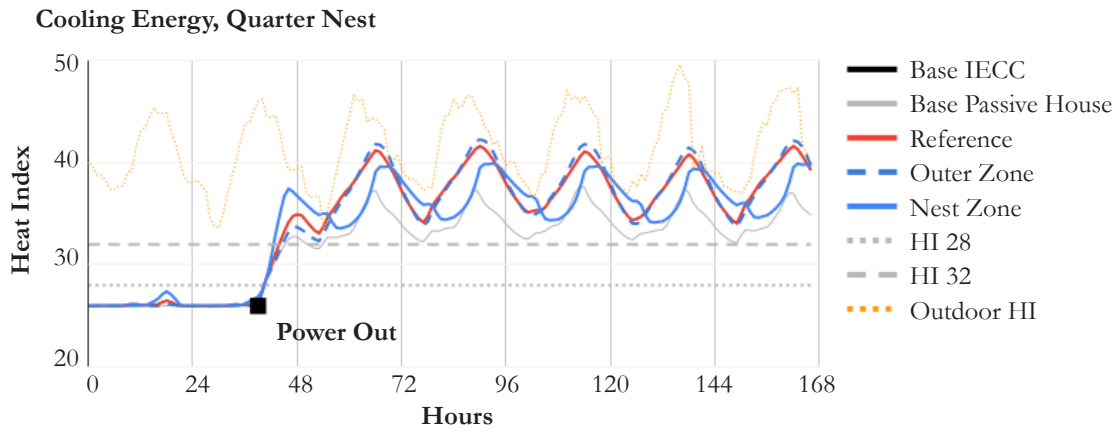
Figure 154. Heat index plot of quarter nest and reference during power outage

Cooling Energy, Half Nest
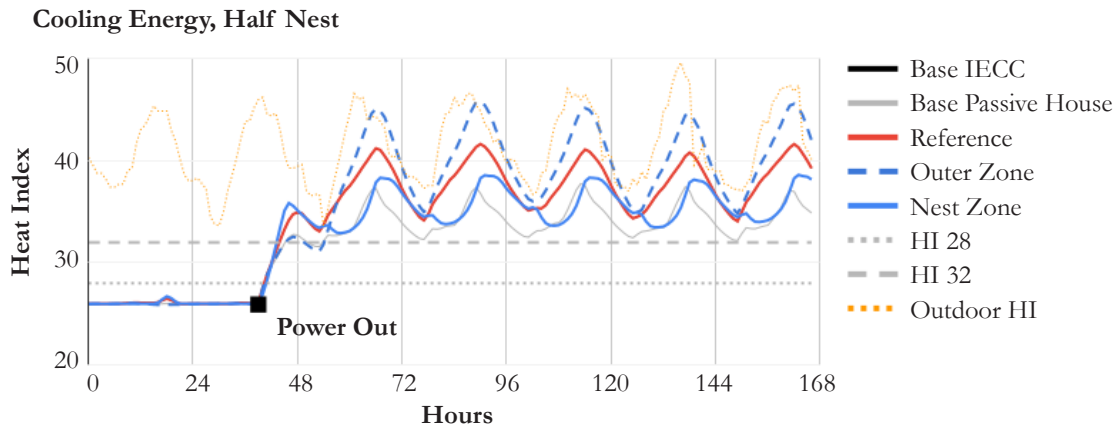
Figure 155. Heat index plot of half nest and reference during power outage

6.6.4. Nest House
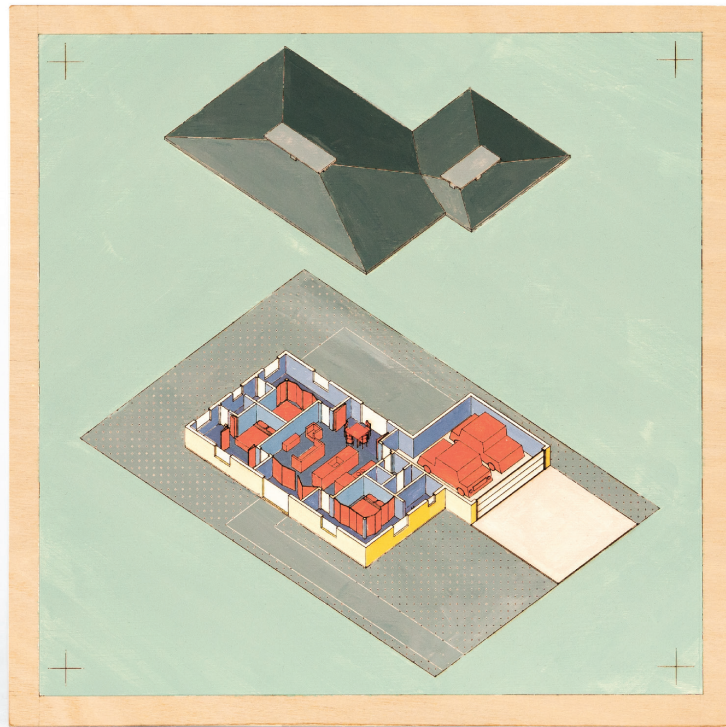
Nest House
Thermo-chromic paint on wood - 12"x12"
No heat applied

Figure 156. Nest House painting - normal conditions

Central, open living space opens to gardens on both sides
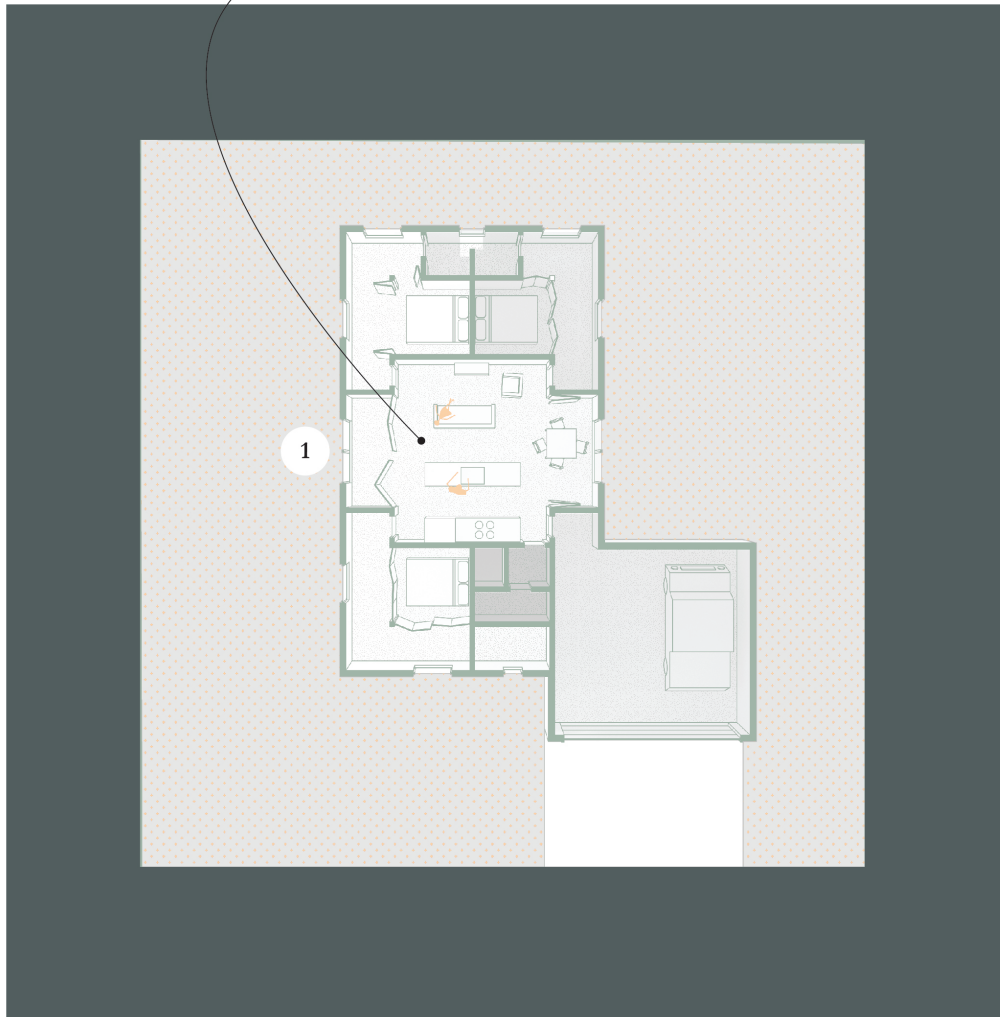
1. Side entrance gives privacy

Figure 157. Nest House plan perspective - normal conditions
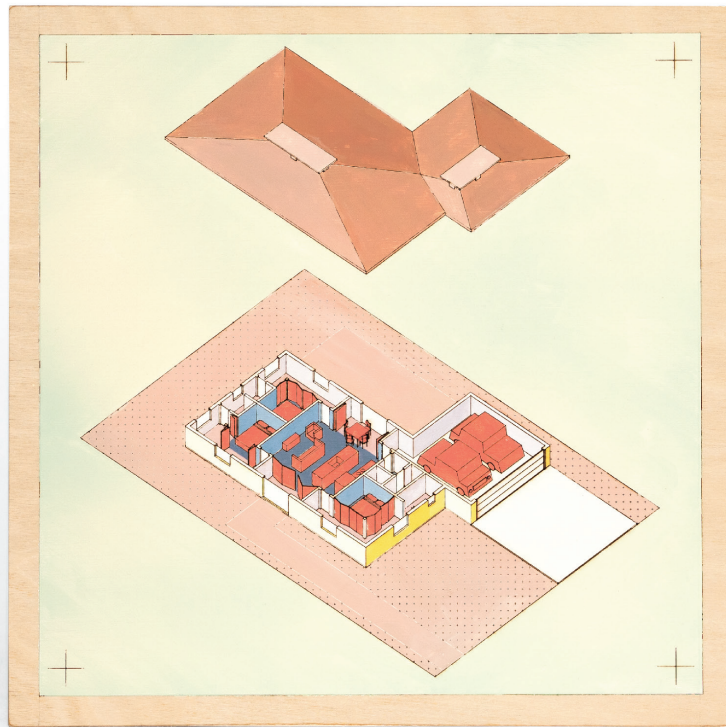
Nest House
Thermo-chromic paint on wood - 12"x12"
Heat applied

Figure 158. Nest House painting - heat wave

Thermal buffer zone

Bi-fold doors close to reduce cooled area.
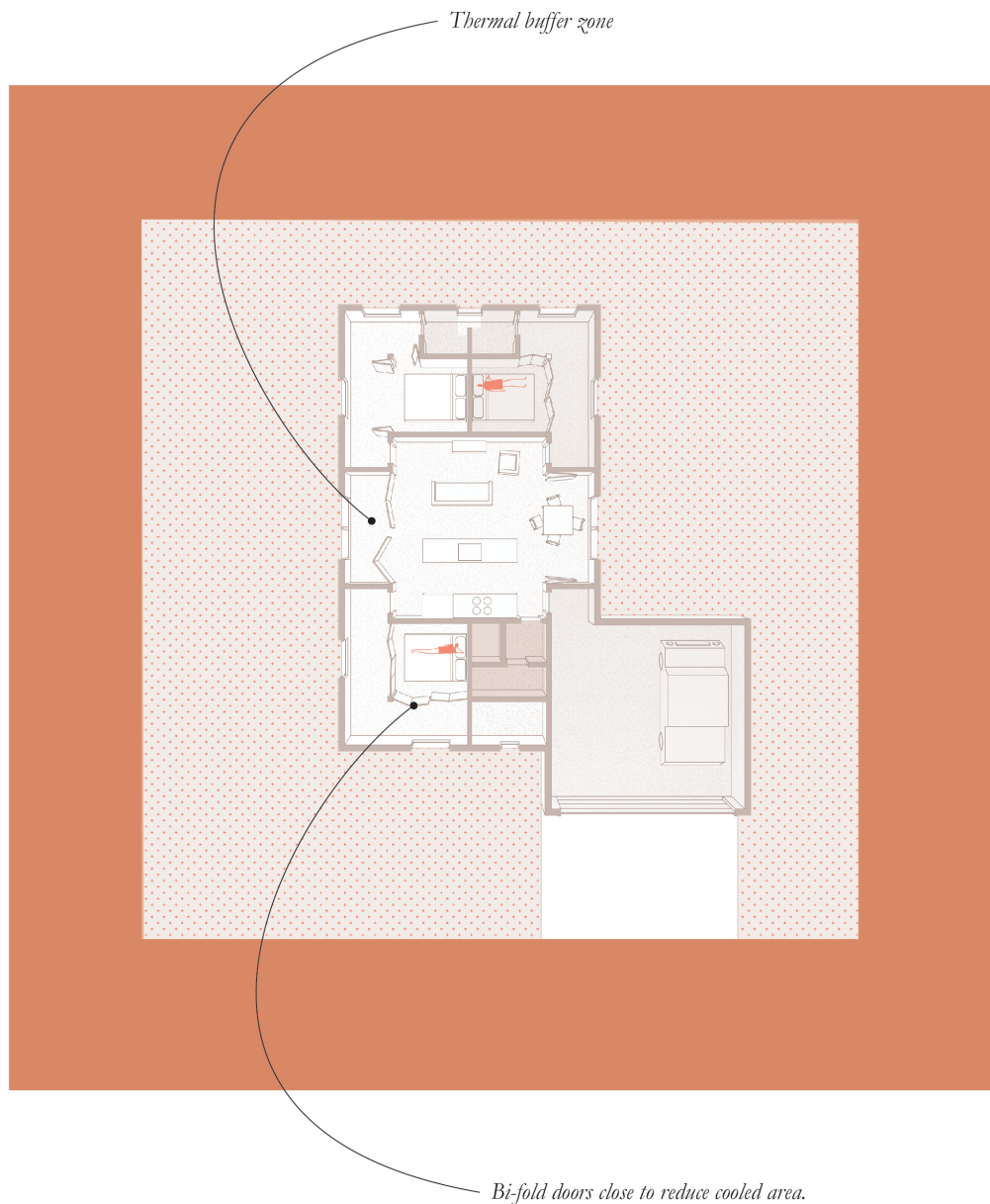
Figure 159. Nest House plan perspective - heat wave

Cooling Energy, Nest House
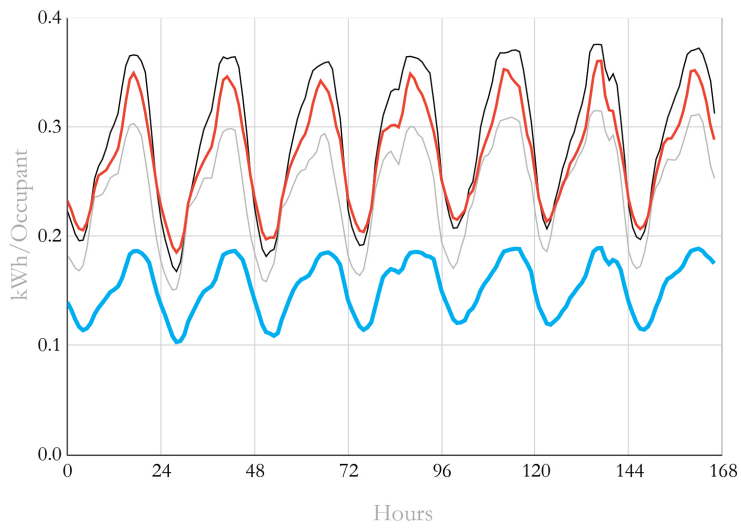
	Cooling Energy / Occupant	
▬ Base IECC	48.8 kWh	0%
▬ Base Passive House	40.1 kWh	-17.8 %
▬ **Nest House**	46.4 kWh	-4.6%
▬ **Nest House (Outer Zone Off)**	**25.6 kWh**	**-47.5 %**

Figure 160. Nest House hot week cooling energy plot

Heat Index, Nest House

Heat Index

60

40

20

0

Power Out

0   24   48   72   96   120   144   168
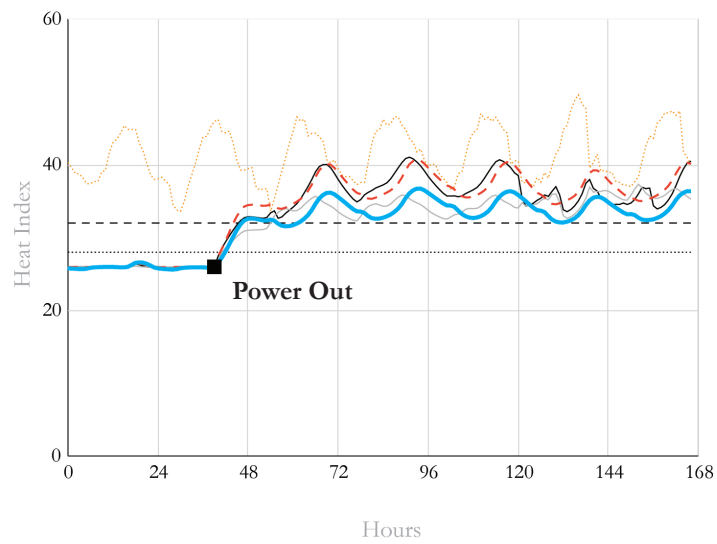
Hours

		Heat Hazard Hours >32
——	Base IECC	122
——	Base Passive House	114
– –	**Nest House (Outer)**	123
——	**Nest House (Inner)**	123
----	Heat Index 28 °C	
– –	Heat Index 32 °C	
----	Outdoor Heat Index	

Figure 161. Nest House power outage heat index plot

203

6.6.5. Huddle House

Huddle House combines the three strategies and shows a building with three homes.
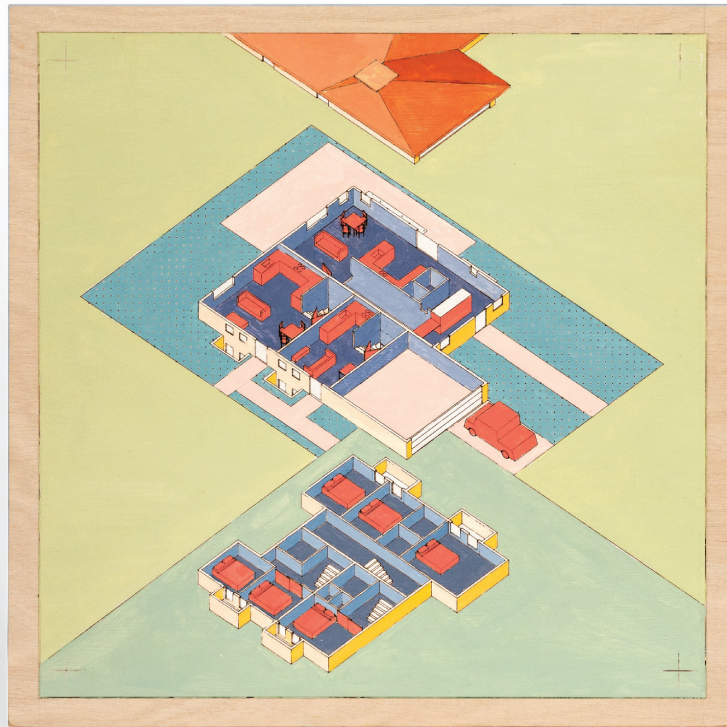
Three House
Thermo-chromic paint on wood - 12"x12"
No heat applied

Figure 162. Three House painting - normal conditions

Canted light-wells and tall windows draw light into sunken bedrooms
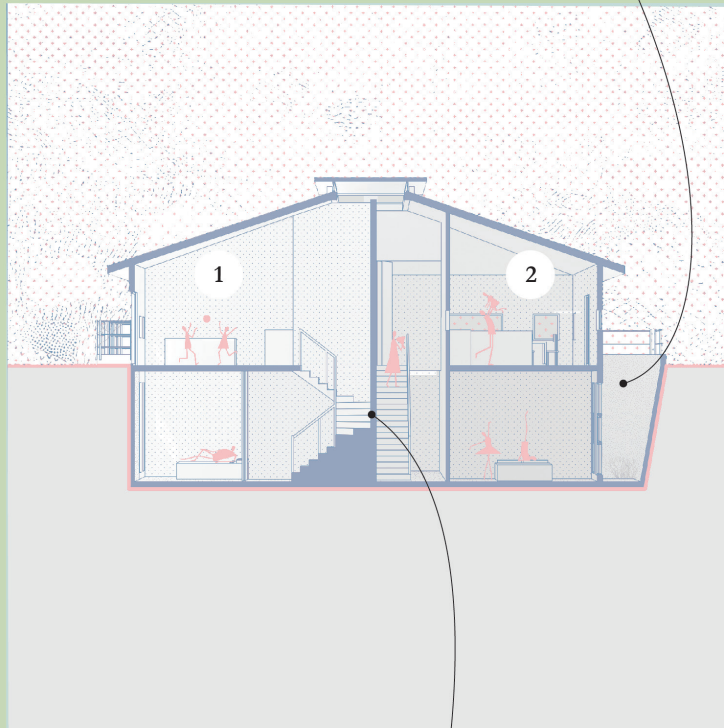
1. One or two bedroom apartment
2. Three bedroom house

Abutting stair-wells create an acoustic buffer between homes

Figure 163. Three House section perspective - normal conditions
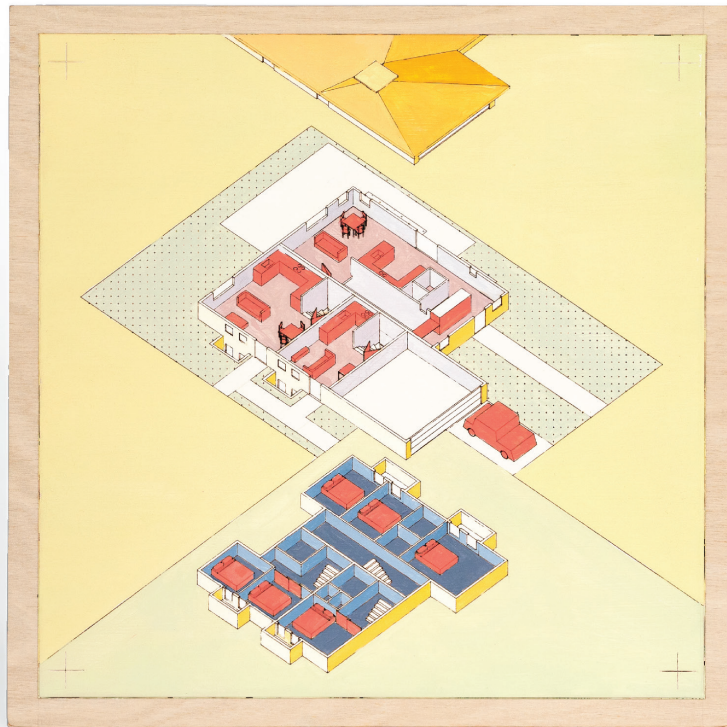
Three House
Thermo-chromic paint on wood - 12"x12"
Heat applied

Figure 164. Three House painting - heat wave
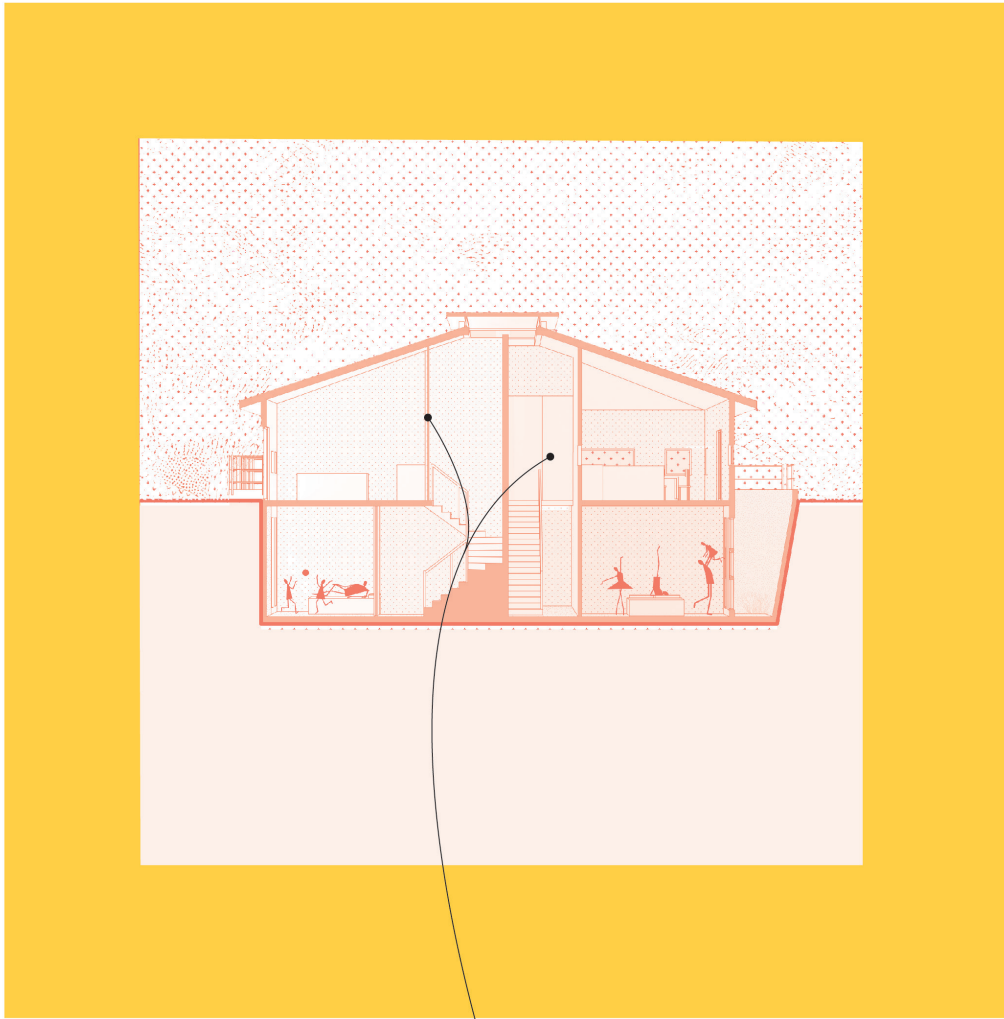
During a heat wave, or even just for the night,
close the upper floor and retreat below

Figure 165. Three House section perspective - heat wave

Cooling Energy, Huddle House
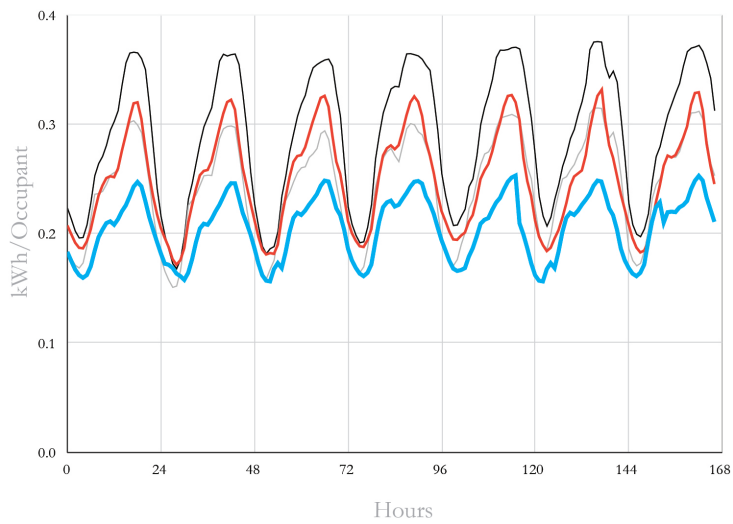
	Cooling Energy / Occupant	
▬ Base IECC	48.8 kWh	0%
▬ Base Passive House	40.1 kWh	-17.8 %
▬ Three House	41.9 kWh	-14.1%
▬ Three House (Upper Zone Off)	**34.4 kWh**	**-29.5 %**

Figure 166. Three House hot week cooking energy plot

Heat Index, Huddle House
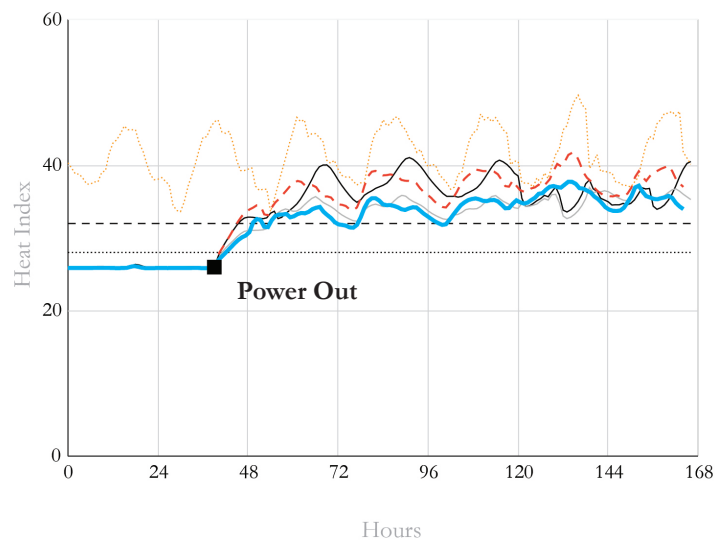
	Heat Hazard Hours >32
—— Base IECC	122
—— Base Passive House	114
– – Three House (Upper Level)	122
—— Three House (Lower Level)	110
- - - - Heat Index 28 °C	
– – Heat Index 32 °C	
- - - - Outdoor Heat Index	

Figure 167. Three House power outage heat index plot

Chapter 7
Heat Resilient Hamlet

Chapter 7. Heat Resilient Hamlet

A proposal for heat resilient housing uses four suburban plots combined with a street on either side. Sited in Phoenix and using IECC constructions, the proposal builds on the strategies expanded in Chapter 6. Energy simulations are performed over the same hot week in a Phoenix climate, yet, the proposal remains somewhat orientation and site agnostic – apart from its intentions to reflect desires of low-density living.
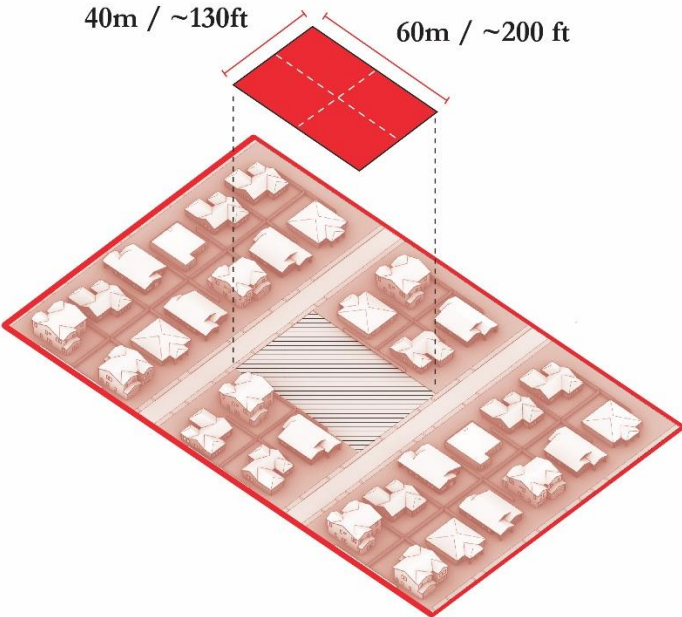
Figure 168. Heat resilient hamlet is sited on four urban plots

The proposal is a collection of homes that, from the street, fits into a low-rise neighborhood.
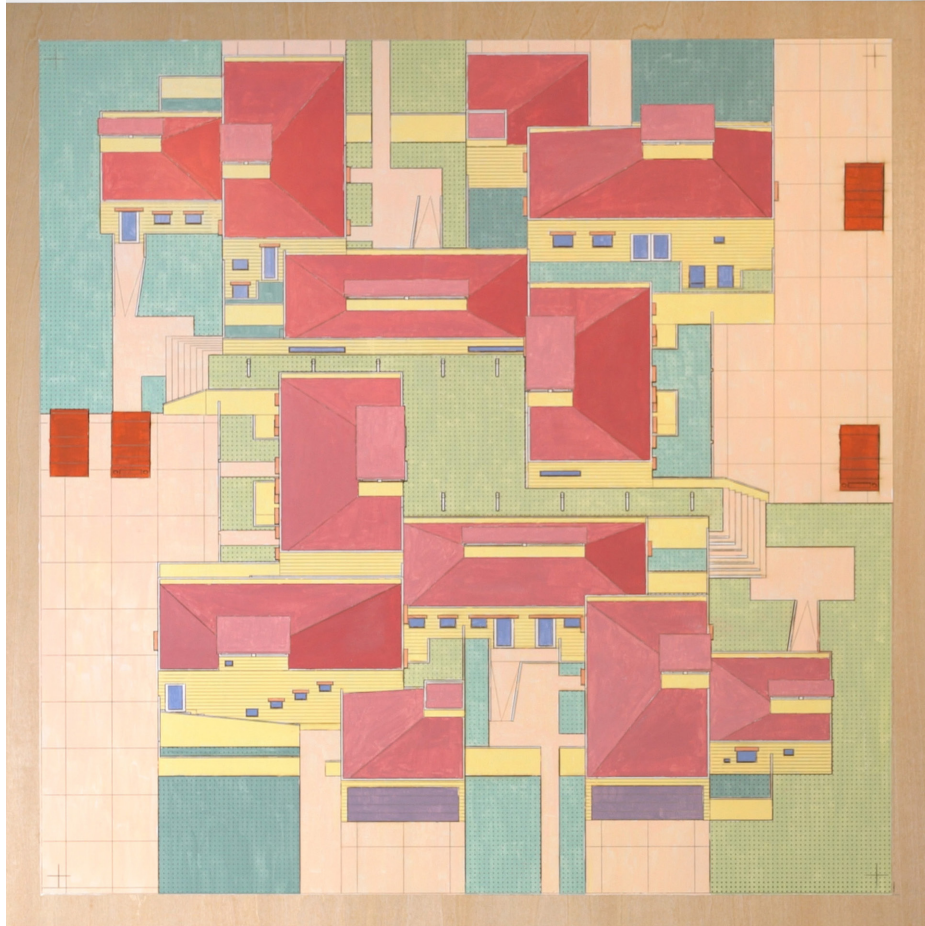
Figure 169. 24"x24" Axonometric Oblique in Thermochromic Paint (No Heat Applied)
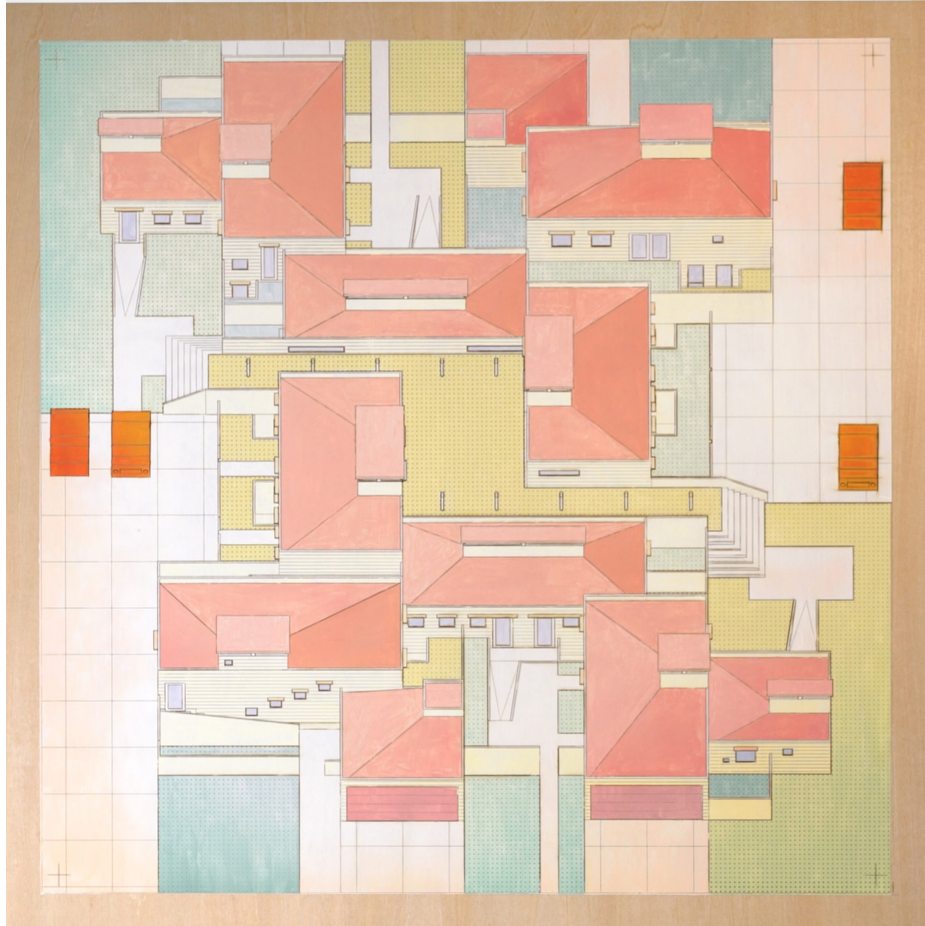
Figure 170. 24"x24" Axonometric Oblique in Thermochromic Paint (Heat Applied)

The larger units have basement rooms, and studios remain on one level though slightly sunken into the ground. Driveways on each side give access to the apartments at the back.
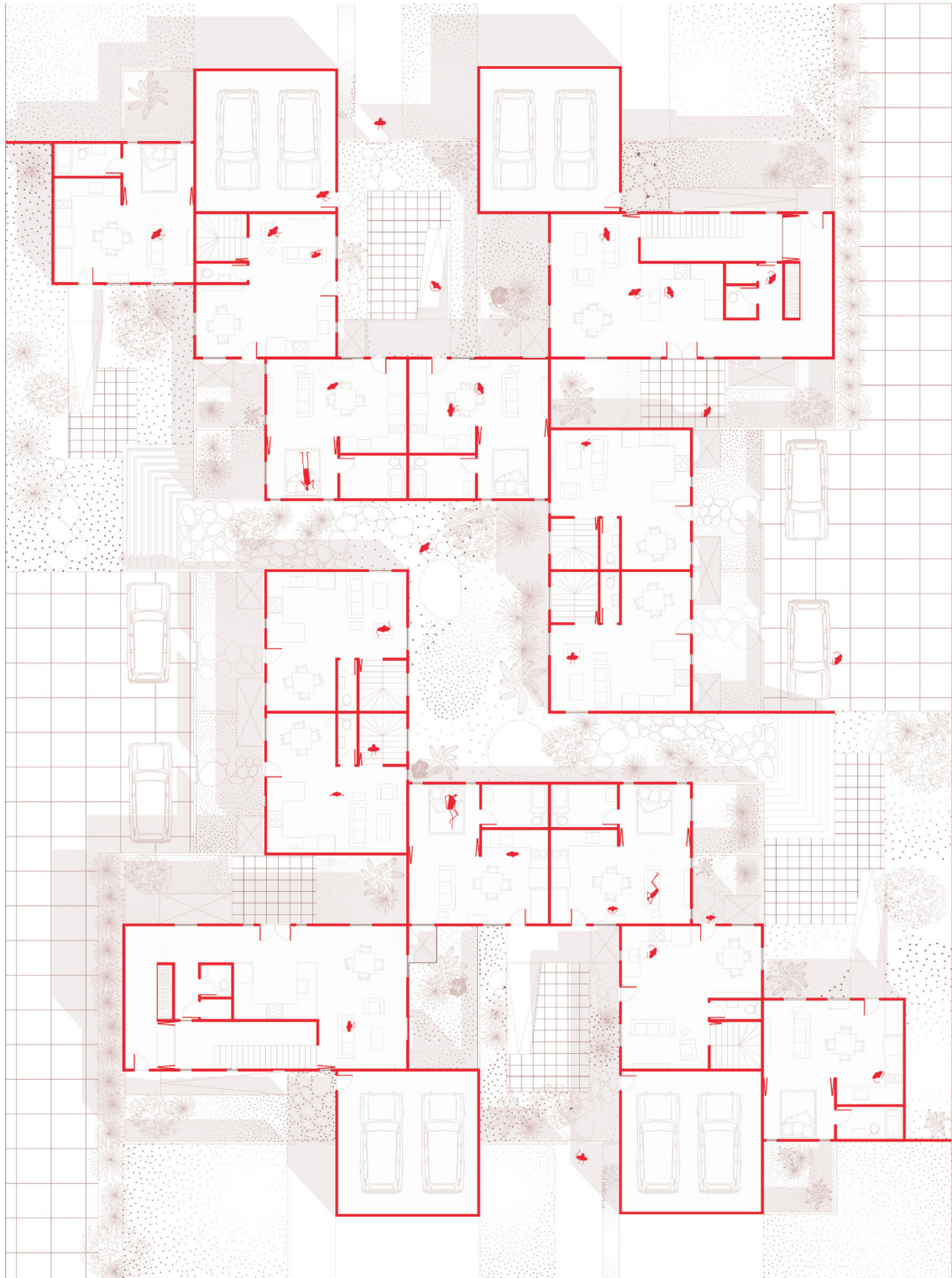
Figure 171. Ground plan of the heat resilient hamlet

Many of the homes prioritize a sense of privacy and individuality through both the entrance and views to private gardens preserving desired aspects of low density living.
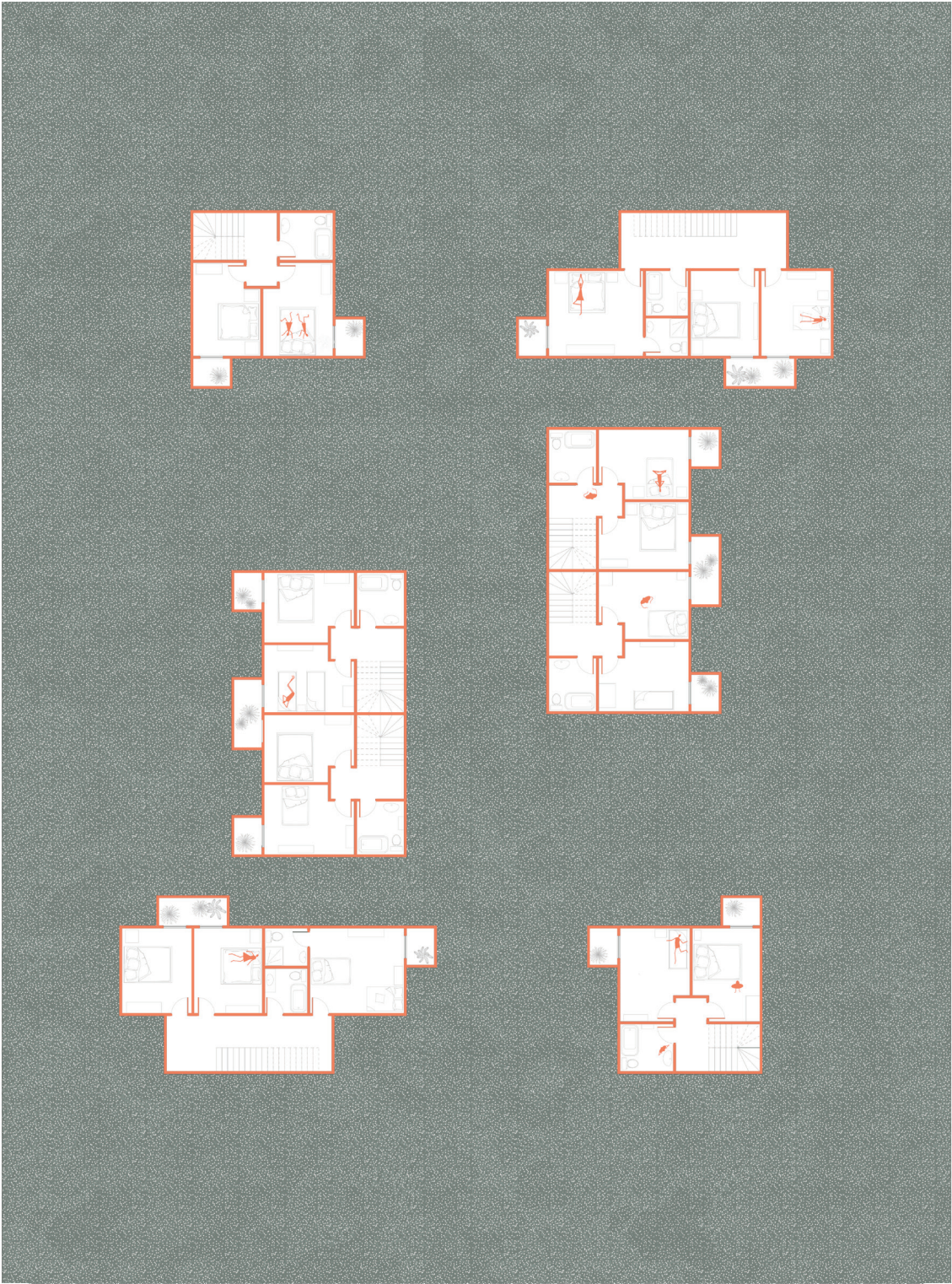
Figure 172. Basements plan of the heat resilient hamlet

Three Bedroom Homes

Size:	~1600 ft²
Assumed Occupancy:	3.5

One/Two Bedroom Homes

Size:	~800 ft²
Assumed Occupancy:	2.5

Studio Homes

Size:	1600 ft²
Assumed Occupancy:	1.5

Total Site Occipancy: ~30
Approximately doubling the site density
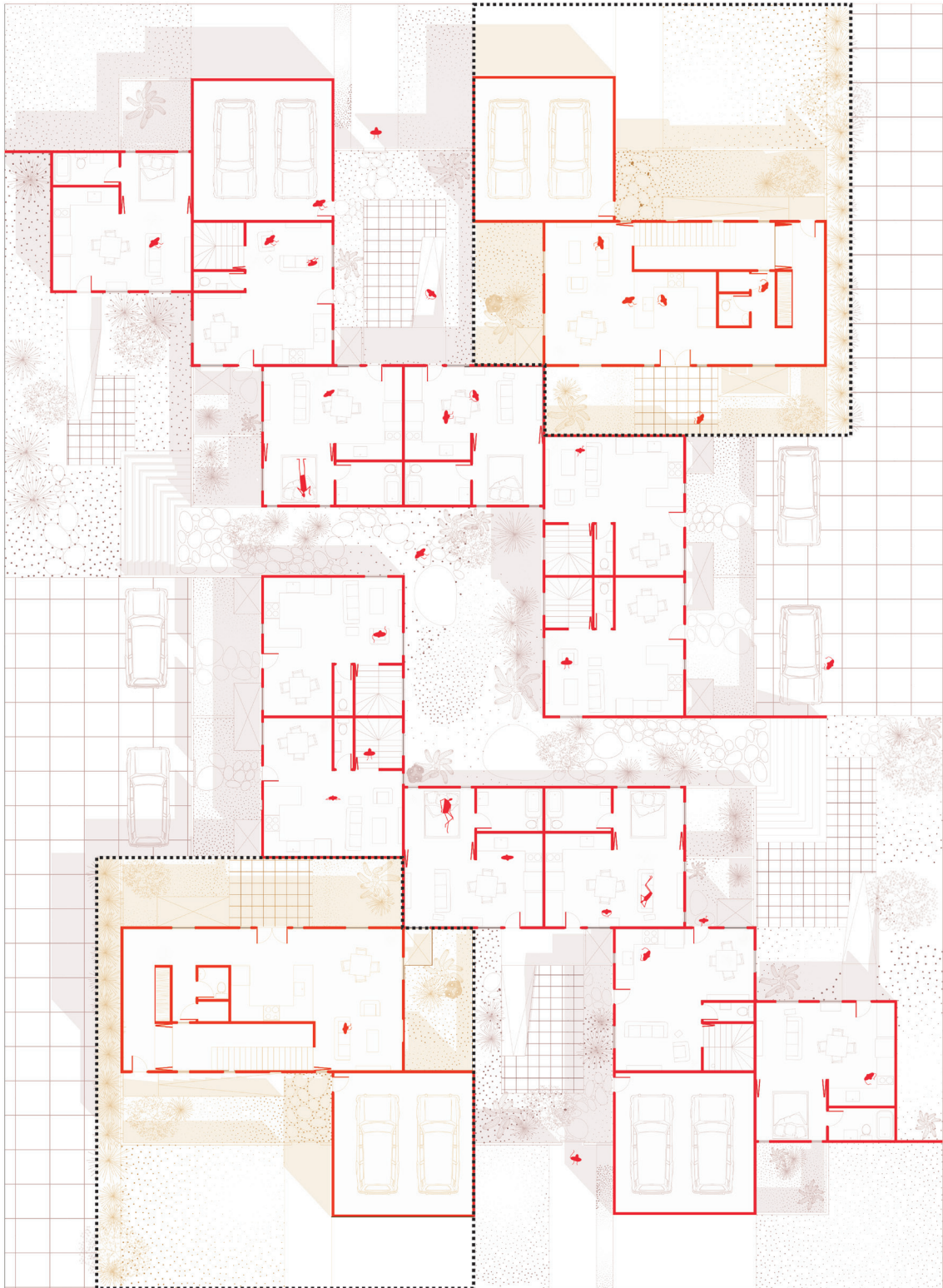
Figure 173. Larger three-bedroom homes
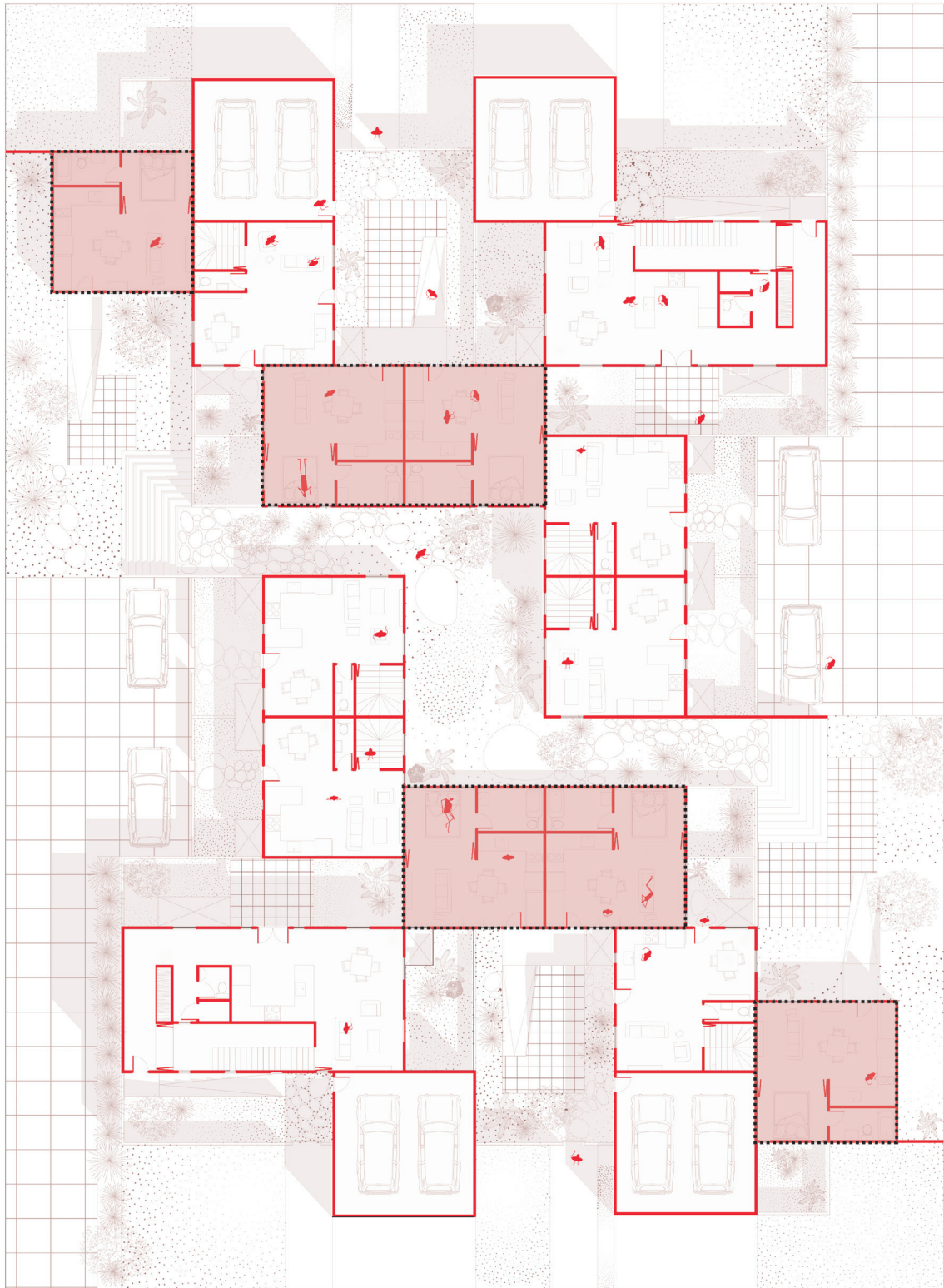
Figure 174. One/two-bedroom homes
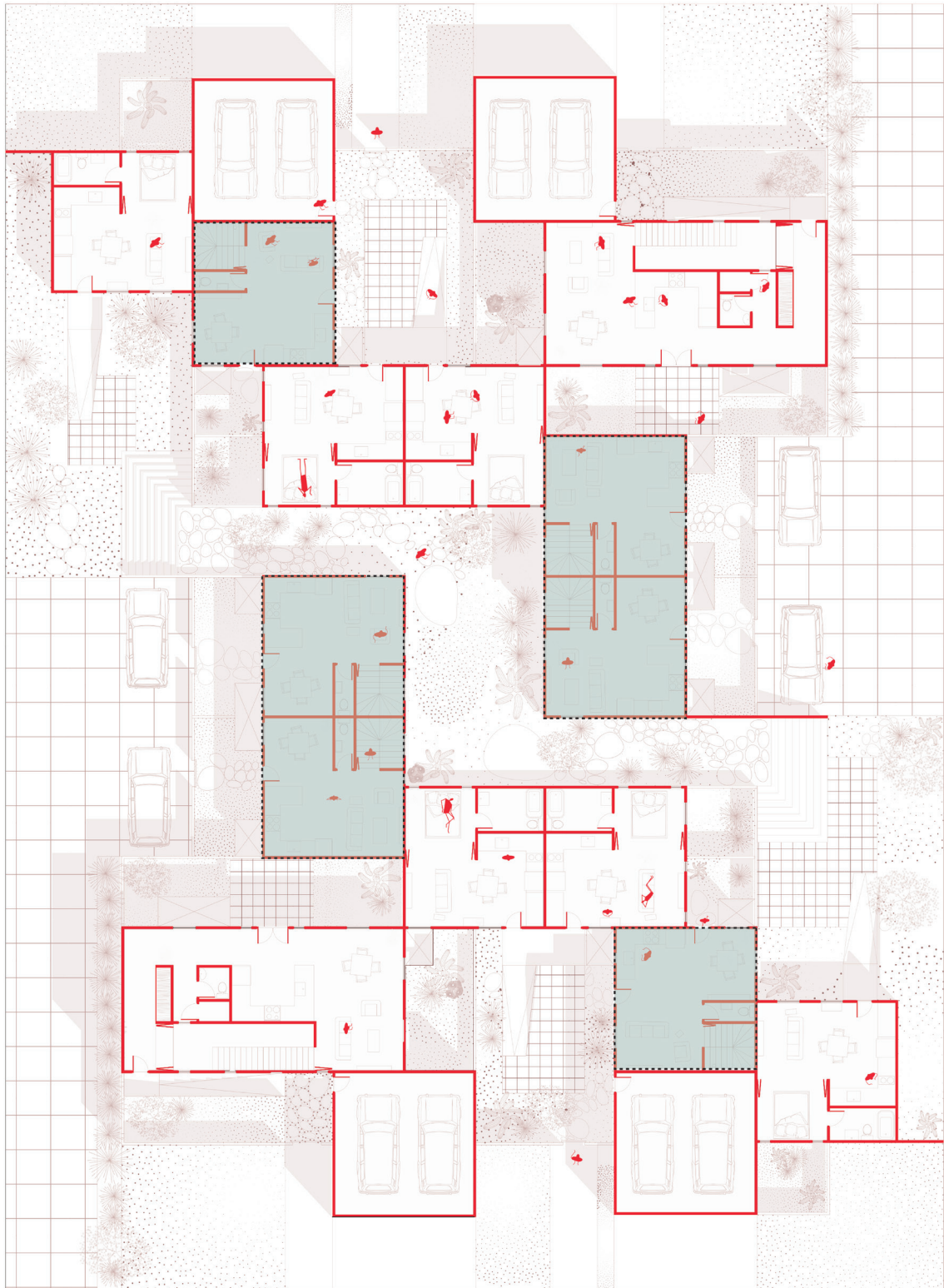
Figure 175. Studio apartments
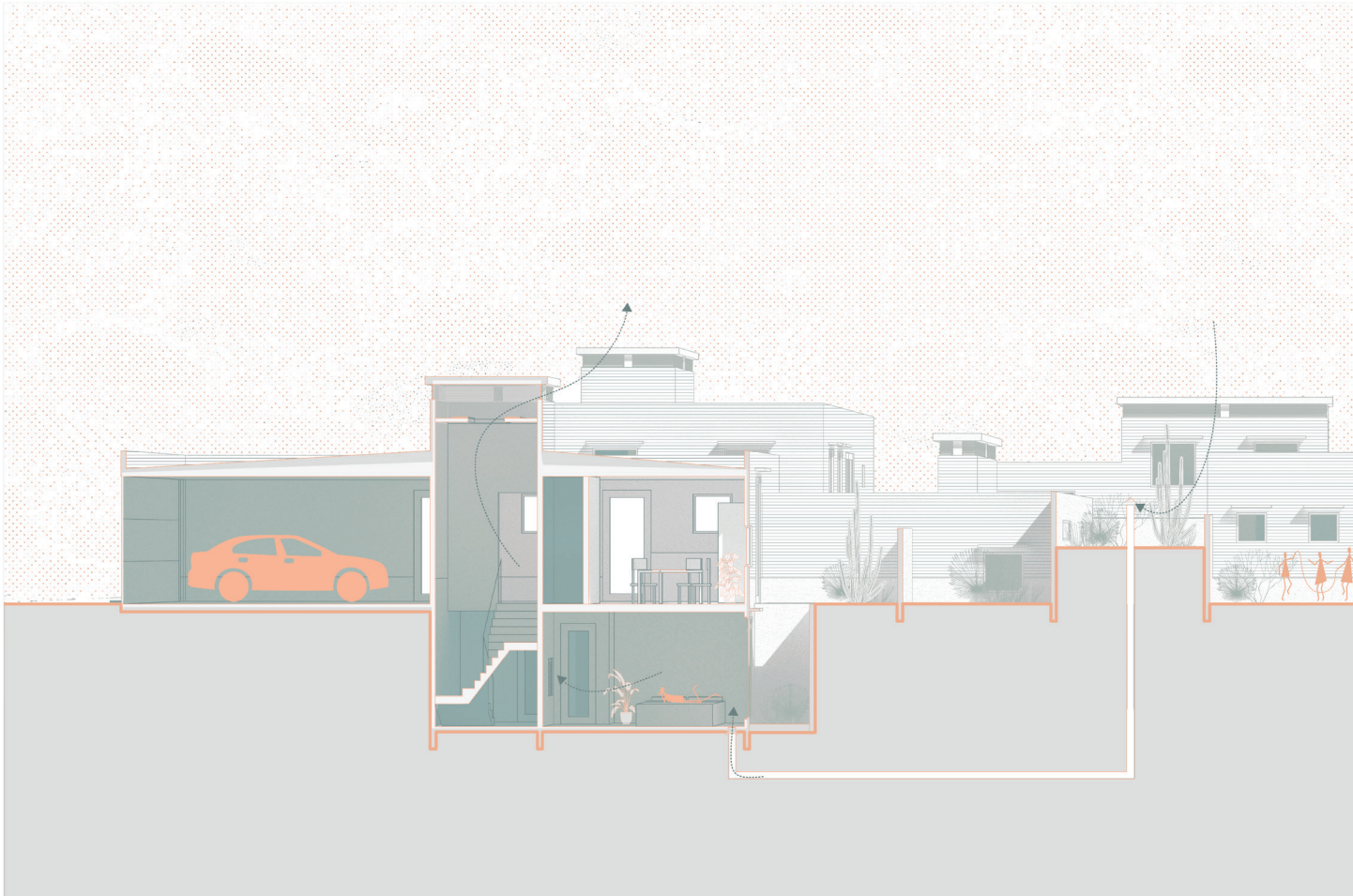
Figure 176. Section Perspective
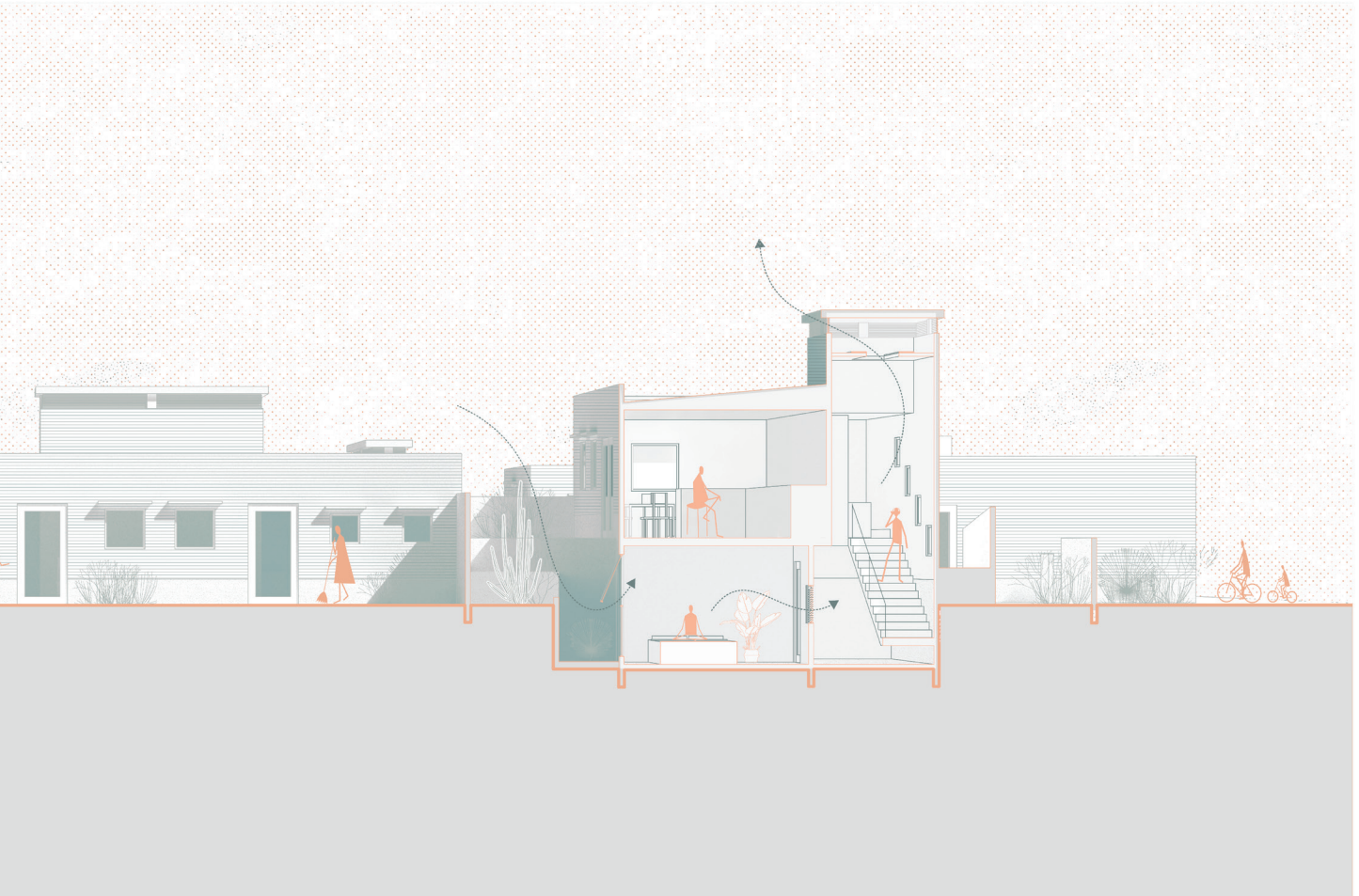
The collection of buildings gives a reduction of 6 percent in total cool energy and a modest peak cooling reduction.

With upper floors and non-resilience space uncooled or free-running, total energy is reduced by 40% and a 43% decrease in peak cooling is seen.
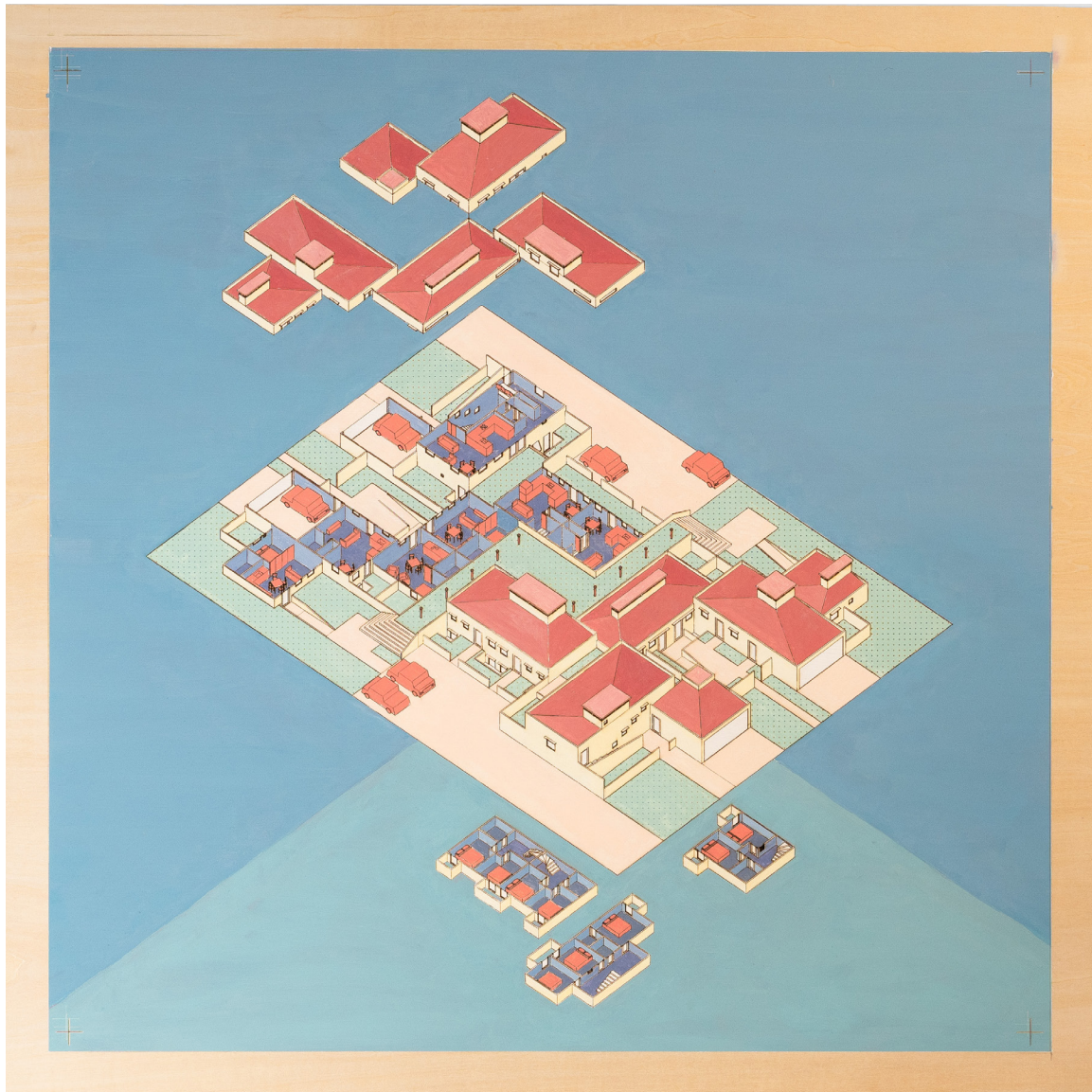
Figure 177. 24"x24" Exploded Axonometric Thermochromic Paint (No Heat Applied)

Cooling Energy, Hamlet Houses
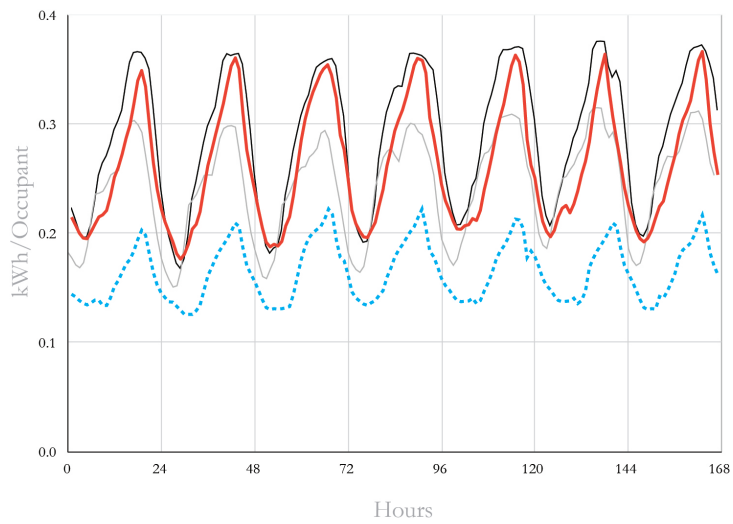
	Cooling Energy / Occupant	
■ Base IECC	48.8 kWh	0%
Base Passive House	40.1 kWh	-17.8 %
Hamlet Houses	**45.8 kWh**	**-6.1%**
-- Hamlet Houses (Cool Zone Only)	**28.6 kWh**	**-41.39%**

Figure 178. Hamlet houses' cooling energy

During a power outage, the resilient spaces in the large house's heat index hours improve by 49%, the one and two bedrooms improve by 97%, and the studios improve by 45%
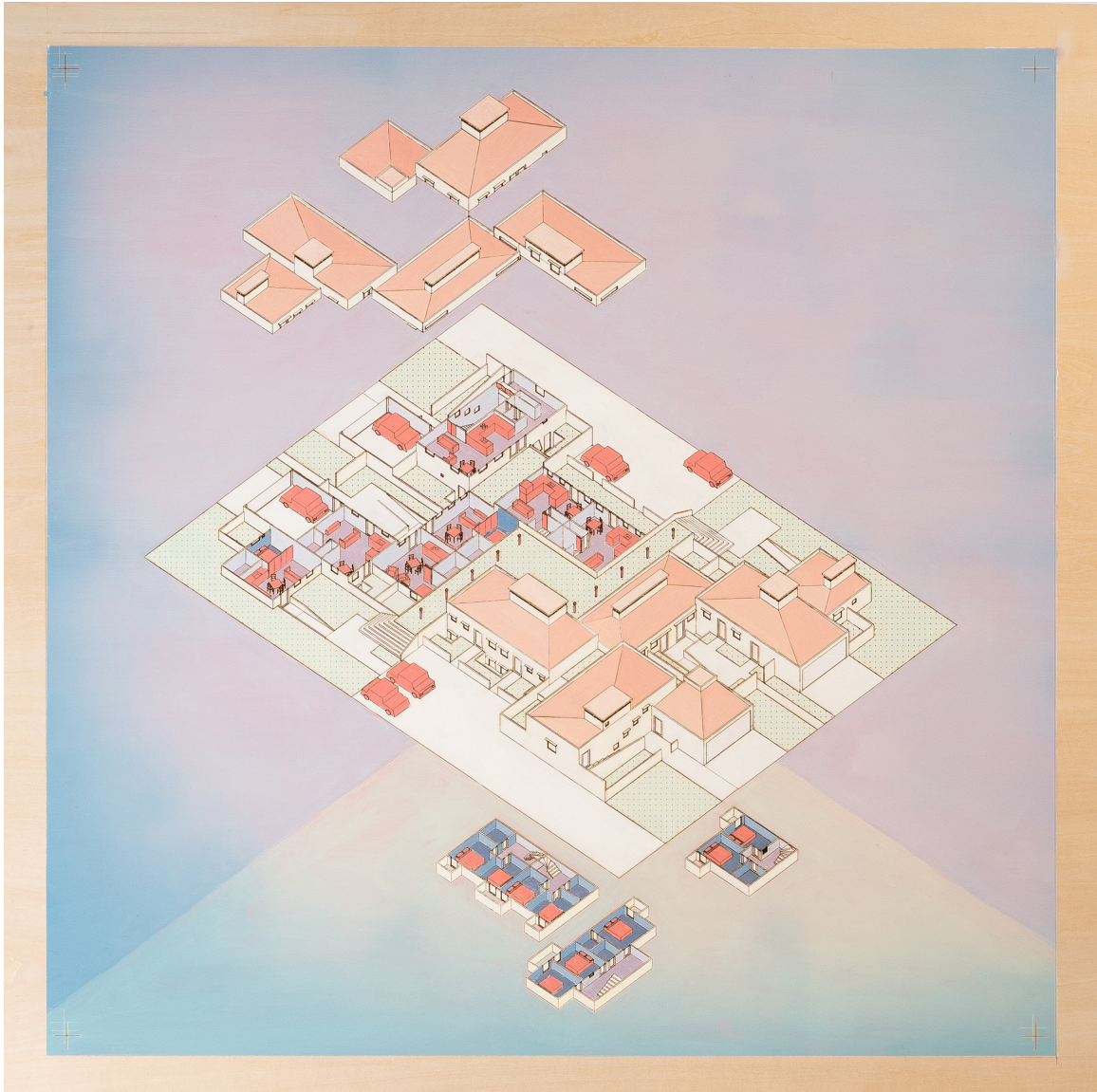
Figure 179. 24"x24" Exploded Axonometric Thermochromic Paint (Heat Applied)

Heat Index, Hamlet Houses
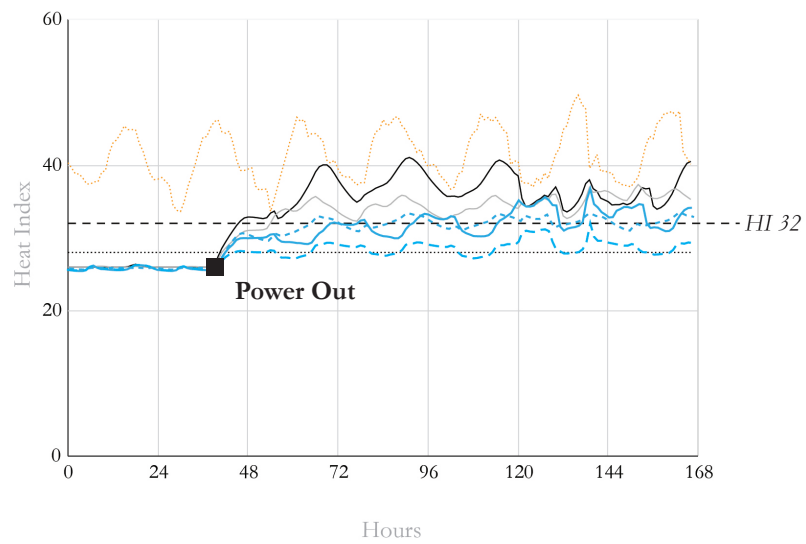
	Heat Hazard Hours >32
—— Base IECC	122
—— Base Passive House	114
—— **3 Bedroom (Lower Level)**	**62**
- - - **1/2 Bedroom (Lower Level)**	**3**
····· **Studio**	**67**
- - - - Heat Index 28 ℃	
— — Heat Index 32 ℃	
- - - - Outdoor Heat Index	

Figure 180. Hamlet houses' heat hazard hours

With passive house materials, cooling energy is reduced by 18% and with full passive house standards applied, total cooling energy is reduced by 28%.

Cooling Energy, Hamlet Houses
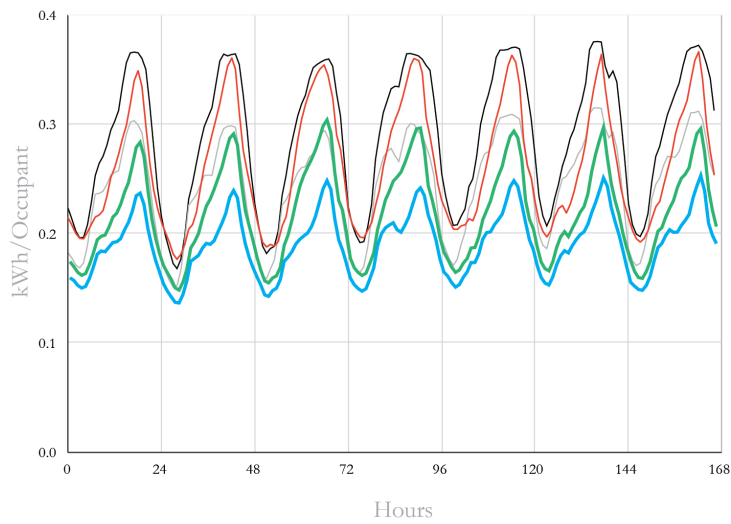
	Cooling Energy / Occupant	
▬ Base IECC	48.8 kWh	0%
▬ Base Passive House	40.1 kWh	-17.8 %
▬ Hamlet Houses	**45.8 kWh**	**-6.1%**
▬ Hamlet Houses (Passive House Materials)	**39.7 kWh**	**-18.6%**
▬ Hamlet Houses (Passive House)	**34.8 kWh**	**-28.6 %**

Figure 181. Hamlet houses' cooling energy with passive house constructions and full standard

If the upper level is un-cooled, the passive hamlet house reduces its cooling energy per occupant by 52.6%

Cooling Energy, Hamlet Houses
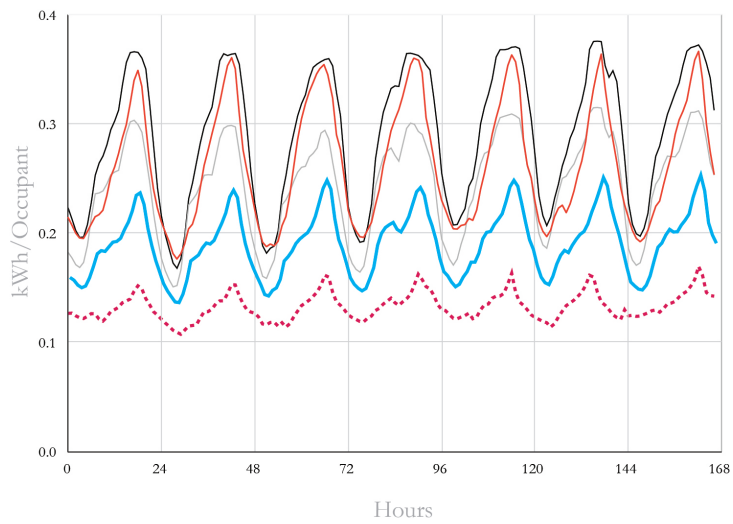
	Cooling Energy / Occupant	
━ Base IECC	48.8 kWh	0%
━ Base Passive House	40.1 kWh	-17.8 %
━ Hamlet Houses	**45.8 kWh**	**-6.1%**
━ Hamlet Houses (Passive House)	**34.8 kWh**	**-34.8 %**
━ Hamlet Houses (Passive House, Upper Off)	**23.1 kWh**	**-52.6 %**

Figure 182. Hamlet houses' cooling energy with passive house standard and resilient cooling applied.

227

An intention of the proposal is to promote resilience through social proximity and to find a balance between privacy and a shared a sense of closeness.

This idealistic scenario shows that if, one or two of the houses are equipped with oversized air conditioners, by gathering together in a home and not cooling the rest, you reduce the cooling energy peak by 36% and total cooling by 35%.
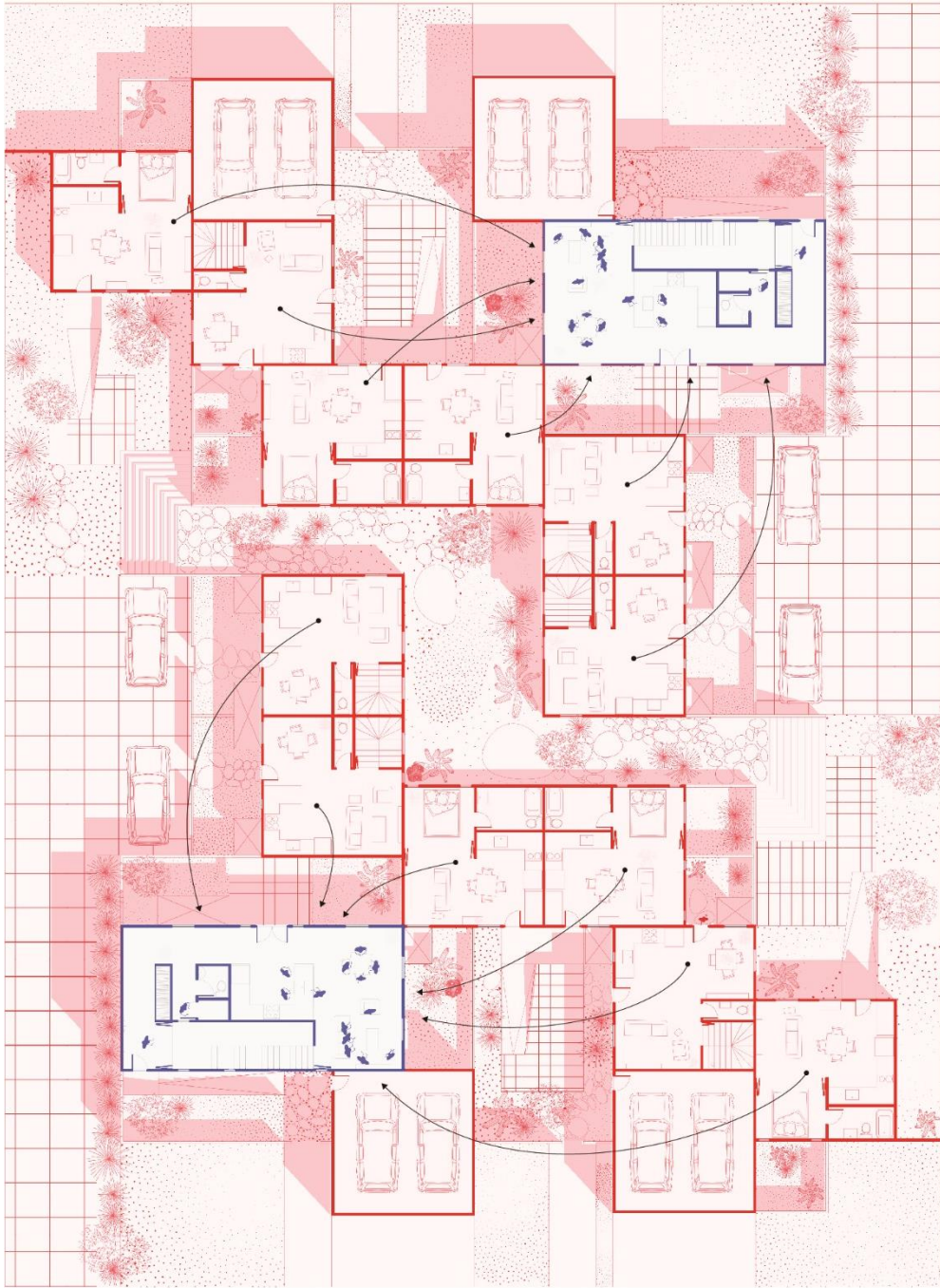
Figure 183. Heave wave Party

Cooling Energy, Hamlet Houses
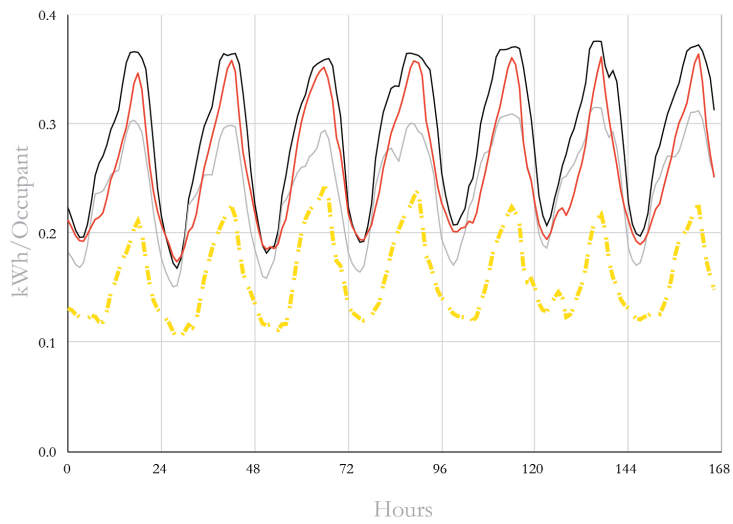
	Cooling Energy / Occupant	
▬ Base IECC	48.8 kWh	0%
▬ Base Passive House	40.1 kWh	-17.8 %
▬ **Hamlet Houses**	**45.8 kWh**	**-6.1%**
▬ **Hamlet Houses (Heat Party)**	**26.8 kWh**	**-45 %**

Figure 184. Heave wave party cooling energy reduction

Chapter 8
Conclusion

Chapter 8. Conclusion

This thesis has been presented in 7 chapters. We began with a vulnerability study that showed a significant increase in cooling energy will be required to maintain comfortable interior conditions in single family homes. This has impacts on both grid demand and on costs for home occupants. Furthermore, single family homes showed significant passive vulnerability where all homes had overheating hours until 2080, apart from the Phoenix Passive house until 2080. The impact on ground coupling and slab insulation, counter to the conventional wisdom in Passive House construction, was elucidated in chapter 3 and expanded on in chapter 4. Ground modeling has significant effects on simulation outcomes, particularly when considering heat resilience and when considering annual metrics like EUI. This highlights the sensitivity of EnergyPlus models and potential for future study and validation. A deep-dive into available ground modeling methods shows a wide spread in results, though does show that methods that do not use the simplified CTF and use a more detailed 2D finite difference method generally agree. The only 1-D method that generally agreed across cases with the two finite difference methods (Kiva and Ground Domain) was the FC method which simplifies model constructions and makes important assumptions about basement and slab constructions. An alternative method of finding monthly ground temperatures was developed and shown to be in reasonable agreement with Kiva and Ground Domain methods while only using CTFs. Chapter 5 presented a toolset that aids in the implementation of these methods in a parametric grasshopper environment which is novel because in the past, ground modeling would either need to be edited by hand directly in the IDF and re-simulated for every iteration or passed through external python code. This toolset allows for more advanced ground modeling in a streamlined environment.

In heat resilience literature, there is discourse on energy efficiency measures versus resilience, similar to the study presented in chapter 3. There is a body of research on heat mitigation retrofits that are concerned largely with materials and building components like insulation and window U-values. Neither of these focus on building form nor on occupants as an active user in the building outside of the opening window and I argue that building form is integral to producing resilience and equally important in partnering with occupants to produce heat resilience. Chapter 6 presents three building form strategies for heat resilience that aim to both reduce cooling energy per occupant and improve passive survivability inside homes during a heat wave and power outage. These strategies were then deployed in the colloquially termed 'heat resilient hamlets' that demonstrated the possibilities of heat resilient homes through the design of a collection of homes with a diversity of unit sizes and types. The design both reduces cooling energy, improves passive resilience, and gestures towards the importance of social capital in disaster resilience that the low-rise, low-density housing typologies of the status quo does not support. In sum, this thesis makes an argument for building form as an essential aspect of housing resilience in future climate extremes and makes a further argument that architecture should partner with occupants to produce the resilience.

Equations

Equations

(1) COP Equation

$$COP \; = \; \frac{|Q_W|}{W}$$

(2) EER from COP Equation

$$EER \; = \; 3.412 \; * \; COP$$

(3) EER Equation

$$EER \; = \frac{|Q_{BTU}|}{W}$$

(4) SEER Equation

$$SEER \; = \frac{Total \; Heat \; Removed \; Over \; Season \; (BTUs)}{Total \; Energy \; Used \; Over \; Season \; (Watt \; hours)}$$

(5) SEER Equation Using Temperature Bins

$$SEER \; = \frac{\sum_{j=1}^{8} \frac{q \, (T_j)}{N_j}}{\sum_{j=1}^{8} \frac{e \, (T_j)}{N_j}}$$

(6) Heat Index Equation

$$Heat \; Index \; = \; C1 \; + \; C2 * T \; + C3 * RH \; - \; C4 * T * RH \; - \; C5 * T2 \; - \; C6 * RH2 \\ + \; C7 * T2 * RH \; + \; C8 * T * RH2 \; - C9 * T2 * RH2$$

(7) Simplified Heat Flux Equation

$$q''_{ko}(t) = \sum_{j=0}^{\infty} X_j T_{o,t-j\delta} - \sum_{j=0}^{\infty} Y_j T_{o,t-j\delta}$$

(8) Indoor Heat Flux Equation

$$q''_{ki}(t) = -Z_o T_{i,t} - \sum_{j=1}^{nz} Z_j T_{i,t-j\delta} + Y_o T_{o,t} + \sum_{j=1}^{nz} Y_j T_{o,t-j\delta} + \sum_{j=1}^{nq} \Phi_j q''_{ki,t-j\delta}$$

---

(9) Outdoor Heat Flux Equation

$$q''_{ko}(t) = -Y_o T_{i,t} - \sum_{j=1}^{nz} Y_j T_{i,t-j\delta} + X_o T_{o,t} + \sum_{j=1}^{nz} X_j T_{o,t-j\delta} + \sum_{j=1}^{nq} \Phi_j q''_{ko,t-j\delta}$$

---

(10) State Space Heat Flux System

$$\frac{d[x]}{dt} = [A][x] + [B][u]$$

$$[y] = [C][x] + [D][u]$$

---

(11) State Space Heat Flux Simplified Matrix Vector Representation

$$\frac{d \begin{bmatrix} T_1 \\ \vdots \\ T_n \end{bmatrix}}{dt} = [A] \begin{bmatrix} T_1 \\ \vdots \\ T_n \end{bmatrix} + [B] \begin{bmatrix} T_{inside} \\ T_{outside} \end{bmatrix}$$

$$\begin{bmatrix} q''_{inside} \\ q''_{outside} \end{bmatrix} = [C] \begin{bmatrix} T_1 \\ \vdots \\ T_n \end{bmatrix} + [D] \begin{bmatrix} T_{inside} \\ T_{outside} \end{bmatrix}$$

---

(12) Two Node RC Heat Flux Equation

$$C\frac{d[T_1]}{dt} = h[A](T_{outside} - T_1) + \frac{T_2 - T_1}{R}$$

$$C\frac{d[T_n]}{dt} = h[A](T_{inside} - T_n) + \frac{T_{n-1} - T_n}{R}$$

$$q''_{inside} = h(T_{inside} - T_2)$$
$$q''_{outside} = h(T_1 - T_{outside})$$

---

(13) Generalized RC Heat Flux For Multiple Nodes

$$
\begin{bmatrix} \dfrac{d[T_1]}{dt} \\ \vdots \\ \dfrac{d[T_n]}{dt} \end{bmatrix}
=
\begin{bmatrix}
A & B & 0 & \cdots & 0 \\
B & A & 0 & \cdots & 0 \\
0 & \ddots & \ddots & \ddots & \vdots \\
\vdots & \ddots & \ddots & \ddots & 0 \\
0 & \cdots & 0 & B & A
\end{bmatrix}
\begin{bmatrix} T_1 \\ \vdots \\ T_n \end{bmatrix}
+
\begin{bmatrix}
\dfrac{hA}{C} & 0 & \cdots & 0 \\
0 & \ddots & \ddots & \vdots \\
\vdots & \ddots & \ddots & 0 \\
0 & \cdots & 0 & \dfrac{hA}{C}
\end{bmatrix}
\begin{bmatrix} T_{outside} \\ T_1 \\ \vdots \\ T_n \\ T_{inside} \end{bmatrix}
$$

$$
\begin{bmatrix} q''_{outside} \\ q''_1 \\ \vdots \\ q''_n \\ q''_{outside} \end{bmatrix}
=
\begin{bmatrix}
0 & \cdots & \cdots & 0 & -h \\
\vdots & & & -h & 0 \\
\vdots & & & & \vdots \\
0 & -h & & & \vdots \\
h & 0 & \cdots & \cdots & 0
\end{bmatrix}
\begin{bmatrix} T_1 \\ \vdots \\ T_n \end{bmatrix}
+
\begin{bmatrix}
0 & \cdots & \cdots & 0 & h \\
\vdots & & & h & 0 \\
\vdots & & & & \vdots \\
0 & h & & & \vdots \\
-h & 0 & \cdots & \cdots & 0
\end{bmatrix}
\begin{bmatrix} T_{outside} \\ T_1 \\ \vdots \\ T_n \\ T_{inside} \end{bmatrix}
$$

$$A = \frac{-1}{RC} - \frac{hA}{C} , B = \frac{1}{RC}$$

---

(14) Outside Heat Balance Equation

$$q''_{solar} + q''_{longwave} + q''_{conv} - \boldsymbol{q''_{ko}} = 0$$

---

(15) Inside Heat Balance Equation

$$q''_{surface\ longwave} + q''_{short\ wave} + q''_{equip\ longwave} + \boldsymbol{q''_{ki}} + q''_{solar} + q''_{conv} = 0$$

---

(16) Other Side Coefficients Contribution Equation

$$T = C2 * C3 * C4 * T_{outdoor\ db} + C5 * T_{ground} + C6 + W_{speed} * T_{outdoor\ db} + C7 * T_{zone+} C8 * T_{past}$$

---

(17) Undisturbed Soil Temperature Equation

$$T(z,t) = T_m - A_s \cdot exp[-z(\frac{\pi}{365\alpha_s})^{1/2}]\ cos\left\{\frac{2\pi}{365}[t - t_0 - \frac{z}{2}(\frac{365}{\pi\alpha_s})^{1/2}]\right\}$$

---

(18) Mean Surface Temperature Equation

$$T_{mean} = \frac{1}{h_e}[h_r T_{ma} - \varepsilon \cdot \Delta R + \beta \cdot S_m - 0.0168 \cdot h_s f b(1 - r_a)]$$

$$h_e = h_s(1 + 0.0168af)$$

$$h_r = h_s(1 + 0.0168a \cdot r_a \cdot f)$$

$$h_s = 5.7 + 3.8u$$

---

(19) Weighted Sum of Average Zone Temp and Mean Surface Temperature

$$\bar{t} = \frac{T_{mean} + (3 * T_{zone\ avg})}{4}$$

---

(20) Amplitude Term

$$T_{amp} = \frac{1}{4}\cos\left(\frac{3(i-9)}{4\pi}\right)$$

---

(21) Correction Term

$$c = \frac{|T_{mean} - T_{zoneavg}|}{8 * (T_{mean} - \bar{t})}$$

---

(22) Outside Ground Temperature Equation (Jerboa Method)

$$T_{outside} = \bar{t} + T_{amp} + c$$

Page intentionally left blank

Bibliography

Bibliography

2017-05-26 Energy Conservation Program: Energy Conservation Standards for Residential Central Air Conditioners and Heat Pumps; Confirmation of effective date and compliance date for direct final rule., Pub. L. No. EERE-2014-BT-STD-0048-0200, 82FR24211 10 CFR Part 430 24211 (2017). https://www.regulations.gov/document/EERE-2014-BT-STD-0048-0200.

"2018 International Energy Conservation Code (IECC) | ICC Digital Codes." Accessed March 28, 2022. https://codes.iccsafe.org/content/IECC2018P4.

"2018 International Energy Conservation Code (IECC) Phoenix Amendments," 2018.

"2020 Florida Building Code, Energy Conservation, 7th Edition | ICC Digital Codes." Accessed March 28, 2022. https://codes.iccsafe.org/content/FLEC2020P1.

AHRI. "2017 Standard for Performance Rating of Unitary Air- Conditioning & Air-Source Heat Pump Equipment." ANSI and AHRI, 2017.

Attia, Shady, Ronnen Levinson, Eileen Ndongo, Peter Holzer, Ongun Berk Kazanci, Shabnam Homaei, Chen Zhang, et al. "Resilient Cooling of Buildings to Protect against Heat Waves and Power Outages: Key Concepts and Definition." *Energy and Buildings* 239 (May 2021): 110869. https://doi.org/10.1016/j.enbuild.2021.110869.

Baniassadi, Amir, Jannik Heusinger, and David J. Sailor. "Energy Efficiency vs Resiliency to Extreme Heat and Power Outages: The Role of Evolving Building Energy Codes." *Building and Environment* 139 (July 2018): 86–94. https://doi.org/10.1016/j.buildenv.2018.05.024.

Baniassadi, Amir, and David J. Sailor. "Synergies and Trade-Offs between Energy Efficiency and Resiliency to Extreme Heat - A Case Study." *Building and Environment* 132 (March 15, 2018): 263–72. https://doi.org/10.1016/j.buildenv.2018.01.037.

Barber, Daniel A. *A House in the Sun: Modern Architecture and Solar Energy in the Cold War.* New York, NY: Oxford University Press, 2016.

Basu, Rupa, and Jonathan M. Samet. "Relation between Elevated Ambient Temperature and Mortality: A Review of the Epidemiologic Evidence." *Epidemiologic Reviews* 24, no. 2 (December 1, 2002): 190–202. https://doi.org/10.1093/epirev/mxf007.

Beals, Bill. "The Building Envelope: Codes, Codes, and More Codes." *Insulation Outlook Magazine* (blog), 2019. https://insulation.org/io/articles/the-building-envelope-codes-codes-and-more-codes/.

Becker, Jonathan A, and Lynsey K Stewart. "Heat-Related Illness" 83, no. 11 (2011): 6.

Bisoniya, Trilok Singh. "Design of Earth–Air Heat Exchanger System." *Geothermal Energy* 3, no. 1 (December 2015): 18. https://doi.org/10.1186/s40517-015-0036-2.

Blazejczyk, Krzysztof, Yoram Epstein, Gerd Jendritzky, Henning Staiger, and Birger Tinz. "Comparison of UTCI to Selected Thermal Indices." *International Journal of Biometeorology* 56, no. 3 (May 2012): 515–35. https://doi.org/10.1007/s00484-011-0453-2.

Bolduc, John, Iram Farooq, Sam Lipson, Owen O'Riordan, Susanne Rasmussen, Nancy Rihan-Porter, Kathy Watkins, Nathalie Beauvais, and Indrani Ghosh. "Resilient Cambridge: Climate Change Preparedness and Resiliency Plan," n.d., 70.

Broadbent, Ashley Mark, Eric Scott Krayenhoff, and Matei Georgescu. "The Motley Drivers of Heat and Cold Exposure in 21st Century US Cities." *Proceedings of the National Academy of Sciences* 117, no. 35 (September 1, 2020): 21108–17. https://doi.org/10.1073/pnas.2005492117.

The Passive House Network. "Building Codes." Accessed February 20, 2022. https://naphnetwork.org/codes/.

"CHAPTER 25-12. - TECHNICAL CODES. | Land Development Code | Austin, TX | Municode Library." Accessed March 28, 2022. https://library.municode.com/tx/austin/codes/land_development_code?nodeId=TIT25LADE_CH25-12TECO_ART12ENCO.

Cole, Helen, and Daniel Immergluck. "Reshaping Legacies of Green and Transit Justice through the Atlanta Beltline." In *The Green City and Social Injustice*. Routledge, 2021.

Colker, Ryan. "The Important Role of Energy Codes in Achieving Resilience." IECC Safe, 2019. https://www.iccsafe.org/wp-content/uploads/19-18078_GR_ANCR_IECC_Resilience_White_Paper_BRO_Final_midres.pdf.

Conlon, Kathryn C., Evan Mallen, Carina J. Gronlund, Veronica J. Berrocal, Larissa Larsen, and Marie S. O'Neill. "Mapping Human Vulnerability to Extreme Heat: A Critical Assessment of Heat Vulnerability Indices Created Using Principal Components Analysis." *Environmental Health Perspectives* 128, no. 9 (September 2020): 097001. https://doi.org/10.1289/EHP4030.

Crawley, Drury B., Curtis O. Pedersen, Linda K. Lawrie, and Frederick C. Winkelmann. "EnergyPlus: Energy Simulation Program." *ASHRAE Journal* 42 (2000): 49–56.

Derradji, Mohamed, and Messaoud Aiche. "Modeling the Soil Surface Temperature for Natural Cooling of Buildings in Hot Climates." *Procedia Computer Science*, The 5th International Conference on Ambient Systems, Networks and Technologies (ANT-2014), the 4th International Conference on Sustainable Energy Information Technology (SEIT-2014), 32 (January 1, 2014): 615–21. https://doi.org/10.1016/j.procs.2014.05.468.

Design Methodology for the Assessment of Overheating Risk in Homes: CIBSE TM59., 2017.

Dickinson, Robert, and Benjamin Brannon. "Generating Future Weather Files for Resilience." *Los Angeles*, 2016, 6.

Dumas, Melissa, Binita Kc, and Colin I. Cunliff. "Extreme Weather and Climate Vulnerabilities of the Electric Grid: A Summary of Environmental Sensitivity Quantification Methods," August 1, 2019. https://doi.org/10.2172/1558514.

"Energy Plus Version 9.6.0 Documentation, Auxiliary Programs." U.S. Department of Energy, September 23, 2021.

"Energy Plus Version 9.6.0 Documentation, Engineering Reference." U.S. Department of Energy, September 23, 2021.

Fischels, Josie. "PHOTOS: The Record-Breaking Heat Wave That's Scorching The Pacific Northwest." *NPR*, June 29, 2021, sec. Environment. https://www.npr.org/2021/06/29/1011269025/photos-the-pacific-northwest-heatwave-is-melting-power-cables-and-buckling-roads.

Fuleihan, Dean, Dominic Williams, Daniel A Zarrilli, and OneNYC Director. "One NYC 2050 Climate Report," n.d., 332.

Garcetti, Mayor Eric. "L.A.'s Green New Deal: Sustainable City PLAn 2019," 2019, 152.

Gidden, Matthew J., Keywan Riahi, Steven J. Smith, Shinichiro Fujimori, Gunnar Luderer, Elmar Kriegler, Detlef P. van Vuuren, et al. "Global Emissions Pathways under Different Socioeconomic Scenarios for Use in CMIP6: A Dataset of Harmonized Emissions Trajectories through the End of the Century." *Geoscientific Model Development* 12, no. 4 (April 12, 2019): 1443–75. https://doi.org/10.5194/gmd-12-1443-2019.

Gronlund, Carina J. "Racial and Socioeconomic Disparities in Heat-Related Health Effects and Their Mechanisms: A Review." *Current Epidemiology Reports* 1, no. 3 (September 2014): 165–73. https://doi.org/10.1007/s40471-014-0014-4.

Gu, Lixing. "Airflow Network Modeling In EnergyPlus." *Building Simulation*, 2007, 11.

Holzer, Peter, Phillip Stern, and Gerhard Hofer. "Annex 80 on Resilient Cooling for Residential and Small Non-Residential Buildings." International Energy Agency, June 2019.

International Code Council. "International Building Code," 2021. https://search.library.wisc.edu/catalog/999907647602121.

Iu, Ipseng, and D E Fisher. "Application of Conduction Transfer Functions and Periodic Response Factors in Cooling Load Calculation Procedures." *ASHRAE Transactions*, 2004, 14.

Jentsch, Mark F. "Climate Change Weather File Generators: Technical Reference Manual for the CCWeatherGen and CCWorldWeatherGen Tools." Sustainable Energy Research Group, November 2012.

Jentsch, Mark F., Patrick A.B. James, Leonidas Bourikas, and AbuBakr S. Bahaj. "Transforming Existing Weather Data for Worldwide Locations to Enable Energy and Building Performance Simulation under Future Climates." *Renewable Energy* 55 (July 2013): 514–24. https://doi.org/10.1016/j.renene.2012.12.049.

Johnson, Daniel P., Austin Stanforth, Vijay Lulla, and George Luber. "Developing an Applied Extreme Heat Vulnerability Index Utilizing Socioeconomic and Environmental Data." *Applied Geography* 35, no. 1–2 (November 2012): 23–31. https://doi.org/10.1016/j.apgeog.2012.04.006.

Klinenberg, Eric. *Heat Wave: A Social Autopsy.* Chicago, IL: Univeristy of Chicago Press, 2002.

Klingenberg, Katrin. "Passive House (Passivhaus)." *Sustainable Built Environments*, 2020, 23. https://doi.org/10.1007/978-1-0716-0684-1_351.

Kolokotroni, M., I. Giannitsaris, and R. Watkins. "The Effect of the London Urban Heat Island on Building Summer Cooling Demand and Night Ventilation Strategies." *Solar Energy* 80, no. 4 (April 2006): 383–92. https://doi.org/10.1016/j.solener.2005.03.010.

Kruis, Neal, and Moncef Krarti. "Three-Dimensional Accuracy with Two-Dimensional Computation Speed: Using the Kiva™ Numerical Framework to Improve Foundation Heat Transfer Calculations." *Journal of Building Performance Simulation* 10, no. 2 (March 4, 2017): 161–82. https://doi.org/10.1080/19401493.2016.1211177.

Kusuda, T, and Paul R Achenbach. "Earth Temperature and Thermal Diffusivity at Selected Stations in the United States," 1965, 236.

Lacaton & Vassal. *Transformation de 530 Logements.* 2017. Building, Bordeaux, France.

Larwa, Barbara, and Krzysztof Kupiec. "Heat Transfer in the Ground with a Horizontal Heat Exchanger Installed – Long-Term Thermal Effects." *Applied Thermal Engineering* 164 (January 5, 2020): 114539. https://doi.org/10.1016/j.applthermaleng.2019.114539.

Lazzarini, Michele, Annalisa Molini, Prashanth R. Marpu, Taha B. M. J. Ouarda, and Hosni Ghedira. "Urban Climate Modifications in Hot Desert Cities: The Role of Land Cover, Local Climate, and Seasonality: URBAN CLIMATE OF DESERT CITIES." *Geophysical Research Letters* 42, no. 22 (November 28, 2015): 9980–89. https://doi.org/10.1002/2015GL066534.

Lukinbeal, Christopher, Patricia L. Price, and Cayla Buell. "Rethinking 'Diversity' Through Analyzing Residential Segregation Among Hispanics in Phoenix, Miami, and Chicago." *The Professional Geographer* 64, no. 1 (February 1, 2012): 109–24. https://doi.org/10.1080/00330124.2011.583584.

"Migrant Workers Bear the Brunt of Extreme Heat in Kuwait," August 2021. https://www.who.int/news-room/feature-stories/detail/migrant-workers-bear-brunt-extreme-heat-kuwait.

"Mission & History: Passive House Alliance U.S.," 2022. https://www.phius.org/about/mission-history.

Mitchell, Robin. "THERM 7 / WINDOW 7 NFRC Simulation Manual." National Fenestration Rating Council, July 2017.

Miutori, Mami, and Deberati Guha-Sapir, eds. "Economic Losses, Poverty & Disasters 1998-2017." Center for Research on the Epidemiology of Disasters, 2018.

Mulville, Mark, and Spyridon Stravoravdis. "The Impact of Regulations on Overheating Risk in Dwellings." *Building Research & Information* 44, no. 5–6 (August 17, 2016): 520–34. https://doi.org/10.1080/09613218.2016.1153355.

Myrup, Leonard. "A Numerical Model of Urban Heat Island." *Journal of Applied Meteorology* 8 (July 24, 1969). https://doi.org/10.1175/1520-0450(1969)008<0908:ANMOTU>2.0.CO;2.

Nahlik, Matthew J., Mikhail V. Chester, Stephanie S. Pincetl, David Eisenman, Deepak Sivaraman, and Paul English. "Building Thermal Performance, Extreme Heat, and Climate Change." *Journal of Infrastructure Systems* 23, no. 3 (September 1, 2017): 04016043. https://doi.org/10.1061/(ASCE)IS.1943-555X.0000349.

Norman, Jonathan, Heather L. MacLean, and Christopher A. Kennedy. "Comparing High and Low Residential Density: Life-Cycle Analysis of Energy Use and Greenhouse Gas Emissions." *Journal of Urban Planning and Development* 132, no. 1 (March 2006): 10–21. https://doi.org/10.1061/(ASCE)0733-9488(2006)132:1(10).

O'Brien, William, and Isis Bennet. "Simulation-Based Evaluation of High-Rise Residential Building Thermal Resilience." *ASHRAE Transactions; Atlanta* 122 (2016): 455–68.

"Passive Survivability and Back-up Power During Disruptions | U.S. Green Building Council." Accessed March 8, 2022. https://www.usgbc.org/credits/new-construction-core-and-shell-schools-new-construction-retail-new-construction-data-48.

"PHIUS+ Certification Guidebook v2.0." PHIUS, February 2019. https://www.phius.org/PHIUS+2018/PHIUS+%20Certification%20Guidebook%20v2.0_final.pdf.

Pinel, Patrice, and Ian Beausoleil-Morrison. "Coupling Soil Heat and Mass Transfer Models to Foundations in Whole-Building Simulation Packages," 2012, 14.

Popovich, Nadja, and Winston Choi-Schagrin. "Hidden Toll of the Northwest Heat Wave: Hundreds of Extra Deaths." *The New York Times*, August 11, 2021, sec. Climate. https://www.nytimes.com/interactive/2021/08/11/climate/deaths-pacific-northwest-heat-wave.html.

Porritt, S. M., P. C. Cropper, L. Shao, and C. I. Goodier. "Ranking of Interventions to Reduce Dwelling Overheating during Heat Waves." *Energy and Buildings*, Cool Roofs, Cool Pavements, Cool Cities, and Cool World, 55 (December 1, 2012): 16–27. https://doi.org/10.1016/j.enbuild.2012.01.043.

Richardson, Roger. "Measurement, Testing, Adjusting, and Balancing of Building HVAC Systems." ASHRAE, 2017. https://ashrae.iwrapper.com/ASHRAE_PREVIEW_ONLY_STANDARDS/STD_111_2008_RA_2017.

Rothfusz, Lans P. "The Heat Index 'Equation' (or, More Than You Ever Wanted to Know About Heat Index)," 1990, 2.

Rothstein, Richard. *The Color of Law: A Forgotten History of How Our Government Segregated America*, 2017. https://www.epi.org/publication/the-color-of-law-a-forgotten-history-of-how-our-government-segregated-america/.

Santamouris, M, N Papanikolaou, I Livada, I Koronakis, C Georgakis, A Argiriou, and D.N Assimakopoulos. "On the Impact of Urban Climate on the Energy Consumption of Buildings." *Solar Energy* 70, no. 3 (2001): 201–16. https://doi.org/10.1016/S0038-092X(00)00095-5.

Seem, John, E. "Modeling of Heat Transfer in Buildings." PhD, Univeristy of Wisconsin, 1987.

"Status of State Energy Code Adoption - Residential | Building Energy Codes Program." Accessed March 28, 2022. https://www.energycodes.gov/status/residential.

Stephenson, D G. "Room Thermal Response Factors." *ASHRAE* 73, no. 1 (1967): 15.

Suerich-Gulick, Frank, Anna Halepaska, and Salmaan Craig. "Cascading Temperature Demand: The Limits of Thermal Nesting in Naturally Ventilated Buildings." *Building and Environment* 208 (January 2022): 108607. https://doi.org/10.1016/j.buildenv.2021.108607.

Sun, Kaiyu, Wanni Zhang, Zhaoyun Zeng, Ronnen Levinson, Max Wei, and Tianzhen Hong. "Passive Cooling Designs to Improve Heat Resilience of Homes in Underserved and Vulnerable Communities." *Energy and Buildings* 252 (2021): 111383. https://doi.org/10.1016/j.enbuild.2021.111383.

Tretter, Eliot, and Moulay Sounny-Slitine. "Austin Restricted: Progressiveism, Zoing, Private Racial Covenants, and the Segregated City." Institute for Urban Policy Research and Analysis, 2012.

Troup, Luke. "Morphing Climate Data to Simulate Building Energy Consumption," 2020, 8.

US Department of Commerce, NOAA. "Heat Index Chart." NOAA's National Weather Service. Accessed May 13, 2022. https://www.weather.gov/ffc/hichart.

"U.S. Energy Codes Adopted by States," September 29, 2021. https://www.cove.tools/u-s-energy-codes-adopted-by-states-2021.

U.S. Green Building Council. *LEED Reference Guide for Building Design and Construction.*, 2019.

Wilburn, Matt. "ANSI/ASHRAE/IES Standard 90.1-2019," 2019, 368.

Wright, Graham S, and Katrin Klingenberg. "Climate-Specific Passive Building Standards," July 2015, 88.

Xing, Lu. "Estimations of Undistrubed Ground Temperatures Using Numerical and Analytical Modeling," 2010.

York, Abigail, Joseph Tuccillo, Christopher Boone, Bob Bolin, Lauren Gentile, Briar Schoon, and Kevin Kane. "Zoning and Land Use: A Tale of Incompatibility and Environmental Injustice in Early Phoenix." *Journal of Urban Affairs* 36, no. 5 (December 1, 2014): 833–53. https://doi.org/10.1111/juaf.12076.

Yusof, Mohd Hazwan, Sulaiman Mohd Muslim, Muhammad Fadhli Suhaimi, and Mohamad Firdaus Basrawi. "The Effect of Outdoor Temperature on the Performance of a Split-Unit Type Air Conditioner Using R22 Refrigerant." Edited by S.A. Abdul Karim, N. Zainuddin, M.H. Yusof, and N. Sa'ad. *MATEC Web of Conferences* 225 (2018): 02012. https://doi.org/10.1051/matecconf/201822502012.

Zhai, V, A Pirani, and S. L Connors. "IPCC, 2021: Summary for Policymakers. In: Climate Change 2021: The Physical Science Basis. Contribution of Working Group I to the Sixth Assessment Report of the Intergovernmental Panel on Climate Change," 2021.

Zheng, Guozhong, Ke Li, and Yajing Wang. "The Effects of High-Temperature Weather on Human Sleep Quality and Appetite." *International Journal of Environmental Research and Public Health* 16, no. 2 (January 2019): 270. https://doi.org/10.3390/ijerph16020270.

Appendix

Appendix

Section 8.1. Notes on earth tubes and power-outage ventilation

Those of you who are eagle eyed will see that a key aspect of the presented work overlooks something essential – ventilation. In grid-on scenarios, there is no problem, the DOAS system provides adequate replacement air for air quality to the tune of 10L/s per occupant. In the event of a power outage, the story is different. Part of what makes such a dramatic improvement in passive survivability in earth coupled zones is that fresh, hot air is not being introduced into the zone. At the moment, it is reasonable to say that infiltration (modeled to 5 ACH_{50} in an IECC construction in Phoenix) will passively allow some amount of air exchange preventing serious health concerns. However, with tighter and tighter envelopes, especially in the Passive House Standard, air will quickly become stale with raised CO_2 levels, high humidity (from occupant breathing/sweating/etc.), and odors. In Figure 176, an earth tube was drawn protectively as a nod towards solving this ventilation problem. The intention being that during a power outage, an earth tube provides tempered fresh air to occupied basement zones.

If the Chapters 1-7 the "strong-form" of the thesis, please consider this short appendix section a "weak-form" exploration of the efficacy of earth tubes (added the night of thesis submission!). This work was done for the final project of Les Norford's 4.421-Space Conditioning for Low-Carbon Building's course taken concurrently with the thesis work. In this section, I look briefly at an analytical approach which references the Trilok Singh Bisoniya 2015 paper "Design of earth–air heat exchanger system" through the development of a few Python scripts in Grasshopper.[113] I then show results that relate directly to the work in Chapters 6 and 7 with the addition of the earth tube EP object which was implemented using the workflow outlined in Figure 110.

8.1.1. Earth tubes

The earth tube is part of a larger world of earth-air heat exchange methods that buildings have used for centuries. Some of the most famous are labyrinth types and are found in contemporary projects like the Norman Foster's Spaceport America building which uses a labyrinth to pre-cool air for conditioning or the Ewha Women's University building designed by Dominique Perrault that uses heat exchangers in the earth coupled walls to ventilate the building. The earth tube, or Canadian well, is generally used in the kind of low-rise, low-density buildings that are the focus of this thesis. They work by drawing air, either passively or with a fan, through a pipe that is buried below ground which, as we know, has a more stable temperature than the surface conditions and is generally cooler than summer temperature peaks. The air exchanges heat with the ground through the tube and ideally enters the zone as close to ground temperature as possible.

8.1.2. Analytic approach

Two Python scripts aid the exploration of the analytic earth tube method, the first is used to determine ground temperatures, both the surface mean and temperatures at varying depths that use equations 17 and 18. Figure 185 shows the component with inputs for an EPW file and depth in meters. The figure also includes ground temperatures for six weather scenarios in Phoenix showing that ground temperatures could rise by 2 over four degrees Celsius in a worst-case scenario by 2080 which has an impact when considering efficacy of earth tubes in future climates. The second Python component accepts earth tube characteristics and outputs the temperature of air leaving the earth tube in both winter and summer, as well fan power for the earth tube. Note that the Darcy friction factor is calculated using the Moody approximation, which has a higher margin of error and a narrower physical window of accuracy than some other approximations.

---

[113] Trilok Singh Bisoniya, "Design of Earth–Air Heat Exchanger System," *Geothermal Energy* 3, no. 1 (December 2015): 18, https://doi.org/10.1186/s40517-015-0036-2.
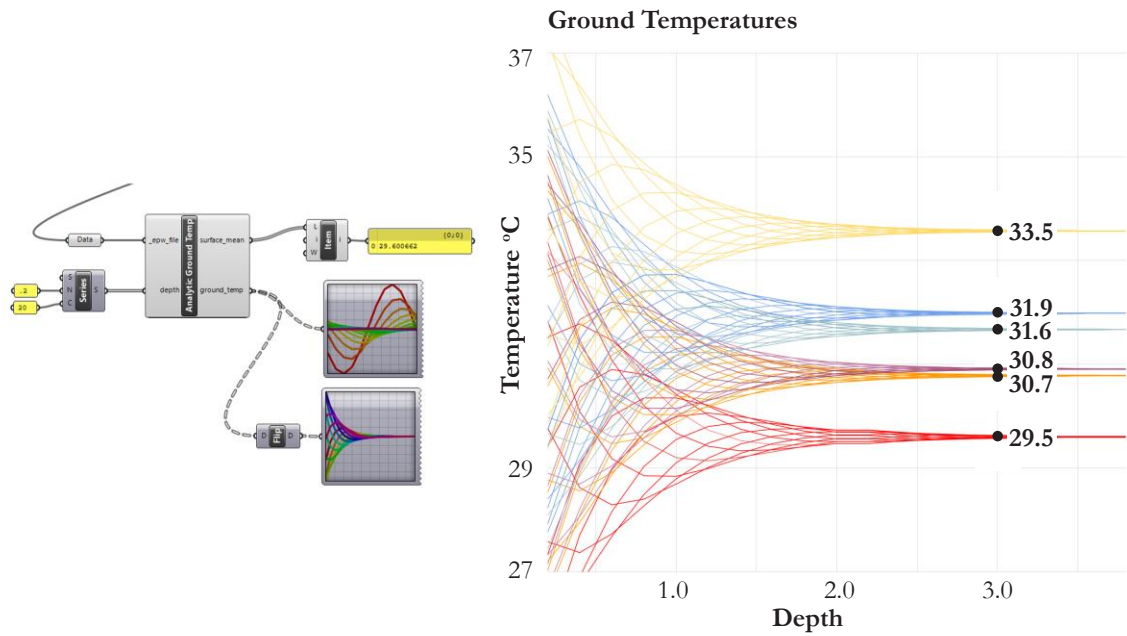
Figure 185. Analytic ground temperature component (left), ground temperatures at depths for five morphed weather scenarios (right)
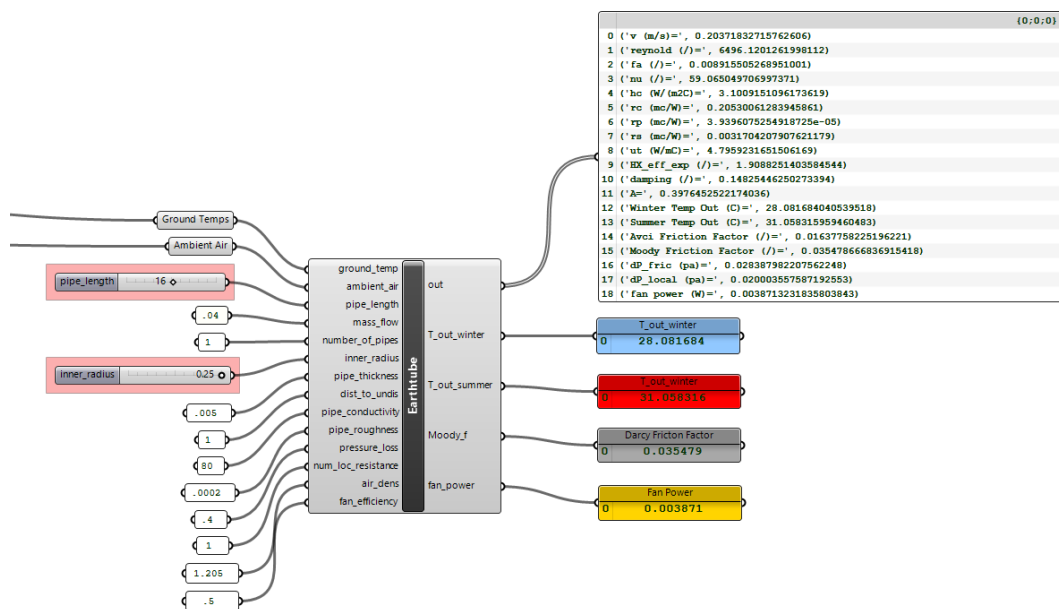

Figure 186. Analytic earth tube component.

With the components from Figure 185 and Figure 186, we can feed a series of dry bulb values and ground temperatures from different climate warming scenarios to understand a range of temperatures supplied by the earth tube. Note the difference between the RCP 4.5 morphed files and A2 files in Figure 187. This likely says more about the morphing methods than the actual warming scenario. Most importantly across scenarios is the large temperature delta that can be realized with an earth tube which, in this case, had a diameter of .28m, a length of 20m, and was buried 3m below ground.
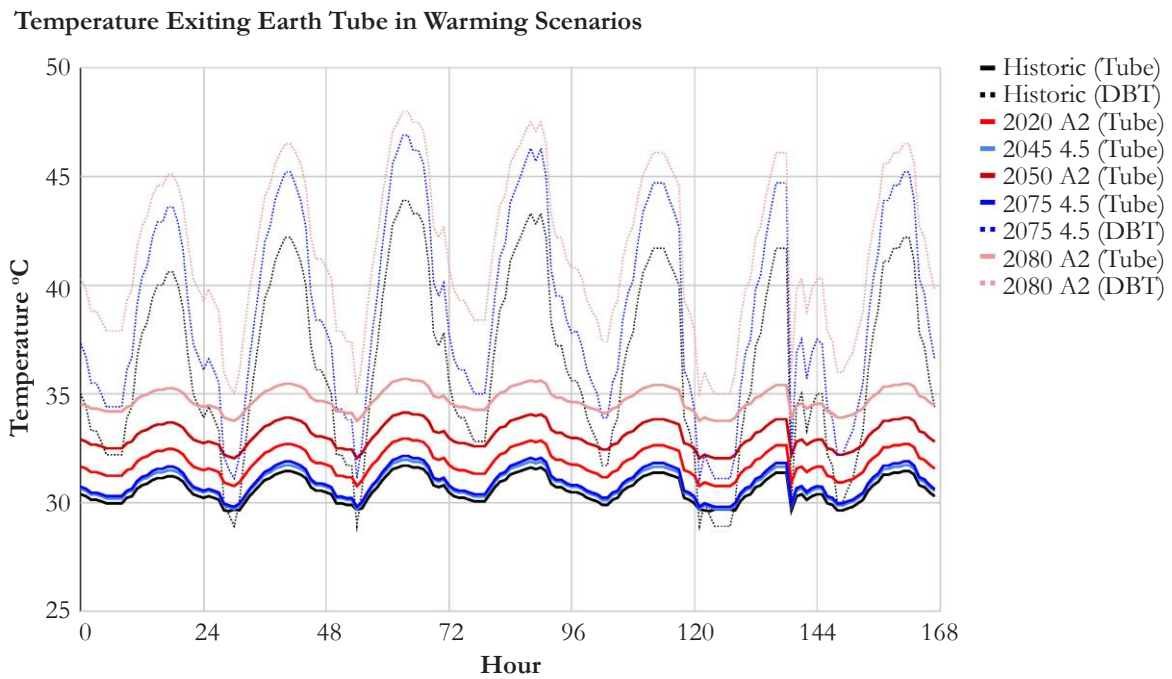
Temperature Exiting Earth Tube in Warming Scenarios

Figure 187. Earth tube supply temperatures and dry bulb temperatures for 6 warming scenarios.

8.1.3. Analytic Earth Tube Design Space

The analytical model allows for an easy exploration of the design space, and so a small multi-objective optimization problem was formulated using tube length and radius as variables. The objectives for minimization are the tube supply temperature and the fan power. Figure 188 shows the design space which reveals several interesting relationships. First, smaller radius and longer pipes lead to lower supply temperatures which are visualized as darker greens. However, smaller radii and longer pipes lead to greater fan power. This is important because the design spaces are oppositional and an optimal solution sits between them
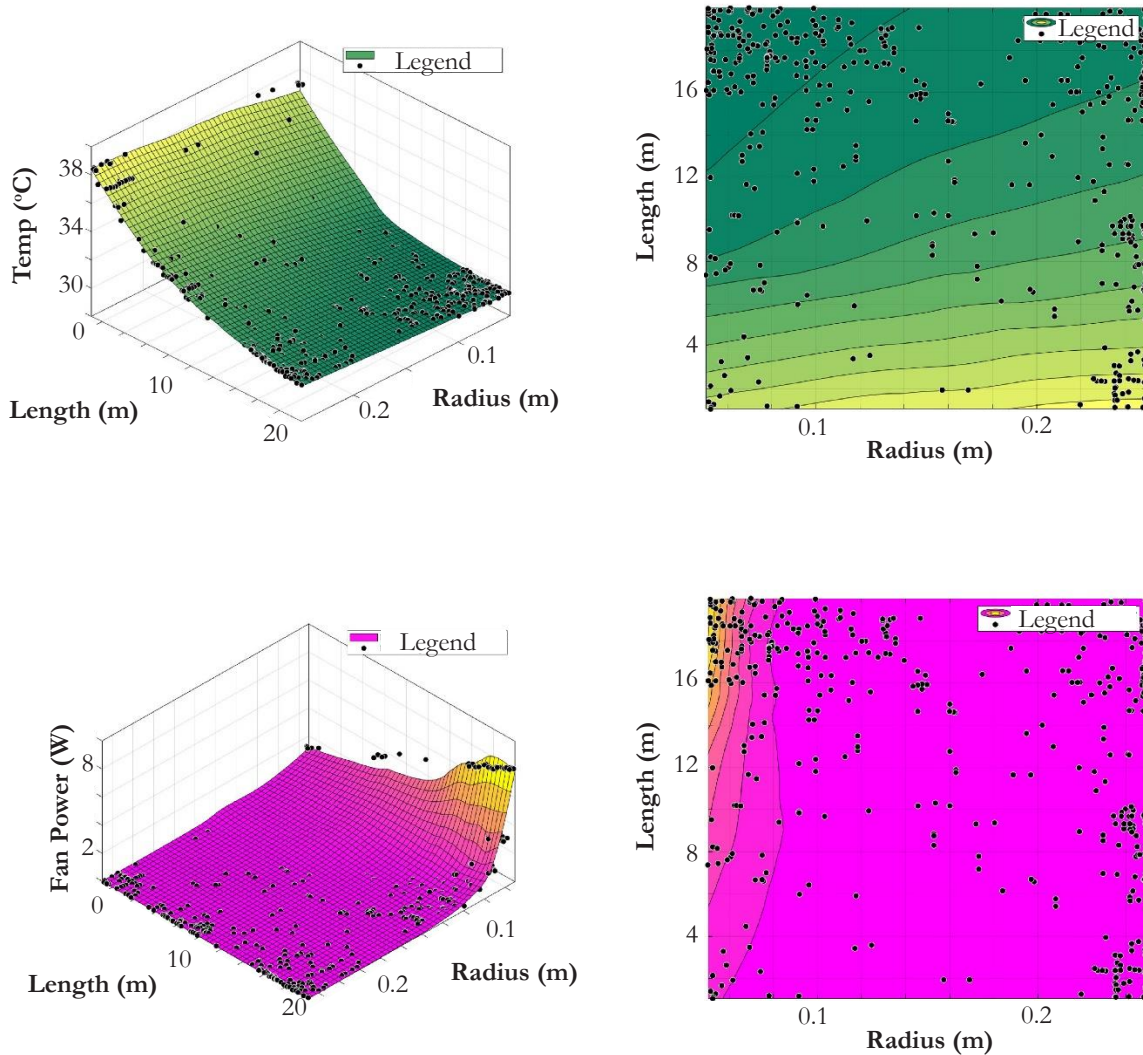

Figure 188. Analytic earth tube design space.

8.1.4. Energy Modeling

EnergyPlus has an earth tube object which is simple to use, and takes similar inputs as the analytic model. For the energy model, Basement 4 from 6.3.2 was used (Figure 125 and Figure 126) and simulated in historic and 2050 A2 weather. Important characteristics for the earth tube are shown in Table 37. In the first case (Figure 189.) the plots are shown with no ventilation. In the second (Figure 190.) plots show ventilation on all floors, and in the third (Figure 191.) plots show the earth tube implementation in the below grade bedrooms.

Table 37. Earth Tube Characteristics

Fan Pressure	20 N/m2
Fan Efficiency	.5
Pipe Radius	.14m
Pipe Thickness	.01m
Pipe Length	20m
Pipe Conductivity	80 W/m^{o}C
Pipe Depth	2m
Soil Condition	Heavy and Dry

Heat Index: No Ventilation, Historic

Heat Index: No Ventilation, 2050
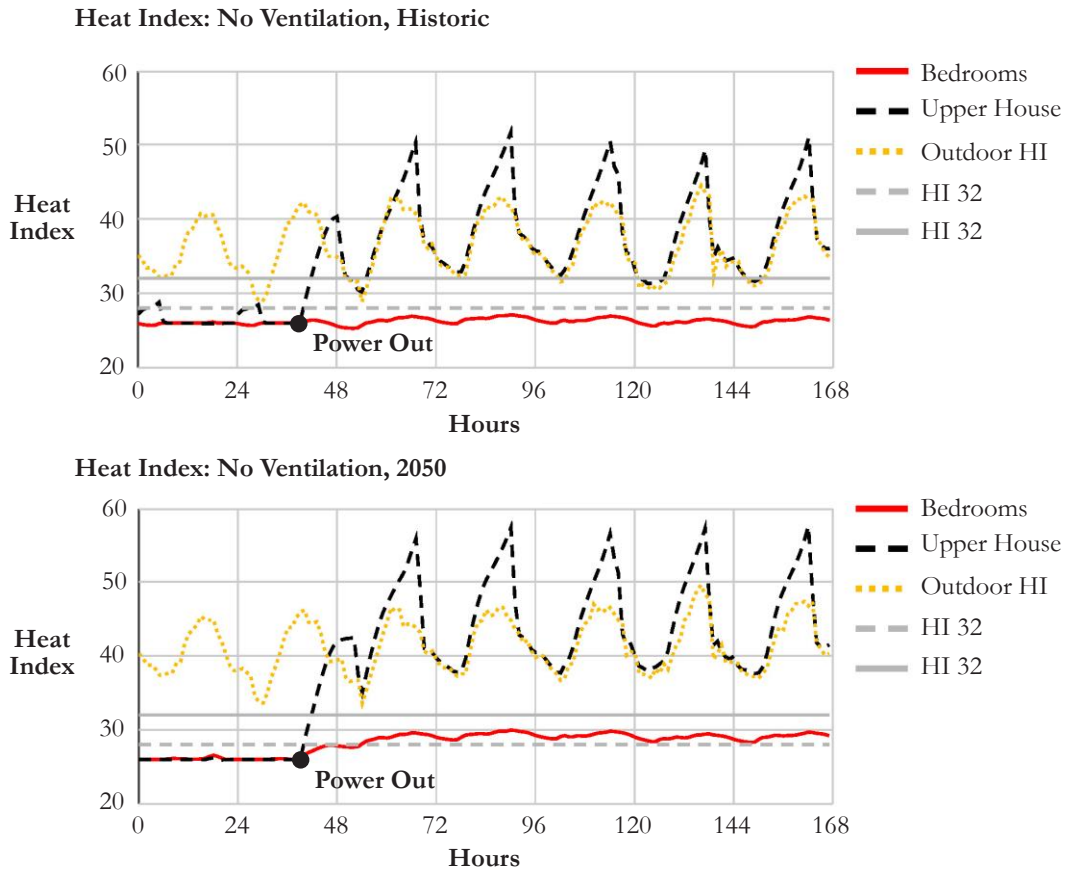
Figure 189. House with below grade bedrooms and no ventilation during a power outage.

249

Heat Index: Natural Ventilation, Historic

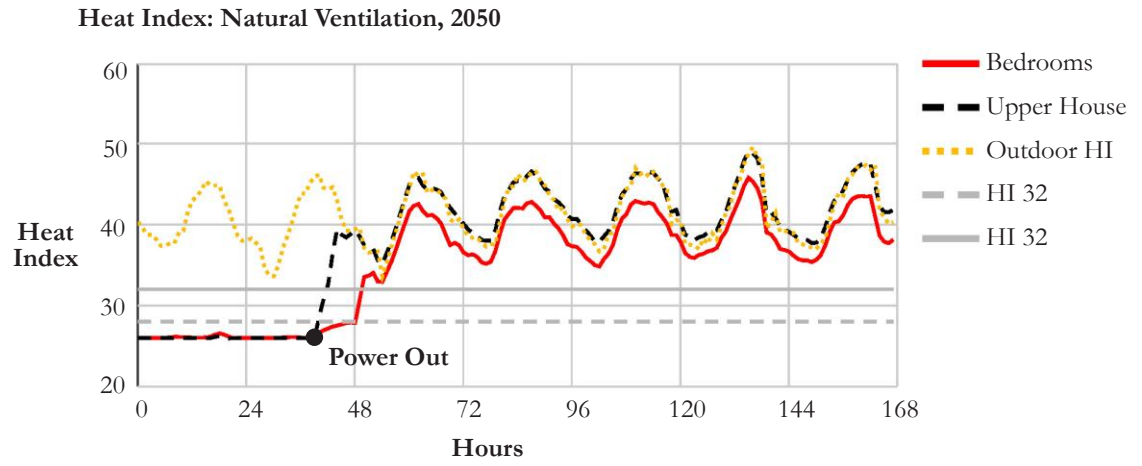
Heat Index: Natural Ventilation, 2050
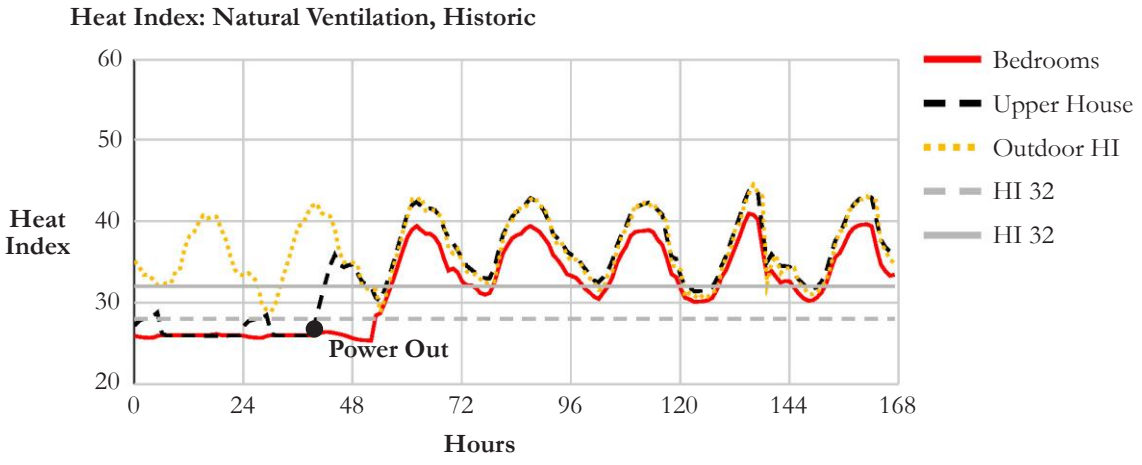
Figure 190. House with below grade bedrooms and natural ventilation during a power outage

250

Heat Index: Earth Tube Ventilation, Historic

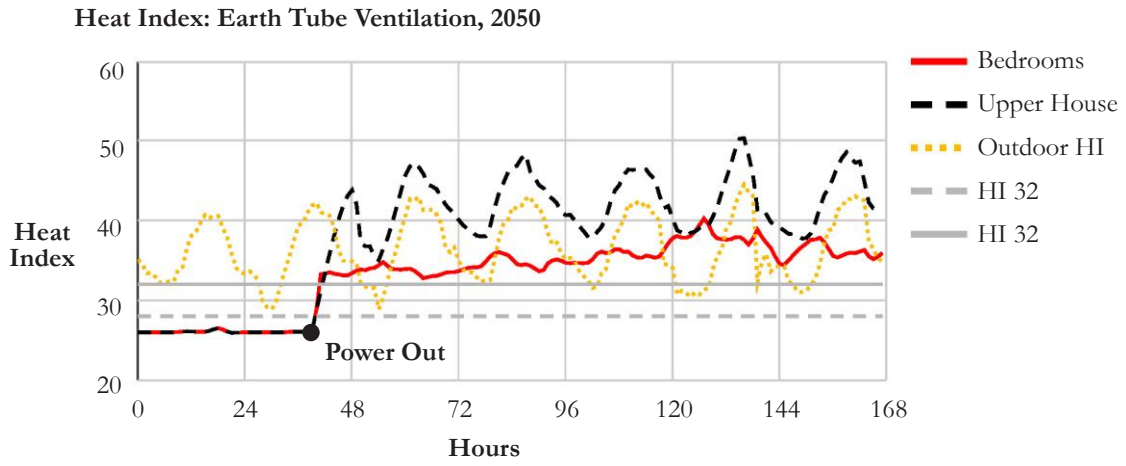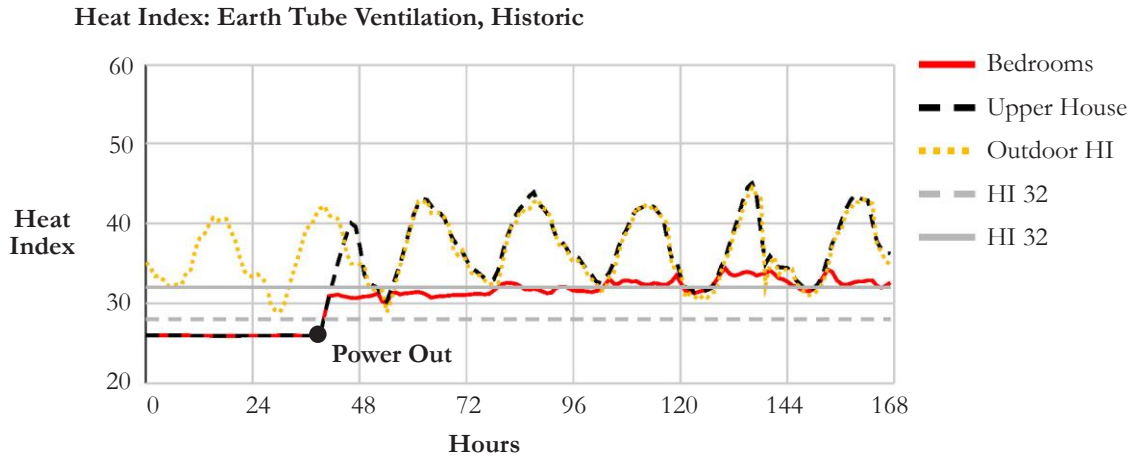**Heat Index: Earth Tube Ventilation, 2050**

Figure 191. House with below grade bedrooms and earth tube ventilation during a power outage

Figure 191 shows that while the heat index in the lower bedrooms increase from Figure 189, it is greatly reduced form the totally naturally ventilating all spaces during a heat wave (Figure 190). Consistent with the conclusions of this thesis, passive survivability is greatly impacted by the prospect of future extremes. This is supported by the 2050 scenario in Figure 191 where heat index hours are greatly increased from historic weather. As, such the earth tube offers a viable ventilation solution for these below-grade, indeed any, zones as a resiliency measure, particularly in buildings with very tight envelopes.

8.1.5. EnergyPlus Earth Tube Design Space

Finally, using the same variables as were used in the analytic example, a multi-objective optimization was run on the energy model. The earth tube temperature supply objective was kept the same, but the fan power objective was changed to the sum of fan energy (J) over the hot week. The resulting design spaces match those from the analytic model.
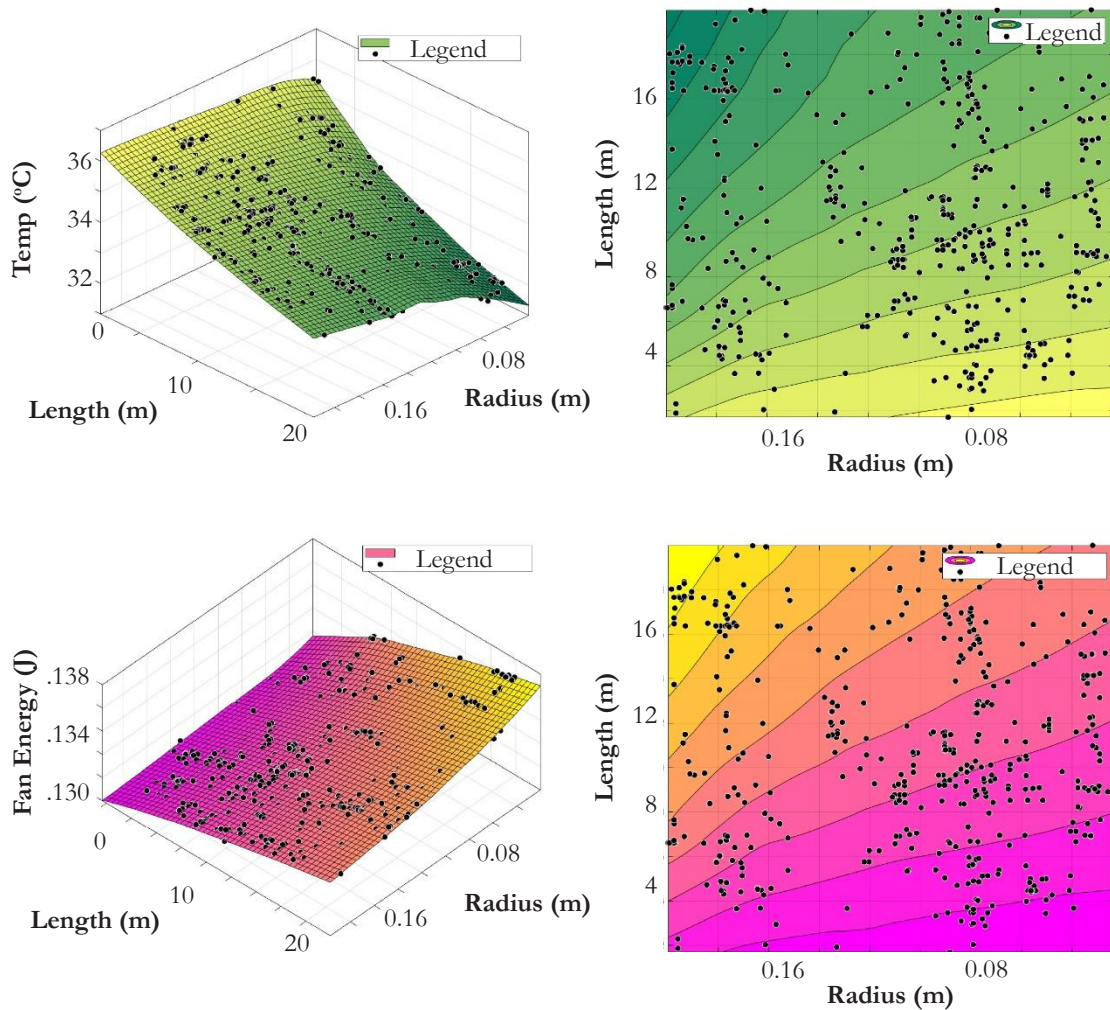

Figure 192. EnergyPlus earth tube design space

252

Page intentionally left blank

Figure 193. Photo of final review (Credit Sheng-Hung Lee)

Torridity Tamed